Single Molecule Studies on the Sec-Translocase

Küsters, Ilja

Stellingen bij het proefschrift:

Theses pertaining to the dissertation:

Single Molecule Studies on the Sec-Translocase

by Ilja Küsters

1. A second copy of SecYEG as an anchor for SecA is not required.

2. a) "There are as many facets of truth as there are ideas. Therefore, before declaring that a particular idea is false, one must try to discover its latent fragment of truth." *Acharya Mahapragya*
   b) In respect of the multitude of conflicting studies on the functional oligomeric state of SecA, it should be considered that neither side is completely wrong.

3. Functional immobilization of biological membranes will be crucial in the development of cybernetic organisms.

4. "Low hanging fruit projects" including single molecule approaches do not exist.

5. Methods with single particle resolution can reveal the number of active proteins of an ensemble, an often neglected but crucial parameter.

6. a) "We are trying to unravel the Mighty Infinite using a language which was designed to tell one another where the fresh fruit was." *Terry Pratchett*
   b) In interdisciplinary networks that include chemists, physicists and biologists, every party talks a different language. Communication scientists are, however, not invited.

7. A model including dynamic changes in the oligomeric state of SecA during protein translocation can merge previously conflicting data. To observe these dynamic changes, the protein translocation process must be observed with single molecule resolution in time.

8. Re-inventing the wheel at the nanoscale is as inefficient as the attempt to build lasting biological nanomachines. The toolbox is full enough; let's stick things together!

9. "Nothing will benefit human health and increase chances for survival of life on Earth as much as the evolution to a vegetarian diet." *Albert Einstein*

For my parents

Cover design: Ilja Küsters

Cover front: "A remarkably unsuccessful attempt to functionally immobilize fluorescently labeled inner membrane vesicles of *E. coli* on amino-silaned glass." 2D confocal scans displayed as height-field plot and rendered by the Persistence of Vision Ray-tracer sofware (POV-Ray, www.povray.org).

Cover back: artist impresstion of *E. coli* and the bacterial protein translocation machinery. The image was created and rendered using POV-Ray. Quote: Title of the fourth part of the book "The Hitchhiker's Guide to the Galaxy" by Douglas Adams.

University of Groningen
Zernike Institute
for Advanced Materials

This Ph.D. study was carried out in the Department of Molecular Microbiology of the Groningen Biomolecular Sciences and Biotechnology Institute (GBB), University of Groningen, The Netherlands. It was finanically supported by NanoNed, a national nanotechnology program coordinated by the Dutch Ministry of Economical Affairs and the Zernike Institute for Advanced Materials.

ISBN: 978-90-367-4938-1

ISBN: 978-90-367-4944-2 (electronic version)

Printed by OffPage, Amsterdam

Printing of this thesis was supported by generous contribution from the University of Groningen and the Groningen Biomolecular Sciences and Biotechnology Institute (GBB).

rijksuniversiteit
groningen

Single molecule studies on the Sec-translocase

Proefschrift

ter verkrijging van het doctoraat in de
Wiskunde en Natuurwetenschappen
aan de Rijksuniversiteit Groningen
op gezag van de
Rector Magnificus, dr. E. Sterken,
in het openbaar te verdedigen op
vrijdag 17 juni 2011
om 11.00 uur

door

Ilja Küsters

geboren op 8 februari 1977
te Düsseldorf, Duitsland

Promotor:	Prof. dr. A.J.M Driessen
Beoordelingscommissie:	Prof. dr. A. M. van Oijen
	Prof. dr. ir. S. J. Tans
	Prof. dr. D.J. Slotboom

Table of Contents

CHAPTER 1

General Introduction

SECA, A REMARKABLE NANOMACHINE

Ilja Kusters and Arnold J.M. Driessen

Published in *Cellular and Molecular Life Sciences*, 2011,
DOI 10.1007/s00018-011-0681-y

Abstract

Biological cells harbor a variety of molecular machines that carry out mechanical work at the nanoscale. One of these nanomachines is the bacterial motor protein SecA that translocates secretory proteins through the protein conducting membrane channel SecYEG. SecA converts chemically stored energy in form of ATP into a mechanical force to drive polypeptide transport through SecYEG and across the cytoplasmic membrane. In order to accommodate a translocating polypeptide chain and to release transmembrane segments of membrane proteins into the lipid bilayer, SecYEG needs to open its central channel and the lateral gate. Recent crystal structures provide a detailed insight into the rearrangements required for channel opening. Here, we review our current understanding of the mode of operation of the SecA motor protein in concert with the dynamic SecYEG channel. We conclude with a new model for SecA mediated protein translocation that unifies previous conflicting data.

1. Introduction

In bacteria, proteins are synthesized in the cytosol at the ribosomes. A major share of these proteins, i.e. about 30%, needs to be transported across or into the cytoplasmic membrane to function at the cell-surface. This process is essential for nutrition uptake, motility and energy conversion as well as pathogenesis. Secretory and membrane proteins are recognized by their N-terminal signal sequences or hydrophobic transmembrane segments (TMS) when emerging as nascent chains at the ribosome and are targeted via two separate routes to the evolutionary conserved protein-conducting channel SecYEG. This hetero-trimeric complex is embedded in the cytoplasmic membrane and allows both the insertion of membrane proteins into and passage of secretory proteins across the membrane barrier. Secretory proteins are mostly translocated post-translationally after their synthesis is completed on the ribosome, but secretion can also occur co-translationally [1]. They appear from the ribosome as nascent polypeptide chains bearing a N-terminal signal sequence and are recognized by the molecular chaperone SecB which binds to the mature region of the preprotein [2]. SecB keeps the preproteins in a partially unfolded and therefore translocation competent state and targets them to the SecYEG bound motor protein SecA [3]. Subsequent binding of ATP to SecA causes the insertion of the signal sequence of the preprotein into the SecYEG channel and the release of SecB. Next, SecA catalyzes the step-wise translocation of the polypeptide chain through multiple cycles of ATP binding and hydrolysis [4-6]. Membrane proteins are targeted via a different route to SecYEG and are integrated into the cytoplasmic membrane in a co-translational manner. The hydrophobic core of TMSs is recognized by the bacterial homologue of the signal recognition particle (SRP) when emerging from the ribosome. Subsequently, SRP targets the ribosome-nascent chain complex to SecYEG where translation at the ribosome provides the driving force for the insertion of the membrane protein (for review see [7]). The Sec-translocase is a large machinery that involves not only SecA and SecYEG, but also another heterotrimeric complex SecDFyajC that stimulates protein translocation by an as yet unknown mechanism. Here we will only focus on the core elements of the translocase and discuss our current insights in the mechanism of protein translocation.

2. The protein conducting channel SecYEG

2.1. SecYEG structure

Protein secretion in bacteria and import of proteins into the endoplasmic reticulum is mediated by a protein-conducting channel that is conserved throughout the three kingdoms of life. This hetero-trimeric integral membrane protein complex is termed SecYEG in prokaryotes and the Sec61 complex in eukaryotes. It consists of one major subunit with 10 TMS, SecY or Sec61α, and smaller subunits that are located at the exterior of the channel. Several crystal structures of archaeal and bacterial Sec-complexes provide detailed structural insight into organization and dynamics of

SecYEG and its homologues. The TMS of SecY assemble into a clamshell-like fold with TMS 1-5 and 6-10 forming the two half-shells that are connected by a flexible hinge between TMS 5 and 6 (Fig 1) which contains a short loop called HL-1 that was suggested by molecular dynamic simulations to be the flexible link that allows opening of the clamshell [8]. SecE appears to stabilize the channel by embracing the clamshell as a clamp. SecG is a non-essential subunit that associates peripherally with the channel [9]. The number of TMS of SecE and SecG varies among the organisms but the functional relevance of the additional TMS is unclear. SecE of *Escherichia coli* (*E. coli*) consists of three TMS while the homologue Sec61γ of the archaeon *Methanocaldococcus jannaschii* has only one TMS. However, an *E. coli* SecE mutant with the two extra TMS truncated is fully functional [10]. The tilt of the SecY TMS creates an hourglass-shaped pore with a funnel-like entrance of 20-25Å that narrows down to a central constriction of around 4Å. This pore ring consists of 6 hydrophobic isoleucine residues and restricts access to the periplasmic side in the closed conformation. Opening of this constriction is necessary to accommodate a translocating polypeptide chain and will result in the formation of a water filled pore if no translocating polypeptide would occupy the channel. The *trans*-side of SecYEG is occluded by an α-helical segment of SecY, called the plug domain that folds back into the periplasmic cavity of the channel (Fig 1). Point mutations that reduce the dependence on signal-sequence recognition map to both pore ring and plug domain [11-13] but the full contribution of these structural elements to channel function and quality control is poorly understood.

SecYEG and its homologue Sec61αβγ were found to form higher oligomeric states in biochemical [14-16] and structural [17-20] studies. The functional relevance of the observed predominantly dimeric and tetrameric species remains unclear. Analysis of the first cryoEM structures of eukaryotic translocation channels led to the hypothesis that an aqueous pore is formed at the interface between oligomers [21-25]. This suggestion was further fueled by the hypothesis that large segments of the SecA motor protein inserts into the channel [4]. Based on the *M. jannaschii* SecYEβ X-ray structure it was proposed that a single SecYEG heterotrimer forms the active translocation channel. Several biochemical and biophysical studies support this hypothesis. First, in a site-specific cross-linking study, a translocation substrate was located to the interior of a single SecY channel [26]. In a second study, introduction of different cross-linkers into the lateral gate prevented fusion of several SecYEG into a bigger pore and created single SecYEG channels with defined maximum pore size. Formation of disulfide bonds with short crosslinks abolished passage of polypeptide chains whereas crossing with longer crosslinking reagents permitted passage [27]. In analogy, cryoEM studies of the homologous Sec61p complex of mammals and yeast suggest that it is monomeric when associated with the ribosome and a translocating nascent chain [28].

SecYEG was also suggested to be dimeric based on the observation that covalently linked SecYEG dimers are functional in protein translocation [26]. Osborne and co-

workers proposed that SecA is anchored to one copy of SecYEG while translocating a polypeptide through the second protomer of a SecYEG dimer. A SecA-SecYEG co-crystal of components of the thermophilic bacteria *Thermotoga maritima* contradicts this view as in this structure SecA is fully docked to monomeric SecYEG and only a few N-terminal residues are close to the presumed membrane interface (Fig 2D) [29]. This structure indicates that SecA is anchored to the SecYEG channel that is promoting passage of the translocating polypeptide chain and that only few SecA residues could interact with a neighboring SecYEG protomer in a putative SecYEG dimer. However, the corresponding residue on SecA that is cross-linked to SecY [26] is far away from the binding interface with SecYEG in the co-crystal suggesting that substantial conformation changes in SecA are needed to bring the two residues close enough to be crosslinked (Fig 2C and D).

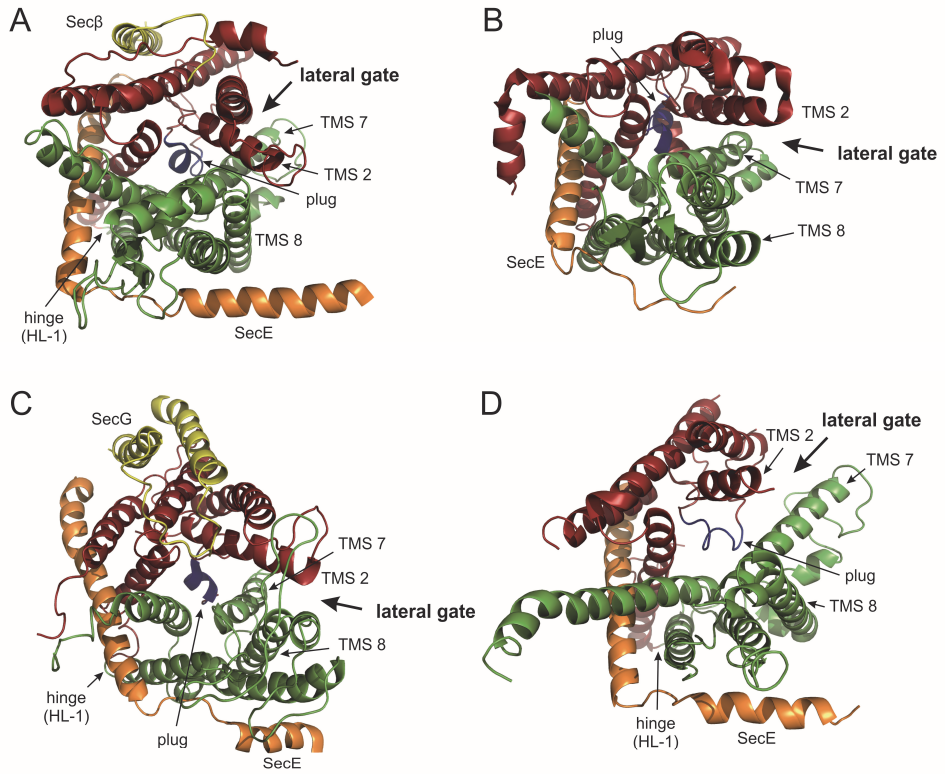

***Figure 1**: Crystal structures of SecYEG in top-view from the cytoplasm. SecY TMS 1-6 (red), TMS 7-10 (green), plug domain (blue), SecE (orange), SecG/β (yellow). (a) SecYEβ from M. jannaschii (PDB accession code: 1RH5). (b) SecYE from T. thermophilus co-crystallized with a Fab fragment (not shown) bound to the C5 loop of SecY (2ZJS). (c) SecYEG from T. maritima co-crystallized with SecA (not shown) (3DIN). (d) SecYE from P. furiosus. In the crystal, the C-terminal α-helix of a neighboring SecY molecule (not shown) inserts partially into the channel inducing opening of the lateral gate (3MP7).*

As the membrane surface is absent in any crystal structure of SecYEG, Deville et al. modeled a second SecYEG copy to the monomeric SecA-SecYEG co-crystal by tilting the two SecYEG protomers relative to each other to achieve an interaction with the SecA N-terminus [30].

2.2. SecYEG binding sites

The cytoplasmic side of SecYEG constitutes a combined binding interface for post- and co-translational protein translocation modes. The SecA ATPase was shown by *in vivo* photo-cross-linking to bind the cytoplasmic loops (C2 and C4-6) although to a different extent depending on the stage of the translocation cycle [31]. In two studies, site-specific disulfide formation between SecA and the C4/C5-loop of SecY was observed [32,33] while a peptide scanning assay revealed a SecA binding site at the interface between TMS4 and the C3 loop of SecY that is close to SecG [32]. Direct contact of SecA and SecG was observed by cross-linking and protease protection [34] but this interaction seems to be non-essential as SecG merely stimulates protein translocation. The *T. maritima* SecA-SecYEG co-crystal provides insight into SecA binding in presence of ADP-BeF_x, a structural analog of an intermediate of ATP-hydrolysis [29]. Surprisingly, the majority of SecA residues identified by biochemical approaches to bind SecYEG are not in the proximity to the respective SecY residues in the structure. One example is residue 255 on *E. coli* SecY that was cross-linked to residue 48 on *B. subtilis* SecA via disulfide bridge formation [26]. The corresponding residues in the *T. maritima* co-crystal (residues 251 on SecY and 43 on SecA) are about 50 Å apart while a disulfide bond is 2 Å in length (Fig 2C and D) [26]. In this structure, SecA is crystalized in the closed conformation with the preprotein binding domain (PBD) moved towards the NBF2 (compare Fig 2 A and B), a conformational change that renders residue 255 of SecY hidden by the PBD (Fig 2C). Thus, SecA must undergo a dramatic conformational change to allow for disulfide bridge formation. On the other hand, if SecA would be bound to SecYEG in the open conformation (Fig 2A), the PBD would not hide residue 255 and would therefore render this position accessible from the cytoplasm. Thus if needed, the binding of a second SecA protomer of a SecA dimer could occur explaining the observed crosslink. Another example is Arg357 in the C5 loop of *E. coli* SecY that was found to be essential for the initiation of post-translational protein translocation [35] but not for SecA binding [32,35,36]. Although the corresponding residue of *T. maritima* SecY (Arg346) is only ~9 Å away from a SecA residue in the SecA-SecYEG co-crystal, no extensive contacts between SecA and SecY are made in this region of the structure. Taken together, these observations suggest that the occupation of SecYEG binding sites by SecA is dynamic during the protein translocation cycle. Ribosome binding occurs at similar sites on SecYEG as for SecA binding. Apparently, these sites play a general role in recruiting ligands, which are essential for channel functioning. The two SecY loops C4 and C5 [17,37-40] as well as the cytoplasmic SecG loop and the N-terminal region of SecE [17] contact the ribosome. Point mutations in loops C4 and

C5 including Arg357 substitutions eliminate ribosome binding [39]. In a recent study, the bacterial homologue of the signal recognition particle (SRP), FtsY, was found to bind to SecY loops C4 and C5 [40]. Hence, SecA, ribosome and SRP use overlapping binding sites on SecY. Occupation of these sites must be dynamic when all components cooperate during membrane protein insertion into the cytoplasmic membrane.

2.3. Opening of the channel

The interface between the tips of the two SecY clamshell-halves is shaped by TMS 2-3 and 7-8 and forms the so-called lateral gate (Fig 1). Opening of this gate is indispensable to expand the channel to accommodate a translocating polypeptide chain during protein secretion [27] and to allow insertion of signal sequences and TMS of integral membrane proteins into the lipid bilayer [41]. Indeed, the signal-sequence of a precursor protein was found to cross-link to TMS 2 and TMS 7 of the yeast SecY homologue Sec61p during posttranslational protein import into the ER [42]. Insertion of a signal-sequence into the lateral gate would result in opening of the hydrophobic constriction as three of the six pore ring residues are located on TMS 2 and 7. However, to allow passage of an α-helical TMS, a gap in the lateral gate of 10-12Å is required. Three X-ray structures provide different views of partially opened translocation channels. SecYE of *Thermus thermophilus* was co-crystallized with a Fab antibody fragment bound to the C5 loop of SecY that induced opening of the cytosolic part of the lateral gate (Fig 1B) [33]. In the closed conformation represented by the *M. jannaschii* structure (Fig 1A), TMS 2 is in close proximity to both TMS 7 and 8 while the TMS 8 of *T. thermophilus* SecY moved away from TMS 2 suggesting a 'preopen' state of the channel. Binding of SecA (ADP-BeF_x) in the *T. maritima* SecYEG-SecA co-crystal induced separation of both cytosolic and periplasmic parts of the lateral gate although further opening would be required to allow insertion of a TMS in α-helical conformation (Fig 1C) [29]. Apparently, the lateral gate opens by a rigid body movement of TMS 6-10 relative to TMS 1-5. This process may be initiated by insertion of a SecA segment, called the two-helix-finger, into SecYEG nearby SecY loops C4 and C5 (Fig 2D). In a recent X-ray structure, two *Pyrococcus furiosus* SecYEβ crystallized as such that the C-terminal helix of one SecY partially inserts into the neighboring SecYEβ thereby functioning as a nascent chain mimic (Fig 1D) [43]. As the result of this insertion, the lateral gate is opened throughout its entire length and the cytoplasmic entrance as well as the pore ring is expanded. While the plug domain still occludes the channel, the pore ring is widened to 13.6 Å where in the *M. jannaschii* structure a 4.6 Å diameter was determined (compare Fig 1A and 1D) [11,43].

In vivo [44] and *in vitro* [45] cross-linking experiments suggest extensive plug movement by around 20-27Å to the C-terminal loop of SecE to allow unrestricted passage of polypeptide chains through the channel. However, immobilization of the plug inside the channel by chemical cross-linkers that allowed displacement of maximal 13Å did not abolish protein translocation *in vitro* indicating that movement of the plug to the periplasmic side of SecE is not necessary [46]. As for the physiological

role of the plug domain, three hypothesizes have been proposed. First, stabilization of the closed conformation has been suggested by instability of SecYEG upon plug deletion [47] and by molecular dynamics simulations [8]. Secondly, in the closed conformation, the plug domain prevents ion leakage through the SecYEG channel acting as a seal [48]. However, deletion of yeast Sec61p and *E. coli* plug domains resulted in thermolabile but viable cells with no significant growth or translocation defects [47,49]. Third, deletion of the plug domain and many point mutations along the plug cause a reduced fidelity of signal sequence recognition (*prlA* phenotype) [47,50,51] and affect membrane protein topology [51]. Therefore, the plug may be involved in proofreading of preproteins and TMSs and mediate channel gating. Furthermore, the plug has been proposed to function as an adjustable flap to protect the emerging preprotein from periplasmic proteases or to assist in folding [52].

Many of the Prl mutations, identified by genetic studies to suppress translocation defects caused by defective signal sequences, reside inside the SecYEG channel [12,13,53]; for review see [54]. Apparently, this *prlA* phenotype is caused by destabilization of the SecY-E interaction that facilitates channel opening [12,55]. Inserted signal peptide, SecA and the ribosome are thought to stabilize the open state of the channel through multiple interactions with SecYEG [11]. Interestingly, PrlA mutants that were shown to bind SecA more tightly also exhibited an enhanced activity in protein translocation assays [56] and were less dependent on the proton motive force (PMF) [57]. Therefore, weaker SecY-E interactions may allow tighter SecA binding by facilitating channel opening leading to exposure of additional or stronger binding sites for SecA. As SecA binding to SecYEG results in a conformational change in SecA that stimulates its ATPase activity [58,59], it appears that a tighter binding of SecA stimulates the initiation of protein translocation, thus allowing a more efficient translocation of wild type preproteins as well as preproteins carrying a defective signal sequence. Therefore, the mechanism of proofreading of the translocation substrates may reside in the regulation of SecA's ATPase activity by conformational states of SecYEG that responds to the physical properties of the signal peptide.

3. The translocation motor SecA

3.1. Cellular localization + binding partners

The ATP dependent motor protein SecA is an essential element of the bacterial translocase engaged in transfer of polypeptides across the cytoplasmic membrane. As a soluble peripheral subunit, it associates with the membrane channel SecYEG and generates the driving force for the transport of secretory proteins and large periplasmic loops of membrane proteins [60]. Binding to signal sequences, unfolded preprotein substrates, anionic phospholipids, SecB and SecYEG allosterically stimulates the ATPase activity of SecA and couples the motor function to the translocation process [58,61].

Localized to the cytosol, SecA is a targeting factor that recognizes signal sequences and the SecB chaperone loaded with the preprotein and binds preproteins destined for secretion [62,63]. On the other hand, SecA was shown to assist in folding of proteins lacking signal sequences [64]. Since preproteins are secreted essentially unfolded, such general chaperone function excludes cytoplasmic proteins from the secretion pathway and adds an additional quality control mechanism to the highly specific secretion process [64]. This suggested moonlight function may further be one reason for the relatively high cytoplasmic concentration of SecA (8 μM [65], corresponding to ~13000 SecA copies per *E. coli* cell assuming an average volume of 2.75 μm^3 per cell [66]) compared to the approximately 500 copies of SecYEG present in a bacterial cell [67].

3.2. Structure of SecA

The SecA protomer consists of functionally and structurally separate domains that act in concert to couple substrate recognition to cellular localization and motor action. The nucleotide-binding domain (NBD) consists of two essential nucleotide-binding folds, NBF1 and NBF2 (also termed intramolecular regulator of ATP hydrolysis 2, IRA2), that sandwich ATP for hydrolysis (Fig 2). The two specificity domains are termed preprotein cross-linking domain (PPXD) or preprotein binding domain (PBD) and C-terminal domain (CTD) [68]. Preproteins bind to the PBD [69-71] the C-terminal linker (CTL) and to the α-helical scaffold domain (HSD) [72]. The CTD is involved in SecB [3,73-75] and lipid binding [76] and consists of an α-helical wing domain (HWD), the CTL that is coordinated with a zinc-ion [75] and HSD that contacts all other domains of SecA (Fig 2).

SecA is a member of the superfamily 2 DEAD (DExH/D) proteins because of its motor domain that has all nine conserved motifs of DNA/RNA helicases included in this family [62,77-79]. Both NBF1 and NBF2 are essential for ATP binding and hydrolysis [80] and form RecA-like binding folds containing Walker A and Walker B motifs [81]. NBF2 regulates the hydrolysis reaction at NBF1 [80,82,83] when a single ATP is bound between the motor sub-domains as common in DEAD-box helicases [84,85]. The ATPase activity of cytosolic SecA is inhibited by the intramolecular regulator of ATP hydrolysis 1 (IRA1), a helix-loop-helix structure of the HSD that contacts both NBF2 and PBD. SecA mutants lacking IRA1 or bearing defects in IRA1/NBF2 interactions display increased ATPase activity independent of preprotein binding [86]. The mechanism of ATPase stimulation by preprotein binding utilizes a conserved electrostatic salt bridge called Gate1 that regulates the access to the nucleotide binding site [59]. Motions with the motor domain are induced by ATP binding and ADP release, respectively [83,85,87] and these conformational changes are thought to be transmitted to the two specificity domains PBD and CTD which directly contact the NBD [70,83]. The preprotein binding domain inserts into NBF1 as a stem-like structure while the CTD contacts both NBF1 and NBF2 via an extended helix of the HSD (Fig 2A and B) and inhibits the ATPase activity [86-89].

Motions of PBD [29,59,70,90] and CTD [4,29,86,88,89] have been suggested to be transferred to the preprotein to push it through the SecYEG channel [4,29,77,90]. PBD displacement relative to the HWD is a major conformational change observed in SecA crystal structures (compare Fig 2 A and B) but whether this motion is dependent on nucleotide or preprotein binding remains unclear [68]. Yet, it seems conceivable that SecA mediates the directed movement of polypeptide segments through the SecYEG channel by coupling motor action to specific substrate and SecYEG interaction.

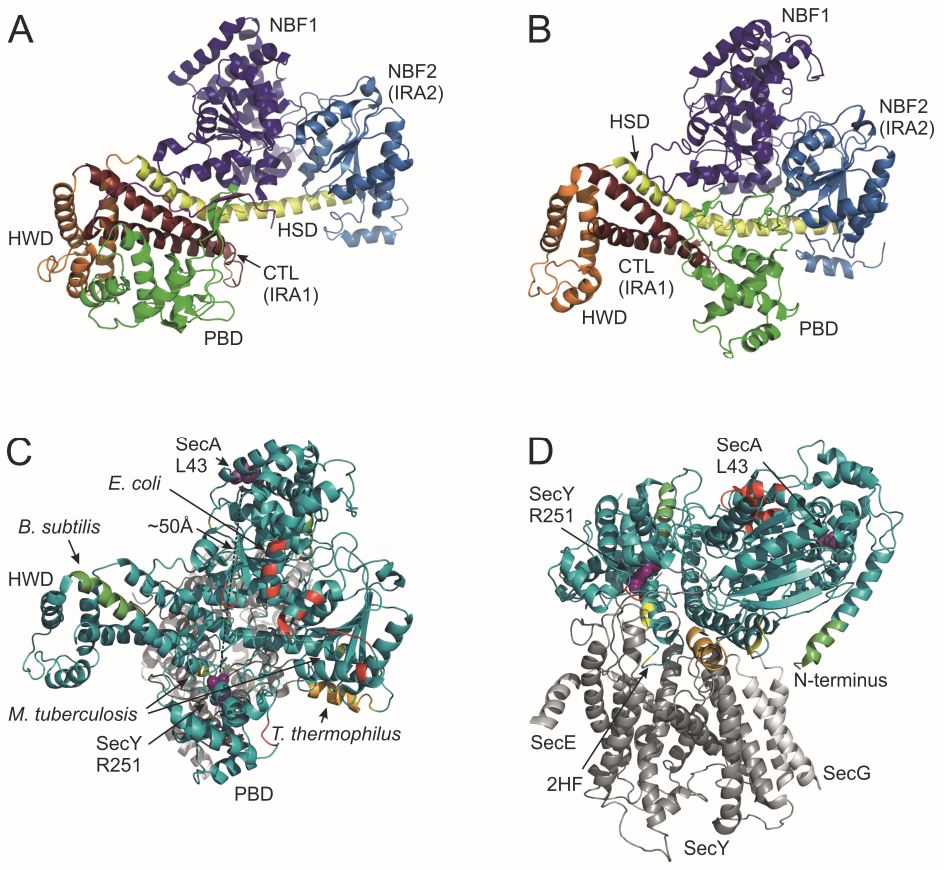

Figure 2: *Conformational changes in SecA crystal structures and SecA dimerization interfaces. (a) SecA protomer from B. subtilis (1M6N). (b) SecA from T. maritima co-crystallized with SecYEG (not shown) (3DIN). (c) Top view (cytoplasmic side) of the SecA-SecYEG co-crystal as in (b) with residues implicated in dimerization in dimeric SecA structures of E. coli (red, 2FSF), B. subtilis (green, 1M6N), T. thermophilus (orange, 2IPC) and M. tuberculosis (yellow, 1NL3). Residues SecY251 and SecA43 that were previously crosslinked [26] are shown as spheres. SecA is displayed in cyan and SecYEG in gray. (d) Side view of (c).*

3.3. The second protomer and the dimerization interface

Soluble SecA forms homo-dimers and is expected to be mostly dimeric in the cytosol [65,91,92]. Several high-resolution structures of SecA from various species have been solved: eight by X-ray crystallography and one by NMR [70]. Additionally, medium and low resolution structures obtained by cryo-EM [93-95], atomic force microscopy (AFM) [93], small angle X-ray scattering [96] and small angle neutron scattering [97] provide insight in SecA oligomerization and its conformational changes. Although the majority of structures show SecA as a homo-dimer, dimerization interface and orientation of the second protomer differs greatly among the structures [84,93-100]. Furthermore, the diameter of observed SecA dimer particles in electron microscopy varies from 10 to 15 nm demonstrating significant conformational differences. In most of the structures, SecA is organized as an antiparallel dimer with its C-domains at the extreme ends. Exceptions are the parallel dimer structure from *T. thermophilus* [99] and one structure from *B. subtilis* that shows a single protomer in the asymmetric unit although a crystallographic dimer can be recognized [85]. The variety of dimerization interfaces implies that either multiple dimeric conformations are possible or some of the observed dimers do not reflect the physiological state of cytosolic SecA. Since for some structures high salt concentrations were present during crystallization, monomerization and re-dimerization according to the crystal confinements could have occurred. This hypothesis is supported by the observation that dimerization occurs via electrostatic and hydrophobic interactions [91,95,98,100,101]. If cytosolic SecA would indeed form multiple dimeric states they might either all support its role as targeting factor [68] or display SecA's different functions as, for example, chaperone for cytosolic proteins. The hypothesis of diverse conformational states of SecA dimers is supported by a study suggesting the existence of multiple equilibriums of SecA dimers in solution [91]. It is tempting to speculate further that the observed dimerization interfaces are part of the catalytic cycle of dimeric SecA during protein translocation. Alternatively, the different dimeric conformations in solution may be irrelevant if only the SecYEG bound state is stabilized and critical for function [68]. Interestingly, in the *T. maritima* SecA-SecYEG co-crystal, residues that were implicated for dimerization in the *E. coli* and *B. subtilis* SecA crystal structures are exposed to the cytoplasmic surface and would allow binding of a second SecA protomer via this interface (Fig 2C and D). The residues thought to be important for dimerization in the *T. thermophilus* and *M. tuberculosis* SecA crystals, however, are in close proximity to the SecY-SecA binding interface, thus would not allow SecYEG binding of SecA dimers in a configuration as presented in these SecA crystals (Fig 2C and D). In several studies, dimerization and orientation of the second protomer in solution was examined. Intermolecular cross-linking studies at the C-terminus confirm dimerization of SecA [102] and are in agreement with the antiparallel orientation of three of the observed structures [100,103] as well as a FRET study [104].

3.4. Ligands modulate SecA dimerization

The oligomeric state of SecA in solution, bound to SecYEG and when engaged in protein translocation has been investigated in a multitude of studies with various methods. Yet, contradicting results, their interpretations and physiological relevance caused a long lasting controversy. Briefly, oligomerization of SecA in solution is dynamic and the dissociation constant K_d that was previously estimated to be around 0.1 μM [91] has been determined by an equilibrium technique to 0.76 nM [105]. This monomer-dimer equilibrium of SecA in solution may be modulated by ligands such as signal peptides, anionic lipids or nucleotides although contradicting results do not allow firm conclusions. However, the sensitive nature of the monomer-dimer equilibrium is apparent in the presence of factors such as detergents, salt or temperature [91,106,107]. The oligomeric state of SecYEG-bound SecA has been investigated mainly in detergent or other artificial environments that may have compromised its native condition. However, an important contribution to this subject has been made by a model of SecA bound to SecYEG derived from a medium-resolution X-ray structure (Fig 2C and D) [29]. Monomeric SecA from *T. maritima* is bound to a single SecYEG trimer of the same organism. The most prominent change is the rotation of the PBD of about 80° toward the NBF2 (Fig 2B) compared to the *B. subtilis* SecA structure (Fig 2A) which is considered to present the closed form of SecA [85]. Another structure of dimeric SecA from *B. subtilis* alone was suggested to be the open form and had the PBD rotated to a lesser extent [100]. In the SecA/SecYEG complex lacking a substrate, PBD movement from CTD to NBF2 results in a clamp like structure that may enclose a preprotein. Moreover, the PBD rotation creates a pore in SecA that aligns with the SecYEG channel. Crystallization was achieved in presence of ADP-BeF_x, a structural analog of an ATP hydrolysis intermediate step, and the model may present an intermediate state of protein translocation. However, the necessary use of detergent suggested to be responsible for the loss of the second SecYEG subunit may also have caused dissociation of the SecA dimer especially since detergents were shown to monomerize SecA [106,107]. Therefore, interpretations derived from this model concerning the mechanism of SecA protein translocation activity need to be confirmed in a more physiological environment. In a recent study, the oligomeric state and binding of SecA to SecYEG is investigated in equilibrium under physiological buffer conditions and SecA is found to bind as a dimer [105]. During catalysis, SecA appears to be dimeric as demonstrated by *in vitro* protein translocation activity assays. Intermolecular cross-linked SecA dimers were shown to be fully active in protein translocation [102,108,109] and more active than non cross-linked species under conditions that favor monomerization [105]. Furthermore, mutants of SecA with a monomer-dimer equilibrium shifted towards the monomeric form display low or no protein activity [103,107,110,111] and hetero-dimers composed of active and non-active SecA monomers were completely inactive [92]. The translocation chaperone SecB interacts with dimeric SecA [73,112] and with the C-termini of both protomers [73,113]. Moreover, SecA reaches maximal coupling of

ATP hydrolysis with preprotein translocation when two of its protomers bind SecB [112]. The two SecA protomers were shown to bind SecB separately by a disulfide crosslinking study [114]. The multitude of contradicting results, methods and interpretations causes an ongoing debate on the oligomeric state of SecA during protein translocation. Therefore, it is important to focus this discussion on the SecA that is actively engaged in translocation and bound to SecYEG.

4. Energy – fueling translocation

After targeting of a preprotein to SecYEG bound SecA, energy in the form of both ATP and PMF is consumed at different stages of the translocation reaction [5,115,116]. ATP hydrolysis occurs at the DEAD-motor domain of SecA with ADP-release being the rate-limiting step for the subsequent catalysis [83,117]. The ATPase activity of cytosolic SecA [86] is stimulated by binding to SecYEG and preproteins [58,59] and is inhibited by azide [118]. Thus, ATP is hydrolyzed throughout the reaction and is essential for the initiation of protein translocation [5]. Although protein translocation through the Sec-system requires polypeptide chains that are largely unfolded, tightly folded protein domains can be translocated by SecA accompanied by elevated ATP consumption. Therefore, a chaperone-like and ATP dependent unfolding activity has been proposed for SecA [64,119].

The PMF is not essential for protein translocation but has stimulating effects on different stages of the reaction cycle. During initiation of preprotein translocation, the insertion and possibly also orientation of the signal-sequence in the translocation channel is affected by the PMF [120]. Protein translocation can be driven by the PMF alone when the inserted polypeptide chain is not attached to SecA [5,6,115,121]. Furthermore, SecA de-insertion from the membrane (i.e., a SecA conformational change) is accelerated in presence of the PMF either by stimulating ADP release from SecA [122,123] or by promoting conformational changes in SecY [14,57,115]. In absence of PMF and SecA, translocating preproteins can slide backwards towards the cytoplasmic side of the channel [5,120]. However, the PMF does not promote preprotein movement in an electrophoretic manner as stretches of both positively and negatively charged amino acids inhibit protein translocation [124]. Clusters of particularly positive amino acids appear to inhibit SecA's ATPase activity by a yet unknown mechanism. Overall it seems as if the PMF supports the unidirectional movement of preproteins at stages where SecA does not contact the translocating polypeptide chain, and promotes the catalytic cycle by stimulating conformational changes in the translocon. In this respect, protein translocation by PrlA mutants shows a remarkably reduced PMF-dependence, and this has led to the suggestion that the PMF modulates the channel opening [57].

5. On the mechanism of SecA mediated protein translocation

5.1. Brownian ratchet, power stroke, peristalsis and subunit recruitment models

Despite the multitude of structural and biochemical details revealed over the last two decades, the exact mechanism of SecA mediated protein translocation is unknown. The suggested mechanisms can be summarized in four models: i) Brownian ratchet; ii) power stroke; iii) peristalsis and iv) subunit recruitment model. Besides this general mode of SecA function, the oligomeric states of SecA and SecYEG in these models are a matter of controversy. After reviewing the four conflicting previous models we propose a new model combining core elements of all four models into one unifying hypothesis that is supported by recent data.

In analogy to protein import into the endoplasmatic reticulum, a ***Brownian ratchet*** mechanism was proposed for protein secretion [125]. Here, SecA would only mediate channel opening thereby enabling the preprotein to diffuse into the SecYEG pore. Spontaneous backsliding of the preprotein is prevented by ATP dependent trapping by SecA, thus allowing diffusion only in one direction similar to the action suggested for BiP (for review see [126]). This hypothesis was recently revived by a study that suggests that preprotein translocation occurs in a single rate-limiting step which is dependent on preprotein length [127]. This idea is opposed to another study in which the translocation rate is independent of the length of the polypeptide chain [128], but also by observations that translocation occurs in steps [4-6]. Obviously, the Brownian ratchet model, cannot explain the observed step-size of protein translocation.

Based on early observations that preproteins are translocated in steps of defined size, SecA was suggested to act as a ***power stroke motor*** [5,6,128,129]. According to this model, ATP hydrolysis and the resulting conformational changes are directly coupled to mechanical pushing of the polypeptide chain through the SecYEG channel. To accomplish mechanical pushing, multiple contacts between preprotein and SecA are comprehensible and support this hypothesis [69-71]. Furthermore, a structural domain of SecA, the so-called two-helix finger, was shown to interact with the preprotein during protein translocation [130]. In the SecA-SecYEG co-crystal of *T. maritima* this two-helix finger is partially inserted into the cytoplasmic opening of the channel (Fig 2D) [29]. Furthermore, a tyrosine residue in this domain that can be substituted only by another bulky hydrophobic residue is important for protein translocation. It has been suggested that the tyrosine residue interacts with the translocating protein through side-chain interactions. However, the observation that long stretches of glycine residues can be translocated rather suggests main chain interactions as a key step [124]. Moreover, since the possible conformational change of the two-helix finger and the resulting lever arm is relatively small, a single movement of the two-helix finger alone could not drive the translocation of the observed 2-2.5 kDa segments [5]. Surprisingly, residues suggested to mediate dimerization in the *M. tuberculosis* SecA crystal reside in the two-helix finger (Fig 2D).

A more defined power stroke model is the inchworm model previously proposed for monomeric DEAD helicases that move along nucleic acids by means of their two nucleotide binding sites (NBS). One of the NBS (henceforth called NBS1) is bound tightly to the DNA while the other NBS (NBS2) is bound weakly. Upon ATP binding and hydrolysis, the weakly bound NBS2 dissociates from the DNA and is moved to a position ahead on the DNA strand by a power stroke motion. At its new position, NBS2 forms a tight interaction with the DNA and the previously tightly bound NBS1 loosens its interaction. A new cycle of ATP binding and hydrolysis would move the NBS1 ahead on the DNA [81,131,132]. Since the DEAD motor of SecA shares a high homology with monomeric helicases, a similar model was proposed for SecA mediated protein translocation [133]. In analogy to the helicases, the translocation machinery would transport the preprotein by means of two substrate binding sites of which one would anchor the polypeptide chain by a tight interaction and the other would dissociate from the substrate to grab a consecutive segment. Monomeric SecA, however, has only one preprotein binding site and thus could not move the preprotein alone. Therefore, the second binding site was proposed to reside on SecYEG [26,107] although experimental evidence is missing. Importantly, in the absence of SecA translocating polypeptides can move freely within the channel [5], thus SecYEG does not seem to form a stable anchor for the preprotein. Moreover, for the observed translocation of preprotein segments of approximately 85Å length [5,6], a very large conformational change of monomeric SecA would be necessary to provide a lever arm of suitable length. Dimeric SecA, on the other hand, has two peptide binding domains and movement of one protomer relative to the other may allow SecA to move along the polypeptide chain similarly to DEAD helicases with their two substrate binding sites. One SecA protomer could trap the polypeptide chain in the channel while the other protomer moves back to grab a consecutive segment of the preprotein.

A combination of power stroke and Brownian ratchet model is the ***peristalsis model***. It suggests binding of dimeric SecA to a SecYEG dimer such that a large vestibule is created between channel and motor protein [60,126]. A central opening as observed in the crystal structures of dimeric SecA of *B. subtilis* [85], *M. tuberculosis* [98] and *T. thermophilus* [99] was proposed to trap the polypeptide chain of a preprotein after ATP binding to SecA. Subsequently, an ATP driven power stroke motion would reduce the volume of the vestibule and thereby force the channel to open enabling the trapped preprotein segments to diffuse into the SecYEG channel. Thus, the actual translocation reaction is driven by Brownian motion while the power stroke merely promotes channel opening. Backsliding of the preprotein is prevented by closure of the central opening in the SecA dimer. This peristalsis model assumes the symmetric docking of the two SecA protomers onto two copies of the SecYEG channel. The orientation of SecA and SecYEG in the co-crystal, however, is opposed to the idea of a symmetric $SecA_2$-$SecYEG_2$ complex. Thus, new structural data are required to support this hypothesis.

A different model based on numerous observations on the sensitive nature of the SecA monomer-dimer equilibrium suggests a ***subunit recruitment mechanism*** [106]. This model is similar to the 'active rolling' model proposed for ATP-dependent helicases that are homologous to SecA. In this 'rolling' model, a monomeric helicase is bound to the nucleic acid polymer and recruits another protomer to bind the upstream segment of the nucleic acid strand. Thus, movement along the polymer is mediated by oligomerization of the helicases that only appears in presence of nucleic acids [134-136]. The observation that phospholipids induce monomerization of SecA while the presence of signal-peptides causes SecA to dimerize has lead to the hypothesis that polypeptide transport is mediated by recruitment of a second SecA protomer onto a SecYEG bound SecA monomer [106]. However, the presence of synthetic signal peptides caused monomerization of SecA in two other studies [107,137], but it should be emphasized that these were observations in the absence of SecYEG involving non-physiological amounts of synthetic signal peptide. Rather, in the presence of SecYEG and a translocating preprotein, SecA does not seem to monomerize [105]. Yet, the sensitive nature of the SecA monomer-dimer equilibrium that is maintained in the SecYEG bound state [105] may support a subunit recruitment mechanism.

5.2. The reciprocating piston model

A unifying model would have to include that a protein translocation cycle comprises two discrete steps, one ATP dependent and one that only requires SecA binding to the translocon [5,6]. ATP binding to SecA is thought to fuel a power stroke motion whereas the translocation event upon SecA (re-)binding likely underlies a different mechanism. Another element of our model are conformational changes in SecA that have been interpreted as insertion-deinsertion cycle as large parts of SecA become accessible from the periplasm for small probes [138] and are protected against proteases [4,139]. Considering the inner dimensions of SecYEG and the bulkiness of SecA, it is unlikely that the latter penetrates entirely and deep into the channel or even reaches the periplasm. The conformational changes in SecA may trigger a partial channel opening, thus allowing small molecules to diffuse through SecYEG. The previously interpreted inserted state could result from a densely packed conformation that is resistant against the applied proteases. However, the two helix finger of SecA inserts partially into the entry funnel of SecYEG in the SecA-SecYEG co-crystal [29] which may represent an intermediate state of the conformational cycle that SecA undergoes during protein translocation. As previously mentioned, several studies have come to the conclusion that SecA functions as a dimer [92,102,108,110] while other studies suggest that monomeric SecA plays a role in protein translocation [29,103,107]. SecA was found to bind SecYEG in both monomeric [15,29,107] and dimeric form [15,16,102,110] and the SecA monomer-dimer equilibrium is sensitive to a wide range of ligands and agents such as salt and detergents (see previous section). Together with the observation that SecA dissociates from the preprotein upon ATP

hydrolysis [5], these data suggest that protein translocation includes cycling of SecA via a monomeric intermediate.

In an attempt to unify previous conflicting studies while integrating recent developments we propose a reciprocating piston model for protein translocation (Fig. 3). First, a cytosolic SecA dimer binds with high affinity to the SecYEG channel (step 1) [102,110] leading to a conformational change and an elevated ATPase activity of SecA (step 2) [58,59]. Based on recent data [105] we propose a model of dimeric SecA binding to SecYEG where one SecA is anchored to SecYEG while the other protomer interacts with the bound SecA alone. Interestingly, the preprotein binding domain (PBD) of SecYEG-bound SecA undergoes a dramatic conformational change resulting in a clamp-like structure (compare Fig. 2A and B) [29]. Docking of a second SecA protomer onto the SecA-SecYEG structure brings both PBDs into close proximity enabling the transfer of polypeptide segments from one SecA protomer to the other [105]. In the cytosol, the molecular chaperone SecB maintains the translocation competent state of newly synthesized preproteins by binding to their mature region thereby keeping them partially unfolded (for SecB review see [140]).

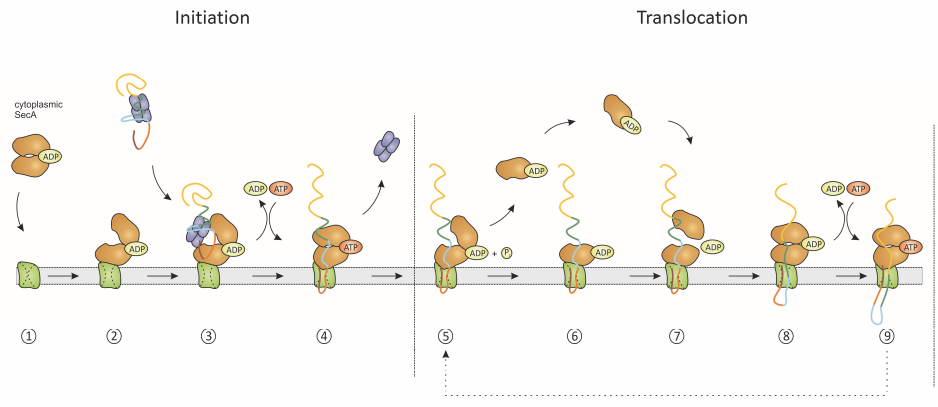

Figure 3: *The reciprocating piston model of SecA-mediated protein translocation. The polypeptide chain of the preprotein is colored differently to illustrate distinct segments that are translocated in steps of defined size*

Homo-tetrameric SecB targets the preprotein to SecYEG- bound SecA [2] by interacting with both C-termini of the SecA dimer (step 3) [73,112,113]. The SecA protomers bind SecB separately (step 3) [114]. Upon binding of ATP to SecA, signal sequence and adjacent mature region of the preprotein are inserted into the SecYEG channel in a hairpin-like structure (step 4) [141-143]. During this step, dependent on ATP binding to SecA, SecB is released from the complex [73] which completes the initiation of protein translocation. ATP hydrolysis causes dissociation of SecA from the preprotein [5] and possibly also monomerization of the SecA dimer whereas one SecA protomer remains bound to SecYEG preventing backsliding of the partially

translocated polypeptide chain (step 5). Additionally, ATP hydrolysis leads to the conformational change in the SecYEG-bound SecA that has been interpreted as de-insertion (step 6) [4], a step that is accelerated by the PMF [14,57,115,122,123]. The dissociated SecA monomer can exchange with the soluble SecA pool or re-bind to the trapped preprotein (step 7) and the SecYEG-bound SecA protomer would cause the observed ATP-independent translocation of a 2-2.5 kDa preprotein-segment (step 8) [5,6].This step may resemble elements of the previously proposed peristalsis model [60] and subunit recruitment mechanism [106]. Binding of an 'upstream' preprotein segment by the soluble SecA protomer and subsequent dimerization could compress the polypeptide chain in the complex thereby forcing it into the channel. Here, Brownian motion would drive movement of the polypeptide chain while directionality is given by the bound, previously soluble, SecA protomer. Next, binding of ATP to SecA results in a power stroke motion accompanied by insertion of SecA into SecYEG [4,29,139] and translocation of another 2-2.5 kDa preprotein segment (step 9). The steps 5-9 are repeated until the preprotein is fully translocated across the membrane. In total 4-5 kDa of the polypeptide chain are transported in each catalytic cycle, which corresponds to around 25-30 amino acids [5,6]. To elucidate the exact mechanism of SecA function, in particular the ATP independent translocation step, new biophysical techniques are required that enable the analysis of protein translocation at the single molecule level with time resolution.

Scope of this thesis

Over the last two decades, a multitude of biochemical and biophysical studies on the oligomeric state of the subunits of the bacterial translocase have been conducted. Yet, due to conflicting results and interpretations, the topic remains in dispute. In part, this is due to the different experimental conditions and techniques employed to investigate the matter and the challenge to determine oligomeric states at or in the membrane interface. The scope of this thesis is to determine the quaternary structure of SecA and SecYEG in a native like environment that sustains the activity of the entire translocation system. To this end, new fluorescence based methods are developed and applied to monitor the oligomeric state of proteins within or associated with the lipid bilayer. Purification, site specific fluorescent labeling and functional reconstitution of the translocon allowed the assessment of protein translocation *in vitro* (chapter 2 and 8). In order to monitor ligand-membrane receptor interactions in equilibrium and with single molecule sensitivity, a recently developed method, termed DCFBA, was modified (chapter 3). DCFBA was used to determine the quaternary structure of SecA when bound to SecYEG being actively engaged in protein translocation (chapter 4). The oligomeric state of SecYEG embedded in the lipid bilayer of giant unilamellar vesicles was investigated by fluorescence cross-correlation spectroscopy in chapter 5. To address kinetic parameters of the translocation reaction, new immobilization techniques for membrane vesicles were developed that sustain the activity of (membrane) proteins (chapter 6 and 7). Furthermore, DCFBA is applied to measure protein translocation activity with single molecule sensitivity in chapter 7.

CHAPTER 2

PURIFICATION AND FUNCTIONAL RECONSTITUTION OF THE BACTERIAL PROTEIN TRANSLOCATION PORE, THE SECYEG COMPLEX

Ilja Kusters, Geert van den Bogaart, Janny de Wit, Viktor Krasnikov, Bert Poolman, and Arnold Driessen

Published in *Methods of Molecular Biology* (2010) 619:131-43

Abstract

In bacteria, proteins are secreted across the cytoplasmic membrane by a protein complex termed translocase. The ability to study the activity of the translocase *in vitro* using purified proteins has been instrumental for our understanding of the mechanisms underlying this process. Here, we describe the protocols for the purification and reconstitution of the SecYEG complex in an active state into liposomes. In addition, fluorescence based *in vitro* assays are described that allow monitoring translocation activity discontinuously and in real time.

1. Introduction

Protein translocation across the cytoplasmic membrane of bacteria is mediated by a protein complex termed translocase (for review *see* [60]). Translocase consists of the membrane embedded protein conducting channel SecYEG [144], the associated soluble motor protein SecA [2,4], and a chaperone, SecB. Secretory proteins synthesized at the ribosome are bound as nascent chains by SecB which prevents their folding and aggregation. SecB targets these so-called precursor proteins to the SecYEG bound SecA [2,145]. Subsequent protein translocation is driven by SecA motor through repeated cycles of ATP binding and hydrolysis whereby the precursor protein is threaded through the SecYEG pore [5]. Major advances in our understanding of this process have been achieved by studying the function of the components of the translocase by *in vitro* methods. In this chapter we describe methods to express, purify, and functionally reconstitute the translocase into proteoliposomes and assays to monitor *in vitro* translocation activity discontinuously and in real time.

2. Materials

2.1. Isolation of Inner Membrane Vesicles (IMVs)

1. LB broth supplemented with 0.1 mg/mL ampicillin
2. *E. coli* SF100 transformed with pET84 (for over expression of SecYG295C EG with N-terminal His-Tag on SecY, ApR)
3. Isopropyl-β-d-thiogalactopyranoside (IPTG), 1 M
4. PMSF 100 mM in 96% Ethanol, 1 M Dithiothreitol (DTT),100 mg/mL DNase and RNase each.
5. Cell disrupter (French press)
6. Tris-sucrose: 50 mM Tris-HCl pH8, 20% (w/v) sucrose
7. Tris-sucrose for sucrose gradient: Tris-sucrose with 55, 51, 45 and 36 % (w/v) sucrose
8. Hepes-KOH pH 7, 50 mM

2.2. Purification and Fluorescent Labelingof SecYEG

1. Buffer S: 50 mM Hepes-KOH pH 7, 20% (v/v) glycerol, 100 mM KCl, 2% (w/v) n-Dodecyl-β-maltoside (DDM)
2. Buffer W: Buffer S with 0.1% DDM and 10 mM Imidazol
3. Buffer E: Buffer W with 0.3 M Imidazol
4. HIS-Select Nickel Affinity Gel (Sigma-Aldrich)
5. Fluorescein-maleimide (Invitrogen, Molecular Probes), 100 mM in dimethylformamide
6. Bio-Spin Chromatography column, empty (Bio-Rad)

2.3. Reconstitution of SecYEG into E. coli Total Lipid Liposomes

1. SecYEG-buffer: 50 mM Tris pH 8, 50 mM KCl, 10% glycerol, 1 mM DTT

2. *E. coli* total lipids (Avanti Polar lipids, Inc.) 4 mg/mL in SecYEG-buffer
3. Bio-Beads SM-2 adsorbents (Bio-Rad), washed and equilibrated (see step 5 of Section 3.3)
4. Bio-Spin Chromatography column, empty (Bio-Rad)
5. Bath sonicator or membrane extruder

2.4. Purification of SecA

1. LB broth supplemented with 0.1 mg/mL ampicillin
2. *E. coli* DH5α transformed with plasmid pMKL18 (unpublished, gift of R. Freudl, SecA gene cloned in pUC19 vector, expression of SecA, ApR) [146].
3. Cell disrupter (French press)
4. SecA buffer: 50 mM Tris-HCl pH 7.6, 10% glycerol, 1 mM DTT and SecA buffer supplemented with 1 M NaCl
5. FPLC system (ÄKTA explorerTM, GE Healthcare or equivalent)
6. HiTrap Q HP columns (5 mL)
7. CentriprepR YM-50 centrifugal filter unit (Millipore)
8. Superdex 200 XK26/60 column (GE Healthcare)
9. SDS-PAGE

2.5. Purification of ProOmpA from Inclusion Bodies

1. LB broth supplemented with 0.1 mg/mL ampicillin
2. *E. coli* DH5α transformed with pET503 (over expression of proOmpA C290S, ApR)
3. Isopropyl-β-d-thiogalactopyranoside (IPTG), 1M
4. Tris-HCl pH 7, 50 mM
5. Sonicator MSE Soniprep 150 (Sanyo Biomedical Europe) or other cell disruptor.
6. ProOmpA buffer: 8 M urea, 50 mM Tris-HCl pH 7.0

2.6. Fluorescent Labeling of ProOmpA

1. Tri(2-carboxyethyl)phosphine (TCEP, Invitrogen) 100 mM in 100 mM Tris-HCl, pH 7.0 (*see* Note 1)
2. Fluorescein-5-maleimide (Invitrogen) 40 mM in dimethylformamide (DMF), (*see* Note 2)
3. ProOmpA in 8 M urea 1 mg/mL in 50 mM Tris-HCl pH 7
4. Dithiothreitol (DTT), 1 M, cold Acetone (−20°C) and 20% (w/v) trichloroacetic acid
5. ProOmpA buffer: 8 M urea, 50 mM Tris-HCl pH 7

2.7. In vitro Translocation of Fluorescently Labeled ProOmpA (Discontinuously)

1. 10-fold Translocation buffer: 500 mM HEPES-KOH pH 7.4, 300 mM KCl, 5 mg/mL BSA, 100 mM dithiothreitol (DTT), 50 mM $MgCl_2$
2. *E. coli* inner membrane vesicles (IMVs) or proteoliposomes with reconstituted SecYEG
3. Purified *E. coli* SecA, SecB (*see* Note 3) and fluorescently labeled proOmpA

4. Energy mix (50 mM creatine phosphate, 0.1 mg/mL creatine kinase), 100 mM ATP in 100 mM Tris-HCl pH 7.5, and 1 mg/mL proteinase K, 20% (w/v) trichloroacetic acid
5. (TCA), cold Acetone (−20°C)
6. Materials for running a 12% SDS-PAGE gel and 2x SDSPAGE loading buffer
7. Roche Lumi-imager F1 (Roche Diagnostics) or equivalent imager

2.8. In vitro Translocation of Fluorescently Labeled ProOmpA (Real Time)

8. Materials from 1 to 4 from Section 2.7.
9. Spectrofluorometer, e.g. Aminco Bowman Series 2 (SLM Instruments).

3. Methods

All components of the Sec translocase can be purified and reconstituted to yield an active *in vitro* translocation system. The SecYEG complex reconstituted into liposomes together with SecA represents the minimal translocase that is sufficient for protein translocation [144,147]. SecG co-purifies with SecE with SecY and enhances the translocation efficiency [144,147]. Several methods for the reconstitution of membrane proteins into proteoliposomes have been described. Here, we describe a mild method for the reconstitution of SecYEG that leads to a high number of protein-containing proteoliposomes with a homogeneous SecYEG distribution and little, if any, protein aggregates. We made use of a dual-color laser-scanning confocal microscope and dual-color fluorescent-burst analysis (DCFBA, for review and description of the method see [148]) to determine the distribution of reconstituted SecYEG among proteoliposomes supplemented with the fluorescent lipid analog DiD. The fluorescent signal distribution of individual proteoliposomes follows a log normal distribution indicating a random reconstitution and the absence of large lipid-free SecYEG aggregates (Fig. 1). In addition, 80% of SecY co-migrates with DiD containing liposomes. The remaining 20% may be assigned to small proteoliposomes with non-detectable DiD content or proteoliposomes with high protein/lipid ratio that migrate with some distance from the center of the confocal volume. The presence of small SecYEG aggregates cannot be excluded. With the method described here, 30–40% of the liposomes contain SecYEG (see Note 4) as determined with DCFBA (number of DiD containing liposomes co-migrating with SecY, data not shown). Protein translocation into proteoliposomes or IMVs can be assayed *in vitro* in two ways: i.e., by (i) protection of translocated precursor proteins from an externally added protease and (ii) fluorescent quenching of fluorophores attached to the precursor-protein once it is inside the vesicles. While in the first method translocated (protease protected) precursor proteins are visualized by SDS-PAGE and in gel fluorescence (Fig. 3) or Western blotting, the second method allows real time observation of fluorescently labeled precursor proteins. Here, fluorescein derivates attached to proOmpA are quenched when translocated together with the precursor protein into the IMVs (Fig. 4) or proteoliposomes resulting in a decreasing total fluorescence. This

decrease is observed only when the system is energized with ATP and when SecA is present [149].

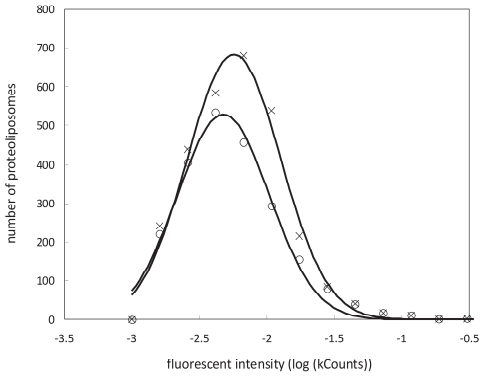

Figure 1: *Distribution of reconstituted SecYEG in liposomes and in vitro translocation of proOmpA. Distribution of fluorescein labeled and reconstituted SecYEG in liposomes of E. coli total lipids supplemented with the hydrophobic fluorophore DiD. Single proteoliposomes were detected by a dual-color laser-scanning confocal microscope. The fluorescent intensities of the SecY signals alone (×) and the SecY signals that overlapped with the DiD signals (corresponding to the SecY containing liposomes, o) are shown. Both data sets are fitted to a log normal distribution (solid and dashed lines). The overlap of both curves shows that 80% of SecY co-migrates with DiD containing liposomes.*

3.1. Isolation of Inner Membrane Vesicles (IMVs)

1. One liter of LB supplemented with 0.1 mg/mL ampicillin is inoculated with a starting OD600 nm of 0.05 of an overnight culture of *E. coli* SF100 transformed with pET84 and grown at 37°C.
2. Expression of SecYEG is induced at an OD600 nm of approximately 0.6 by addition of 0.5 mM IPTG. The cells are grown for 2 h longer and collected by centrifugation.
3. The pellet is resuspended in 10 mL Tris-sucrose, frozen in liquid nitrogen and stored at −20°C (*see* Note 5).
4. To prevent proteolysis all further steps are carried out at 4°C.
5. The suspension is defrosted in ice water and supplemented with 1 mM PMSF, 2 mM DTT, 1 mg/mL DNase and RNase each (*see* Note 6).
6. Cells are lysed by two passages through a cell disrupter (French press) at 8000 psi. After the first passage the PMSF concentration is raised to 2 mM.
7. Unbroken cells are removed by 15 min centrifugation at 5000 *g* and membranes are collected from the supernatant by ultracentrifugation at 125,000 *g* for 90 min.
8. The pellet is resuspended to a total volume of 2.4 mL Tris-sucrose and 800 µL is loaded on each of a sucrose gradient consistent of 0.9 mL 55%, 2 mL 51%, 1.4 mL 45%, and 0.9 mL 36% Tris-sucrose (*see* Note 7). The gradients are centrifuged for 30 min at 250,000 *g* at 4°C.
9. The upper brownish band at around 45% sucrose contains the IMVs and is removed from the gradient and diluted 5-fold with 50 mM Tris-HCl pH8. The IMVs are recollected by ultracentrifugation (250,000 *g*, 30 min 4°C).
10. The IMVs are resuspended in 0.5 mL 50 mM Hepes-KOH pH7, frozen in liquid nitrogen and stored at −80°C.

3.2. Purification and Fluorescent Labeling of SecYEG with Fluorescein-Maleimide

1. All steps are carried out at 4°C.
2. Two milligram IMVs (Fig. 2, lane 2) are diluted to 1 mL with Buffer S followed by 30 min incubation under gentle mixing. Non-solubilized material is removed by 30 min centrifugation (14,000 *g*).
3. If no fluorescent labeling is required, proceed with step 6.
4. The supernatant is supplemented with 2 mM TCEP and incubated for 30 min.
5. Three times 5 μL fluorescein-maleimide is added, each addition followed by 30 min incubation under gentle mixing. The labeling is continued for 2 h (*see* Note 2).
6. The NiNTA beads (150 μL) are washed according to the specifications of the manufacturer and equilibrated with Buffer W. Subsequently, the beads are added to the labeling reaction or solubilized membranes. The suspension is incubated for 1 h under gentle mixing.
7. An empty BioSpin column is used to separate the beads from the solution and to perform washing and elution steps. The NiNTA beads are washed five times with 1 mL Buffer W and SecYEG is eluted with 300 μL Buffer E (*see* Note 8 and Fig. 2, lanes 4–7 and 8–9).

3.3. Reconstitution of SecYEG into E. coli Total Lipid Liposomes

1. All steps are carried out at 4°C or on ice.
2. In order to form small unilamellar vesicles, 1 mg liposomes is sonicated for 15 min in a bath sonicator or extruded through a polycarbonate filter with a pore size of 200 nm.
3. Solubilization of the liposomes is achieved by incubation with 0.2 % dodecylmaltoside (DDM) for 15 min on ice.
4. Depending on the protein concentration, up to 100 μL of purified SecYEG (for protein concentrations of <0.2 mg/mL) is added to the solubilized liposomes and incubated under gentle mixing for 30 min.
5. Two times 100 mg Bio-Beads are washed twice in methanol, twice in ethanol, and thrice in demineralized water which is evaporated using a vacuum centrifuge or 80°C oven after the last washing step. The Bio-Beads are equilibrated with 100 μL SecYEG-buffer prior use.
6. The suspension from step 4 is added to 100 mg Bio-Beads and incubated for 5 h under gentle mixing.
7. A short centrifugation step (30 s, 8000 *g*) separates the Bio-Beads from the solution which is transferred to a fresh tube containing 100 mg equilibrated Bio-Beads. The reconstitution reaction is incubated over night under gentle mixing.
8. An empty BioSpin chromatography column is used to separate the beads from the solution and the Bio-Beads are washed with 2 mL SecYEG-buffer. The flow-through and wash fractions are pooled and the proteoliposomes are collected by ultracentrifugation (250,000 *g* for 30 min at 4°C).
9. The proteoliposomes are resuspended in 100 μL SecYEG buffer, frozen in liquid nitrogen and stored at −80°C.

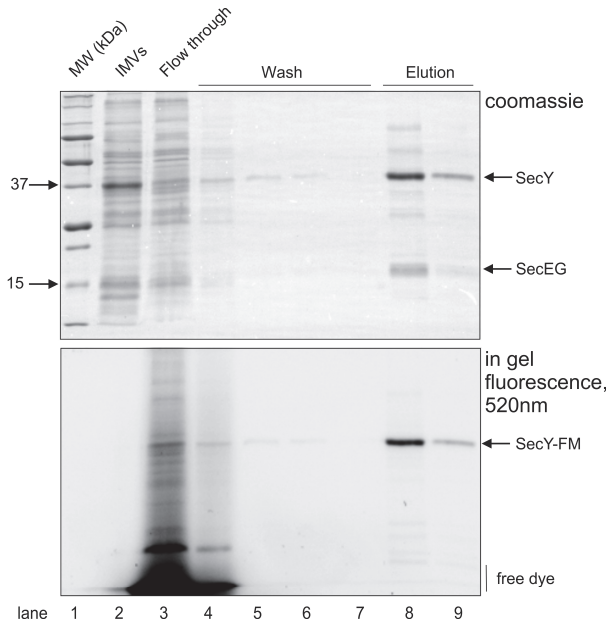

Figure 2: *Labeling and purification of SecYEG as described in Section 3.2. Coomassie stained gel and in-gel fluorescence (520 nm). IMVs: inner membrane vesicles containing overexpressed SecYEG, Fth: flow through. SecY migrates around 37 kDa, SecE and SecG as double band around 15 kDa. Specific labeling of SecY with fluorescein (SecY-FM) is displayed by in-gel fluorescence at 520 nm.*

3.4. Purification of WT-SecA

1. Five milliliters of an overnight culture of *E. coli* DH5α transformed with pMKL18 is inoculated in 300 mL LBAmp supplemented with 0.5% glucose for 8 h at 37°C.
2. 20 mL of the over day culture is added to 1 L of LB-Amp and the cells are grown over night at 37°C.
3. The cells are collected by centrifugation and resuspended in 20 mL Buffer A. DNase, RNase (each 1 mg / mL), 1 mM PMSF, and 2 mM DTT are added (*see* Note 6).
4. Cell-lysis is achieved by two passes through a French press at 8000 psi. Membranes and unbroken cells are removed by ultracentrifugation at 125,000 *g* for 1 h at 4°C.
5. The supernatant is supplemented with 150 mM NaCl and diluted with Buffer A to a protein concentration of 5 mg/mL.
6. Two HiTrap Q HP columns (5 mL) are combined, assembled in a FPLC system, and equilibrated with 50 mL SecA buffer supplemented with 150 mM NaCl.
7. The cell free extract is loaded on the columns at a flow rate of 1 mL/min.
8. The columns are washed with 100 mL SecA buffer containing 180 mM NaCl at a flow rate of 2 mL/min and elution is achieved with 100 mL of a linear gradient from 180 to 400 mM NaCl in SecA buffer.
9. Using ultrafiltration (Centriprep YM-50) the SecA containing fractions are concentrated to 5 mL.
10. A Superdex 200 XK26/60 column is equilibrated with 360 mL SecA buffer at a flow rate of 0.5 mL/min (overnight) and the concentrated SecA fractions are loaded and eluted with SecA buffer at the same flow speed.
11. Purity of SecA can be analyzed on a 10% SDS-PAGE where it migrates at a mass of around 100 kDa.

3.5. Purification of ProOmpA from Inclusion Bodies

1. One liter of LB supplemented with 0.1 mg/mL ampicillin is inoculated with 25 mL of an overnight culture of *E. coli* DH5α transformed with pET503.
2. At an OD600 nm of approximately 0.6 proOmpA expression is induced by addition of 1 mM IPTG and the cells are grown for 2 h longer.
3. The cells are collected by centrifugation, washed once in 100 mL 50 mM Tris, pH7, and resuspended in 5 mL of the latter buffer.
4. Cells are lysed by sonication (20 cycles of 30 s sonication and 30s pause) and the inclusion bodies are separated from the lysate by centrifugation (1500 *g* for 7 min at 4°C).
5. The proOmpA pellet is resuspended in 10 mL proOmpA buffer, frozen in liquid nitrogen, and stored at −80°C (*see* Note 9).

3.6. Fluorescent Labeling of ProOmpA

1. Steps 2–4 are carried out at room temperature.
2. Urea dissolved proOmpA is reduced by addition of 2 mM TCEP and incubation for 30 min.
3. A 100-fold molar excess of fluorescein-5-maleimide is added and the labeling reaction is incubated for 2 h in the dark (*see* Note 2).
4. In order to end the labeling reaction, 10 mM DTT is added and incubated for 30 min.
5. ProOmpA is precipitated by addition of two volumes 20% (w/v) TCA and incubation for 30 min on ice. The precipitate is collected by centrifugation (16,000 *g*, 30 min, 4°C).
6. The pellet is washed with 1 mL ice cold acetone and recollected by centrifugation (16,000 *g* for 15 min at 4°C) (*see* Note 10).
7. ProOmpA-fluorescein is resuspended in 50 µL proOmpA buffer, frozen in liquid nitrogen, and stored at −80°C (*see* Note 11).

3.7. In vitro Translocation of Fluorescently Labeled ProOmpA (Discontinuously)

1. The translocation mixture consists of 5 µL 10-fold translocation buffer, 3.2 µL energy mix, 50 µg/mL IMVs or 10 µL proteoliposomes, 80 µg/mL SecB, 50 µg/mL SecA, and 20 µg/mL proOmpA-fluorescein and is adjusted to a final volume of 49 µL with demineralized water. The mixture is incubated for 3 min at 37°C prior to the start of the translocation reaction by addition of 2 mM ATP.
2. After 1 to 20 min time intervals, the translocation is stopped by adding 40 µL of the reaction mixture to a vial containing 5 µL 1 mg/mL proteinase K followed by incubation for 15min on ice (*see* Fig. 3, lanes 5–10).
3. Four microliters of the reaction mixture is mixed with 4 µL 2x SDS-sample buffer and serves as a standard (10%) to determine the translocation efficiency (*see* Fig. 3, lanes 1–4).
4. In order to precipitate the proteins, 100 µL 20% TCA is added and incubated on ice for 30 min. The precipitate is then collected by centrifugation (16,000 *g* for 30 min at 4°C), washed with 1 mL ice cold acetone, and recollected by centrifugation (16,000 *g* for 15 min at 4°C) (*see* Note 10).

5. The pellet (often invisible) is resuspended in 15 µL 2x SDS sample buffer and boiled at 95°C for 4 min.
6. Both the 10% standard (see step 3) and the various translocation mixtures are run on a 12% SDS-PAGE and in-gel fluorescence is visualized using the Roche Lumi-imager F1. With appropriate software, the proOmpA-fluorescein bands can be quantified and related to the 10% standard to determine the translocation efficiency. An example of a discontinuous *in vitro* translocation assay is shown in Fig. 3.

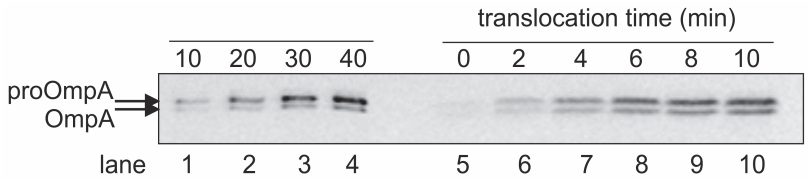

Figure 3: *In vitro translocation of fluorescein-labeled proOmpA into IMVs containing over expressed SecYEG as described in Section 3.7. ProOmpA is partially processed by leader peptidase yielding the mature OmpA which is the lower protein band.*

3.8. In vitro Translocation of Fluorescently Labeled ProOmpA (Real Time)

1. An Aminco Bowman Series 2 spectrofluorometer is set as followed: excitation wavelength 490 nm, emission 520 nm, slitwidths 4 nm, and for measuring mode time traces of 10 min with a 1 s sampling time.
2. A translocation mixture (*see* step 1 of Section 3.7) of 150 µL is preincubated in a 120 µL thermo stated microcuvette at 37°C for 3 min before the reaction is started by addition of 2 mM ATP. An example of a real time *in vitro* translocation assay is shown in Fig. 4.
3. This method can be combined with the discontinuous assay (*see* Section 3.7) by taking samples at different time points (Fig. 4, reversed triangles) and proceeding from Section 3.7 step 2.

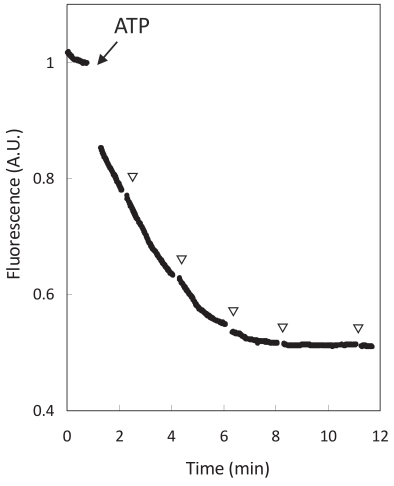

Figure 4: *Real time in vitro translocation of proOmpA labeled with fluorescein into IMVs containing over expressed SecYEG as described in Section 3.8. Translocation of proOmpA-fluorescein is induced by addition of ATP and results in quenching of the fluorescein inside the vesicles. For comparison, samples were taken at the indicated time points and treated as described in Section 3.7 and shown in Fig. 3.*

4. Notes

1. TCEP is very acidic. Adjust pH with 1 M NaOH.
2. Maleimide and fluorescein are light sensitive. Protect from light as much as possible. Wrap vials in aluminum foil.
3. SecB with C-terminal His-tag can be purified by NiNTA chromatography. SecB is not essential for *in vitro* translocation but enhances the efficiency.
4. SecYEG containing proteoliposomes can be separated from empty liposomes by spinning through a sucrose gradient made of 40%, 30%, 20%, 10% (w/v) Tris-sucrose in equal volumes (*see* **Note 7**). The upper band contains the proteoliposomes.
5. Cells in Tris-sucrose can be stored at −20°C for several months.
6. PMSF is not stable in water. Proceed with the next steps as soon as possible.
7. The sucrose gradient is made by gently pipetting the different sucrose solutions on top of each other starting with 55% (w/v) sucrose.
8. Incubating the beads with elution buffer for 15 min increases the elution efficiency.
9. ProOmpA from inclusion bodies is usually sufficiently pure for the described translocation assays. In order to purify proOmpA further, it can be applied on a HiTrapTM Q HP column (GE Healthcare) equilibrated with proOmpAbuffer at pH 8. Under these conditions, proOmpA does not bind to the column and elutes with the wash fractions while other proteins stay bound to the column.
10. To remove all acetone the pellet can be incubated for up to 10 min at 37°C.
11. This procedure removes most of the free fluorescein-5-maleimide. For further cleaning repeat steps 5–7.

Acknowledgements

This work was supported by NanoNed, a national nanotechnology program coordinated by the Dutch Ministry of Economical Affairs and the Zernike Institute for Advanced Materials.

CHAPTER 3

DUAL-COLOR FLUORESCENCE-BURST ANALYSIS TO STUDY PORE FORMATION AND PROTEIN–PROTEIN INTERACTIONS

Geert van den Bogaart, Ilja Kusters, Jeanette Velásquez, Jacek T. Mika, Victor Krasnikov, Arnold J.M. Driessen and Bert Poolman

Published in *Methods* (2008) 46: 123-130

Abstract

Dual-color fluorescence-burst analysis (DCFBA) enables to study leakage of fluorescently labeled (macro) molecules from liposomes that are labeled with a second, spectrally non-overlapping fluorophore. The fluorescent bursts that reside from the liposomes diffusing through the focal volume of a confocal microscope will coincide with those from the encapsulated size-marker molecules. The internal concentration of size-marker molecules can be quantitatively calculated from the fluorescence bursts at a single liposome level. DCFBA has been successfully used to study the effective pore-size of the mechanosensitive channel of large-conductance MscL and the pore-forming mechanism of the antimicrobial peptide melittin from bee venom. In addition, DCFBA can be used to quantitatively measure the binding of proteins to liposomes and to membrane proteins. In this paper, we provide an overview of the method and discuss the experimental details of DCFBA.

1. Introduction

Membrane pores are a class of proteins that form holes in membranes that can be functionalized with a gate to allow regulated transport. They range from very small proteins, such as the ~2 kDa a-helical antimicrobial peptides [150], up to very large protein complexes, such as the ~50 MDa nuclear pore complex [151]. There is a considerable interest in membrane pores as defects in the protein(s) can cause numerous diseases [152]. Moreover, membrane pores offer interesting applications in targeted drug delivery [153], and pore-inducing peptides offer potential as new antibiotics [154]. A variety of assays are available to measure the translocation of molecules through membrane pores in order to obtain information on their structure and activity.

Electrophysiology (e.g. patch-clamp, black lipid membranes) can be used to probe the ion conductance through membrane pores but does not allow direct measurement of fluxes of neutral solutes. In addition, direct translocation of macro-molecules cannot be readily observed, because of their limited charges relative to the free ions in solution. However, macro-molecule translocation can be observed indirectly through blocking of the channel conductance, although formally translocation cannot be distinguished from mere association to the channel [155-157]. Also, it can be technically very challenging to embed the membrane pores in membrane structures that are large (>1 μm for patch-clamp) and stable enough to allow for patch-clamp or black lipid membranes.

Alternatively, translocation through membrane pores is measured via leakage of (macro-) molecules from liposomes that bear the membrane pores of interest. The leaked molecules are separated from the molecules that are still encapsulated by use of a variety of non-equilibrium techniques, such as size-exclusion chromatography, filtration or centrifugation [158,159]. The extent of leakage is determined by quantification of both the leaked and encapsulated fractions, e.g. using radioactivity or fluorescence. As it involves a separation step, this technique does not enable to monitor the leakage immediately and it is difficult to obtain kinetic information.

Leakage from liposomes can be measured directly with fluorescence- based assays, where liposomes are loaded with a fluorophore such as calcein, a highly self-quenched fluorescein derivative [160,161]. As the fluorophore leaks from the liposomes, it is diluted into the external solution and the fluorescence increases because of decreased self-quenching. This enables to follow the leakage directly in a single reaction and no separation step is needed. The main limitation of this approach is that only self-quenching fluorophores can be used. Thus, leakage of fluorophore-labeled macro-molecules cannot be measured with the assay, because generally they cannot be concentrated enough for self-quenching (typically 25–100 mM). In addition, leakage assays based on separation or self-quenching provide bulk information; i.e. only the average leakage is determined. For instance, in the case where only a fraction of the

marker molecules leaks out, one cannot distinguish between full leakage from part of the liposomes or partial leakage from all liposomes.

Obtaining single liposome resolution is essential to probe for heterogeneities in the population and can provide important information on the life-time or the number of active pores. Therefore, single liposome detection provides single pore information when the number of pores per liposome is limited. Recently, we introduced a fluorescence-burst assay, called dual-color fluorescence burst analysis (DCFBA) that allows leakage of fluorophores to be assessed at a single liposome level [162]. In this review, we demonstrate that DCFBA can be successfully applied to measure the binding of proteins to membranes and to obtain quantitative information on protein–protein interactions.

1.1. Principle of DCFBA

DCFBA enables to measure the leakage of fluorescently labeled size-marker molecules from liposomes. The liposomes are labeled with a second, spectrally separated, lipophilic probe (Fig. 1a). Although liposomes, with diameters typically ranging from 50 to 400 nm, are relatively large compared to the encapsulated sizemarkers, they still diffuse, albeit with a low diffusion constant, i.e. ~2.3 $\mu m^2 s^{-1}$ for a 200 nm liposome [162]; for the water soluble Alexa fluor 488, the diffusion constant is 435 $\mu m^2 s^{-1}$ (succinimidyl ester; 643 Da; 25 °C) [163]. The size-marker molecules also diffuse, but their motion is confined by the liposome. The fluorescent bursts that reside from the liposomes diffusing through the focal volume of a confocal microscope will therefore coincide with those from the size-marker molecules (Fig. 1b). If the size-marker molecules leak from the liposomes (Fig. 1c), for instance through membrane pores, their motion is no longer limited by the liposomes and the fluorescent bursts no longer coincide (Fig. 1d). Thus, a decrease in the level of coincidence indicates passage of the size-marker molecules through membrane pores. If the size-marker molecules are too large to pass through the membrane pores, the bursts will still coincide (Fig. 1e–f).During a measurement time of about 10 min, typically 100– 1000 fluorescent bursts are observed and each is originating from a liposome passing through the focal volume of the microscope. As both the fluorescence signals of the size-marker molecules and the lipophilic probes are linearly related to the number of fluorophores in the focal volume, the internal concentration of size-marker molecules in the liposomes can be calculated from the fluorescent intensities of the bursts. Thus, a list of typically 100–1000 internal size-marker concentrations is obtained from a DCFBA experiment. Pore formation can be induced by auto-insertion of antimicrobial peptides or a-hemolysin [150,164] or gating of pores reconstituted in liposomes [165], as was performed for the mechanosensitive channel of large-conductance MscL from Escherichia coli [162].

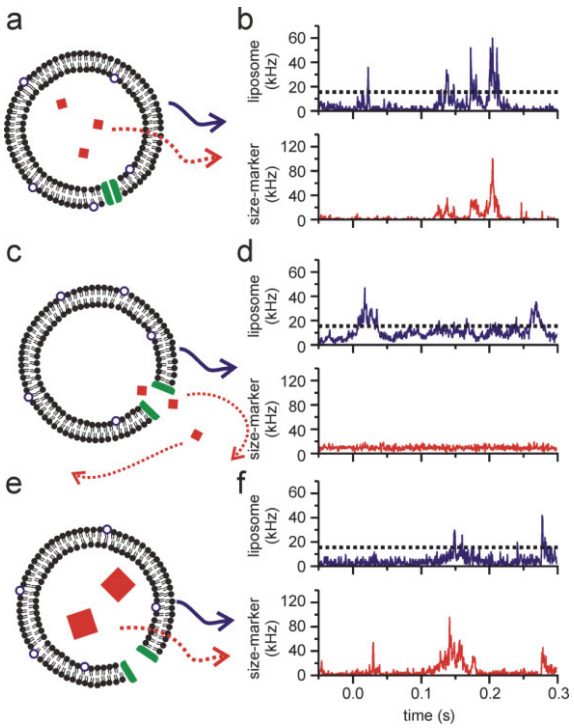

Figure 1: *Principle of dual-color fluorescence-burst analysis. (a) Liposomes are labeled with a fluorescent lipid analog (blue, ○) and loaded with size-marker molecules that are labeled with a spectrally non-overlapping second fluorophore (red, filled squares). The motion of the size-marker molecules (red dotted arrow) is confined by the liposomes (blue solid arrow). (b) The fluorescent bursts, resulting from the diffusion of the liposomes (a) through the detection volume of a dual-color confocal microscope are recorded for about 10 min. The bursts coincide, since the sizemarker (red, lower panel) is liposome (blue, upper panel) associated. The dotted line indicates the threshold used for the calculation of the internal concentrations of the size-marker molecules (see Fig. 2). (c) Same as (a), but now after opening of a membrane pore (green) and leakage of the size-marker molecules. (d) The fluorescent bursts no longer coincide, since the size-marker molecules are no longer liposome associated. (e) Same as (c), but now the size-marker molecules do not pass through the pore, and the fluorescent bursts (f) still coincide. By varying the size-marker molecules, the pore-size can be determined. By varying the lipid composition of the membrane, one can obtain detailed information on the mechanism of pore formation and the channel properties, e.g. as described in [13,15].*

1.2. Comparison with other methods

DCFBA uses two spectrally separated fluorophores to study the association to liposomes. The use of two fluorophores to study intermolecular interactions was first employed in fluorescence cross-correlation spectroscopy (FCCS) [166]. FCCS measures temporal correlations of two fluorescent signals to determine the level of coincidence. In addition to FCCS, several other techniques exist that do not use temporal correlations but use coincidence or burst selection instead. One of these techniques is confocal fluorescence coincidence analysis (CFCA), which uses a relatively simple statistical algorithm to quantitatively compare the coincidence of the bursts and uses this to measure the relative concentration of interacting particles [167-169]. CFCA has been applied to measure DNA restriction enzyme activity [167,168] and to characterize quantum dots using a very similar experimental setup as for DCFBA [169]. CFCA offers simplicity in analysis and faster data acquisition than FCCS. The main difference between CFCA and DCFBA is that in the former technique the whole fluorescence trace is analyzed, whereas the latter uses an arbitrary threshold to select the fluorescent bursts. In this context, two-color coincidence

detection (TCCD [170]), where thresholds are applied to select the fluorescent bursts, is rather similar to DCFBA.

With TCCD, the bursts in the two fluorescence channels are recognized using two arbitrary thresholds and the fraction of events that are coincident is calculated. TCCD has been proven extremely sensitive, especially in the case of a low fraction of coincidence or a high background and it has been used to study DNA hybridization [170] and the activity of telomerase [171]. Interestingly, TCCD was recently used to study the oligomerization of αβ-heterodimers of the T-cell receptor in the membranes of T-cells [172]. The main difference between DCFBA and TCCD is that with DCFBA a single threshold is applied to select liposomes that are labeled with multiple fluorophores, whereas TCCD uses two thresholds to study the fraction of coincidence between two fluorescence signals. DCFBA offers the advantage over TCCD that the distribution of the ratios of coincidence is obtained, and not only the fraction of coincidence. This is particularly useful in the case of a variable number of fluorophores, as is the case for liposomes because of their heterogeneous size-distribution and encapsulation efficiency. DCFBA allows for determining the internal size-marker concentration in the liposomes, with single liposome resolution.

1.3. Instrumentation

DCFBA can be performed on any dual-color confocal microscope where two spectrally different fluorophores can be separately detected. For the excitation, two lasers [162,164,166] or two-photon excitation [168,173] can be used, the latter offering the advantage of simplified alignment. A high degree of overlap of the two focal volumes of the microscope is essential, especially if the liposomes are smaller than the focal volume. The focal volume can be below 1 fl and is equal to $\pi^{3/2}\ \omega_{xy}^2\ \ \omega_z$ where ω_{xy} and ω_z are the lateral and axial radii of the confocal volume, respectively. The bin-time t_d should be small enough to allow for detection of single events of liposomes diffusing through the focal volume and hence should be smaller than ω_{xy}^2/D, or typically below 10 ms.

One of the main requirements for DCFBA is that the liposome concentration is low enough to avoid detection of multiple events, i.e. the average number of liposomes present at the same time in the focal volume should be well below 1. Since the focal volume is typically smaller than 1 fl, the liposome concentration should be lower than 1 nM. Assuming an average surface area per lipid of 0.7 nm^2 (for 1,2-dioleoyl-sn-glycero-3-phosphocholine (DOPC) [174,175]) and a molecular weight of 700 Da, a liposome with a radius of 200 nm consists of roughly 1 million lipid molecules and has a molecular weight of 700 MDa. This means that the maximum concentration of lipids for DCFBA is about 0.7 mg ml^{-1}. In practice, DCFBA was successfully applied to liposome concentrations ranging from 50 μg ml^{-1} to 1 mg ml^{-1}.

1.4. Liposomes

The liposomes need to be labeled with for instance a lipophilic probe. Dialkylcarbocyanine dyes are fluorescent probes that mimic lipid molecules and consist of a charged fluorophore conjugated to two acyl chains. They are available in a range of colors, for example, DiO (Invitrogen, Carlsbad, CA, Table 1) and DiD. Other fluorescent lipid analogs are the NBD labeled phospholipids (7-nitro- 2,1,3-benzoxadiazole, λ_{ex} = 465 nm, λ_{em} = 534 nm). In addition to fluorescent lipid analogs, many fluorophores which are poorly soluble in an aqueous environment can be used to label the liposomes. The lipophilic probe marker can be incorporated into the liposomes by adding it to the lipid solution in organic solvent and prior to liposome formation. Alternatively, because many lipophilic probes are poorly soluble in an aqueous buffer, they can be added to the liposome suspension to auto-insert in the membrane, although this may lead to staining heterogeneities and hence artifacts in the measurements. Each liposome should have a sufficient number of fluorescent lipid analogs to allow for clear detection. On the other hand, the fluorescence signal should be low enough to avoid any saturation of the detection system. The optimal amount of lipophilic probe is strongly dependent on the lipid composition, most likely because the fluorescence quantum yield is dependent on the microenvironment and the charge of the lipid membrane.

Table 1

Fluorophore pairs suitable for DCFBA

Lipophilic probe	λ_{ex} [a]	λ_{em} [b]	Size-marker probe	λ_{ex} [a]	λ_{em} [b]
DiO	484	501	Alexa fluor 633	632	647
			Cy5	647	665
DiD	648	670	Alexa fluor 488	495	519
			Cy2	492	506

[a] Excitation wavelength in nm, [b] Emission wavelength in nm.

We use molar DiO or DiD to lipid ratios ranging from 1:40,000 (~25 fluorophores per liposome) for liposomes composed of negatively charged lipids up to 1:4000 (~250 fluorophores per liposome) for those composed of zwitterionic lipids.

The size of the liposomes is found to be a non-critical parameter, and DCFBA was even performed with whole *Lactococcus lactis* cells [164]. For this, GFP was expressed as a leakage marker and the membrane was labeled with the fluorescent lipid analogue DiD. Thus, DCFBA can be used as an alternative to flow cytometry and can be used to measure expression of GFP or leakage of fluorophores from cells [176]. A general

problem with the whole-cell assay was that the cells were labeled by addition of DiD to the cell suspension and this resulted in heterogeneities in and among the samples. This led to a broad distribution and poor reproducibility of the results and sensitivity of the assay was low. An alternative for membrane labeling would be the tagging of an integral membrane protein with a red fluorescent protein such as mCherry [177].

1.5. Size-marker molecules

One of the merits of DCFBA is that any molecule can be used as a leakage marker that can be fluorescently labeled and encapsulated into the liposomes. They can range from the smallest fluorophore available, NBD (164 Da), up to nm-sized quantum dots. Two major conditions are: (i) the fluorescence of the size-marker does not spectrally overlap with the fluorescence of the lipophilic probe. (ii) The size-marker is not too hydrophobic (or strongly cationic when anionic lipids are used), such that it (transiently) associates with the membrane. The latter can be easily checked by adding (free) size-marker molecules to the liposome suspension and performing a DCFBA measurement. We used the fluorescent lipid analog DiO and labeled the size-marker molecules with either Alexa fluor 633 (Invitrogen, Table 1) or Cy5 (GE Healthcare, Waukesha, WI). Alternatively, we used the fluorescent lipid analog DiD in conjunction with Alexa fluor 488 or Cy2 [162,164]. Fluorophore-labeled dextran molecules are commercially available in a wide range of sizes, from 1 up to 2000 kDa and they are often used as size-markers to determine pore-sizes [178-181]. However, with dextrans it is difficult to accurately determine pore-sizes because: (i) dextrans are polydisperse and a particular sample may have a broad distribution of molecular weights with a spread of typically ~50%; and (ii) in an aqueous solution, dextrans form ellipsoids with shortest radii of ~2.0 nm and relatively independent of their size [182]. Therefore, soluble proteins of known structure are a better alternative to dextrans for the determination of pore-sizes. Proteins can be labeled with fluorophores at either specific or aspecific positions. In particular, cysteines can be labeled using fluorophores conjugated to thiol-reactive groups, such as maleimides or iodoacetamides. Since the number of freely accessible cysteines in proteins is often limited, labeling at specific positions can be achieved by engineering single cysteine mutants [183]. Alternatively, primary amines (N-termini, lysines) can be labeled using fluorophores conjugated to amine-reactive groups, such as succinimidyl esters, N-hydroxysuccinimide (NHS)-esters or isothiocyanates. Also, primary amines can be labeled with maleimides in a basic environment (pH > 8) [162].

The presence of unlabeled size-marker molecules does not pose a problem for DCFBA, because they cannot be detected and do not interfere with the measurements. However, the presence of free label (unbound to a size-marker molecule) and the presence of more than one label per size-marker molecule can affect DCFBA measurements. To overcome these problems, an excess (>10x) of protein relative to the label should be used for the labeling reaction. In addition, unbound dye can be removed from the size-marker molecules using size-exclusion chromatography [162].

The labeling efficiency can be determined by comparing the absorption of the protein to that of the label (e.g. molar extinction coefficient ε = 73 cm^{-1} mM^{-1} for Alexa fluor 488 at 494 nm, and ε = 159 cm^{-1} mM^{-1} for Alexa fluor 633 at 621 nm). The tryptophan and tyrosine absorption of the protein at 280 nm can be calculated using for instance the ProtParam tool (http://www.expasy.org/tools/protparam.html) [184]. Absorption of the dye molecules at 280 nm should be corrected for (ε = 76 cm^{-1} mM^{-1} for Alexa fluor 488 and ε = 30 cm^{-1} mM^{-1} for Alexa fluor 633).

1.6. Encapsulation

The same criteria as for the lipophilic probes apply for the number of size-marker molecules which are encapsulated in the liposomes, and there should be a sufficient number of molecules present to detect a significant signal, but not too many to avoid saturation. The encapsulation efficiency can be estimated from the fraction of fluorescence bursts from the liposomes that do not have a coinciding fluorescence burst from the size-marker molecules [162]. The encapsulation efficiency is typically between 0% and 40% [162], but this is largely dependent on the electrochemical properties of the size-marker molecules, the lipid composition of the membrane and the ionic strength of the medium [185]. Generally, anionic molecules are encapsulated ~10-fold more efficient in liposomes composed of zwitterionic than of negatively charged lipids. The concentration of the size-marker molecules needed for sufficient encapsulation is thus dependent on the experimental conditions (size-marker, lipid composition, buffer), but usually concentrations between 5 and 100 μM can be easily reached.

Encapsulation can be achieved using four different approaches: (i) The solution of the size-marker molecules is mixed with the detergent-solubilized lipids. The detergent is subsequently removed by adsorption to polystyrene beads (e.g. Bio-Beads, Bio-Rad, Hercules, CA), dilution or dialysis [186]. (ii) The aqueous solution of size-marker molecules is added to the lipid solution in organic solvent which is subsequently removed [187]. This method is not very suitable for the encapsulation of proteins, since the presence of organic solvent denatures the macro-molecules. (iii) Encapsulation in the liposomes is obtained by rehydration of a dried lipid film with the aqueous size-marker molecule solution [164,188]. (iv) The size-marker molecules are encapsulated by freeze-thawing of preformed liposomes. This method is especially useful in the case where the membrane pores are reconstituted in the liposome [162]. In all approaches, multiple cycles of freezing the liposomes in liquid nitrogen and subsequent thawing at temperatures between 20 and 100°C greatly enhance the encapsulation efficiency [36]. As all methods result in a heterogeneous population of liposomes with many multilamellar structures, they need to be extruded through a polycarbonate filter with defined pore-sizes, which results in unilamellar liposomes of a more discrete size and increases the encapsulation efficiency [185]. The non-encapsulated size-marker molecules can be removed from the liposomes using centrifugation (e.g. 300,000xg for 15 min) or size-exclusion chromatography.

1.7. DCFBA analysis

DCFBA measurement results in fluorescent intensity traces from both the liposomes and the size-marker molecules (Fig. 2a). The analysis is based on the identification of the fluorescent bursts originating from the liposomes diffusing through the focal volume, using an arbitrary fluorescence threshold $I_{threshold}$. The threshold should be high enough to allow for identification of liposomes passing through the focal volume and to distinguish these events from the background noise. Since each liposome is labeled with multiple (25–250) fluorophores, the bursts are of relatively high intensity.

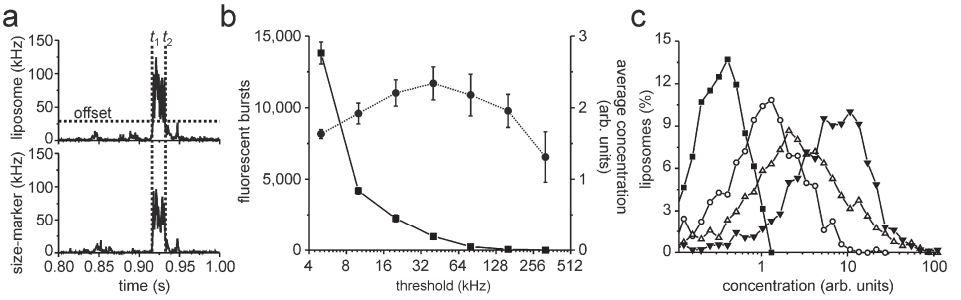

Figure 2: *DCFBA measurements in liposomes loaded with Alexa 633-labeled glutathione. (a) Between t1 and t2, the fluorescent intensity of the liposome is above the threshold (dotted line) and the total intensities of both the fluorescent lipid analog (upper panel) and the size-marker molecules (lower panel) are calculated for each burst. (b) The threshold should be taken such that only significant events from liposomes diffusing through the focal volume are taken into account. A too low an threshold results in lower average concentrations (filled circle, dotted line, right axis), since non-significant bursts are taken into account (filled square, solid line, left axis) and a too high an threshold results in poor statistics. (c) Histogram analysis of liposomes loaded with 0 (filled square), 1 (open circle), 5 (open triangle) and 10 (closed triangle) μM of Alexa 633-labeled glutathione. The concentration of glutathione was determined using Eq. (1). Adapted from [13].*

We generally use values for the threshold between 20% and 40% of the maximum intensity, with lower values leading to more burst events but also to lower size-marker/liposome ratios (Fig. 2b). To allow direct comparison of two samples (e.g. closed vs. open pores), the threshold needs to be kept constant. Given that the intensities of both the fluorescent lipid analog and the size-marker molecules are linearly proportional to the number of fluorophores, the concentration Ci of size-marker molecules inside the liposome can be calculated for each burst *i*:

$$C_i = \frac{\int_{t_1}^{t_2} I_{\text{size-marker}}\,\mathrm{d}t}{\left(\int_{t_1}^{t_2} I_{\text{liposome-marker}}\,\mathrm{d}t\right)^{\frac{3}{2}}} \quad (1)$$

where $I_{liposome}$ and I_{size}-marker are the fluorescence signals from the liposomes and the size-marker particles, respectively, and $I_{liposome}$ is above $I_{threshold}$ between t_1 and t_2. The 3/2 is a scaling factor because the fluorescent lipid analogs are associated with the

surface of the liposome, whereas the size-marker molecules are volume encapsulated and they scale to the powers of 2 and 3, respectively [162,164]. Since C_i is a multiplicative parameter, it is a log-normal function [189]. C_i is in arbitrary units, but is linearly proportional to the internal concentration. Using the fluorescence per particle or a calibrant conversion factor for liposomes with a known internal concentration of fluorophores, C_i can be converted to real units (Fig. 2c).

1.8 FCS

The same fluorescence trace can be used for both DCFBA and fluorescence correlation spectroscopy (FCS). FCS is a well established technique to measure the concentrations and mobility of biomolecules and is based on the temporal correlation of the fluorescent intensity trace [190,191]. FCS can be used to calculate the diffusion speed of liposomes and size-marker molecules. Because free size-marker molecules move faster through the focal volume than those encapsulated in liposomes, FCS can be also used to quantify leakage, using a two component fit (Fig. 3) [162]. The disadvantage of FCS relative to DCFBA is that only information on the ensemble average is obtained. Also, FCS is more sensitive to artifacts arising from big aggregates of fluorophores, since these have a relatively large contribution to the final correlation. In principle, FCCS [166,173] can be used to determine the leakage of size-marker molecules from liposomes too. However, in our experience, it is difficult to use FCCS to quantify leakage from liposomes and the reproducibility and sensitivity are relatively low, especially if a large fraction of the liposomes does not contain size-marker molecules or active pores.

1.9. Laser-scanning DCFBA

For sufficient statistics on the population of liposomes, typically about 100–1000 bursts should be recorded during a DCFBA measurement, depending on the heterogeneity of the sample. The diffusion constant of a 200 nm liposome is 2.3 $\mu m^2 s^{-1}$ [162], and this means that at a lipid concentration of 1 mg ml^{-1}, the acquisition time is at least 5 min and kinetic processes faster than this acquisition time cannot be followed. However, the measurement time can be 10- to 100-fold decreased by stirring or moving the sample [167]. Alternatively, the probe beams can be moved and this approach was used to study the pore formation of cytolytic peptides in erythrocytes using a laser-scanning confocal microscope [180]. For a laser-scanning DCFBA measurement, two confocal images of the size-marker molecules and the liposomes are simultaneously recorded (Fig. 4). To achieve less than one event per pixel, the dwell-time of the laser-scanning should be smaller than $\omega 2/D$ (<<10 ms). Because confocal images contain both spatial and temporal information, the diffusion of the liposomes and size-marker molecules can be obtained by a spatial-temporal correlation of the images [192].

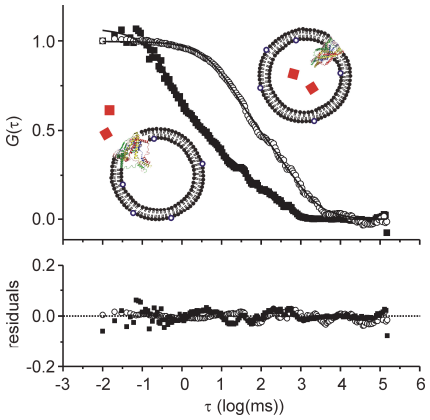

Figure 3: *FCS was used to determine the leakage through the MscL pore. Alexa fluor 633-labeled bovine pancreas trypsin inhibitor (BPTI) was encapsulated in the liposomes and the fluorescence auto-correlation was measured (open circle, upper inset). Upon opening of MscL (by labeling of Cys22 at the constriction site of the pore with MTSET [45]) and the release of BPTI, the movement of BPTI (lower inset; red squares) was no longer limited by the liposomes (blue open circles). Curves were fitted with a two component model (solid lines), with a slow component attributed to size-marker molecules still encapsulated in the liposomes and a fast component corresponding to the free molecules. The lower panel shows the residuals of the fit. Adapted from [13].*

2. Results

The pore-sizes of the mechanosensitive channel MscL from *E. coli* and the antimicrobial peptide melittin from bee venom were determined using DCFBA. MscL is an osmolyte pore protein that functions as a safety valve for the cell, opening upon a decrease in the external osmolyte concentration and preventing cell lysis. It forms a very large pore in the membrane with 2.5–4 nS conductivity [193]. We determined the effective pore-size of MscL reconstituted in DiO-labeled liposomes, using a range of size-marker molecules (Fig. 5). A cysteine was engineered at the constriction site of the pore (MscL G22C); this mutant is pushed open when the Cys-22 site is labeled with a charged thiol-specific reagent [194].

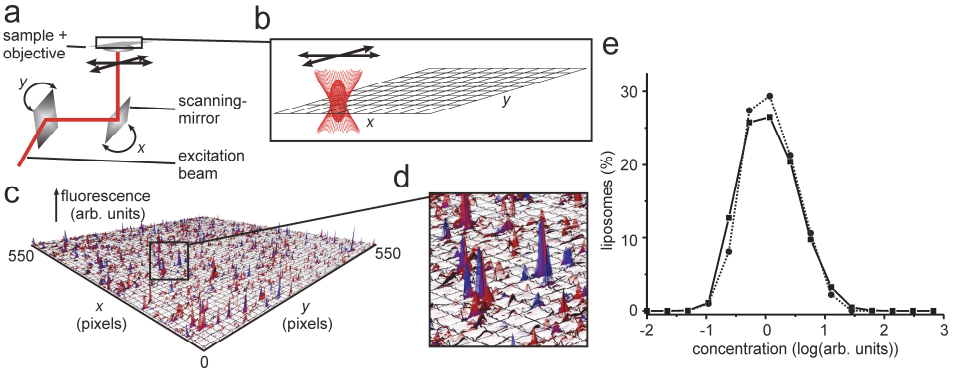

Figure 4: *Laser-scanning DCFBA. (a) Cartoon showing the setup for the scanning of the probe beam in lateral x and y directions using two scanning-mirrors. (b) Close-up of the detection volume. (c) Laser-scanning DCFBA measurement of a total area of 100 x 100 µm, with a step size of 0.2 µm. The peaks indicate the fluorescent signal from the liposomes (red) and the size-marker molecules (blue). (d) An enlargement of some of the fluorescent bursts from panel c to indicate the overlap of the bursts. (e) Comparison of DCFBA measurements on liposomes with encapsulated Alexa fluor 633-labeled glutathione in the static (circles, dotted line) and scanning (squares, solid line) mode. For both samples, ~1500 bursts were analyzed.*

For compounds smaller than 3 nm (proteins up to ~7 kDa), the internal size-marker concentrations C_i (Eq. (1)) shifted to lower values upon opening of MscL, indicating that these size-marker molecules were able to pass through MscL, whereas for larger compounds no change in C_i was observed [162]. The single liposome resolution of DCFBA was used to estimate the reconstitution efficiency of MscL. Importantly, only about 50% of the liposomes leaked their full content, whereas the others were not affected. This indicated that about half of the liposomes did not incorporate a functional MscL channel. Based on the protein to lipid ratio, we expected an average number of 10 MscL channels per liposome. Thus, the reconstitution efficiency was less that 10%, and this number was in accordance with published data [162].

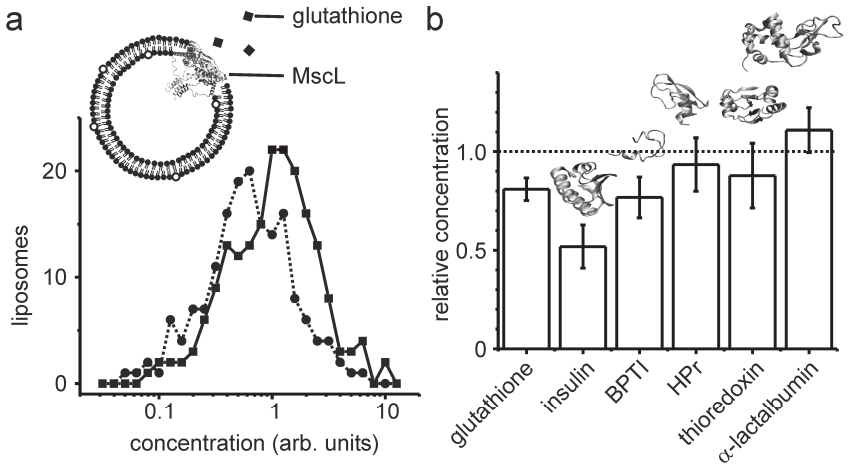

Figure 5: *The effective pore-size of MscL. (a) DCFBA was performed on liposomes with MscL reconstituted and the membrane labeled with the fluorescent lipid analog DiO (squares, solid line). After chemically opening of MscL (circles, dotted line), the internal concentration of Alexa fluor 633-labeled glutathione decreased due to leakage through MscL (inset). Because not all liposomes contained an active MscL channel, there was still a large fraction of liposomes with glutathione encapsulated and considerate overlap between the two histograms. (b) A number of size-marker molecules was tested: Alexa fluor 633-labeled glutathione (1.4 kDa); insulin (6.8 kDa); bovine pancreas trypsin inhibitor (BPTI, 7.6 kDa); HPr of the PEPdependent sugar:phosphotransferase system (10.2 kDa); thioredoxin (12.6 kDa) and a-lactalbumin (15.3 kDa). The y-axis shows the relative concentration after opening of MscL. Molecules smaller than HPr leaked out, whereas larger molecules did not. The error bars indicate the standard deviation. Adapted from [13].*

Melittin is a 26 residues lytic peptide that kills bacterial cells by auto-inserting into their membranes and forming pores [195-197]. We determined the effective pore-size for various lipid compositions as a function of melittin concentration (Fig. 6). For neutral, bilayer- forming lipids, there was a positive correlation between the melittin concentration and the pore-size, whereas for negatively charged or non-bilayer forming lipids, the pore-size was independent of the melittin concentration and was at least 5 nm (Fig. 6a) [164]. In addition, melittin caused membrane fusion or aggregation, which was observed as the decrease of the number and the increase of the

intensities of the fluorescent bursts. Importantly, the collective information from a DCFBA experiment enables to distinguish membrane fusion from lysis. Treatment of the liposomes with the detergent Triton X-100 resulted in the disappearance of the bursts and a total homogenization of the sample (Fig. 6b). The 10–100 lm-sized giant unilamellar vesicles (GUVs) have been proven useful for studying lytic peptides and also allow to distinguish pore-formation and fusion from lysis [197,198].

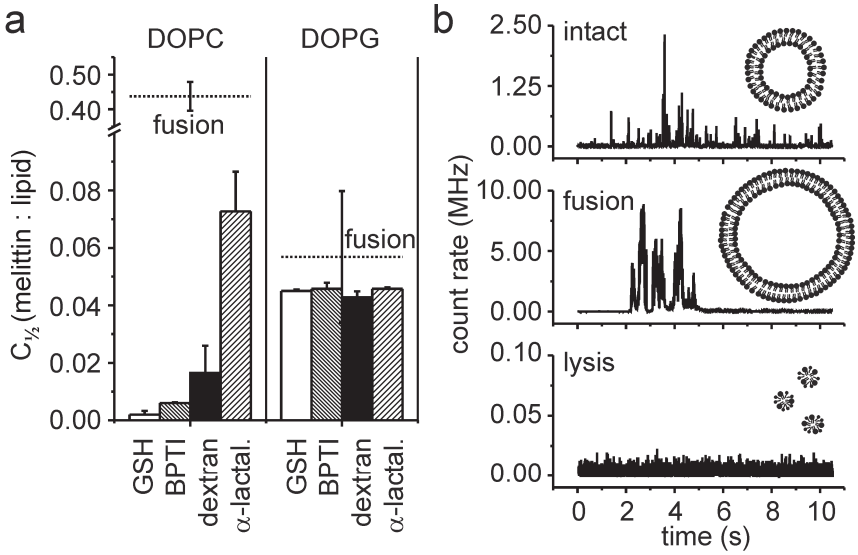

Figure 6: *Pore formation of melittin. (a) Melittin action depends on the lipid composition of the membrane. The $C_{1/2}$ values for leakage and fusion are shown, defined as the melittin to lipid ratios where the average internal concentration of size-marker molecules in the liposomes (bars) or the number of bursts (fusion) decreased 50%, respectively. For liposomes composed of the zwitterionic DOPC, an increasing melittin to lipid ratio is needed for leakage of larger size-marker molecules, whereas for liposomes composed of the negatively charged DOPG, leakage is a-specific. As size-markers, fluorophore labeled glutathione (GSH), bovine pancreas trypsin inhibitor (BPTI), dextran (10 kDa) and a-lactalbumin were used. (b) Fluorescent intensity trace of DiO-labeled DOPG liposomes (upper panel). At high concentrations, melittin induces fusion of the liposomes, as is apparent from the decrease of the number of peaks and the increase of the intensity per peak (center panel; melittin to lipid ratio of 0.06). Addition of 1% (w/v) of Triton X-100 results in lysis of the liposomes and diminishes all fluorescent bursts (lower panel). Adapted from [15].*

Because of their large size, the leakage of size-marker molecules from GUVs takes place in seconds to minutes timescale and can be followed using fluorescence microscopy [197]. In addition, experiments with GUVs allow to determine the effect on the viscoelastic properties of the membrane [198] that cannot be assessed with DCFBA. Compared to experiments with GUVs, DCFBA offers the advantage of improved statistics, as generally 100–1000 of liposomes are measured. Moreover, for DCFBA sub μm-sized vesicles can be used that are more stable and less tedious to handle than GUVs.

In principle, these results could also be obtained with alternative approaches, such as the calcein dequenching assay or techniques that involve a separation step (see Section 1). However, DCFBA offers three advantages: (i) only ~1 μg of liposomes is needed for a measurement and therefore, many measurements can be done with just one batch of liposomes. (ii) More importantly, information on the population level of liposomes is obtained and not just the average extent of leakage and this was used to determine the reconstitution efficiency of MscL [162]. (iii) DCFBA can be used to discriminate between leakage, fusion and lysis in a single experiment, as was shown by melittin induced fusion of liposomes [164].

2.1. Ligand binding

DCFBA can be used to study the binding of components to membrane proteins reconstituted in liposomes. In this case, liposomes have to be prepared bearing the fluorescently labeled receptor and the ligand must be labeled with a spectrally separated fluorophore. To have a limited background resulting from unbound ligand molecules, the affinity should be high enough (<0.1 μM). As fluorescence allows single molecule detection, DCFBA is much more sensitive than binding assays based on radioactivity (reviewed in [199]), and this makes DCFBA especially useful to study systems with a high binding affinity. An advantage of DCFBA relative to other fluorescence-based binding assays such as FCCS and fluorescence resonance energy transfer (FRET) is that single liposome resolution is obtained and this enables to study the population distribution and oligomerization behavior.

DCFBA was successfully used to determine the binding of the Cy5-labeled SecA ATPase to the Alexa fluor 488-labeled SecYEG protein channel of the protein secretion system from *E. coli* ([60] for review, Fig. 7). The ratio of SecA over SecYEG is obtained from the fluorescent bursts:

$$C_i = \frac{\int_{t_1}^{t_2} I_{SecA}\,\mathrm{d}t}{\int_{t_1}^{t_2} I_{SecYEG}\,\mathrm{d}t} \qquad (2)$$

This equation is similar to Eq. (1), apart from that no volume-surface normalization is needed since both receptor and ligand are associated to the surface of the liposomes. By varying the concentration of unlabeled SecA, a binding constant of 4 nM was determined, in agreement with literature values [200]. This technique can also be applied to study the oligomerization of the various components of the Sec system or the interaction of proteins with the surface of the liposomes.

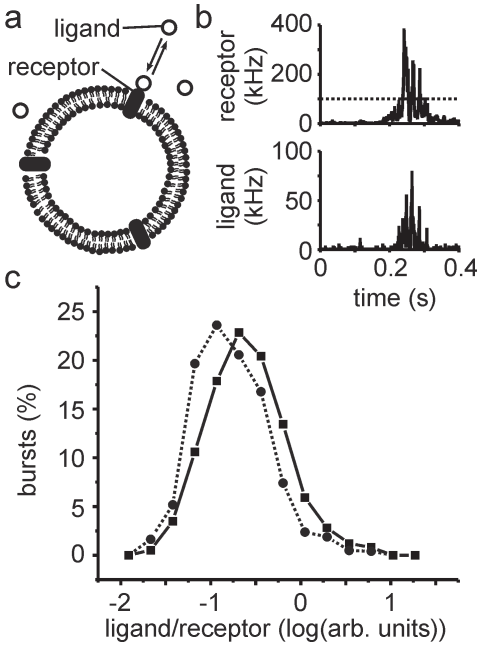

Figure 7: *DCFBA to probe binding of SecA to the membrane reconstituted SecYEG complex. (a) DCFBA can be used to determine the binding between a fluorophore-tagged ligand and a liposome associated receptor that is labeled with a spectrally different fluorophore. (b) Upon binding, the fluorescent bursts of the receptor and the ligand overlap. Here, we present the binding of 10 nM of Cy5-labeled SecA motor protein to the Alexa fluor 488-labeled SecYEG translocon from E. coli; the Alexa 488 was on the SecY subunit. (c) Histogram presents the ratio of ligand to receptor from panel b (squares, solid line, Eq. (2)). Upon addition of a 100-fold excess of unlabeled SecA (circles, dotted line), the ratio shifted to lower values.*

3. Concluding remarks

The fluorescent burst technique DCFBA enables to measure leakage of fluorophores from liposomes. It is especially useful for studying membrane pores as one obtains single liposome information. Measurements can be done with a small amount of material (1–10 μg liposomes) and in a few seconds time span if the acquisition is sped up using probe-scanning or sample stirring. Furthermore, one can distinguish between fusion/aggregation, lysis and pore formation in a single experiment. Binding to membrane proteins can also be measured with DCFBA, provided that the interaction of binding partners is of sufficiently high affinity. DCFBA has been proven useful to characterize mechanosensitive channel proteins [162] and antimicrobial peptides [164] and in the future we plan to use it to unravel the pore formation and channel properties of other proteins.

Acknowledgments

We are grateful to the Dutch Science Foundation (NWO), Grant No. ALW-814.02.002, NanoNed, a national nanotechnology program coordinated by the Dutch Ministry of Economical Affairs, and the Zernike Institute for Advanced Materials for financial support.

CHAPTER 4

QUATERNARY STRUCTURE OF SECA IN SOLUTION AND BOUND TO SECYEG PROBED AT THE SINGLE MOLECULE LEVEL

Ilja Kusters, Geert van den Bogaart, Alexej Kedrov, Victor Krasnikov, Faizah Fulyani, Bert Poolman and Arnold J.M. Driessen

Published in *Structure*, 2011, 19:430-9

Abstract

Dual-color fluorescence-burst analysis (DCFBA) was applied to measure the quaternary structure and high affinity binding of the bacterial motor protein SecA to the protein-conducting channel SecYEG reconstituted into lipid vesicles. DCFBA is an equilibrium technique that enables the direct observation and quantification of protein-protein interactions at the single molecule level. SecA binds to SecYEG as a dimer with a nucleotide- and preprotein-dependent dissociation constant. One of the SecA protomers binds SecYEG in a salt-resistant manner, while binding of the second protomer is salt-sensitive. Since protein translocation is salt-sensitive we conclude that the dimeric state of SecA is required for protein translocation. A structural model for the dimeric assembly of SecA while bound to SecYEG is proposed based on the crystal structures of the *Thermotoga maritima* SecA-SecYEG and the *Escherichia coli* SecA dimer.

Introduction

Protein secretion in bacteria is mediated by a multi-protein complex termed translocase. It consists of the protein-conducting channel SecYEG and the motor protein SecA (for review see [60]). Post-translational protein translocation starts with the binding of the mature region of the secretory protein (preprotein) by the molecular chaperone SecB [2], whereupon it is targeted to the SecYEG-bound SecA [3]. Upon ATP binding to SecA the signal sequence of the preprotein inserts into the SecYEG channel and SecB is released. Next, SecA mediates the step-wise translocation of the preprotein through multiple cycles of ATP-hydrolysis [4-6].

The functional oligomeric state of SecA during the protein translocation cycle is still a matter of controversy. In solution, SecA forms a homo-dimer and is expected to exist mainly as a dimer in the cytosol [65,91]. The monomer-dimer equilibrium can shift towards the monomeric form in the presence of certain lipids [106,107], detergents [106,107] or synthetic signal peptides [107,137], although signal peptides also have been shown to induce oligomerization of SecA [106]. When bound to lipids, SecA is mainly dimeric and can be monomerized by the addition of nucleotides [97]. Since in none of these studies SecYEG was present, it is not clear if these observations are functionally relevant for SecA when actively engaged in preprotein translocation. However, these studies clearly demonstrate the sensitive nature of the monomer-dimer equilibrium of SecA in solution.

Detergent-solubilized SecYEG has been used to determine the oligomeric state of SecYEG- bound SecA, using native gel-electrophoresis and size exclusion chromatography. The functional oligomeric state of SecYEG is not known but it was suggested to be monomeric [14,16], dimeric [14,16,201-203] and tetrameric [18,19]. SecA can bind both as monomer or dimer to SecYEG-dimers in detergent solution when the latter is stabilized by crosslinking or by an antibody [15,16]. Only monomeric SecA was found on detergent-solubilized SecYEG when a preprotein was trapped in the pore prior to membrane solubilization [15]. Since detergents affect the monomer-dimer equilibrium of SecA [106,107] and because SecYEG is not in its native membrane environment, the exact functional implications of these observations have also remained obscure. The experimental conditions, in particular the SecA concentration, seem to be crucial and may have led to conflicting results on the oligomeric state of SecA bound to SecYEG. When SecA was used at a concentration far below its physiological concentration (5 nM compared to 8 μM), no dimeric SecA was found by chemical crosslinking to bind liposome-reconstituted SecYEG [107]. In contrast, dimeric SecA was detected to bind inner membrane vesicles (IMVs) as shown by chemical crosslinking [102,110] and surface plasmon resonance (SPR) [102]. Recently, SecA has been crystallized bound to SecYEG in the presence of ADP-BeF_x, a structural analog of an intermediate state of ATP-hydrolysis [29]. This structure in which both SecA and SecYEG are monomeric may represent a specific intermediate in

the catalytic cycle, but since detergent and high salt were present throughout the crystallization, the conditions employed will favor the dissociation of the SecA dimer.

The oligomeric state of translocation engaged SecA has also been investigated by activity assays, e.g. the *in vitro* preprotein translocation and preprotein-stimulated SecA translocation ATPase. Mutants of SecA with a monomer-dimer equilibrium strongly shifted towards the monomer showed a very low translocation activity or no activity at all [103,107,110,111]. On the other hand, chemically crosslinked SecA dimers have been shown to be fully active in protein translocation [102,108]. Furthermore, hetero-dimers formed from active and non-active SecA monomers were completely inactive [92]. These studies suggest that dimeric SecA is involved at least in an initial step of protein translocation. Overall, it seems that SecA can bind as a monomer as well as a dimer to SecYEG.

Here, we present an equilibrium method to determine the oligomeric state of proteins when bound to their membrane receptor in a dynamic *in vitro* system. This method, dual-color fluorescence-burst analysis (DCFBA) was recently employed to determine the pore size of the mechanosensitive channel of large conductance MscL [162] and the pore-forming mechanism of the antimicrobial peptide melittin from bee venom [164] (for DCFBA review see [148]). Now we have used DCFBA to quantitatively measure the binding of SecA to membrane-reconstituted SecYEG at low nano-molar concentration, and to monitor the oligomeric state of SecA when functionally involved in preprotein translocation. The method is based on a quantitative coincidence analysis of the fluorescent bursts that reside from single liposomes containing fluorescently labeled SecYEG and SecA labeled with a second, spectrally separated fluorophore diffusing through the focal volume of a confocal microscope (Figure 1A). Our data show that dimeric SecA is driving protein translocation.

Results

SecA binding to SecYEG and liposomes monitored by DCFBA

DCFBA is a fluorescence correlation spectroscopy method wherein the fluorescent bursts that reside from fluorescently labeled proteins that diffuse through the focal volume of a confocal microscope coincide with those from another protein labeled with a second spectrally well-separated fluorophore (Figure 1A). We determined the binding stoichiometry of SecA to SecYEG using DCFBA and employing a dual-color laser scanning confocal microscope with a 488 nm and a 633 nm laser for excitation of fluorescein-maleimide (FM) and Atto647N simultaneously. The pinholes and laser beams are spatially aligned to a high degree of overlap of the two detection volumes allowing the simultaneous detection of co-migrating fluorophores with single molecule resolution (Figure 1B). To employ the method to the protein translocase, the translocation pore $SecY_{C295}EG$ was labeled with the fluorescent probe Atto647N (647

nm and 669 nm for excitation and emission, respectively) at the unique cysteine position C295 and reconstituted into 100 nm-sized liposomes composed of *E. coli* lipids. SecA was labeled with FM (494 nm/521 nm) at its native cysteine residues.

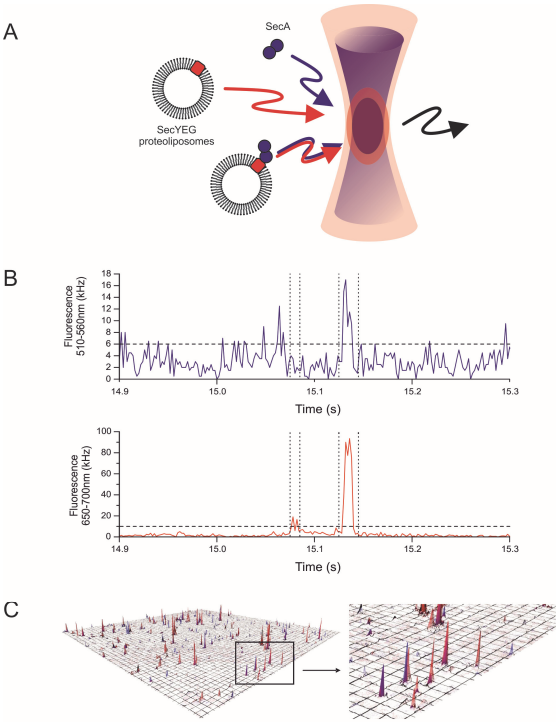

Figure 1: *Principle of DCFBA of SecA-SecYEG binding. (A) Schematic of the principle of DCFBA. Complexes of the blue fluorophore-labeled motor protein SecA and liposome reconstituted with the red fluorophore labeled SecYEG co-migrate through the two aligned laser foci of a dual-color laser-scanning confocal microscope. (B) Recording of fluorescent bursts resulting from proteoliposomes containing fluorescently labeled SecYEG (lower panel; red) and SecA, labeled with a spectrally separated fluorophore (upper panel; blue), passing the detection volumes of a dual-color confocal laser-scanning microscope. Binding of SecA to its membrane receptor SecYEG leads to co-migration and overlap of the discrete fluorescent bursts. The ratio of the SecA/SecYEG peak surface represents a direct measure of the relative binding stoichiometry. Peaks are selected for analysis by use of noise thresholds (dashed lines). (C) Laser scanning DCFBA, height field plot of confocal images of SecA-FM (blue peaks) and SecYEG-Atto647N containing proteoliposomes (red peaks). Peak height represents the fluorescence intensity.*

To determine the SecA binding to SecYEG, SecA-FM was incubated with the proteoliposomes bearing SecYEG-Atto647N (SecYEG-Atto-PL) and the fluorescent bursts resulting from SecYEG-Atto-PL and SecA-FM passing through the confocal volumes of the two aligned laser beams were recorded using the scanning mode of the microscope (Figure 1C). This allowed identifying the overlap of the fluorescent bursts from SecYEG and SecA (Figure 1B) also at very low SecA concentrations when SecA-SecYEG complexes are only infrequently encountered. Thus, the ratio c of SecA over SecYEG could be calculated for each individual burst i from the overlapping fluorescent burst using a simple division:

$$C_i = \frac{\int_{t1}^{t2} I_{SecA}\,\mathrm{d}t}{\int_{t1}^{t2} I_{SecYEG}\,\mathrm{d}t} \quad \text{(eq. 1)}$$

where I_{SecA} and I_{SecYEG} are the fluorescence intensities of the SecA-FM and SecYEG-Atto647N channels, respectively. These are above noise thresholds between

times t_1 and t_2. The average ratio c of SecA-FM over $SecY_{C295}EG$-Atto647N derived from the overlapping fluorescent bursts is an arbitrary unit for the binding stoichiometry of SecA to SecYEG. This ratio was determined as a function of the concentration of SecA-FM and this resulted in a binding curve (Figure 2A, dashed line). As a control for binding of SecA-FM to lipids [106,107], we used empty liposomes composed of *E. coli* lipids supplemented with the fluorescent lipid analog DiD (Figure 2B, dashed line). The binding of SecA to the empty liposomes increased with the concentration, evident as a linear, non-saturable increase of the average ratio SecA/DiD. The data from the binding experiments of SecA to SecYEG were fitted using the Hill-equation, including a linear parameter to account for this background binding to empty lipids. The obtained a dissociation constant (K_d) of 3.6 ± 1.2 nM is in good agreement with the values obtained in earlier studies using surface plasmon resonance (2 nM) [200]. This result validates DCFBA as a technique to study protein binding and confirms the high binding affinity of SecA to membrane-embedded SecYEG.

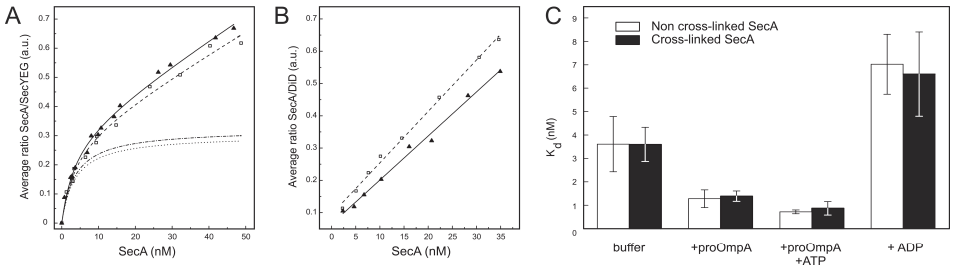

Figure 2: *Saturable binding of SecA to SecYEG. (A) Binding of SecA-FM to SecYEG-Atto647N containing proteoliposomes. The average ratio of SecA/SecY fluorescence was calculated using DCFBA (eqn 1) yielding an arbitrary unit for the binding stoichiometry. Crosslinked SecA-FM (triangles) and non crosslinked SecA-FM (squares) bind with identical ratios. Data points were fitted using the Hill-equation (straight and dashed lines) and the linear non-saturable binding parameter was subtracted from the fit (dotted lines). (B) Binding of SecA-FM to empty liposomes composed of E. coli lipid extract supplemented with 10^{-4} molar % of the fluorescent lipid analog DiD. The linear increase of the average ratio SecA/DiD indicates that SecA binds non-specifically to the lipid membrane. c) Binding affinities of crosslinked and non crosslinked SecA to SecYEG in presence or absence of translocation ligands. Error bars: s.d.*

SecA is dimeric during the rate-limiting step of protein translocation

Previously, chemically crosslinked SecA dimers were shown to be fully active in protein translocation [102,108]. Crosslinking is conveniently realized by oxidation of the C-terminal cysteines and forces SecA to stay dimeric throughout the protein translocation reaction without comprising its activity [102]. The three C-terminal cysteines of SecA are coordinated by a Zn^{2+}-ion in a zinc-finger like motif. In the presence of an excess of zinc, these cysteines are protected against labeling with the fluorescent alkylating agent FM, whereas labeling can occur at a cysteine at position 98. After removal of Zn^{2+} by the chelator EDTA, FM-labeled SecA was chemically

crosslinked into a stable dimer by oxidation with copper phenanthroline [102] (Figure 3B). Addition of dithiothreitol (DTT) reduces the disulfide bonds and SecA can monomerize. The crosslinked SecA was tested in *in vitro* translocation assays using the fluorescently labeled fusion protein proOmpA-DhfR-Atto550 and urea-treated IMVs of an *E. coli* strain containing overexpressed levels of SecYEG (Figure 3A).

Figure 3: *Functional crosslinked SecA dimer. (A) In vitro protein translocation with crosslinked SecA. Translocation of fluorescently labeled proOmpA-DhfR into urea-treated inner membrane vesicles was assayed with limiting*

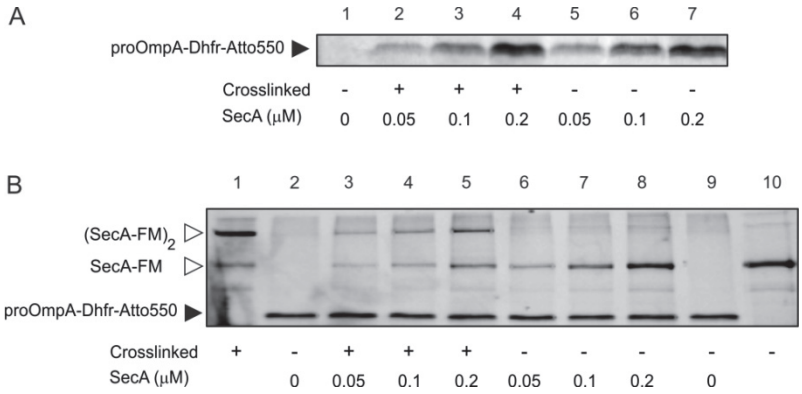

concentrations of SecA-FM. Equal amounts of proOmpA-DhfR (black arrow) were translocated by both cross- and non crosslinked SecA. The SecA concentration is shown for the monomer. (B) Chemically crosslinked SecA dimers are stable throughout the translocation reaction. Fractions of the completed in vitro protein translocation reactions shown in panel a) were run on SDS-PAGE under non-reducing conditions without prior protease treatment. Covalently crosslinked SecA remained dimeric [(SecA-FM)₂] after the reaction, whereas non crosslinked SecA dimers dissociated in SDS and migrate as monomers (SecA-FM, white arrows). Equal amounts of proOmpA-DhfR-Atto550 were used for the translocation reactions (black arrow).

Translocated proOmpA-DhfR-Atto550 is protected against an externally added protease and was visualized on SDS-PAGE by fluorescent imaging. Since absorption spectra of FM and Atto550 overlap, proOmpA-DhfR-Atto550 and SecA-FM can be visualized simultaneously (Figure 3A). Crosslinked SecA migrates at around 200 kDa, and this state was maintained during the translocation reaction conditions (Figure 3B). The efficiency of proOmpA-DhfR-Atto550 translocation was nearly identical for the crosslinked and non crosslinked SecA (Figure 3A) indicating that all subunits of the crosslinked SecA dimer are active. Importantly, under the conditions tested, SecA is the limiting factor, which is evident by a linear increase of the translocation efficiency with the SecA concentration (Figure 3A, compare lanes 2-4 and 5-6). These observations demonstrate that the fluorescently labeled SecA is active for protein translocation, and that SecA is dimeric during protein translocation, at least during a rate-limiting step. However, these experiments cannot exclude that SecA monomerizes at a later step of protein translocation that is not rate limiting.

SecA binds SecYEG as a dimer throughout protein translocation

To further determine the oligomeric state of SecA when bound to SecYEG, the binding of the covalently crosslinked FM-labeled SecA dimer was compared with the non crosslinked SecA at low nano-molar concentrations. The binding curves of crosslinked and non crosslinked SecA obtained by DCFBA are virtually identical suggesting that also the non crosslinked SecA binds as a dimer. Both curves saturate at SecA/SecYEG ratio of approximately 0.3 when the linear non-saturable binding parameter is subtracted from the fit (Figure 2A). No significant difference in nonspecific lipid binding of the crosslinked and non crosslinked SecA-FM was observed, as assayed with *E. coli* liposomes labeled with the fluorescent lipid analog DiD (Figure 2B). The data strongly suggest that the non crosslinked SecA binds SecYEG as a dimer. To determine the oligomeric state of translocation-engaged SecA, the binding reactions were supplemented with the preprotein proOmpA with (Figure S1) and without ATP (Figure S2) or with ADP (Figure S3). In all cases the binding curves of the crosslinked and non crosslinked SecA dimer were identical and saturated at a ratio of about 0.3. The dissociation constants of SecA binding to SecYEG in absence or presence of translocation ligands and nucleotides were derived from the DCFBA-binding curves. Interestingly, the sensitive DCFBA technique allowed the detection of a 2.8-fold increase in the affinity of SecA to SecYEG in the presence of proOmpA (Figure 2C, 1.39 ± 0.22 nM and 1.28 ± 0.38 nM for crosslinked and non crosslinked SecA, respectively, which compares to a value of 3.6 nM in the absence of proOmpA). Addition of proOmpA plus ATP leads to further affinity increase (0.87 ± 0.29 nM and 0.72 ± 0.08 nM for crosslinked and non crosslinked SecA, respectively). On the other hand, addition of ADP resulted in a two-fold decrease of the affinity of SecA to SecYEG compared to binding in the absence of translocation ligands and nucleotides (6.6 ± 1.8 nM and 7.02 ± 1.28 nM for crosslinked and non crosslinked SecA, respectively).

SecA binds SecYEG as a monomer in the presence of high salt or urea

We investigated the binding and oligomeric state of SecA at salt concentrations that were previously shown to favor dissociation of the SecA dimer in solution. In the presence of 500 mM NaCl, crosslinked SecA still binds SecYEG with high affinity (Figure 4) although with a somewhat reduced ratio (0.27) compared to the binding in absence of NaCl (0.32). In contrast, the non crosslinked SecA binds with a substantially reduced ratio to SecYEG (0.18, Figure 4) in the presence of high NaCl. The same 1.5-fold reduced ratio of non crosslinked SecA binding to SecYEG was observed in presence of 1 M urea (Figure S4).. Considering the crosslinking efficiency of about 70 %, (Figure 3B), the reduction in the ratio suggests that in the presence of 500 mM NaCl or 1 M urea non crosslinked SecA binds mostly as a monomer. As anticipated, the unspecific binding of SecA to liposomes in presence of 500 mM NaCl was significantly reduced as assayed with empty *E. coli* liposomes labeled with the

fluorescent lipid analog DiD (data not shown). Consequently, the linear parameter in the binding of SecA to SecYEG containing proteoliposomes was reduced

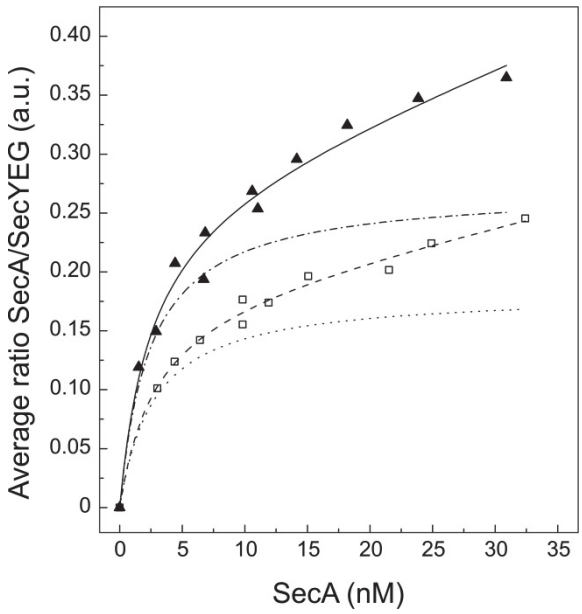

Figure 4: *High salt sensitivity of binding of the SecA dimer to SecYEG. Binding of crosslinked (triangles) and non crosslinked SecA (squares) to SecYEG in the presence of 500 mM NaCl. Data points were fitted using the Hill-equation (straight and dashed lines) and the linear non-saturable binding parameter was subtracted from the fit (dotted lines).*

Measuring oligomerization of soluble proteins with low (sub micro-molar) dissociation constants by standard methods is often limited by low detection sensitivity. Indeed, previous attempts to determine the dissociation constant for SecA dimerization were unsuccessful because of the limited sensitivity of sedimentation velocity centrifugation, yielding estimates in the range of 100 nM [91] to < 0.6 µM [204]. Fluorescence cross-correlation spectroscopy (FCCS) enables the detection of hetero-dimers of protein subunits labeled with two spectrally distinct fluorophores at low nano-molar concentrations [205]. Simultaneously, the concentration of all fluorescent species is determined. A dilution series of a mixture of SecA-Atto488 and SecA-Cy5 with a high degree of dual-color hetero-dimers was subjected to FCCS measurements to determine the dissociation constant for SecA dimerization. The binding curve resulting from the relative concentration of dual-color SecA hetero-dimers plotted against the SecA concentration revealed a K_d for the dissociation of the SecA dimer of 0.74 ± 0.09 nM (Figure 5A). This implies that both dimerization of SecA in solution and binding of dimeric SecA to SecYEG occur at similarly low nano-molar concentration, underlining the importance of dimeric SecA in the translocation cycle. To investigate the influence of NaCl on dimerization of SecA in solution, dual-color (DC) SecA (28 nM) was treated with various NaCl concentrations and measured by FCCS. Evidently, the relative concentration of dual-color SecA hetero-dimers

decreased with increasing NaCl concentrations (Figure 5B). At 500 mM NaCl the vast majority of SecA was monomeric. This observation indicates that SecA only binds SecYEG as a monomer when previously monomerized in solution. To assay the influence of high salt on the translocation activity of crosslinked and non crosslinked SecA, we performed *in vitro* translocation experiments with varying NaCl concentrations. Inhibition of protein translocation was observed at > 200 mM NaCl (Figure 6). Interestingly, the translocation efficiency was affected significantly more with non crosslinked SecA compared to crosslinked SecA (compare lane 2-6 with lane 7-11, Figure 6) demonstrating that stably dimeric SecA is more efficient in protein translocation at high salt concentrations.

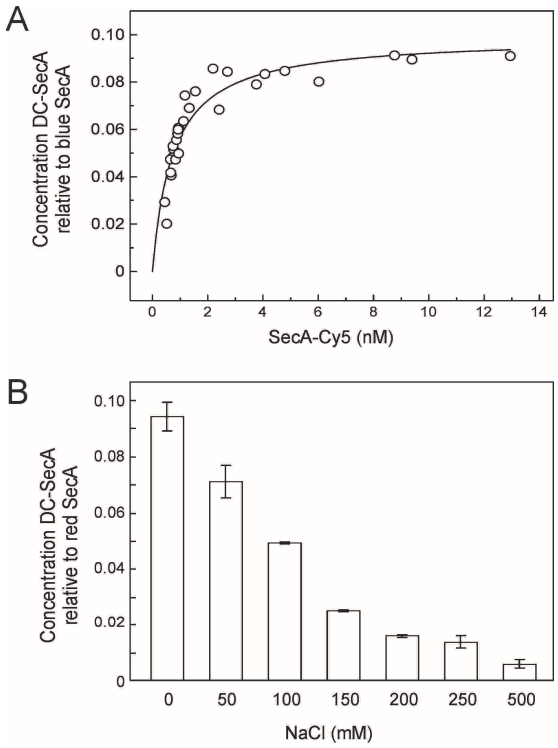

Figure 5: *Dimerization of SecA in solution. (A) Dimerization of SecA in suspension monitored by fluorescence-cross-correlation spectroscopy (FCCS). The relative concentration of dual-color SecA hetero-dimers decreases when a mixture of SecA, labeled with two distinct fluorophores, is diluted to low nano-molar concentrations. The dissociation constant was calculated from the Hill-fit. (B) Influence of NaCl on the dimerization of SecA in suspension monitored by FCCS. SecA (28 nM) was incubated with different NaCl concentrations, and the relative concentration of dual-color SecA hetero-dimers was determined by FCCS. Error bars; s.d*

.

Protein translocation requires cycling of SecA

To examine the apparent Michaelis-Menten constant K_M of SecA for protein translocation, we performed *in vitro* translocation experiments with varying SecA concentrations under the same conditions as used in the DCFBA measurements. The translocation of fluorescently labeled proOmpA into proteoliposomes containing SecYEG saturated at high nano-molar concentration with an apparent K_M of 106 ± 16 nM (Figure 7). Compared to the high binding affinity of SecA to SecYEG, this

relatively low apparent K_M demonstrates that an excess of SecA is necessary for efficient protein translocation

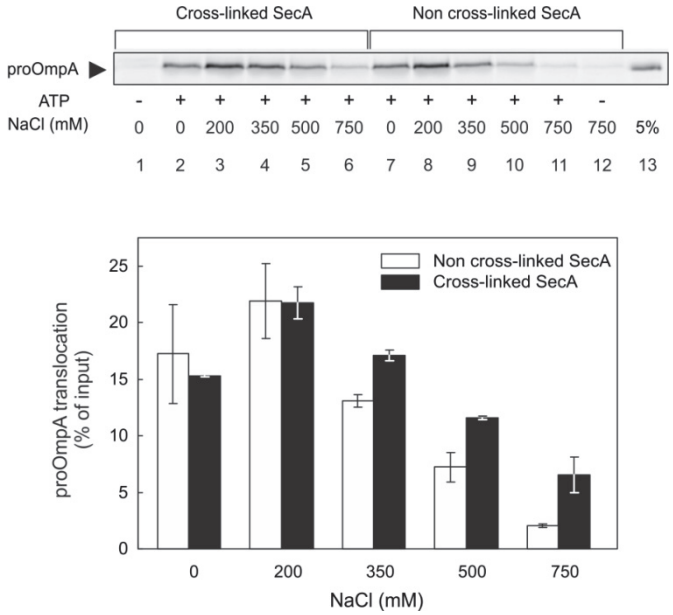

***Figure 6**: High salt sensitivity of protein translocation. In vitro protein translocation in the presence of NaCl. Crosslinked SecA (lane 2-6) is less inhibited by increasing NaCl-concentrations than non crosslinked SecA (lane 7-11). NaCl concentrations were 0, 200, 350, 500, and 750 mM for lane 2-6 and 7-11, respectively. Reactions in lane 1 and 12 were without ATP (digestion controls). Lane 13: 5% of input material. Graph represents quantified bands from two independent experiments. Error bars show the spread.*

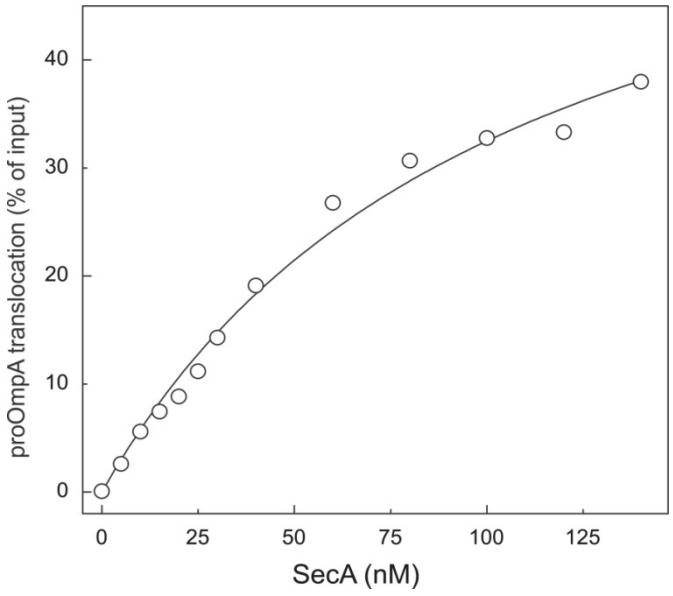

***Figure 7:** SecA dependence of protein translocation. In vitro protein translocation of proOmpA-FM into SecYEG containing proteoliposomes as a function of the SecA concentration. Solid line presents a fit using the Michaelis-Menten equation.*

Discussion

Measuring the quaternary structure and high affinity binding of ligands to their membrane receptors under physiologically relevant conditions has been a challenge up to date. The low detection sensitivity for proteins as well as the handling of membrane proteins, detergent-solubilized or embedded in an elastic and sensitive membrane environment, has hampered such analysis. Here, we employ dual-color-fluorescent-burst analysis (DCFBA) to probe the quaternary structure of the motor protein SecA when bound to its membrane embedded receptor, the protein conducting channel SecYEG. Simultaneously, the method allowed the determination of the binding affinity of SecA to SecYEG for various steps of the translocation cycle.

In this study, we show by employing an *in vitro* translocation assay that crosslinked (covalent dimer) and non crosslinked (noncovalent dimer) SecA have identical activity, yet being the limiting factor. This result demonstrates that, at least during the rate-limiting step, SecA is dimeric in protein translocation. To investigate whether SecA monomerizes at a later, not rate-limiting, step of the translocation cycle, we used fluorescently labeled SecA in the crosslinked and non crosslinked form for a binding assay followed by DCFBA. The average ratio of SecA over SecYEG as determined from the binding curves was virtually identical for all translocation conditions (no translocation ligands, preprotein, preprotein plus ATP, ADP) which implies that also non crosslinked SecA binds as a dimer (Figure 2, Figure S1-3). Previous studies concluding that SecA functions as a dimer [92,102,108] were recently opposed by a crystal structure of a monomeric SecA-SecYEG complex [29] from *Thermotoga maritima*. This structure, however, was obtained in detergent and at high salt concentration, both conditions that favor dissociation of the SecA dimer [91,106,107] (this study). Interestingly, the residues mediating dimerization of *E. coli* SecA [84] are highly conserved and the corresponding residues of the *T. maritima* SecA are exposed to the cytoplasmic surface in the SecYEG bound state [29] (compare Figure 8A and B). It is therefore possible that a second SecA protomer associates with these structurally conserved motifs of SecYEG bound SecA. We visualized such SecA dimer by docking a duplicated copy of the *T. maritima* SecA protomer onto the SecA-SecYEG structure (Figure 8C) using the coordinates of the *E. coli* dimer (Figure 8D). It is likely that the second protomer has a different conformation as the SecYEG-bound protomer as nucleotide binding induces a dramatic structural change in SecA, e.g. rotation of the preprotein binding domain (PBD) by around 80° [29]. However, the cytoplasmic surface of SecYEG-bound SecA seems less affected by these changes and readily allowed docking of the second SecA protomer to the conserved dimer interface of the *E. coli* SecA. Interestingly, in this antiparallel dimer arrangement, the two PBD come in close proximity, which would enable transfer of preprotein segments from one protomer to the other. It should be emphasized, however, that the dimerization interfaces in the crystal structures of various SecA proteins differ substantially [84,85,98,99,104,206] and it remains unclear which dimeric conformation is physiological relevant (for review see [207]).

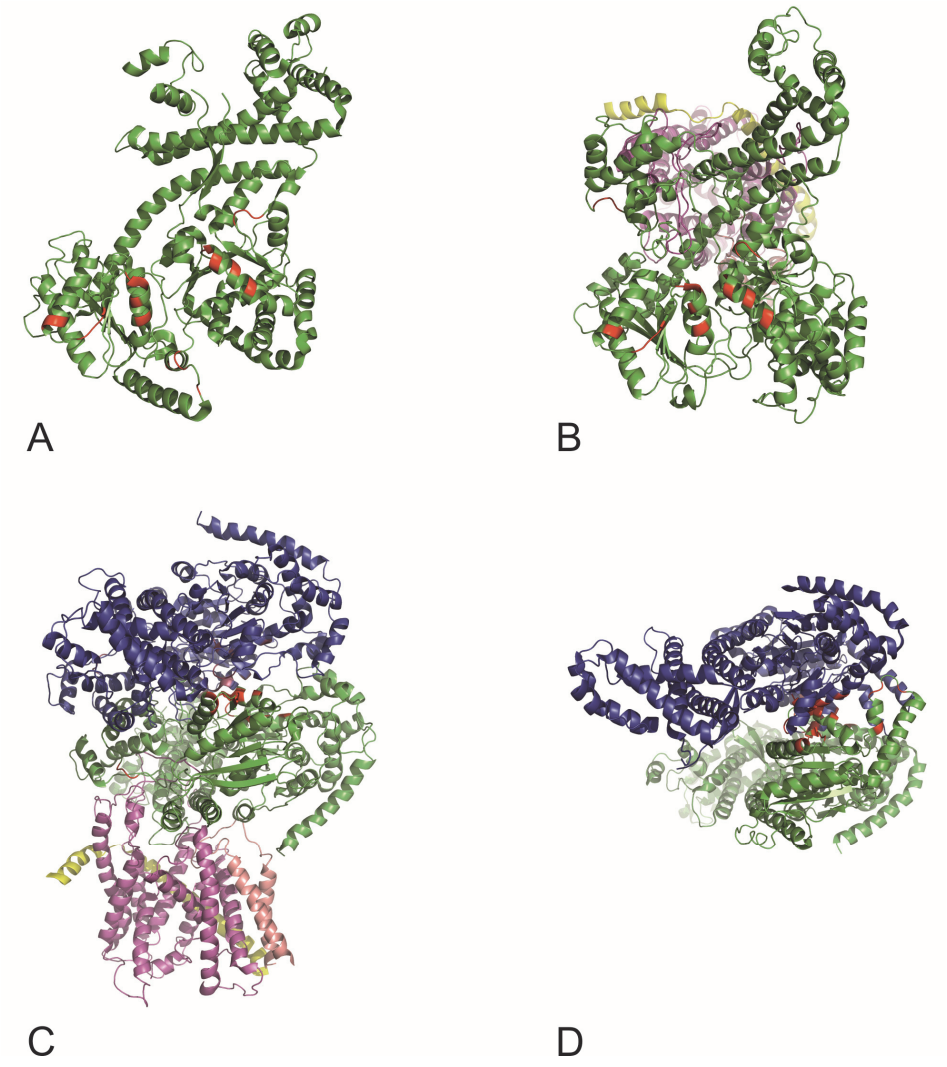

Figure 8: *Structural model for the dimeric SecA bound to SecYEG. Structures of the E. coli and T. maritima SecA and a structural model for the dimeric SecA bound to SecYEG. The dimer interface of E. coli SecA (A, residues in red) [84] (PDB accession code 2FSF) is highly conserved and exposed on the cytoplasmic surface of SecYEG bound SecA of T. maritima [29] (PDB accession code 3DIN). Docking of a second copy of the T. maritima SecA onto the monomeric SecYEG bound protomer (C) using the coordinates of the E. coli SecA dimer (D). The SecA protomers are shown in green and blue, respectively. The T. maritima SecY, SecE and SecG are shown in purple, yellow and pink, respectively.*

Importantly, the orientation of the SecA monomer in the SecA-SecYEG structure is not compatible with several of the proposed crystallographic SecA dimers and also contradicts some biochemical crosslinking studies aimed at elucidating the orientation of the SecA dimer. Our model also fits the crystal structure of the *B. subtilis* SecA dimer [85]. The corresponding residues in the HSD that are involved in dimerization

in the *B. subtilis* SecA dimer are exposed to the cytoplasm in the *T. maritima* SecA-SecYEG co-crystal (Figure S5A+B). The flexible N-terminus of SecA that has been implicated in dimerization of the *B. subtilis* SecA, however, is oriented towards the membrane in the SecA-SecYEG structure. It should however be noted that there is conflicting evidence on the importance of the N-terminus. In one study [103], an N-terminal deletion in the *E. coli* SecA led to monomerization and inactivation of SecA, while in other studies [109,208] a similar mutant was found to be dimeric and fully functional. Additionally, the genetically fused head-to-tail (N- to C-terminus) [109] or chemically crosslinked (C- to C-terminus) SecA dimers (Figure 3) [102] are fully active in protein translocation. Thus, the involvement of the extreme termini in physiological dimerization remains obscure.

The *E. coli* SecA dimer has also been crosslinked via introduced cysteines at position 11/611 and 637/801 [108] while retaining some activity and at 636/801 [209] resulting in inactivation of the protein. The residues 611, 636, 637 and 801 are localized at the binding interface of the *T. maritima* SecA-SecYEG and thus cannot participate both in SecYEG binding and SecA dimerization (Figure S5C). Hence, both the structure and our model are compatible with this crosslinking data. Similarly, the residues implicated in dimerization of the anti-parallel dimer crystallized from *M. tuberculosis* are close or within the SecA-SecYEG binding interface and thus cannot participate in dimerization as depicted in Figure 8. Also, the short helix that participates in the formation of the parallel *T. thermophilus* SecA dimer is oriented sideways in the *T. maritima* SecA-SecYEG structure (Fig S5A+B). Finally, the ring-like structures of membrane bound SecA observed by AFM are difficult to conceive with our model. Importantly, our model of SecA dimerization is compatible with the *T. maritima* SecA-SecYEG co-crystal, the *E. coli* and *B. subtilis* SecA dimer structures and is supported by various C- and N-terminal crosslink studies. Furthermore, it combines previous conflicting functional studies that reported binding of monomeric and/or dimeric SecA to SecYEG [15,16,102,107,110]. The interaction between SecA and SecYEG may involve only one protomer of the SecA dimer while the second copy does not interact with SecYEG directly as shown in Figure 8C. Therefore, also association of monomeric SecA is possible and the relevant quaternary structure of the SecA-SecYEG complex is determined by the sensitive nature of the SecA monomer-dimer equilibrium. We now show that binding of monomeric SecA to SecYEG is salt resistant while binding of the second protomer is salt sensitive (Figure 4). In earlier studies on the oligomeric state of the SecYEG bound SecA, the experimental conditions varied considerably. The use of detergents [15,16], low protein concentration [107] or non-equilibrium methods (gel-filtration, native gel-electrophoresis) may have shifted the monomer-dimer equilibrium of SecA towards the monomeric form. It is well established that an increasing salt concentration leads to monomerization of SecA in solution [91]. Therefore, to probe the binding of monomeric SecA to membrane-embedded SecYEG, we performed the DCFBA binding assay in the presence of 500 mM NaCl (or 1 M Urea). For all conditions, non

crosslinked SecA bound with significantly lower ratio to SecYEG than crosslinked SecA indicating salt-resistant monomeric SecA binding. Considering a crosslinking efficiency of about 70 %, the 1.5-fold lower ratio of non crosslinked SecA binding to SecYEG at 500 mM NaCl implies that the majority of SecA is bound as a monomer. We performed FCCS experiments with SecA labeled with two spectrally distinct fluorophores confirming that increasing salt concentrations shift the monomer-dimer equilibrium of SecA towards the monomeric state (Figure 5B). The salt-sensitivity suggests that electrostatic interactions play a critical role in dimerization. Indeed, the *E. coli* SecA dimer is stabilized by 15 hydrogen bonds although the primary dimer interface involves hydrophobic contacts [84]. Remarkably, the affinity (K_d of 0.74 nM) for dimerization (in solution) is significantly higher than the affinity of SecA for SecYEG. This implies that at SecYEG saturating concentrations, SecA will bind as a dimer. Our quantitative assessment of the dissociation constants indicate that the monomer-dimer equilibrium of SecA in solution determines the oligomeric state of the SecYEG bound SecA and that SecYEG does not induce SecA monomerization.

DCFBA is based on the quantification of fluorescent bursts that reside from fluorescently labeled proteins diffusing through the two laser foci of a dual-color confocal microscope (Figure 1A). Co-migrating proteins, labeled with two spectrally distinct fluorophores, will result in fluorescent bursts whose intensities depend on the position within the confocal excitation volume and the number of fluorophores in the complex (Figure 1B). Thus, changes in the relative stoichiometry of the co-migrating proteins can be addressed by quantifying the intensity of overlapping fluorescent bursts and calculating the relative ratio of one color over the other. In comparison with similar methods that use coincidence or burst selection, such as confocal fluorescence coincidence analysis (CFCA, [167-169]) or two-color coincidence detection (TCCD, [170-172]), DCFBA offers several advantages. Two arbitrary thresholds are used to select the overlapping bursts and not only the fraction of coincidence is revealed but the relative concentration of co-migrating fluorophores is determined with single particle resolution. This is in particular important when complexes with a variable number of fluorophores are present as is the case using liposomes with heterogeneous size distribution and membrane protein content. However, DCFBA underlies a single particle analysis and at higher (> 20 nM) nano-molar concentration on average, more than one fluorescent species resides in the focal volume leading to an increasing degree of coincidental co-migration with increasing particle number. Therefore, a concentration dependent linear increase in co-migrating fluorescent particles is observed at high nano-molar concentrations.

The activity of monomeric wild type SecA, as assayed by *in vitro* translocation, in the presence of high salt is significantly more inhibited than that of the dimeric, crosslinked, SecA (Figure 6). This is in agreement with earlier studies where SecA mutants with the monomer-dimer equilibrium shifted towards the monomeric state had low or no activity at all [103,107,110,111]. The increase of translocation activity in the presence of 200 mM NaCl is most likely due to a significant reduction in

proteoliposome aggregation, which occurs under *in vitro* translocation assay conditions as observed by fluorescence microscopy (data not shown). In line with the above observations, in previous studies hetero-dimers composed of active and non active SecA monomers were shown to be entirely inactive [92]. Overall, our data now show that SecA is dimeric throughout the protein translocation cycle and that monomeric SecA has a low or no translocation activity.

Does a single SecA dimer bound to SecYEG mediate the translocation of an entire preprotein or are repeated cycles of SecA dimer binding and dissociation from SecYEG required for complete translocation? Our data on the *in vitro* translocation assay with varying SecA concentrations and the affinity cascade of SecA for SecYEG in presence of translocation ligands provides evidence for a cycling model. Remarkably, the affinity of SecA to SecYEG increases significantly in the presence of preprotein and by the addition of ATP. In contrast, in the presence of ADP, there is a reduction in the binding affinity, confirming previous reports [56]. The apparent K_M derived from the *in vitro* translocation assay with varying SecA concentrations (106 nM, Figure 7) is about 30-fold higher than the K_d for SecA binding to SecYEG (3.6 nM, Figure 2) and even more than 150-fold higher than the K_d for the dissociation of the SecA dimer (0.74 nM, Figure 5A). The large difference between the K_d and apparent K_M indicates that a single SecA bound to SecYEG is highly inefficient in protein translocation *in vitro* and suggests that cycles of SecA binding and complete dissociation from the SecYEG channel are required for protein translocation. Our observations support the notion that protein translocation is driven by repeated nucleotide binding and hydrolysis driven cycles of SecA binding and dissociation [5,6]. Future studies should address the question how the two protomers contribute to the protein translocation reaction during the catalytic cycle of SecA.

Experimental Procedures

Chemical and reagents

Fluorescein-maleimide and DiD were purchased from Molecular Probes (Invitrogen), maleimide derivatives of Atto647N, Atto550 and Atto488 from Atto-Tec, (57076 Siegen, Germany) and Cy5-maleimide from GE-Healthcare. Cation exchange chromatography was performed on HiTrap SP HP and gel filtration on Superdex 200 XK26/60 or NAP5 columns from GE Healthcare. HIS-Select Nickel Affinity Gel (P6611) was purchased from Sigma-Aldrich. N-Dodecyl-β-maltoside (DDM) was purchased from Anatrace. *E. coli* total lipid extract was purchased from Avanti and acetone-ether washed as described elsewhere [210]. Bio-Beads SM-2 adsorbents, Micro Bio-Spin 6 and empty Bio-Spin chromatography columns were purchased from Bio-Rad.

Protein purification and reconstitution

SecB and proOmpA were purified as described elsewhere [211]. SecA was purified via a single step cation exchange chromatography. Cell free extract (in 20 mM Hepes-KOH, pH 6.5) of *E. coli* DH5α carrying plasmid pMKL18 [210] grown overnight in LB to OD 0.6 was applied on a HiTrap SP HP column equilibrated with buffer A (20 mM Hepes-KOH, pH 6.5, 10 % glycerol). The column was washed with buffer A supplemented with 100 mM NaCl and elution was achieved by a NaCl gradient in buffer A. SecA eluted around 400 mM NaCl. Prior to labeling with a 20-fold molar excess of fluorescein-maleimide (FM) at pH 7, SecA was incubated for 30 min with a 10 fold molar excess of $ZnCl_2$. The labeling reaction was stopped after 3 h by addition of 1 mM DTT. In order to remove the Zn^{2+}, a 10 fold molar excess of EDTA was added followed by 30 min incubation. Prior to the labeling of WT-SecA with Atto488 and Cy5, Zn^{2+}-ions were chelated by incubation for 30 min with a 10-fold molar excess of EDTA. Fluorescently labeled SecA was then purified on a Superose 12 column with Buffer B (50 mM Tris-HCl, pH 7.6, 10 % (v/v) glycerol, 50 mM KCl). Crosslinking of SecA was achieved by incubation with 0.5 mM copper phenanthroline (CuPhe) for 30 min at room temperature (RT). To remove CuPhe, SecA was applied on a Micro Bio-Spin 6 gel filtration column equilibrated with Buffer B. $SecY_{(C295)}EG$ purification, labeling with Atto647N-maleimide and reconstitution into total *E. coli* lipid extract is described elsewhere [211]. The labeling efficiency of both SecA-FM and $SecY_{(C295)}EG$-Atto647N was determined by UV-Vis spectroscopy and corrected for the fluorophore absorption at 280 nm as specified by the manufacturer of the fluorophores. Labeling efficiency was 100 % for SecA-FM and approximately 80 % for $SecY_{(C295)}EG$-Atto647N.

In vitro protein translocation

The *in vitro* protein translocation assays were essentially performed as described elsewhere [211] with the following variations: For assaying crosslinked SecA-FM the translocation mixture contained urea treated IMVs of *E. coli* SF100 overexpressing $SecY_{(C295)}EG$, and 2 mM ATP. Translocation assays were performed in the absence of SecB. Indicated concentrations of crosslinked or non crosslinked SecA were added to the mixture and the volume was corrected with buffer B. After 3 min incubation at 37 °C the reaction was started by the addition of 20 µg/mL proOmpA-DhfR-Atto550 (unfolded DhfR domain). For *in vitro* translocation in the presence of NaCl at RT, a translocation mixture with $SecY_{(C295)}EG$ containing proteoliposomes, 100 nM crosslinked or non crosslinked SecA and 20 µg/mL proOmpA-FM was adjusted to the indicated NaCl concentration and incubated for 10 min at RT before the reaction was started by addition of 2 mM ATP and continued for 45 min at RT. The translocation mixture for K_M determination was composed of $SecY_{(C295)}EG$ proteoliposomes, 80 µg/mL SecB, 20 µg/mL proOmpA-FM, indicated SecA concentrations and carried out at RT as described above.

Binding reactions and sample preparation

Binding of SecA-FM to $SecY_{(C295)}$EG-Atto647N reconstituted into *E. coli* liposomes was performed as follows: SecA-FM (2-80 nM) was incubated with proteoliposomes containing $SecY_{(C295)}$EG-Atto647N in buffer C (50 mM Hepes-KOH, pH 7.6, 30 mM KCl, 2 mM $MgCl_2$) for 12 min at RT. For the DCFBA measurements, a microscope sample of 10 µL was prepared with a silicone press-to-seal spacer (Invitrogen). For the fluorescence cross-correlation spectroscopy (FCCS) experiments, equimolar amounts of SecA-Atto488 and SecA-Cy5 were mixed and incubated with 500 mM NaCl for 30 min on ice to dissociate SecA dimers. Buffer exchange to buffer C and formation of SecA-heterodimers was achieved by gel filtration (NAP5 column, GE Healthcare). A 30 min ultra-centrifugation at 400,000 ×g ensured the absence of aggregates in the sample.

Fluorescence spectroscopy, DCFBA and FCCS analysis

All fluorescence measurements were carried out on a dual-color laser scanning confocal microscope (LSCM). The LSCM was based on an inverted Axiovert S 100 TV microscope (Zeiss) and combined with a galvanometer optical scanner (model 6860, Cambridge Technology). The two laser beams (488 nm, argon ion laser, Spectra-Physics; 633 nm, He-Ne laser, JDS Uniphase) were focused by a Zeiss C-Apochromat infinity corrected 1.2 NA 40× water-immersion objective. The fluorescence was collected through the same objective, separated from the excitation beams by a beam pick-off plate (BSP20-A1, Thor-Labs), split into two channels by a dichroic beam splitter (585 DCXR, Chroma Technology), and finally directed through emission filters (HQ 535/50 and HQ 675/50, Chroma Technology) and pinholes (diameter of 30 µm) onto two avalanche photodiodes (SPCM-AQR-14, EG&G). For the laser-scanning dual-color fluorescent burst analysis (lsDCFBA, for review see [148]) measurements, the two aligned laser beams were moved simultaneously with the galvanometer optical scanner through the sample well above the surfaces of the sample holder. Two confocal images (60 × 60 µm) of SecA-FM and $SecY_{(C295)}$EG-Atto647N containing proteoliposomes were recorded simultaneously. The fluorescent bursts originating from the proteoliposomes and SecA-FM were identified using arbitrary fluorescence thresholds as described [148]. Software for DCFBA can be downloaded at www.bogeert.com/DCFBA/publish.htm. The dwell-time of the laser scanning was 200 µs and the pixel step was 110 nm. Typically, in 4 consecutive scans, 100-1000 burst were recorded for sufficient statistics. A dilution series of SecA-FM was subjected to FCS measurements and confocal scans. The concentration of SecA-FM was calculated from the amplitude of the FCS curve and plotted against the total fluorescence from the corresponding scan. The resulting calibration curve was used to determine the concentration of SecA-FM in the scans from binding assays. The fluorescence cross-correlation spectroscopy (FCCS) and data analysis were performed as described elsewhere [212].

For the analysis, a number of controls were performed to ascertain that quenching does not occur during the measurement. The fluorescent intensity (counts per molecule, cpm) of crosslinked and non crosslinked SecA as determined by FCS showed identical cpm. Furthermore, the total fluorescence as derived from the confocal scans was comparable for both species at similar protein concentration. The Atto647N fluorophore that is insensitive to environmental changes was attached to a periplasmic loop of SecY, keeping it far away from the cytoplasmic SecA binding site. This, besides the spectral separation of fluorescein and Atto647N, further diminishes the chance for Förstner Resonance Energy transfer (FRET) between fluorophores on SecA and SecY. Finally, background fluorescence originating from fluorescent molecules diffusing far from the center of the confocal excitation volume and dark current were filtered out by the arbitrary thresholds as described [148].

Acknowledgements

This work was supported by NanoNed, a national nanotechnology program coordinated by the Dutch Ministry of Economical Affairs and the Zernike Institute for Advanced Materials, and by the Chemical Sciences division of The Netherlands Organization for Scientific Research (NWO-CW).

Supplementary Information

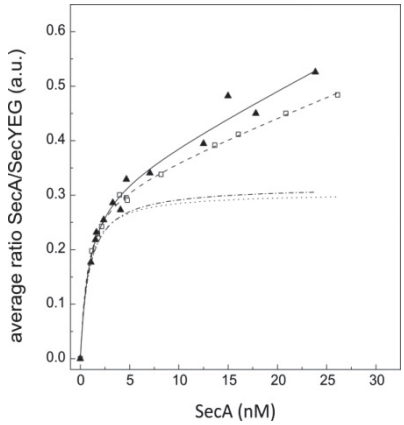

Figure S1: *Binding of SecA-FM to SecYEG-Atto647N containing proteoliposomes in presence of proOmpA and 1mM ATP. Data points were fitted using the Hill-equation (straight and dashed lines) and the linear non-saturable binding parameter was subtracted from the fit (dotted lines).*

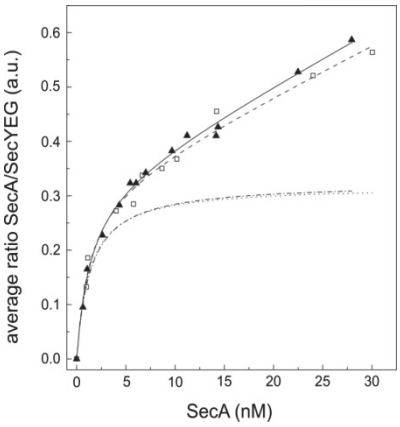

Figure S2: *Binding of SecA-FM to SecYEG-Atto647N containing proteoliposomes in presence of proOmpA. Data points were fitted using the Hill-equation (straight and dashed lines) and the linear non-saturable binding parameter was subtracted from the fit (dotted lines).*

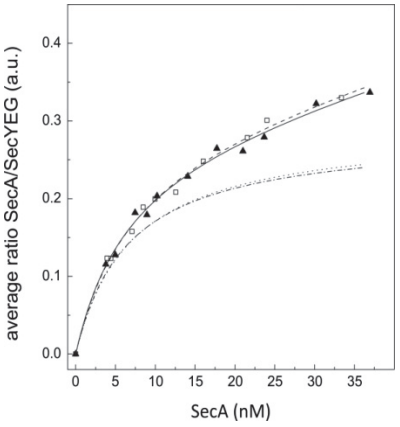

Figure S3: *Binding of SecA-FM to SecYEG-Atto647N containing proteoliposomes in presence of 1 mM ADP. Data points were fitted using the Hill-equation (straight and dashed lines) and the linear non-saturable binding parameter was subtracted from the fit (dotted lines)*

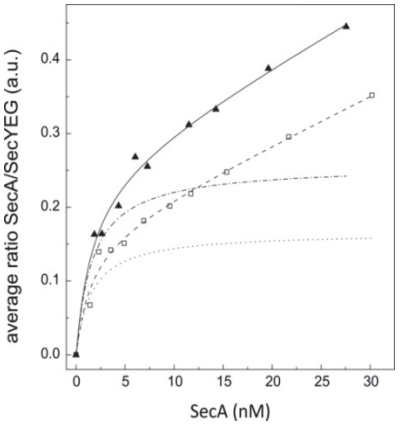

Figure S4: *Binding of SecA-FM to SecYEG-Atto647N containing proteo-liposomes in presence of 1 M Urea. Data points were fitted using the Hill-equation (straight and dashed lines) and the linear non-saturable binding parameter was subtracted from the fit (dotted lines).*

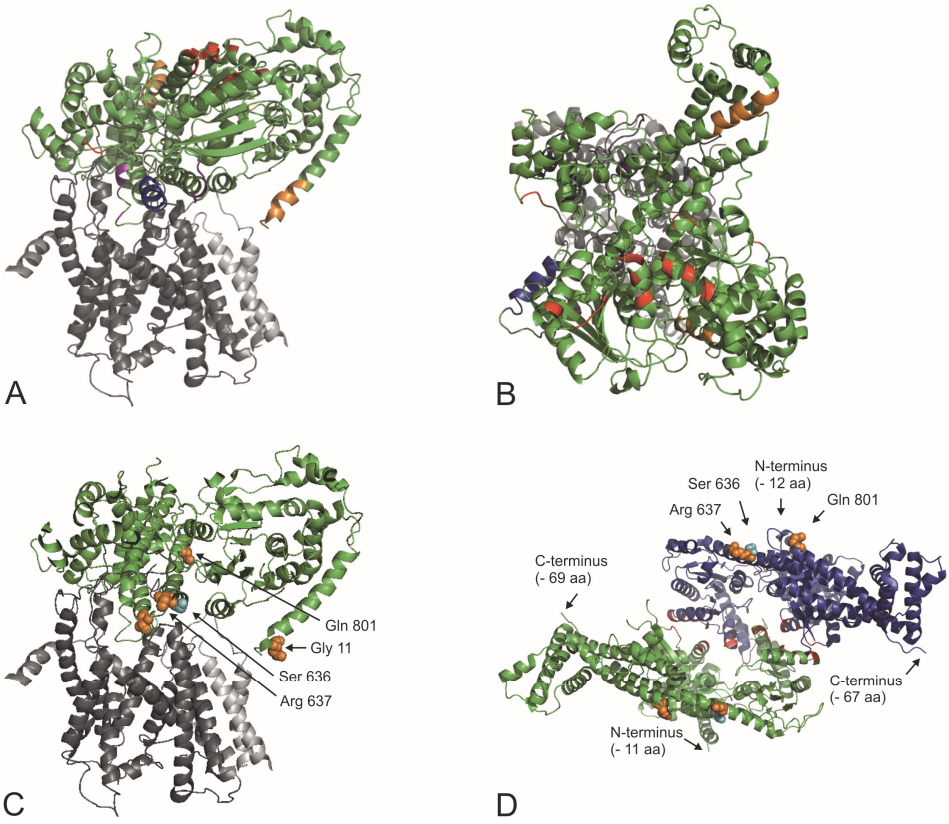

Figure S5: *Comparison of the T. maritima SecA-SecYEG co-crystal to SecA dimerization interfaces described by structural and biochemical studies. A) Side view of the T. maritima SecA-SecYEG co-crystal [29] with residues implicated in dimerization from dimeric SecA crystal structures from E. coli (red) [84], B. subtilis (orange) [85], T. thermophilus (blue) [99] and M. tuberculosis (magenta) [98]. SecYEG is coloured in gray and SecA in green. B) Top view (cytoplasm) of A). C) Side view of the T. maritima SecA-SecYEG co-crystal with corresponding residues found to crosslink E. coli SecA dimers in solution depicted as spheres. Residue numbers are from E. coli SecA. Orange spheres [108], cyan sphere [209]. D) Crystal structure of E. coli SecA dimer [84] with residues as indicated in C). Not resolved N- and C-termini are indicated.*

CHAPTER 5

A single Copy of SecYEG is Sufficient for Preprotein Translocation

Alexej Kedrov, Ilja Kusters, Victor V. Krasnikov, and Arnold J.M. Driessen

Submitted

Abstract

The heterotrimeric SecYEG complex comprises a protein-conducting channel in the bacterial cytoplasmic membrane. SecYEG functions together with the motor protein SecA in preprotein translocation. Here we have addressed the functional oligomeric state of SecYEG when actively engaged in preprotein translocation. We reconstituted functional SecYEG complexes labeled with fluorescent markers into giant unilamellar vesicles at a natively low protein-to-lipid ratio. Förster's resonance energy transfer and fluorescence (cross-) correlation spectroscopy with single-molecule sensitivity allowed for independent observations of the SecYEG and preprotein dynamics, as well as complex formation. In the presence of ATP and SecA up to 80% of the SecYEG complexes were loaded with a preprotein translocation intermediate. Neither the interaction with SecA, nor preprotein translocation resulted in the formation of SecYEG oligomers whereas such oligomers can be detected when enforced by crosslinking. These data imply that the SecYEG monomer is sufficient to form a functional translocon in the lipid membrane.

Introduction

A major share of the bacterial proteome localizes at the cell surface or is targeted to the periplasm. Most of these proteins are synthesized in the cytosol with a N-terminal signal sequence (preproteins) and are transported across the bacterial cytoplasmic membrane by the Sec translocon [60]. In *Escherichia coli*, nascent preproteins are captured by the chaperone SecB [213], maintained in their unfolded state and delivered to the Sec complex (Fig. 1A). Next, preproteins are actively translocated via the SecYEG channel in a process that is fueled by ATP hydrolysis by the motor protein SecA [62]. During the last two decades, a multitude of biochemical data collected on various aspects of the translocon function has led to a detailed insight in the mechanism of preprotein translocation. The structure of the SecYEG channel in several conformations, including a free closed state and a SecA-bound state has been elucidated by X-ray crystallography [11,29,33]. Recent cryo-EM studies visualized monomeric Sec61p and SecYEG complexes bound to a ribosome translating a secretory protein [28]. The structural data suggests that a single copy of the SecYE(G) complex is sufficient to form a pore in the membrane, but several biochemical studies indicate that the translocon is a highly dynamic structure and that oligomers of SecYEG are formed during the catalytic cycle. SecYEG dimers were shown to be ubiquitous in native and synthetic membranes when over-expressed [14,18,20], but also at endogenous levels [214]. A dynamic equilibrium between SecYEG monomers and dimers in the membrane has been suggested, that is shifted towards SecYEG dimers or higher oligomers upon the interaction with SecA and preproteins [14,19,20]. Two-dimensional crystals of the *E. coli* SecYEG showed a dimeric architecture with the C-terminal helix of SecE forming the dimerization interface [9], also termed as the "back-to-back" dimer. On the other hand, tag-based co-purification experiments suggested that SecYEG forms a monomeric complex with the preprotein in native membranes [215], though also dimers were suggested to interact with the preprotein [14]. In a complementary approach, monomers of SecYEG reconstituted in nano-discs were shown to be competent in SecA binding and SecA ATPase activity, but no translocation activity was determined [216]. Since many of these experiments studied the SecYEG complex in the detergent-solubilized or an otherwise restricted state, it has remained unclear if the monomer represents the functional state in translocation. Recently, an effort has been made to investigate the SecYEG oligomeric state at the single-molecule level in lipid membranes [30]. Based on semi-quantitative results it was stated that dimerization is required for efficient translocation, but only minor differences in translocation efficiency between SecYEG monomers and crosslinking-stabilized dimers were demonstrated. In order to resolve this question, a quantitative approach is required that thoroughly tests the various hypotheses.

Here, we establish a novel quantitative *in vitro* assay for protein translocation with single-molecule sensitivity using fluorescence (cross-) correlation spectroscopy (FCS/FCCS) and Förster's resonance energy transfer (FRET) measurements. For the

first time we describe the properties of functional translocons in a non-invasive manner at the single-molecule level, and address the oligomeric state of SecYEG in the lipid environment at different stages of the functional cycle. Our results strongly suggest that a single copy of the SecYEG complex is sufficient both for SecA binding and preprotein translocation.

Results

Formation of SecYEG-containing giant unilamellar vesicles

Giant unilamellar vesicles (GUVs) are well-suited for a range of *in vitro* studies, including microscopy and electrophysiology [217]. Here, we aimed to establish a GUV-based system for studying the SecYEG translocon by means of ultra-sensitive microscopy, in particular FCS [218]. An FCS experiment on integral membrane proteins generally requires planar lipid bilayer, so that the protein diffusion occurs in a two-dimensional space. GUVs of tens of microns in diameter represent a suitable system ensuring both the relevant environment for the protein and a flat surface within the observation volume of a confocal microscope. We screened different mixtures of synthetic phospholipids and probed their propensity to form stable GUVs [217]. Lack of surface undulations, homogeneity and the ubiquity in the preparation were the primary criteria. The SecYEG activity is critically dependent on the content of anionic lipids in the membrane [219-221], so we supplied liposomes with DOPG and cardiolipin. Mixing DOPG (20 mol %), cardiolipin (10 mol %), DOPE (30 mol %) and DOPC (40 mol %) allowed for efficient GUV formation both from empty liposomes and after SecYEG reconstitution. This lipid composition was selected for further experiments. The purified SecYEG reconstituted into synthetic lipid membranes (Fig. 1B) showed a high translocation activity, which even exceeded the activity of SecYEG reconstituted in the polar lipid extract of *E. coli* (Fig. 1C). Stimulation of the translocon activity by certain lipid compositions has been previously described [220], although no comparison between synthetic and native lipids has been carried out. Replacing the cardiolipin fraction with DOPG did not affect the translocation efficiency (Fig. S1).

For fluorescence measurements we used the variant, $SecY_{C295}EG$, that contained a single cysteine residue in the periplasmic loop connecting transmembrane segments 7 and 8 of SecY. This residue could be efficiently conjugated with maleimide-derivative fluorophores, such as AlexaFluor 488-C_5-maleimide or Atto 647N-maleimide with a labeling efficiency of about 90%. Prepared proteoliposomes contained fluorophore-labeled $SecY_{C295}EG$ at a molar protein-to-lipid ratio of 1:30,000. This ratio is substantially lower than those used in conventional bulk experiments and it allowed eliminating effects of unspecific interactions due to molecular crowding. To form GUVs we used a modified protocol for gentle hydration of desiccated proteoliposomes [222] that allowed for spontaneous and efficient GUV formation. The protein translocation activity of the SecYEG-containing proteoliposomes after the

dehydration/rehydration cycle was retained at essentially the same level as that of untreated proteoliposomes (Fig. 1D). Thus, $SecY_{C295}EG$ was functionally reconstituted in GUVs and these were further used to examine SecYEG dynamics.

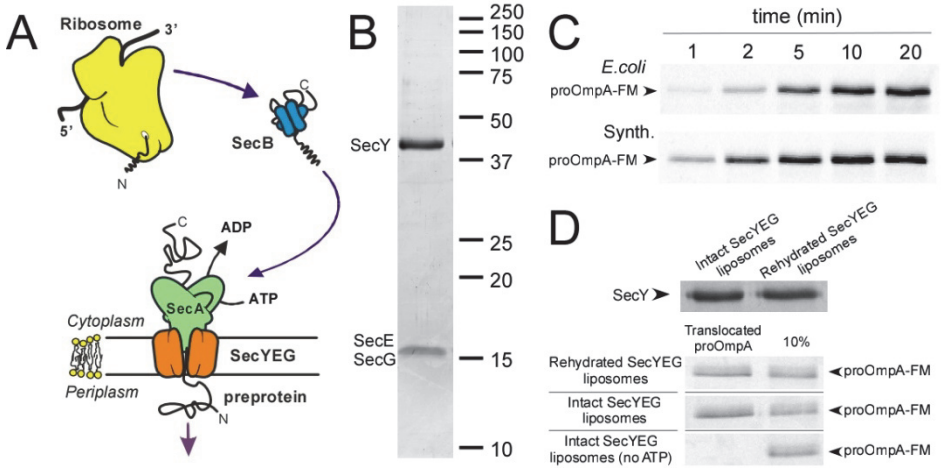

Figure 1. Purification and membrane reconstitution of SecYEG translocon. *(A) Scheme of the Sec translocase of bacteria, with SecYEG as membrane-embedded protein-conducting channel, and an unfolded preprotein that is actively translocated by the SecA ATPase. The SecB chaperone prevents the preprotein from folding or aggregation after leaving the ribosome and delivers it to the SecYEG:SecA complex. (B) Coomassie-stained SDS-PAGE of purified SecYEG reconstituted into liposomes made of synthetic lipids. (C) SecYEG translocation activity in model membranes. SecYEG reconstituted into liposomes composed of synthetic lipids (10 mol % cardiolipin, 20 mol % DOPG, 30 mol % DOPE, 40 mol % DOPC) showed a faster rate of translocation as compared to SecYEG reconstitution into E. coli polar lipids, as monitored by the translocation of proOmpA$_{C295}$-fluorescein into the membrane vesicles. (D) Sucrose protects the SecYEG functional state upon dehydration. SecYEG-containing proteoliposomes (protein-to-lipid molar ratio 1:1,000) were desiccated overnight under vacuum and rehydrated prior the translocation reaction. The SecYEG level was identical in intact and rehydrated proteoliposomes as judged from SDS-PAGE (upper panel). The activity of SecYEG was tested by conventional translocation assay [149] and compared with the untreated controls (lower panel). No decrease in the SecYEG translocation activity was observed upon the dehydration/rehydration step suggesting that SecYEG retained its functional state.*

After 10 min rehydration, GUVs of different sizes ranging up to 50 μm in diameter could be observed by means of phase-contrast and scanning confocal microscopy (Fig. 2A-C). We tested the permeability of the GUVs for large molecules using fluorescently labeled SecA-Atto 647N as a reporter. SecA-Atto 647N was added to the solution after GUV formation and this resulted in an intensive fluorescence signal in the GUVs exterior only (Fig. S2). The concentration of SecA-Atto 647N was measured inside the GUVs by FCS after 20 min, and no signal was detected in at least 90% of the vesicles (Fig. S2). This implied that the SecYEG complexes exposing their cytoplasmic surface towards the GUVs interior were not accessible for SecA binding and thus do not participate in translocation.

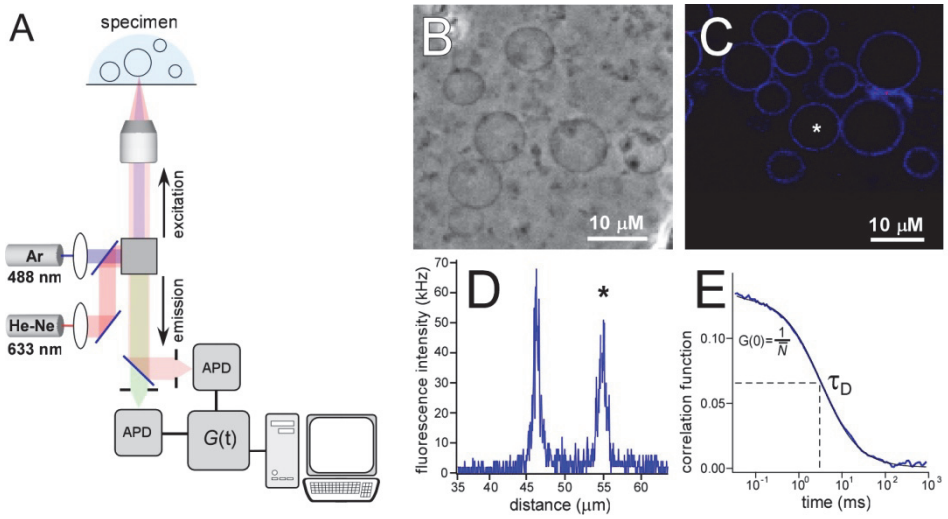

Figure 2. Fluorescence correlation spectroscopy on SecYEG-containing vesicles. *(A) Scheme of the home-built dual-laser confocal microscope used to study GUV-incorporated SecYEG. Dual-laser excitation was used for FCCS measurements, and the argon laser was used for FRET studies. Synthetic lipids allow for GUV formation in presence of reconstituted SecYEG complexes as monitored in phase-contrast (B) and fluorescent modes (C). A selected GUV (white asterisk) was scanned through its center in Z-direction parallel to the optical axis to locate lower and upper membrane planes (D). The fluorescence signal was measured on the upper plane (black asterisk) and used to calculate the auto-correlation curve (E). The protein concentration* $\overline{N}$ *and the diffusion time* τ_D *were extracted from the experimental data and used for further analysis (see text for details)*

To monitor the membrane-embedded $SecY_{C295}EG$ the laser beam was focused on the GUV surface (Fig. 2C, D). The fluorescence intensity of AlexaFluor 488-labeled $SecY_{C295}EG$ molecules diffusing through the focal volume was recorded and further used to build the auto-correlation curve (Fig. 2E). Curves were fitted assuming two-dimensional diffusion within the planar bilayer providing a diffusion coefficient of $(2.6\pm0.6)*10^{-8}$ cm^2/s. The measured diffusion coefficient of $SecY_{C295}EG$ was within the range typical for multi-spanning membrane proteins [223]. It was also close to the value of $3.1*10^{-8}$ cm^2/s that was theoretically calculated using Saffmann-Delbrück model [224] assuming the SecYEG radius of 2 nm, lipid bilayer thickness of 4.5 nm, and the bilayer viscosity around 0.1 Pa·s. The auto-correlation function G(t) yielded the concentration of $SecY_{C295}EG$ complexes reconstituted in the lipid membranes, since the amplitude G(0) equals the reciprocal of the particles number in the focal volume (Eq. 1; Fig. 2E). The reconstitution procedure ensured a low density of $SecY_{C295}EG$ in the membranes, so that normally about 10 molecules were observed within the observation volume. This value was optimal for FCS measurements, as it allowed both for sufficient statistics and sensitivity in the fluorescence fluctuations [225]. An accurate measure of the $SecY_{C295}EG$ surface density by FCS provided the unique opportunity to determine the actual molar protein-to-lipid ratio in the membranes. The observation volume radius around 200 nm corresponded to the

membrane area of ≈120,000 nm² that accommodated in total ≈350,000 lipid molecules of the bilayer. Thus, the actual protein-to-lipid ratio was 1:35,000 in agreement with the ratio used for reconstitution, and the SecYEG surface density was 100 molecules/μm². Importantly, the $SecY_{C295}EG$ density in the GUVs correlated well with that in *E. coli* membrane considering 300 SecYEG copies per bacterium [226] with dimensions of 1 x 3 μm and a corresponding surface area of 2.5 μm².

Monitoring SecYEG:preprotein complex formation

A fusion protein proOmpA-DhfR that consists of the unfolded OmpA protein precursor (proOmpA) and dihydrofolate reductase (DhfR) domain was used to study the translocation reaction [227]. This protein cannot be fully translocated through the SecYEG channel when the folded DhfR is stabilized by its ligands methotrexate and NADPH. Under those conditions the preprotein remains trapped in the SecYEG channel leaving the DhfR domain exposed at the cytoplasmic side [227] while the unfolded proOmpA is largely translocated through the pore thus forming a stable translocation intermediate (Fig. 3A and S3). A fluorophore conjugated to the translocated proOmpA domain and a spectrally separated fluorophore bound at a loop on the periplasmic side of SecY should allow for FRET. Hence, the translocation of proOmpA through $SecY_{C295}EG$ can be directly observed as an increase in the FRET efficiency between the donor (Cy3) and the acceptor (Cy5) markers conjugated to proOmpA and SecYEG, respectively (Förster's distance for the Cy3/Cy5 donor-acceptor pair > 5 nm). Bulk measurements showed an up to 30% increase in the acceptor fluorescence intensity when the proOmpA-DhfR-Cy3 was trapped in the $SecY_{C295}EG$-Cy5 channel (Fig. 3B), and the FRET signal was strictly ATP-dependent. Labeling the translocated polypeptide chain at different positions modulated the FRET efficiency as this determined the distance of the donor fluorophore to the $SecY_{C295}EG$-linked acceptor (Fig. 3B). The maximum signal was observed when labeling proOmpA at residues 282 and 290 suggesting that these residues are in close vicinity to the SecYEG periplasmic interface. Placing the fluorophore either near the DhfR domain (residue 315) trapped at the cytoplasmic side of SecYEG or within the translocated proOmpA region (residue 245) led to a minimal FRET efficiency due to their large distance from the acceptor fluorophore at the periplasmic exit of SecYEG channel. Residue 315 of the preprotein resides at the cytoplasmic interface of the membrane, thus being separated from the $SecY_{C295}$ residue by up to 7 nm, which is the sum of the membrane thickness (~4 nm) and dimension of SecA (~3 nm) (Fig. 3A). Residue 245 lies within the translocated part of proOmpA and thus it is distanced from the SecYEG pore.

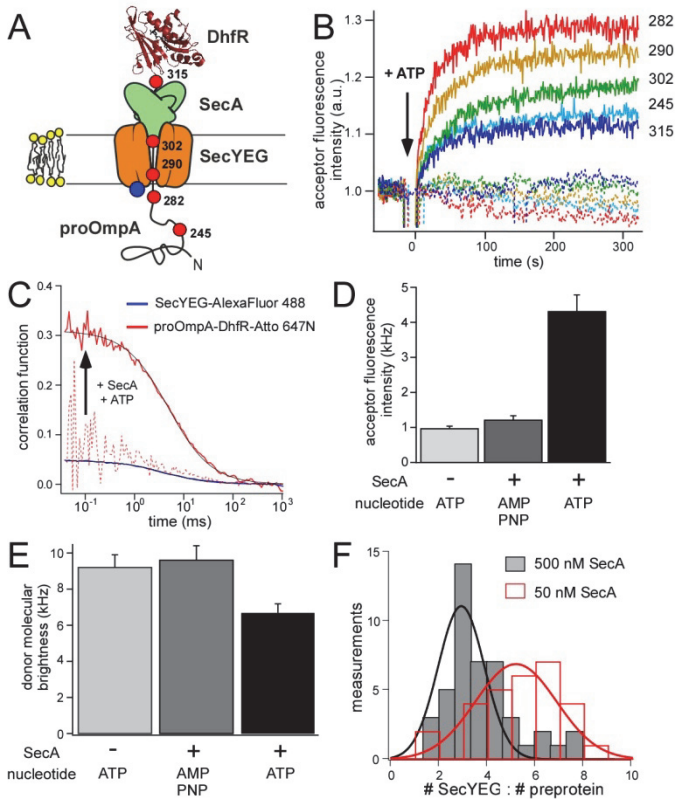

Figure 3. Formation of SecYEG - preprotein complex. *(A) The proOmpA preprotein is trapped in the SecYEG channel by the presence of a folded DhfR domain fused to the C-terminus. A single cysteine residue was introduced at different positions within the proOmpA domain (numbers and red circles) and fluorescently labeled. Complex formation was probed in bulk by measuring FRET efficiency between fluorophores Cy3 and Cy5 conjugated to proOmpA-DhfR variants and $SecY_{C295}EG$ in IMV, respectively. (B) Trapping the preprotein within SecYEG increases the acceptor fluorescence intensity due to FRET. The FRET efficiency depended on the fluorophore position along the proOmpA polypeptide chain (numbers aside). No change in fluorescence was observed in absence of the acceptor fluorophore on $SecY_{C295}EG$. (C) FRET-FCS recordings on the SecYEG:preprotein complex. GUV-embedded SecYEG complexes were monitored using the confocal microscope set-up. When both SecA and ATP were present, FCS recordings on the GUV surface showed a dramatic change in proOmpA-DhfR time-correlated fluorescence. Auto-correlation traces were fitted to two-dimensional diffusion model (black lines; Eq. 1). (D) A four-fold increase in the fluorescence intensity of proOmpA-DhfR-Atto 647N was observed upon trapping within SecYEG. At least 20 GUVs were examined at each condition to calculate the average fluorescence intensity; error bars present SEM values. (E) The molecular brightness of the donor SecYEG-AlexaFluor 488 decreased upon formation of the translocation intermediate (average ± SEM). (F) The fraction of active translocons in GUV membranes. Approximately 80% of the correctly oriented SecYEG complexes were involved in the translocation reaction in presence of 500 nM SecA. Reducing the SecA concentration ten-fold caused a decline in SecYEG:preprotein interaction. Solid lines present fits with normal distributions.*

FRET-FCS-based translocation assay

We further extended the approach to study translocation in GUVs using FCS and FRET to detect SecYEG:preprotein complexes. The AlexaFluor 488 fluorophore introduced into the $SecY_{C295}$ subunit served as a donor in the designed FRET assay. GUVs were supplied with the $proOmpA_{C282}$-DhfR conjugated with the Atto 647N fluorophore (acceptor; Förster distance for the donor-acceptor pair ~ 4 nm), SecB, and 5 mM ATP. Recordings in the blue channel of the $SecY_{C295}$EG-AlexaFluor 488 were used to determine an auto-correlation curve as described above to monitor the

diffusion of the $SecY_{C295}EG$ protein within the membrane (Fig. 3C). The auto-correlation curve of the acceptor fluorophore in the absence of SecA was dominated by the cross-talk between the channels (Fig. 3C, dashed red line). Also the corresponding fluorescence intensity remained at background levels, below 1,000 photons/s (Fig. 3D). After the sample was incubated for 10 min at 37°C in the presence of 0.5 □M SecA the fluorescence intensity of the acceptor fluorophore increased approximately four-fold and the auto-correlation curve acquired a characteristic shape (Fig. 3C, D). The average molecular brightness of the donor $SecY_{C295}EG$-AlexaFluor 488 decreased by about 20% when $proOmpA_{C282}$-DhfR-Atto 647N was trapped in the SecYEG channel (Fig. 3E). The substantial increase in the acceptor fluorescence was in agreement with the bulk translocation experiments (Fig. 3B), but now observed at a much lower protein concentration. The enhanced FRET signal (400% vs. 30%) is likely due to better signal-to-noise ratio when using a confocal microscope instead of the fluorescence spectrophotometer, as well as larger spectral separation of the fluorophores used.

The fluorescence signal recorded in the acceptor channel in the presence of SecA and ATP corresponded to the partially translocated and trapped $proOmpA_{C282}$-DhfR-Atto 647N molecules. The contribution of fluorescence from the membrane-bound $proOmpA_{C282}$-DhfR-Atto 647N to the fluorescence correlation function could be neglected, as their molecular brightness was at least 10-fold lower than that of SecYEG-trapped preproteins. If ATP was replaced by the non-hydrolysable analog AMP-PNP or if no SecA was added, we did not observe either an increase in the acceptor fluorescence (Fig. 3D), or a time-correlated signal. Thus, the approach discriminated stable translocation intermediates from the partially inserted or non-specifically bound preprotein molecules. Decreasing the translocation time down to 3 min caused an increase in the amplitude of proOmpA-DhfR-Atto 647N auto-correlation function, as the number of DhfR-trapped intermediate complexes decreased (Fig. S4).

SecYEG:preprotein complexes are ubiquitous in GUVs

The auto-correlation curves recorded in both channels upon the translocation reaction contained detailed and quantitative information about the protein diffusion rates and the stoichiometry of the interactions. Since the amplitude of the auto-correlation function yields an accurate measure of the number of fluorescent particles (Fig. 2E), the technique could be used to directly quantify the efficiency of translocation intermediate formation expressed as the ratio of the total number SecYEG complexes and trapped proOmpA-DhfR molecules. The most probable SecY:preprotein ratio measured on individual GUVs was 2.8 (Fig. 3F, grey bars; n=45). The vesicles manifesting higher ratios, i.e. lower translocation efficiency, typically showed a high SecYEG content of 20-30 molecules in observation volume. They likely reflected a minor non-unilamellar fraction comprising less than 10% of the vesicle ensemble. Accounting for the dual membrane topology of the reconstituted

SecYEG complexes and the limited labeling efficiency of the preprotein (~90%), we concluded that at least 76%, i.e. the vast majority of correctly oriented SecYEG complexes was functionally active assuming a stoichiometric complex of proOmpA-DhfR and SecYEG. Reducing the SecA concentration down to 50 nM, i.e. below the K_M value of ~100 nM [105], led to a lowered translocation efficiency (Fig. 3E, red bars).

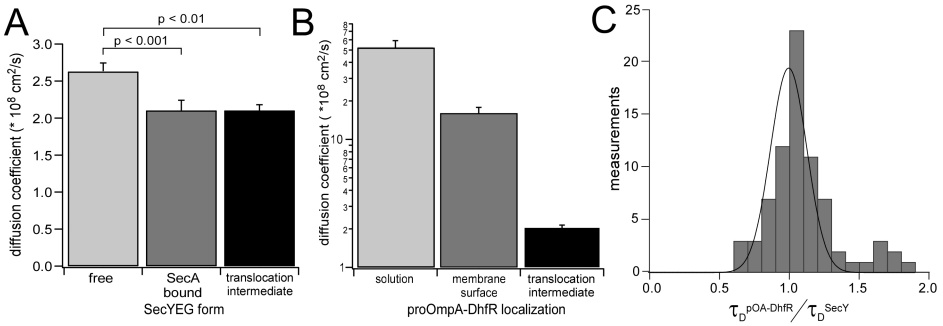

Figure 4. The mobility of SecYEG in the membrane depends on the functional state of the translocon. *(A) The lateral diffusion coefficient of $SecY_{C295}EG$-AlexaFluor 488 in GUV membranes measured using FCS is reduced in presence of the SecA motor protein and when trapping the preprotein proOmpA-DhfR. At least 20 GUVs were examined at each condition to calculate average diffusion coefficients; error bars present SEM values. (B) The mobility of the preprotein $proOmpA_{C282}$-DhfR-Atto 647N depends on its localization. The diffusion coefficient is maximal for three-dimensional diffusion in solution (n=10) and minimal for SecYEG-trapped form (n=77). Membrane-bound proOmpA-DhfR is characterized by the marginal lateral mobility (n=12). Average values for diffusion coefficients are shown; error bars present SEM values. (C) $SecY_{C295}EG$-trapped $proOmpA_{C282}$-DhfR demonstrates the same diffusional mobility as the translocon. The ratio of their diffusion times was calculated for individual GUVs (n=77) based on the FCS-FRET assay. The solid line presents fit with the normal distribution.*

Diffusional mobility of SecYEG and the preprotein

Remarkably, we observed a decrease in the SecYEG mobility in the membrane upon the formation of a proOmpA-DhfR translocation intermediate with a reduction in the SecYEG diffusion coefficient from $(2.6\pm0.6)*10^{-8}$ cm²/s to $(2.1\pm0.7)*10^{-8}$ cm²/s (Fig. 4A). A similar decrease in the mobility was observed if only SecA was added to GUVs. Solely the binding of the large extramembrane protein SecA may affect the mobility of the protein embedded into the highly viscous membrane ($\mu_{membrane} \sim 100*\mu_{water}$). However, the observed change may also occur due to increased molecular crowding and local distortion of the lipid environment upon SecA binding, a SecYEG conformational change [29] or the hypothetical SecYEG oligomerization. We also characterized the mobility of the preprotein $proOmpA_{C282}$-DhfR-Atto 647N depending on its localization, i.e. in solution, membrane-bound, and in the translocation intermediate state (Fig. 4B). The first two states were studied using the direct excitation with the He-Ne laser (633 nm), whereas the third state was analyzed using FRET-FCS measurements, when exciting the $SecY_{C295}EG$-conjugated AlexaFluor 488

donor fluorophore with the Argon-ion laser (488 nm). SecB-bound proOmpA-DhfR in solution showed the highest mobility (D = (51±19)*10^{-8} cm^2/s). Using the Einstein-Stokes equation, this diffusion coefficient could be assigned to a particle of ~4 nm radius. The size estimation agrees well with the dimensions of the SecB tetramer of 3 nm [228] extended by the preprotein coiled around, and it is further supported by the recent EM imaging of SecB:OmpA complex [229]. ProOmpA-DhfR localized at the membrane surface of the GUVs in absence of SecA showed a three-fold lower diffusion coefficient (16±6)*10^{-8} cm^2/s that is similar to the lipid mobility within the bilayer [183]. This implied that most preprotein molecules were bound non-specifically to the lipid bilayer. Even lower diffusion coefficient, (2.1±0.8)*10^{-8} cm^2/s, was measured for the SecYEG-trapped preprotein. Here, the preprotein molecule should remain fluorescent over the time the stable complex was diffusing through the excitation volume of the Argon-ion laser. Indeed, the ratio of the corresponding diffusion times of SecY and proOmpA-DhfR was 0.99 (n = 77, Fig. 4C) supporting the notion that they co-diffused.

Probing the oligomeric state of SecYEG in the membrane

The diffusion characteristics determined by FCS provide a measure for the size of the target molecules, since the diffusion coefficient in solution scales inversely with the molecular radius, as described by the Einstein-Stokes relation. In contrast, diffusion of particles embedded in highly viscous lipid membranes is strongly affected by interactions with the membrane environment, while the dependence on the particle dimensions is logarithmical, i.e. rather weak, according to the Saafmann-Delbrück theory [224]. Thus, using the FCS approach alone would not allow unambiguous discriminating between monomeric and dimeric species of SecYEG in the ensemble. As a control, we prepared a $SecY_{C50}E_{C106}G$ dimer, where $SecE_{C106}$ subunits were cross-linked in presence of copper phenantroline [230], and the $SecY_{C50}$ subunits were labeled with AlexaFluor 488. The diffusion coefficient of this covalently stabilized dimeric SecYEG was (2.4 ± 0.4)*10^{-8} cm^2/s, so the mobility decreased only by 10% as compared to the non-crosslinked SecYEG complex. The confocal microscope can be used for fluorescence cross-correlation spectroscopy (FCCS) measurements when extended with a second, spectrally separated laser beam (Fig. 2A) that is aligned with the 488 nm laser to a high degree of spatial overlap [166,231]. Fluorescence fluctuations of differently labeled diffusing species are monitored and cross-correlated over the measurement time to detect molecular binding/dissociation processes. This method has been recently applied to study interactions on the membrane interface and within the membrane [231,232]. Here, we employed the approach to probe the SecYEG oligomeric state. We tested the sensitivity of the FCCS set-up by monitoring the lateral diffusion of the variants, $SecY_{C148C313}EG$ and the disulfide-bonded covalent dimer $SecY_{C50}E_{C106}G$, which bear both the AlexaFluor 488 and Atto 647N fluorophores. In these cases substantial cross-correlation signal was measured, up to 50% of the auto-correlation amplitude of Atto 647N-labeled species (Fig. S5). Also a

non-zero cross-correlation signal was measured for SecYEG:proOmpA-DhfR complexes in which the $SecY_{C295}EG$ and $proOmpA_{C282}$-DhfR units were labeled, as described above (Fig. S5).

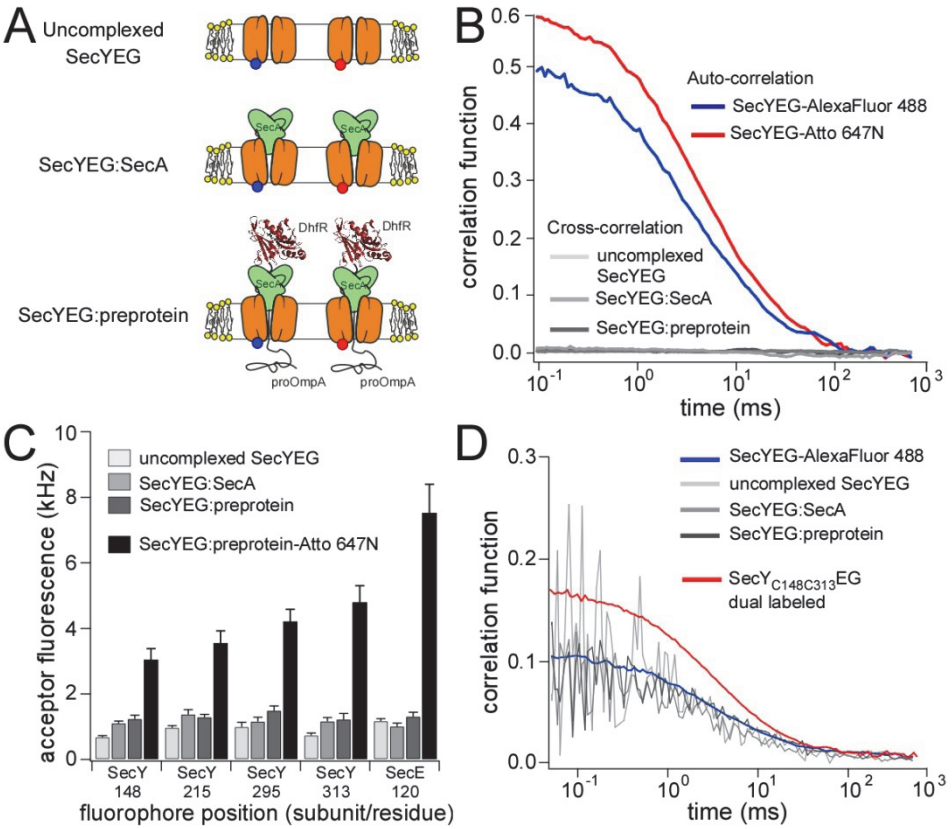

Figure 5. Probing the oligomeric state of SecYEG. *(A) Schematic representation of the studied translocon states. Differently labeled $SecY_{C295}EG$ complexes were co-reconstituted into GUV membranes and SecYEG oligomerization was probed under described conditions. (B) FCS/FCCS analysis of $SecY_{C295}EG$ diffusion. Auto-correlation curves revealed the diffusion of differently labeled $SecY_{C295}EG$ species, while cross-correlation curves reflected presence/absence of dual-labeled complexes. At various functional states of SecYEG no cross-correlation signal was detected suggesting that no dual-labeled SecYEG complexes were formed and no oligomerization occurred. (C) Studying the oligomeric state of SecYEG by FRET. No FRET was detected between SecYEG protomers at different functional states, as the average fluorescence intensity remained at the background level. FRET between AlexaFluor 488-conjugated SecYEG variants and the preprotein $proOmpA_{C282}$-DhfR-Atto 647N confirms the SecYEG functionality. Error bars present SEM values. (D) FRET-FCS analysis of SecYEG oligomerization. If only $SecY_{C295}EG$-AlexaFluor 488 was excited, its fluorescence fluctuations resulted in a characteristic auto-correlation trace, while recordings on the acceptor, $SecY_{C295}EG$-Atto 647N, were dominated by the cross-talk at all studied conditions. $SecY_{C148C313}EG$ conjugated with both AlexaFluor 488 and Atto 647N was used as a reference control, and the corresponding FRET-FCS recording resulted in a sigmoid auto-correlation trace in the acceptor channel.*

We co-reconstituted the $SecY_{C295}EG$ complexes individually labeled with AlexaFluor 488 and Atto 647N fluorophores into GUVs (Fig. 5A), and recorded both the auto- and cross-correlation spectra. SecYEG alone did not show a substantial cross-correlation signal (<5% of the auto-correlation amplitude) suggesting that only monomeric SecYEG complexes were present in the membrane (Fig. 5B). Even though the dynamic equilibrium between SecYEG monomers and dimers has been described earlier [19,20], the low protein concentration in GUVs may favor the monomeric form for the resting SecYEG complexes. Stable association of SecYEG with SecA was triggered by saturating SecA with the non-hydrolysable nucleotide AMP-PNP (5 mM) [4]. Under these conditions also no increase in the SecYEG FCCS signal was detected, supporting previous observations that SecA can interact with the monomeric SecYEG [216]. When proOmpA-DhfR was added and translocation was initiated at 37 °C in presence of ATP, again no change in cross-correlation signal was observed. Since almost all correctly oriented SecYEG was involved in translocation as shown above, the lack of a cross-correlation signal suggests that the translocon is formed by a single SecYEG copy.

To verify these FCCS results, we designed an additional FRET-based experiment to probe the oligomeric state of SecYEG. If differently labeled SecYEG complexes formed oligomers, it would result in a substantial FRET between fluorophores. The FRET efficiency depends strongly on the distance between donor and acceptor fluorophores and reduces dramatically at separations above 5-6 nm. Since the lateral dimensions of a single SecYEG complex are ~4 nm [29], and several models of the dimer organization exist [9,17], we had to ensure that the fluorophores would come in proximity upon putative oligomerization. Several variants of SecYEG were designed bearing single cysteine residues at different locations along the periplasmic side of the channel (Fig. S6). Dual-labeled $SecY_{C148C313}EG$ molecules were used to control the method sensitivity. Within the SecYEG structure conjugated AlexaFluor 488 and Atto 647 were positioned within 3.6 nm (Fig. S6) and resulted in an intensive FRET-FCS signal (Fig. 5B). The acceptor fluorescence intensity measured on GUV membranes was 9.4 ± 0.6 kHz (average ± SEM, n=7).

Designed SecYEG variant were fully functional as measured in the bulk translocation assays [149] (Fig. S1). The AlexaFluor 488-conjugated forms were effective in the formation of a $proOmpA_{C282}$-DhfR intermediate as monitored via FRET in GUVs at low protein-to-lipid ratios (Fig. 5C). Efficient FRET between SecYEG- and the preprotein-bound fluorophores was observed if the donor fluorophore was placed on the $SecE_{C120}$ subunit suggesting that SecYEG subunits remain assembled during the translocation cycle. For each SecYEG variant we prepared GUVs bearing both SecYEG complexes labeled with AlexaFluor 488 and Atto 647N and studied their interactions at the listed conditions (Fig. 5A, C). No FRET signal was detected either upon SecA binding or the translocation reaction, as the fluorescence intensity remained at the background level and the FCS recordings

were dominated by the crosstalk (Fig. 5C, D). Taken together the data strongly suggest that SecYEG actively engaged in translocation is monomeric.

Discussion

The organization of membrane proteins in biological membranes remains an intriguing question in modern cell biology. As an example, the oligomeric state of the translocation pore SecYEG has remained in the focus of intensive debates for two decades [233]. Evidence has been provided for the presence of dimers and higher oligomers of SecYEG in cellular and model membranes but their biological role has remained elusive. Conflicting results from different studies could be reconciled by the dynamic nature of the translocon [14,20], but they also suggest that the experimental outcome may be determined by the conditions employed. In the experiments presented here, we developed an *in vitro* approach to study protein translocation by the bacterial Sec translocon down to single-molecule resolution using fluorescence microscopy. It allowed not only for the detailed and quantitative description of the reaction, but also provided new insights on the oligomeric state of the active SecYEG complex. Only a minor modification of SecYEG was needed to make it amendable for single-molecule fluorescence detection. Neither the introduced cysteine mutations in periplasmic loops, nor the conjugated fluorophores at those positions affected the SecYEG activity. SecYEG complexes were embedded into GUVs at natively low SecYEG-to-lipid ratios [226] and the membrane environment was thoroughly adjusted to contain all components essential for the SecYEG activity. In particular, GUVs contained a substantial amount of cardiolipin that has recently been implicated in SecYEG dimer formation [221]. Importantly, all measurements have been performed on functional SecYEG complexes in the membrane environment and did not require additional sample treatment, such as detergent solubilization or staining, thus avoiding possible artifacts. For the first time, the dynamics of individual components of the reaction (preprotein, SecYEG subunits) could be studied at various stages of the functional cycle. As expected, a reduced mobility of the proOmpA-DhfR preprotein was observed upon its binding to the membrane surface and when it was trapped within the SecYEG channel. While a previous study on SecYEG reconstituted in nano-discs was limited to a demonstration of the interaction of SecYEG with the SecA motor protein [216], our approach allowed monitoring the preprotein translocation reaction for the SecYEG complex. Quantitative analysis of SecYEG:proOmpA-DhfR interactions suggested that the majority of SecYEG was actively involved in translocation. Under none of the experimental condition employed we detected oligomers of SecYEG, while using two different fluorescence-based studies based on either FCCS or FRET approaches.

As a conventional method for studying macromolecular interactions, bulk FRET measurements have been employed previously to probe SecYEG oligomerization. Two different studies were performed on SecYEG complexes labeled at nearby positions either at SecY or SecE subunits and reconstituted into lipid vesicles at protein-to-lipid

ratio of at least 1:5,000 [201] [20]. Though the presence of SecYEG oligomers was reported in both cases, some results remained difficult to interpret. No SecYEG complex dynamics was revealed in FRET experiments in bulk: Thus, either no subunit exchange between SecYEG oligomers was observed [201], or the SecYEG complex remained static upon the functional cycle, in contrast to what was suggested from electron microscopy experiments [20]. Limited protein aggregation upon the reconstitution procedure, which is difficult to assess in bulk assays, might at least partially account for those results. To validate a positive FRET signal, one may test its dependence on the fluorophore positions on SecYEG, expecting that the FRET efficiency is dependent on the oligomer architecture.

Our data strongly suggest that a single copy of SecYEG is sufficient to conduct the translocation reaction. These results argue against a recent model on how the translocon may function that includes two copies of SecYEG arranged in a "back-to-back" orientation [30]. SecYEG dimers were reported as minimal functional units based on studies employing genetically engineered SecY-SecY fusion proteins [26]. This artificial dimer was designed to compensate a point mutation at residue 357 of the SecY subunit that normally renders SecYEG non-functional. When introduced into only one of the two copies of the fused dimer, the point mutation did not inactivate SecYEG, presumably leaving one channel active in translocation. However, since the mutation does not exhibit any dominant negative effects on the neighboring SecYEG channel in this artificial dimer, it rather appears that each channel functions on its own. The hypothesis that one SecYEG protomer would form a translocating pore for the preprotein, while the other would serve for SecA binding [26], predicts that there is a strong functional cooperativity in SecYEG oligomerization as each of these functions specify a critical activity of the SecYEG complex. However, such cooperativity was not observed in a recent study on the functional oligomeric state of SecYEG. Herein, the translocation efficiencies of SecYEG monomers and a covalently cross-linked $SecYE_{C106}G$ dimer were compared [30]. Though it was claimed that SecYEG dimerization is "essential" for preprotein translocation, the original data showed only a two-fold increase in the translocation efficiency for the covalently crosslinked SecYEG dimer. This is consistent with each protomer being independently functional. The relevance of these results for the functional oligomeric state remains uncertain as dimerization is induced artificially by crosslinking while the exact geometry of individual SecYEG protomers with an hypothetical oligomer is unknown. Moreover, the structure of the SecYEG:SecA complex suggests that a single SecYEG channel provides sufficient interface for docking a single SecA molecule above the translocating pore [29]. As it was noted therein, such complex contains a SecYEG monomer and is equipped with all crucial interactions previously determined by cross-linking studies [31,32]. While a single SecYEG complex may serve as a minimal translocon, different roles have been attributed to its oligomerization in bacterial membranes. The SecYEG:SecA interaction may be modulated by another copy of SecYEG present, but that effect is not essential as demonstrated in our current study.

Future research should be focused on the interaction of SecYEG with accessory proteins such as the SecDF complex and YidC that modulate the translocon activity in native cellular membranes and should examine their potential role in SecYEG oligomerization.

Methods

SecYEG purification and labeling

PCR-mediated mutagenesis was used to introduce codons for cysteine residues into the cysteine-less SecYEG gene cluster. Positions for cysteine residues were selected based on the *M. jannaschii* SecYEβ structure [11], and evenly distributed along the protein perimeter on the translocon periplasmic side (Fig. S8). SecYEG variants were cloned in the pET20 vector (Table 1), and over-expressed in *E. coli* SF100 as described elsewhere[210]. Membrane fractions were isolated and inner membrane vesicles (IMVs) were purified by sucrose gradient centrifugation followed by incubation with 0.18 M Na_2CO_3, pH 11 for 30 min on ice [210]. Harvested IMVs were solubilized with 2 % DDM for 30 min in presence of Complete protease inhibitor cocktail (Roche), incubated with Ni^+-NTA agarose beads (Qiagen) for 1 hour and extensively washed using a Bio-Spin Micro column (Bio-Rad) with the buffer solution containing 50 mM Tris-HCl pH 8, 100 mM NaCl, 0.05% DDM, 20% glycerol and 10 mM imidazole. The fluorophore-maleimide conjugation was performed at pH 7.0 to ensure specific labeling of the cysteine residues. Ni^+-NTA agarose-bound SecYEG complex was incubated with 100 μM of either AlexaFluor 488-C_5-maleimide (Invitrogen, USA) or Atto 647N-maleimide (Atto-Tec, Germany) for 2 hours at 4 °C on a rolling bank, followed by extensive washing and elution with the buffer solution containing 300 mM imidazole. For the $SecY_{C148C313}EG$ variant both fluorophores were added to achieve dual labeling. The estimated purity of SecYEG was above 90%, as judged from SDS-PAGE. The amount of free fluorophore that remained during the last washing step never exceeded 5% of the total fluorescence in the elution fraction. SecYEG and fluorophore concentrations were estimated spectrophotometrically. The extinction coefficient for SecYEG at 280 nm was calculated as 71.000 M^{-1} cm^{-1}. Extinction coefficients for fluorophores were as provided by manufacturers. For all SecYEG constructs labeling efficiencies reached up to 90%, while unspecific labeling remained below 5% for AlexaFluor 488 and below 10% for Atto 647N as tested using the cysteine-less SecYEG variant. To obtain a dimeric SecYEG complex, the $SecY_{C50}E_{C106}G$ variant was cross-linked in IMVs in presence of 1 mM Cu-phenanthroline as previously described [230]. No cross-linking occurred via SecY subunit, as tested using the $SecY_{C50}EG$ variant. Fluorescent labeling was performed as described above, either with AlexaFluor 488 alone or together with Atto 647N. Labeling efficiency for the cross-linked $SecY_{C50}E_{C106}G$ was substantially reduced, and did not exceed 70%.

The activity of the reconstituted SecYEG complexes was confirmed by *in vitro* translocation assays as described [149], using the fluorescently labeled precursor of

outer membrane protein A (proOmpA) as a substrate (0.5 μM). The reaction was carried out in presence of the chaperone SecB (4 μM) and motor protein SecA (0.5 μM). The N-terminal end of the SecY subunit contained an enterokinase cleavage site DDDDK followed by the hexa-histidine tag, so its accessibility to externally added enterokinase could be detected by SDS-PAGE as a shift in the apparent molecular mass [220]. Only SecYEG exposing the cytoplasmic domain out of proteoliposomes was subjected to the cleavage. The N-terminus of the oppositely oriented SecYEG was protected by the lumen of the liposome where it is inaccessible for the enterokinase. Fractions of cleaved/non-cleaved SecY were quantified from SDS-PAGE using AIDA software (raytest Isotopenmessgerate GmbH, Germany).

Table 1

Strain / Plasmid	Short description	Source
E. coli SF100	*F-, ΔlacX74, galE, galK, thi, rpsL, strA, ΔphoA(pvuII), ΔompT*	[234]
E. coli DH5α	*supE44, ΔlacU169 (Δ80lacZαM15) hsdR17, recA1, endA1, gyrA96 thi-1, relA1*	[235]
pEK20	Cysteine-less SecYEG	[202]
pET84	SecY(G295C)EG	[236]
pEK20-C50	SecY(A50C)EG	This study
pEK20-C148	SecY(L148C)EG	This study
pEK20-C215	SecY(L215C)EG	This study
pEK20-C313	SecY(G313C)EG	This study
pET2523	SecYE(S120C)G	[20]
pEK20-C148-C313	SecY(L148C, G313C)EG	This study
pEK20-C50-EC106	SecY(A50C)E(L106C)G	This study
pET627	SecYE(L106C)G	[230]
pET501	proOmpA(S245C;C290S;C302S)-DHFR(C334S)	[52]
pET504	proOmpA(S282C;C290S;C302S)-DhfR(C334S)	[52]
pET505	proOmpA(C302S)-DhfR(C334S)	[52]
pET507	proOmpA(S315C;C290S;C302S)-DhfR(C334S)	[52]

Preprotein preparation

ProOmpA and its derived fusion with dihydrofolate reductase (proOmpA-DhfR) were over-expressed in *E. coli* DH5α, purified from inclusion bodies, and stored in 6 M urea [210]. Mutants bearing single cysteine residues in proOmpA domain (Table 1) were fluorescently labeled with Cy3- or Atto 647N-maleimide with an efficiency of ~90%. To achieve the folded form of the DhfR domain the fusion protein was incubated in the presence of methotrexate and NADPH prior the translocation reaction [227].

Bulk FRET measurements on SecYEG:preprotein complex

Variants of proOmpA-DhfR containing single cysteine residues within proOmpA domain were labeled with Cy3-maleimide dye (donor) and whole cells over-expressing $SecY_{C295}EG$ were labeled by Cy5-maleimide (acceptor) as described elsewhere [237]. Inside-out IMVs were generated upon disrupting cells in French press, so the $SecY_{C295}EG$-conjugated Cy5 fluorophore was located in the vesicle lumen. Fluorescence measurements upon the translocation intermediate formation were performed using an Aminco Bowman spectrofluorometer. Donor fluorophore was excited at 525 nm, and FRET efficiency was measured as a change in the acceptor fluorescence at 670 nm.

Confocal microscopy

A home-built confocal microscope [183] was used for FCS/FCCS measurements. An Argon-ion laser at 488 nm was used to excite the AlexaFluor 488 fluorophores, and He-Ne laser at 633 nm - to excite Atto 647N. All measurements were carried out at room temperature. The calibration procedure was carried out as previously described [183,231]. To determine the excitation volumes for both lasers, diffusion of AlexaFluor 488 and AlexaFluor 633 was measured in solution and corresponding auto-correlation curves were fitted using diffusion coefficients of $300*10^{-8}$ and $198*10^{-8}$ cm^2/s, respectively [162,238]. Fluorescence fluctuations on GUV membranes were recorded in series, each containing 10 measurements over 8 seconds. Auto-correlation traces were built for individual measurements within a series, and non-disturbed measurements were averaged and used for further analysis. FCS data acquired on SecYEG within the GUV membranes was analyzed assuming one-component two-dimensional protein diffusion, and auto-correlation traces were fitted to equation:

$$G(t) = \frac{1}{\overline{N}}\left(1 + \frac{t}{\tau_D}\right)^{-1}$$

Eq. 1,

where $G(t)$ is the amplitude of the auto-correlation function, $\overline{N}$ – average number of fluorescent particles in the laser focus, and τ_D – diffusion time. We excluded fast intramolecular dynamics and occasional fluorophore photoconversion from analysis by limiting FCS data to the time range from 10^{-1} – 10^{3} ms. The measured number of particles and the fluorescence intensity were used to estimate the molecular brightness of fluorophores. To assess the co-diffusion of differently labeled proteins the fluorescence intensity in blue and red channels was cross-correlated [166]. The amplitude of the resulting FCCS function is proportional to the concentration of dual-labeled molecular complexes and could be used to determine the protein oligomerization level. Laser beam alignment was controlled using dual-labeled λ-DNA as a reference sample for the FCCS.

Since the detection volumes of the blue and the red channels differ due to the difraction limitation, we determined the ratio of these volumes to calculate the concentration ratios from the autocorrelation amplitudes for FRET-FCS translocation assay. Herein, we performed FCS measurements on membrane-incorporated fluorescent lipid analog 4-(4-(dihexadecylamino)styryl)-N-methylpyridinium iodide, DiA (Invitrogen, USA). Due to its spectral properties the dye could be efficiently excited at 488 nm, and its fluorescence was recorded both in the blue and red channels. The ratio of particle numbers detected in both channels ($N_{blue}/N_{red}=0.95$) was used for correcting the FRET-FCS data.

Acknowledgements

We would like to thank J.A. Lycklama á Nijeholt for helping with cloning experiments, J.G. de Wit for providing pET84 plasmid, J. de Keyzer, A. Garcia-Saez, and G. van den Bogaart for critical comments on the manuscript. This work was financially supported by the Netherlands Foundation for Scientific Research, Chemical Sciences, and NanoNed, a national nanotechnology program coordinated by the Dutch Ministry of Economic Affairs.

Author Contributions

A.K. designed and performed the experiments, analyzed the data and wrote the paper; I.K. designed and performed the experiments and wrote the paper; V.V.K. designed technical aspects of the experiments and analyzed the data; A.J.M.D. designed the experiments, supervised the work and wrote the paper.

Supplementary Information – Methods

Probing SecYEG topology in model membranes

Reconstituting SecYEG into proteoliposomes results in alternately oriented translocons [220]. SecYEG complexes that expose their cytoplasmic surfaces to the lumen of the proteoliposomes do not participate in preprotein translocation as they are unable to bind externally added SecA. To confirm the dual orientation of His_6-tagged SecYEG in the membrane we used partial proteolysis with enterokinase [220]. When the N-terminus of SecY is exposed to the external membrane face, enterokinase will remove the His_6-tag that is linked to SecY via an enterokinase cleavage site. Proteolysis was performed overnight at 25 °C and products were resolved on Coomassie-stained SDS-PAGE. On average 55% SecY in proteoliposomes was accessible for enterokinase (n=11; Fig. S7) and thus correctly oriented. Complete tag loss was observed when the proteoliposomes were destabilized by the detergent DDM. Limited unspecific proteolysis occurred in the DDM-solubilized sample causing the reduction of the total SecY concentration.

GUV formation

Synthetic phospholipids were mixed in the desired ratio in chloroform, dried under vacuum using a rotary evaporator, washed with ethanol and dried again [220]. The lipid film was rehydrated with 5 mM Tris-HCl pH 8.1, 3 mM sucrose to the final lipid concentration of 10 mg/mL, whereupon the liposomes were dispersed using an ultrasonic bath. The polar lipid extract of *E. coli* was prepared via acetone/ether wash from *E. coli* total lipid extract (Avanti Polar Lipids, USA) [210]. Purified SecYEG was reconstituted into the liposomes as described before [210]. Shortly, liposomes (5 mg/mL) were destabilized by 0.5% Triton X-100 and incubated with solubilized SecYEG. Detergent was removed overnight using Bio-Beads SM-2 adsorbents (Bio-Rad), and proteoliposomes were harvested by ultracentrifugation and resuspended in 40 mM KCl, 10 mM Tris-HCl pH 8.1, 6 mM sucrose. To form GUVs for fluorescence measurements pre-formed SecYEG proteoliposomes were deposited on a glass cover slide in a sucrose-containing buffer and desiccated under vacuum for at least 12 hrs. To protect SecYEG from denaturation during the desiccation step [183], proteoliposomes were prepared in presence of 6 mM sucrose that prevented the lipid phase transition under cryogenic and desiccating conditions [239,240]. Upon rehydration with a solution containing 10 mM Tris pH 8.1, 10 mM KCl, 0.5 mM $MgCl_2$, and 6 mM sucrose, numerous GUVs formed within 10 min. Using low salt concentration resulted in the osmotic pressure formed on GUV surfaces that maintained the shape and stability of vesicles. The GUVs were stable for at least a few hours and withstood incubation at 37°C. To study protein translocation and the SecYEG assembly GUVs were additionally incubated with other components of the reaction at 37°C for 10 min and equilibrated at room temperature prior measurements on the confocal microscope.

Supplementary Information – Figures

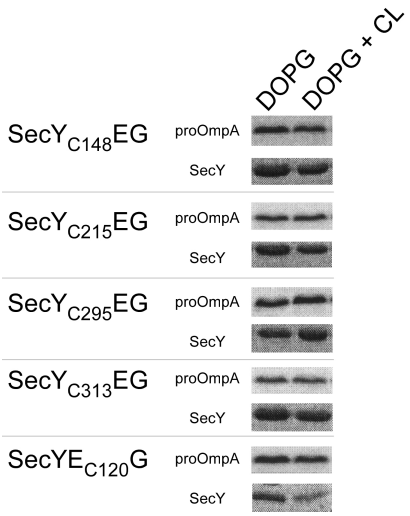

Figure S1. Cardiolipin does not affect SecYEG translocation activity. *Single-cysteine mutants of SecYEG were reconstituted into proteoliposomes containing either 30 mol % DOPG (lane DOPG), or 20 mol % DOPG and 10 mol % cardiolipin (lane DOPG + CL) as anionic lipid fraction, as well as 30 mol % DOPE and 40 mol % DOPC. The SecYEG concentration was adjusted to the same level prior to the translocation assays (lower panels). The activity was tested by measuring the translocation of proOmpA$_{C252}$-FM into proteoliposomes [149]. Inclusion of cardiolipin did not significantly affect the translocation efficiency of the SecYEG variants, as levels of translocated preprotein did not depend on change when cardiolipin was replaced by phosphatidylglycerol*

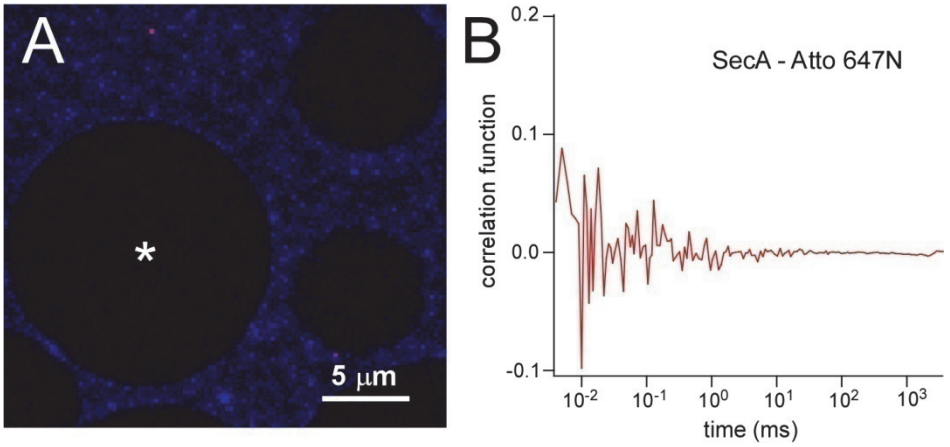

Figure S2. GUVs are non-permeable for SecA. *Fluorescently labeled SecA-Atto 647N was added to GUV-containing solution and incubated for 10 min. The confocal microscope was used for the two-dimensional scanning of the reaction volume using He-Ne laser excitation at 633 nm (A). Intensive fluorescence signal on the outside of the GUVs corresponds to SecA-Atto 647N in solution, while no fluorescence was observed within the GUV interiors (black circles). The auto-correlation curve recorded within the GUV (white asterisk) was determined by background noise (B).*

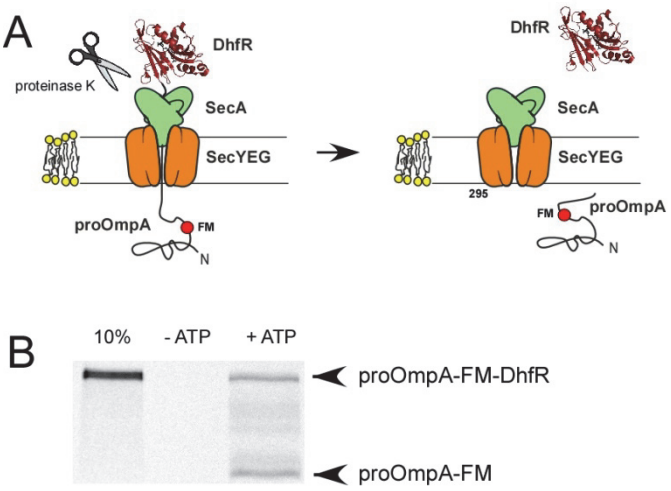

Figure S3. Formation of a proOmpA-DhfR translocation intermediate. *(A) SecYEG:proOmpA-DhfR complex can be dissociated by treatment with proteinase K. (B) ProOmpA$_{C252}$-DhfR was fluorescently labeled with fluorescein-maleimide (FM). The DhfR domain of the fusion protein was pre-folded in presence of methotrexate and NADPH [227]. The fusion protein was translocated into proteoliposomes containing SecY$_{C295}$EG at protein-to-lipid ratio 1:500. After digestion with proteinase K, a prominent band corresponding to proOmpA-FM indicates that the folded DhfR domain was cleaved off by the protease, but not translocated through SecYEG channel, so the stable intermediate was formed upon translocation.*

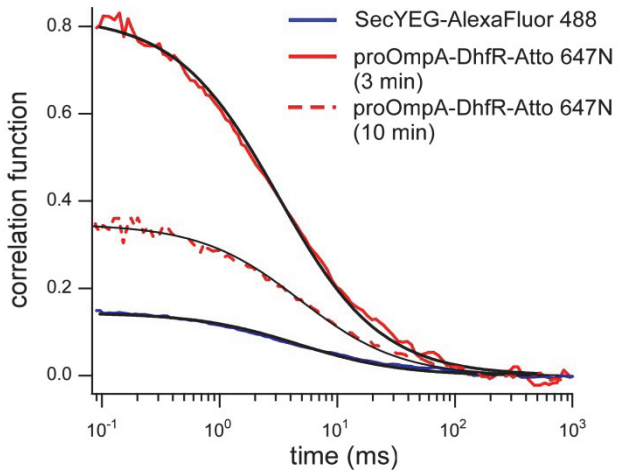

Figure S4. Formation of SecYEG:proOmpA-DhfR complex is a time-dependent process. *SecY$_{C295}$EG-AlexaFluor 488 was reconstituted into GUVs containing 10 mol % cardiolipin, 20 mol % DOPG, 30 mol % DOPE, and 40 mol % DOPC. ProOmpA$_{C252}$-DhfR-Atto 647N was used as a preprotein and trapped translocation intermediates were probed by FRET-FCS as described in main text. Reducing the time for the translocation caused increase in proOmpA-DhfR auto-correlation function amplitude, i.e. less preprotein molecules were translocated to yield a FRET signal. If the reaction was conducted for 3 min, we measured a ratio SecYEG:proOmpA-DhfR of approx. 6, so only ~30% SecYEG contained trapped preprotein. If translocation was performed for 10 min, SecYEG:proOmpA ratio was approx. 2.8. The measurements were performed on Zeiss LSM 710 equipped with the Confocor 3 module.*

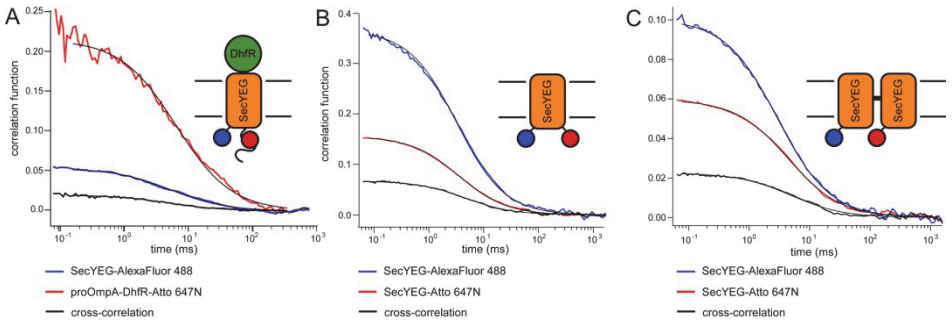

Figure S5. FCCS on SecYEG:preprotein and dual-labeled SecYEG translocons. *(A) ProOmpA$_{C282}$-DhfR-Atto 647N was trapped within SecY$_{C295}$EG translocon in GUV membranes as described in the main text. When exciting SecY$_{C295}$EG-AlexaFluor 488 with the argon-ion laser FRET between fluorophores was detected in SecYEG:preprotein complexes. Auto-correlation functions shown as blue and red lines described diffusion of SecYEG and trapped proOmpA-DhfR, respectively, within GUV membranes. The positive cross-correlation signal (black line) reflected the co-migration of translocon and preprotein molecules. (B) SecY$_{C148SC313}$EG was dual labeled with AlexaFluor 488 and Atto 647N fluorophores and reconstituted into GUV membranes. Both argon-ion and He-Ne lasers were used to excite the conjugated fluorophores. Diffusion of SecY$_{C148SC313}$EG in membranes was monitored by FCS/FCCS. The cross-correlation signal reached up to 50% relatively to the SecYEG-Atto 647N auto-correlation function. (C) To investigate the diffusion properties of covalently stabilized dimeric SecYEG complex the variant SecY$_{C50}$E$_{C106}$G was cross-linked by Cu-phenanthroline to yield a dimeric SecY$_{C50}$E$_{C106}$G disulfide bonded at SecE$_{C106}$ in the "back-to-back" position. The complex was fluorescently labeled at the SecY$_{C50}$ position with AlexaFluor 488 and Atto 647N. The diffusion coefficient was determined as described in the main text. Substantial cross-correlation signal was measured for the dual-labeled artificial SecYEG dimer, though its amplitude was limited by relatively low labeling efficiency for the cross-linked protein (below 70%). The measurements on dual-labeled SecYEG were performed on Zeiss LSM 710 equipped with the Confocor 3 module.*

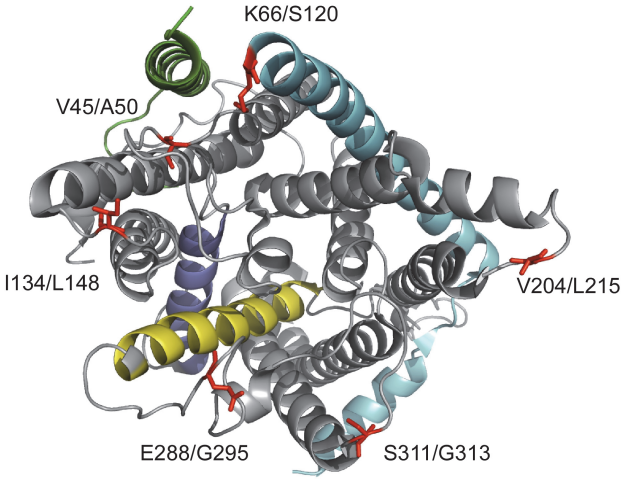

Figure S6. Single cysteine and corresponding fluorophore positions introduced into the SecYEG translocon. *The atomic structure of SecYEβ homologue of M. jannaschii [11] was used to design single- and double-cysteine substitutions into the E. coli SecYEG complex. Positions on the periplasmic membrane face are shown in red, and numbered according to the SecYEβ/SecYEG subunits. The SecY subunit is colored grey, with the lateral gate formed by transmembrane segments 2 (purple) and 7 (yellow). SecE is shown in cyan, and Secβ (SecG) in green.*

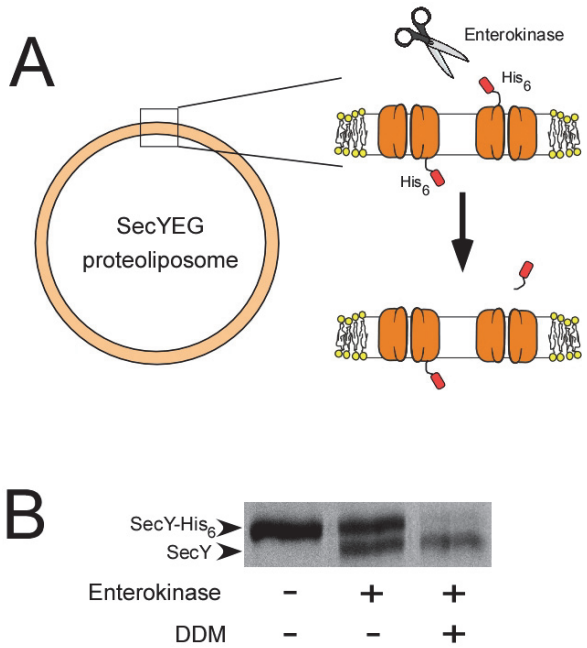

Figure S7. Orientation of membrane-reconstituted SecYEG. *(A) SecYEG topology in liposomes determines its accessibility for the enterokinase protease. (B) Limited cleavage of His_6-tagged SecYEG by enterokinase confirms the dual topology of the SecYEG complex in the membrane. Proteolysis was performed overnight at 25 °C and products were resolved on Coomassie-stained SDS-PAGE. On average 55% SecYEG were correctly oriented, exposing their C-terminal facing the outside of the proteoliposomes thereby being available for cleavage by enterokinase. In the presence of 1% DDM, the liposomes were solubilized and the complete tag degradation occurred confirming the protease functionality.*

CHAPTER 6

TAMING MEMBRANES: FUNCTIONAL IMMOBILIZATION OF BIOLOGICAL MEMBRANES IN HYDROGELS

Ilja Kusters, Nobina Mukherjee, Menno R. de Jong, Sander Tans, Armagan Koçer and Arnold J.M. Driessen

In press in PLOS one

Abstract

Single molecule studies on membrane proteins embedded in their native environment are hampered by the intrinsic difficulty of immobilizing elastic and sensitive biological membranes without interfering with protein activity. Here, we present hydrogels composed of nano-scaled fibers as a generally applicable tool to immobilize biological membrane vesicles of various size and lipid composition. Importantly, membrane proteins immobilized in the hydrogel as well as soluble proteins are fully active. The triggered opening of the mechanosensitive channel of large conductance (MscL) reconstituted in giant unilamellar vesicles (GUVs) was followed in time on single GUVs. Thus, kinetic studies of vectorial transport processes across biological membranes can be assessed on single, hydrogel immobilized, GUVs. Furthermore, protein translocation activity by the membrane embedded protein conducting channel of bacteria, SecYEG, in association with the soluble motor protein SecA was quantitatively assessed in bulk and at the single vesicle level in the hydrogel. This technique provides a new way to investigate membrane proteins in their native environment at the single molecule level by means of fluorescence microscopy.

Introduction

Biological membranes are ubiquitous in all living cells and harbor a unique set of proteins, the membrane proteins. These play a crucial role in critical cellular and physiological processes such as nutrient transport, signaling, and energy-transduction. About 60 % of the human druggable targets are membrane proteins [241]. Despite their importance, the knowledge of the function of membrane proteins lags far behind that of water-soluble proteins. This is due to the fragility of the lipid membrane rendering investigations of membrane proteins in their native environment challenging. At the same time, the high hydrophobicity and tendency to precipitate when extracted from the membrane environment make membrane proteins intrinsically difficult to analyze and handle. A true understanding of membrane protein functioning requires both ensemble and single molecule techniques such as fluorescence spectroscopy [242]. Single-molecule fluorescent spectroscopy methods are non-invasive tools that can be used to investigate protein functioning without the averaging of temporal or population heterogeneity from bulk experiments [243]. Hence, detailed kinetic information, intermediates and rate limiting steps of protein performance can be acquired [244]. For time resolved fluorescence spectroscopy, however, the membrane proteins need to remain in the observation area of a microscope, thus requiring immobilization of membrane protein or entire membranes. Immobilization of biological membranes without affecting the functionality of embedded membrane proteins has been a major challenge up to date due to the fragility of the lipid bilayer. Therefore, new immobilization techniques for the detailed investigation of membrane protein functioning at the single molecule level are crucial.

Surface supported planar lipid-bilayers have been developed to mimic cell membranes and accommodate membrane proteins. They allow the lateral mobility of lipids by a thin layer of water (1-2 nm) between the surface and the lipid bilayer [245]. However, this layer is insufficient to accommodate large soluble loops of membrane proteins and contact with the surface might lead to immobilization and/or even inactivation of the protein. To minimize the interaction with the supporting material, polymers [246] and hydrogels [247] were developed to cushion the bilayer. These polymer supported lipid bilayers improve the lateral mobility of reconstituted membrane proteins [246,248]. Unfortunately, the formation of supported lipid bilayers is limited to certain lipid compositions that promote vesicle fusion and rupture on the supporting material [249]. However, lipids determine the physical and chemical properties of the membrane and may affect membrane proteins in their mobility and function. Lipids were also shown to directly control membrane proteins through specific interactions [250]. Moreover, for this method the required surface modifications and cleaning procedures are time consuming and costly. Thus, more versatile methods are required to study membrane proteins in immobilized membranes.

Surface immobilization of small (50-200 nm) unilamellar vesicles would allow to investigate the functioning of even a single membrane protein over a desired period of time. As these small membrane vesicles appear as diffraction limited spots in a fluorescence microscope, the membrane protein(s) are retained in the observation area albeit diffusing laterally in the lipid bilayer of the vesicles. Possibly due to incompatibility of membranes and embedded membrane proteins with the surfaces, which may result from multiple interactions, these studies are extremely rare. Recently, proteoliposomes (PLs) containing SecYEG channels were immobilized on a surface supported lipid bilayer [251]. However, the activity of the membrane channel was not definitely proven and the method was poorly documented.

Another approach to do single molecule studies on membrane proteins is by generating giant unilamellar vesicles (GUVs) with embedded membrane protein of interest and keeping them in the observation area for a desired period of time. (for review see [252]). Due to their big size (1-15 μm) GUVs have a low curvature and their membrane surface appears practically planar in the observation area of a confocal microscope. Thus, they offer a valuable tool to study the diffusion and oligomeric state of membrane proteins by fluorescence cross-correlation spectroscopy (FCCS). In addition, transport processes across the membranes of these giant vesicles can be investigated by high-resolution fluorescence imaging. However the same property, the size, makes the surface immobilization of GUVs very challenging as they have more available area that can interact with the surface. In most cases direct attachment of GUVs into a surface via surface modifications results in rupture and collapse of the GUV [253]. Besides, their size makes them more fragile to mechanical disturbances in the environment.

An ideal environment for the study of membrane proteins should therefore support a variety of biological membranes without inhibiting the functioning of the membrane-embedded proteins and at the same time should allow single molecule fluorescence measurements by keeping them in the observation area for a desired period of time. The immobilizing material should minimize interactions with the membrane surface and allow the embedded proteins to diffuse freely. As many membrane proteins interact with ligands or substrates, molecules of a wide sizes range should diffuse freely and access the entire membrane surface. At the same time, membrane vesicles of various sizes ranging from small (50-200 nm) up to several micron sized GUVs should be stably immobilized while maintaining their membrane integrity.

In this study we present, for the first time, hydrogels composed of organic gelators for the functional immobilization of membrane proteins both in their native lipid environment and in synthetic lipid environments (PLs, GUVs). Hydrogels composed of self-assembling units of low-molecular-weight gelators based on 1,3,5-cyclohexyltricarboxamide form networks of nano-scaled fibers that are an attractive way to immobilize membrane vesicles [254]. The di-ethylene glycol functionalization of the gelator creates a low interacting fiber surface that minimizes surface

interactions with biological molecules (Figure 1). Moreover, as fiber-fiber interactions are weak, the local mesh size of the gel is adjusted by the vesicles, allowing them to form their own cavity. Importantly, the vesicles are completely surrounded by an aqueous environment and the self-adapting mesh size of the gel allows the free diffusion of macromolecules such as proteins, yet restricts the movement of the membrane vesicle. The fibers of hydrogelators from the same family of gelators were previously shown to immobilize bilayer liposomes composed of zwitterionic synthetic lipids without interacting at the molecular level [254]. Here, we demonstrate that hydrogels based on 1,3,5-cyclohexyltricarboxamide effectively immobilize inverted membrane vesicles (IMVs) from *E. coli*, proteoliposomes (PLs) from native *E. coli* lipids and even several micron sized GUVs composed of a synthetic lipid mixture. The integrity of the lipid bilayer of the different vesicles remains intact during the immobilization procedure. Importantly, the embedded membrane proteins MscL, the mechanosensitive channel of large conductance of *E. coli*, and SecYEG, the protein-conducting channel of bacteria, are fully active. Since these hydrogels are optically transparent, they allow for fluorescent investigations of the activity of the membrane proteins and processes at the membrane interface down to the single molecule level.

Results

The membrane integrity of hydrogel immobilized (proteo-) liposomes is maintained

Hydrogelator molecules based on 1,3,5-cyclohexyltricarboxamide self-assemble into nano-scaled fibers that form a three dimensional interpenetrating network with defined mesh size [254]. Here, we obtained hydrogels (Figure 1A) by cooling a hot solution (130 °C) of 1.3 % gelator 1 in buffer to room temperature. For visualization, liposomes of *E. coli* lipids supplemented with the fluorescent lipid analog DiD were filled with the water-soluble fluorophore Alexa Fluor 488 (AF488) attached to the tripeptide glutathione. Liposomes and proteoliposomes as prepared in this study typically have an average size of around 100 nm as observed by dynamic light scattering and NanoSight particle tracking (data not shown). Immobilization of the filled liposomes was achieved by short vortexing (vigorous shaking) of the liposome suspension in a 1:1 ratio with the preformed gel. Subsequently, the gel was applied onto a microscopic cover slip followed by a resting phase in which the gel "heals", i.e. crosslinks between fibers are re-formed leading to a network with incorporated liposomes.The immobilized liposomes were imaged in the gel using a dual color laser scanning confocal microscope In contrast to the PLs in suspension (Figure 2 C and D) which moved while taking the image, the location of the PLs in the hydrogel was entirely stable within the confocal plane (Figure 2 A and B). Moreover, the fluorescent signals of the two fluorophores DiD and AF488 co-localize and the level of liposome encapsulated AF488 was similar to that of liposomes prior immobilization (Figure S1). The latter was determined by dual-color fluorescent-burst analysis (DCFBA, for

review see [148]), a technique that enables the quantification of co-localizing fluorescent signals and the calculation of relative fluorescence ratios.

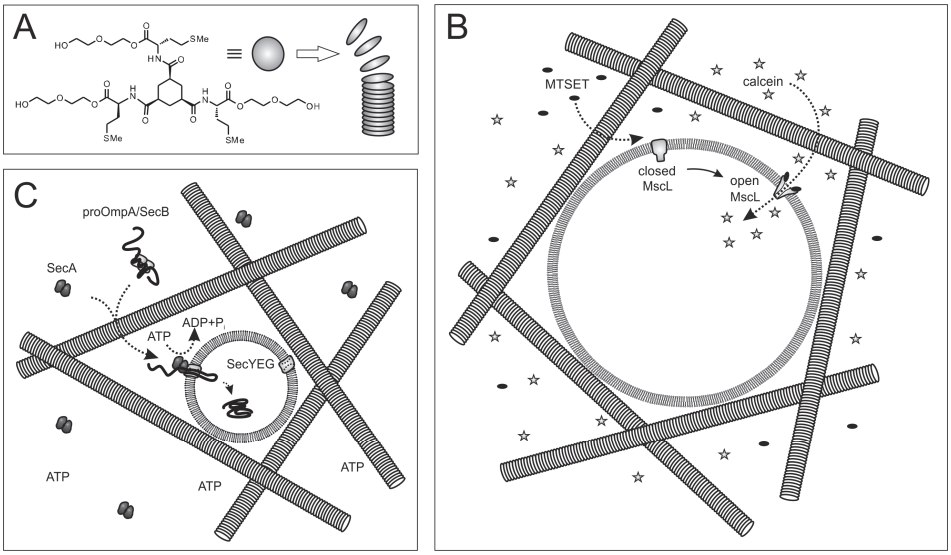

Figure 1: *Hydrogels composed of self-assembling organic gelators immobilize membrane vesicles. (A) Gelator molecule 1 is based on 1,3,5-cyclohexyltricarboxamide and self-assembles into fibers of 20-100nm [254]. (B) Schematic representation of a hydrogel immobilized GUV with embedded MscL channel. The lipid bilayer is impermeable for the soluble fluorophore calcein when MscL occupies the closed conformation. Addition of MTSET triggers the opening of genetically engineered MscL and allows influx of calcein into the lumen of the GUV. (C) In vitro protein translocation into hydrogel immobilized PLs. SecA translocates the fluorescently labeled preprotein proOmpA through the SecYEG channel by multiple cycles of ATP hydrolysis. Inside the PL, proOmpA is protected against an externally added protease. Molecules in (B) and (C) are not drawn in scale.*

Using DCFBA, the fluorescent intensities of encapsulated AF488 and DiD of individual liposomes were determined and the ratio of AF488/DiD was calculated for both liposomes diffusing in solution and immobilized in the hydrogel (Figure S1). The average ratio AF488/DiD is an arbitrary unit for the amount of encapsulated dye per liposome and was found to be similar for both conditions (Figure S1). Thus, no significant leakage of AF488 occurred during immobilization in the hydrogel.

Opening of the mechanosensitive channel of large conductance (MscL) can be observed on a single GUV

To investigate the suitability of the hydrogel for immobilization of very large and fragile membrane systems, we prepared several micron sized GUVs and tested them for membrane integrity and membrane protein activity in the gel. The performance of a hydrogel as described in the previous section was tested for GUV immobilization and monitoring of membrane protein activity. The mechanosensitive channel of large

conductance, MscL, from *E. coli* was reconstituted into liposomes and the resulting PLs were used to generate DiD labeled GUVs [255]. MscL is a bacterial membrane channel protein that senses the increase in the lateral pressure in the membrane due to a hypo-osmotic shock. It functions as a safety valve to release the turgor pressure by opening a large, non-selective pore and releasing molecules and even peptides up to 6.5 kDa [162,193].

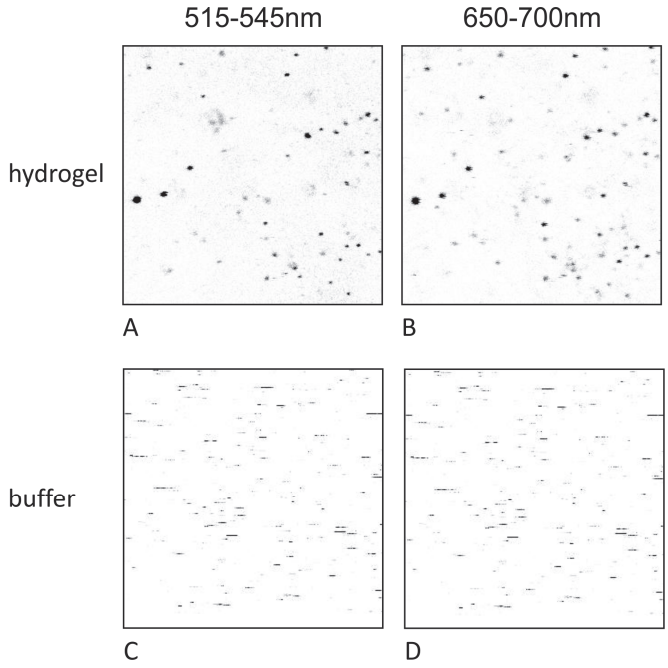

Figure 2: *Liposomes containing fluorescent lipid analog DiD (maximum emission at 670 nm) filled with Alexa Fluor 488 (maximum emission at 517 nm) labeled glutathione, A+B hydrogel immobilized, C+D liposomes in suspension prior immobilization. Images were taken in a Dual-color laser-scanning confocal microscope by scanning an area of 30 x 30 μM in gel or solution.*

Here we used an engineered version of this channel, MscLG22C [256,257]. MscLG22C can be activated by labeling the cysteine at position22 with the charged molecule [2-(trimethylammonium)ethyl]methane thiosulfonate bromide (MTSET). This covalent modification results in the opening and closing of the channel in the absence of its native trigger, i.e. membrane tension [194]. The performance of MscL, embedded in hydrogel immobilized GUVs, was tested by following the triggered influx of a fluorescent dye (calcein) into GUVs through MscL using confocal microscopy. For incorporation of GUVs into the gel, we took advantage of the inherent reversibility of the physical crosslinks that hold the gel together. By vigorous shaking on a vortex mixer, crosslinks between and within fibers are broken, resulting in a viscous suspension. Due to their fragile nature, DiD labeled GUVs containing MscL were embedded in a hydrogel of gelator 1 by first liquefying the preformed hydrogel by vigorous shaking it for 1 min and mixing the hydrogel afterwards with

0.5 volume of GUVs using a pipette..The gel-GUV mixture was applied on a cover slip and incubated for about 10 minutes to ensure gel healing. During this time period, new crosslinks between the fibers are formed and short fibers can assemble and form longer fibers. The DiD stained membrane of an approximately 10 μm sized MscL-GUV was imaged by a two-dimensional scan using a dual laser confocal microscope (Figure 3A, lower panel). Calcein, added to the hydrogel prior to imaging without disturbing the setup, is surrounding the GUVs (Figure 3A, upper panel, first picture). Since MscL was not activated at this point, it stayed closed and calcein could not penetrate into the GUV demonstrating the membrane integrity. Upon the addition of the membrane-impermeable channel activator, MTSET, the channel opened and the gradual time dependent filling up of the GUV was observed (Figure 3A-C). The concentration of calcein inside and outside of the GUV was quantified by a one dimensional cross-section through the center of the GUV at the different time points illustrating MscL channel opening (Figure 3B). Time dependent influx of calcein into the GUV was quantified measuring the calcein fluorescence at the center of the GUV resulting in a kinetic saturating curve (Figure 3C). Equilibration of the calcein concentrations inside and outside of the GUV was reached at around 180 s (Figure 3C), in accordance with the results obtained with PLs in solution (data not shown). Upon addition of buffer containing MTSET, a slight shift in the focal plane was observed resulting from a minor movement of the gel such that a smaller cross-section of the GUV was imaged. As a control, buffer without MTSET was added to MscL GUVs in another gel (Figure S2). No influx of calcein into the GUV could be observed (Figure 3C and S2B) demonstrating the stability of the GUV and the closed state of the MscL channel. Taken together, this data demonstrates that MscL, a mechanosensitive membrane protein, in GUVs is not affected by the hydrogel, which allows single molecule measurements. Moreover, different ways of vesicle immobilization are possible and ensure membrane integrity even of fragile, micron sized vesicles.

The hydrogel does not affect protein-protein interactions

Next, the compatibility of the hydrogel with fluorescently labeled proteins was tested. Here, we focus on the protein translocation system of *E. coli*. This system consists of a multi-protein complex termed 'translocase' that includes a protein conducting channel, SecYEG, embedded in the cytoplasmic membrane and a motor protein, SecA (for review see [60]). Secretory proteins (preproteins) are translocated through the translocase by SecA through multiple cycles of ATP hydrolysis (Figure 1C) [4-6]. Protein translocation of fluorescently labeled preproteins into SecYEG containing IMVs or PLs can be followed in bulk by protease protection [211] and by the formation of a translocation intermediate that can be monitored by FRET between a donor-fluorophore on the trapped preprotein and an acceptor fluorophore attached to the exit of the SecYEG pore (A. Kedrov et al., submitted). Here, using the procedure described above, we mixed proteins and PLs into hydrogels containing 0.65 % gelator 1. While GFP was found freely diffusing in the gel as determined by fluorescence cross

correlation spectroscopy (FCS, data not shown), the very hydrophobic and partially unfolded model preprotein proOmpA labeled with Atto647N bound non-specifically to the gel fibers (Figure 4B).

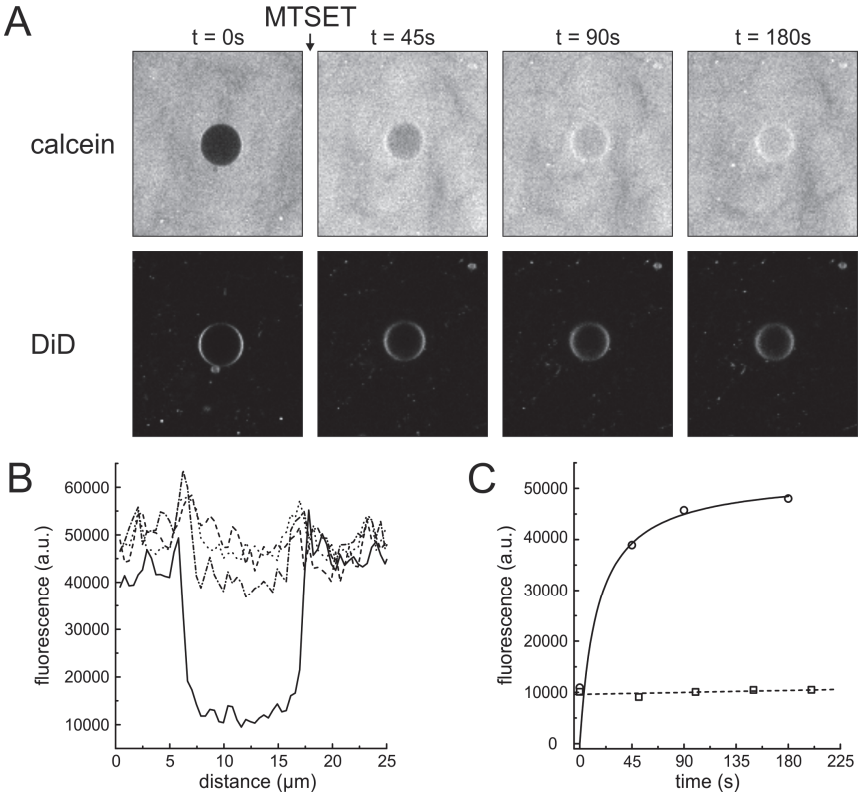

Figure 3: *Opening of the MscL channel monitored on a single hydrogel immobilized GUV supplemented with the fluorescent lipid analog DiD. (A) Addition of MTSET to the top of the hydrogel causes opening of the membrane embedded MscL channel whereupon the soluble fluorophore calcein diffuses into the lumen of the GUV. (B) Calcein fluorescence inside and outside of the GUV quantified by cross-sections through the center of the GUV depicted in (A) at the different time points; t = 0s (straight line), 45s (dash-dot), 90s (dot), 180s (dash). (C) Calcein fluorescence at the center of the GUV (A) at the indicated time points (straight line). Background fluorescence inside a GUV (as shown in Fig S5) did not change upon addition of buffer (dashed line).*

Furthermore, a fraction of the otherwise freely diffusing fluorescein labeled SecA (SecA-FM) interacted with the fibers in absence of SecYEG containing PLs (Figure 4A). However, the non-specific binding of SecA-FM was virtually absent in the presence of immobilized proteoliposomes containing SecYEG-Atto647N that bound SecA-FM specifically (compare Figure 4C and D). This is likely due to the lower concentration of soluble SecA as a large fraction of SecA is bound to the SecYEG-PLs suggesting that the non-specific interaction is dependent on the SecA concentration.

Altogether, this data demonstrates that interaction of a membrane receptor (SecYEG) with its ligand (SecA) can be studied on single liposome level using hydrogel immobilized PLs or IMVs.

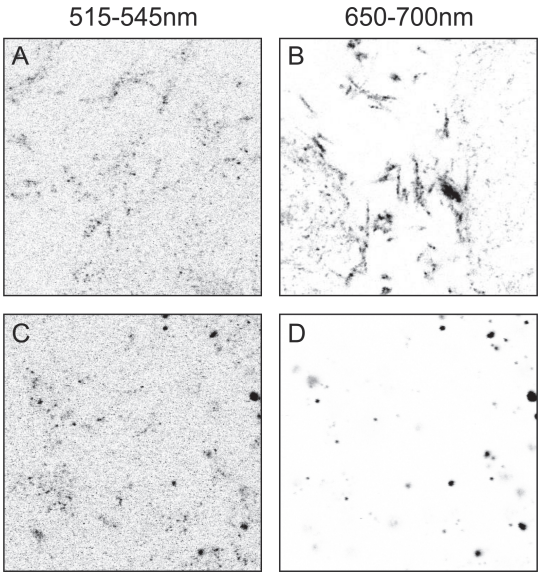

Figure 4: *Protein interactions in the hydrogel. A fraction of SecA-FM (A) and proOmpA-Atto647N in complex with the chaperone SecB (B) bind non-specifically to the OG8 fibers. SecA-FM (C) binding to PLs containing SecYEG-Atto647N (D) is visible as co-localizing signal. In presence of SecYEG-PLs non-specific binding of SecA-FM to the gel fibers is eliminated (A,C).*

Hydrogel immobilized PLs and IMVs are active in protein translocation

The activity of the translocase was examined by *in vitro* translocation of proOmpA-FM into SecYEG-PLs immobilized in a hydrogel composed of 0.65 % gelator 1. ProOmpA-FM in complex with SecB, SecA, PLs and ATP were mixed simultaneously with the pre-formed hydrogel and incubated first at room temperature to heal the gel and then at 37 °C. After 15 min, proteinase K was mixed with the gel to digest non-translocated proOmpA-FM. In order to collect translocated proOmpA, proteins in the gel were precipitated by addition of TCA and analyzed on SDS-PAGE using a fluorescence imager. Significant translocation activity in the hydrogel was observed after 15 min (Figure 5A, lane 4). Translocation activity was reduced to about 30 % compared to translocation in suspension (Figure 5A, lane 2), possibly due to non-specific binding of the substrate proOmpA-Atto647N to the gel fibers (Figure 4B) preventing multiple turnovers of protein translocation. Since the healing of the gel and immobilization of the membranes is completed only after 1-2 min, *in vitro* protein translocation into fully immobilized *E. coli* IMVs was triggered by UV light induced un-caging of NPE-caged ATP (Figure 5B). Unlike the proteoliposomes, in IMVs, the membrane associated leader peptidase cleaves off the signal peptide resulting in the mature OmpA (Figure 5B). Similarly to the PLs, protein translocation activity of IMVs in the hydrogel was reduced to about 20 % compared to translocation in solution after 15 min. However, for the first time, protein translocation was observed

on immobilized vesicles in bulk. This data demonstrates that the translocon is functioning inside the gel, which is compatible with established biochemical methodologies such as TCA precipitation and SDS-gel electrophoresis.

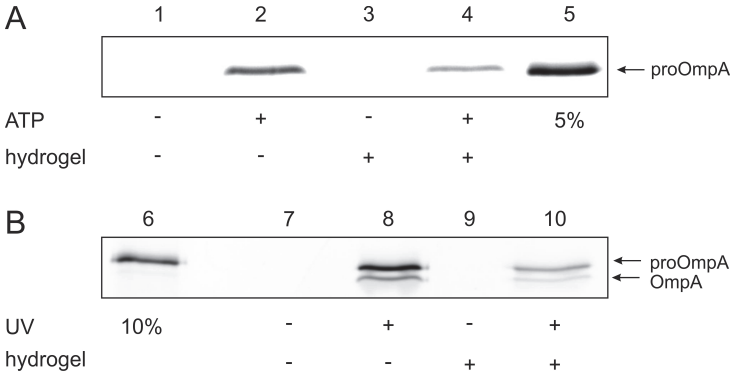

Figure 5: *In vitro protein translocation in a hydrogel composed of gelator 1 and in suspension. Upon addition of ATP, SecA mediates the translocation of proOmpA into the PLs thereby rendering it resistant against an externally added protease (A). Translocation in the hydrogel or in suspension can be triggered by UV light when NPE-caged ATP is present (B). Lane 5, 6 serves as standard 5 and 10% of input material, respectively.*

Protein translocation can be monitored at the single PL level by FRET

Since the chaperone SecB keeps the model substrate proOmpA in a partially unfolded and therefore translocation competent state, substantial non specific interactions of proOmpA with membranes and other surfaces occur. This renders monitoring of protein translocation by means of proOmpA accumulation inside of small vesicles intrinsically difficult. Therefore, to quantitatively assess protein translocation activity at the single liposome level, we performed DCFBA-FRET experiments employing a dual color laser scanning confocal microscope. As proOmpA was labeled with the acceptor fluorophore Atto647N (647 nm / 669 nm, excitation/emission) non-specifically bound proOmpA was not visible when exciting the donor fluorophore with the 488 nm laser line. The ratio of donor and acceptor fluorescence intensity in a FRET experiment can be used to determine FRET efficiencies and by immobilizing PLs in the hydrogel, FRET efficiencies for individual liposomes can be obtained. Proteoliposomes containing fluorescein labeled SecYEG, SecA and the fusion protein proOmpA (C282)-DhfR-Atto647N in complex with SecB were immobilized in a hydrogel of gelator 1 as described in the previous sections (Figure 6). The DhfR domain of the proOmpA-DhfR fusion protein is tightly folded in presence of its ligands NADPH and methotraxate and translocation results in a stable translocation intermediate with the proOmpA-DhfR trapped in the SecYEG channel (Figure 6C) [52,227]. Using fluorescently labeled preprotein and SecY, formation of the translocation intermediate is expected to result in FRET between the donor

fluorophore on SecYEG and the acceptor on proOmpA(C282)-DhfR (Kedrov et al, submitted, Figure 6C).

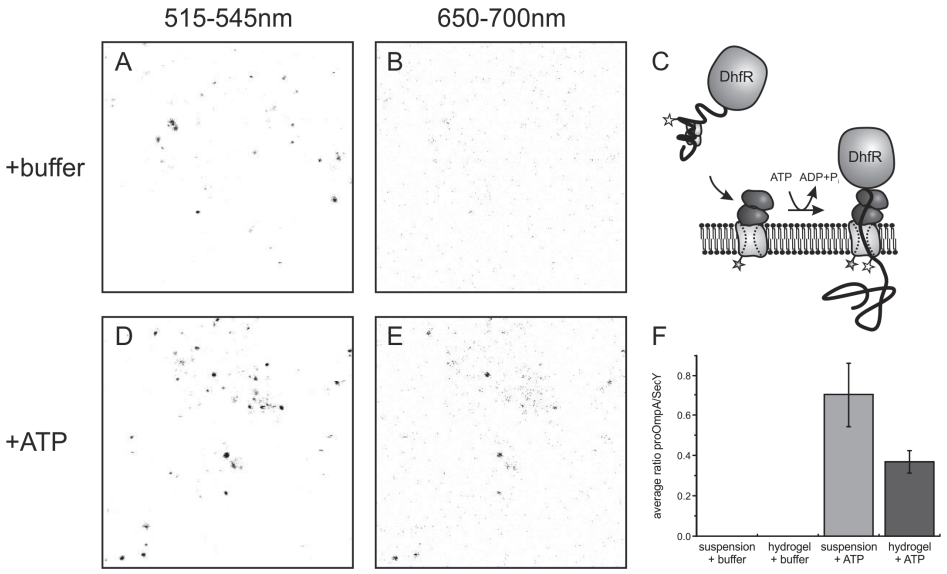

Figure 6: *Activity of hydrogel immobilized PL monitored by DCFBA-FRET. Immobilized proteoliposomes containing SecYEG-FM were excited with a 488 nm laser only and fluorescence at 515-545 nm (A, D) and 650-700 nm (B, E) was recorded simultaneously. (A) PLs containing SecYEG-FM after addition of buffer. (B) The same area as (A) at 650-700 nm shows only background fluorescence. (C) Schematic representation of proOmpA-DhfR intermediate formation. In presence of ATP, SecA translocates the proOmpA domain until the tightly folded DhfR domain stalls translocation resulting in a stable complex. Atto647N on proOmpA serves as acceptor for FRET from a donor fluorophore attached to the exit of the SeYEG channel. (D) PLs containing SecYEG-FM after addition of ATP leading to formation of protein translocation intermediates of proOmpA-DhfR-Atto647N. E) Resulting FRET signals appear as co-localizing fluorescence at 650-700 nm. (F) Quantification of FRET efficiencies by DCFBA in the hydrogel and in suspension is shown in.*

In order to monitor single liposome FRET of translocation intermediates, we performed confocal scans in the gel to record fluorescence signals for blue (donor fluorophore on SecY, Figure 6 A and D) and red fluorescence (acceptor fluorophore on proOmpA-DhfR, Figure 6B and E) simultaneously, using the 488 nm laser only for donor excitation. Co-localizing signals were identified and quantified with DCFBA as the ratio of proOmpA (C282)-DhfR-Atto647N over SecYEG-FM fluorescence. This ratio serves as an arbitrary unit for the FRET efficiency per liposome. In absence of ATP, no ratio of Atto647N/FM could be determined as fluorescence intensities at 650-700 nm did not exceed background levels (Figure 6B and F). However, when ATP was added to the reaction, fluorescent signals at 650-700 nm appeared originating from FRET between fluorophores on SecY and proOmpA-DhfR (compare Figure 6D

and E, respectively). The efficiency of translocation intermediate formation in the hydrogel as determined by the average FRET efficiency per liposome was ~50 % compared to suspension (Figure 6F). This further demonstrates that the translocon is functional when reconstituted in PLs that are immobilized in the hydrogel.

Discussion

To immobilize membrane vesicles with a size ranging from 100 nm to several micrometers such as proteoliposomes (PLs), IMVs and GUVs, a new method employing hydrogels composed of self-assembling low molecular weight gelators was investigated. Here, we demonstrate that the nano-scaled fibers of hydrogels based on 1,3,5-cyclohexyltricarboxamide are efficiently immobilizing (proteo-) liposomes composed of *E. coli* lipids and synthetic lipid mixtures without disturbing membrane integrity. This is evident as the water soluble tripeptide glutathione labeled with AF488 remains inside the liposomes after immobilization. Furthermore, calcein is unable to penetrate hydrogel immobilized GUVs containing a closed MscL channel. In previous studies, leakage of fluorescently labeled glutathione from liposomes was studied in investigations on the pore forming mechanism of the antimicrobial peptide melittin [164] and on the pore size of the mechanosensitive channel MscL [162]. Thus, if membrane integrity had been compromised during liposome or GUV immobilization, significant leakage would have been observed.

The hydrogels presented in this study are inert to factors such as pH, salts and temperature allowing immobilization of membrane vesicles at all physiologically relevant conditions. As the mesh size of the gel fibers is adjusted by the dimensions of the encapsulated particles, membrane vesicles of various sizes can be incorporated. Importantly, the biological activity of embedded membrane proteins in hydrogel immobilized membrane vesicles is preserved. Thus, the hydrogels are to a high degree biologically orthogonal. The fast and easy gel immobilization further allows high throughput sample preparation and single molecule measurements without time consuming surface preparations. Several strategies can be employed to incorporate molecules and vesicles in the gel. While small membrane vesicles and molecules can be vortexed with the gel, immobilization of fragile GUVs is accomplished by first liquefying the gel following by mild mixing with the GUV containing suspension. Furthermore, small molecules can be incorporated in the gel by addition to the top of the gel upon which they diffuse throughout the gel. This is evident by the here presented triggered opening of the MscL channel upon addition of the activator MTSET to the top of the formed gel containing immobilized GUVs. Influx of the soluble fluorophore calcein into single GUVs was followed in time by confocal microscopy providing a new tool to the GUV study tool box and investigation of MscL function in detail and at the single GUV level. This data demonstrates that GUVs are powerful in investigating membrane transport processes as their size allows measurements inside their lumen using confocal microscopy. Moreover, hydrogel

immobilization of GUVs is possible and allows measurements without interference from surfaces as molecules can diffuse freely in the gel and surround the GUVs from all sides.

Immobilization of small membrane vesicles such as PLs and IMVs allows tackling a different set of questions on membrane protein functioning as possible in GUVs. In the latter, due to size, the embedded membrane proteins can move out of the observation plane of a confocal microscope by lateral diffusion in the lipid bilayer. As PLs and IMVs appear as diffraction limited spots, membrane proteins cannot escape from the observation area. Thus, by downscaling the number of membrane proteins per liposome, single membrane proteins can be immobilized in their native environment. We performed *in vitro* protein translocation experiments with hydrogel immobilized PLs and IMVs, both in bulk and on the single vesicle level, and observed significant protein translocation activity although with reduced efficiency. The latter is most likely due to non-specific binding of the partially unfolded model substrate proOmpA to the hydrogel fibers by which multiple translocation events per channel are prevented. In order to determine protein translocation activity inside the hydrogel and on the single liposome level, laser scanning DCFBA was employed. DCFBA provides a high throughput tool to measure a large number of liposomes thus enabling improved statistics. The FRET efficiency per hydrogel immobilized PL was reduced to 50 % compared to liposomes in solution. Trapping of proOmpA-DhfR inside SecYEG blocks the channel for further translocation. Thus, multiple turnovers of protein translocation are prevented and the withdrawal of substrate due to non-specific binding to the fibers may be less severe. It appears, however, that proOmpA-DhfR bound to SecYEG prior immobilization may be ripped off from the PLs during mixing with the gel resulting in a reduction of intermediates. This data, however, demonstrates that hydrogels enable single molecule studies on membrane proteins incorporated in native or synthetic lipid mixtures.

In summary, the biological activity of (folded) proteins in the gel is sustained and macromolecules can diffuse freely in the gel due to its large mesh size. The transparency of the hydrogel allows the application of optical microscopy and processes at the membrane interface or within can be quantitatively assessed at the single vesicle and single molecule level. Thus, hydrogels composed of nano-scaled fibers are a new, generally applicable, immobilization tool for a wide range of native and synthetic membrane systems for the study of membrane proteins, their functioning and interaction with ligands from bulk down to the single molecule level.

4. Material and Methods

Hydrogels

Gelator 1 was synthesized as described in [254]. Preformed hydrogels were obtained by solubilizing 1.3 % (w/v) gelator 1 in buffer (50 mM Hepes-KOH, 30 mM KCl, and 2 mM $MgCl_2$) by heating to 130°C using an oil bath. After cooling to <100°C, the hot suspension was aliquoted to 50 µl and cooled down to room temperature (RT) upon which the gels formed. Incorporation and immobilization of IMVs or PLs was achieved by a short vortexing with one volume IMV/PL containing buffer.

Preparation of 'filled' liposomes, SecYEG reconstitution and in vitro translocation

SecYEG was purified, fluorescently labeled and reconstituted as described [211]. Filling of liposomes was achieved by a procedure similar to SecYEG reconstitution. Addition of 10 µM AlexaFluor488-glutathione (AF488-glu) to detergent solubilized (0.5 % Triton X-100 / 0.2 % n-Dodecyl-β-maltoside) lipids supplemented with DiD (1:100,000 molar ratio) and subsequent detergent removal by polystyrene beads (Bio-Beads SM-2 adsorbents) lead to the formation of AF488-gluthatione filled liposomes. Due to the absorption of AF488-glu to the polystyrene beads, only a fraction of the AF488-glu was encapsulated and virtually no free fluorophore was detected. IMVs, SecA, SecB, proOmpA, proOmpA-DhfR were purified as described elsewhere [211]. *In vitro* protein translocation was essentially performed as described previously [211]. Shortly, after addition or un-caging (2 min of UV, 360nm, 4W lamp) of ATP the translocation reaction was incubated at 37 °C for 15min. Subsequently, proteinase K was added to digest not translocated proOmpA. After 15 min incubation at 37 °C, proteins were precipitated by addition of 10 % TCA (final concentration) for 30 min on ice. Prior centrifugation (16000 x g, 15 min) ten volumes of a 4:1 aceton-water mixture were added to the TCA precipitation to dissolve the organic gelator. The pellet was washed once with the acetone-water mixture, dried at 37 °C and dissolved in SDS-sample buffer before it was applied to SDS-PAGE. The fluorescently labeled proOmpA was visualized in a gel imager (Fuji).

Formation of GUVs containing MscL channels

Phosphatidylcholine (DPhPC, 1,2-Diphytanoyl-sn-Glycero-3-Phosphocholine) and POPG (PG, 1-Palmitoyl-2-Oleoyl-sn-Glycero-3-[Phospho-rac-(1-glycerol)], Sodium salt) were purchased from Avanti polar lipids. DPhPC was chosen as the PC component for our lipid composition for its high mechanical and chemical stability. Cholesterol (3β-Hydroxy-5-cholestene, C27H46O) was obtained from Sigma. MTSET ([2-(trimethylammonio)ethyl] methanethiosulfonate and bio-beads (Bio-Beads SM-2 adsorbents) were from Anatrace and Bio-Rad Laboratories B.V., respectively. Giant unilamellar vesicles (5-20µm) were formed from PLs (150nm) by electroformation as described previously [255]. Briefly, first MscL was produced, isolated and

reconstituted into DPhPC:POPG:cholesterol liposomes (70:25:5 weight ratio) by a detergent-mediated reconstitution method as indicated before [256,257]. The resulting PLs were used to obtain a thin lipid film on the surface of conductive glass slides (ITO). Droplets of 2 µl containing 0.8 mg/ml PLs in 2 mM MOPS-Tris buffer pH 7.0 were applied to the glass surface followed by overnight partial dehydration in a vacuum desiccator at 4 °C. After the PL films were obtained, an electroformation chamber was prepared in NanionVecicle Prep Pro (Nanion Technologies GmbH, Munich, Germany). The chamber was filled with 250 mM sucrose. An AC voltage was applied for 4 hours across the cell unit with stepwise increases from 0.1 to 1.1 V at 12 kHz frequency. At the end, in order to detach glass attached giant unilamelar liposomes, the AC current was lowered to 4 Hz and voltage raised to 2 V for 30 min. Vesicles formed in this way had a diameter of 10- 15 µm. In order to image the GUVs, a fluorescent lipid analogue, the fluorescent lipid analog DiD (650 nm/670 nm, excitation/emission) was added to the vesicles after they were formed. Calcein (497 nm/516 nm, excitation/emission) was used as an external dye for uptake by the GUVs.

Fluorescent measurements

Immobilized (proteo-) liposomes were imaged in a dual-color laser scanning confocal microscope that is described in detail elsewhere [162,164]. The two laser beams (488 nm, argon ion laser; 633 nm, He-Ne laser) were aligned to a high degree of spatial overlap and moved simultaneously with a galvanometer optical scanner through the sample. Two confocal images (30 × 30 µm) of the blue and red fluorescence channels were recorded simultaneously. For the laser-scanning dual-color fluorescent burst analysis (lsDCFBA, for review see [148]) measurements, fluorescent bursts from the spectrally well separated fluorophores (AF488/DiD or FM/Atto647N) were identified using arbitrary thresholds as described [148]. The ratio of the fluorescence of one fluorophore over the other (AF488/DiD and Atto647N/FM, respectively) is an arbitrary unit for the relative stoichiometry of both fluorophore. The DCFBA-software can be downloaded at www.bogeert.com/DCFBA/publish.htm. Hydrogel immobilized GUVs and calcein were imaged in a Confocor3 confocal microscope (Zeiss) using the 488 nm argon ion laser and the 633 nm He-Ne laser.

Supplementary information

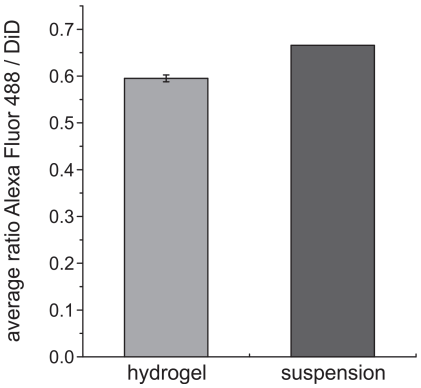

Figure S1: *Membrane integrity of liposomes remains intact during hydrogel immobilization. DCFBA analysis of liposomes filled with the soluble fluorophore AF488-glutathione and supplemented with the fluorescent lipid analog DiD determines the relative stoichiometry of the co-localizing fluorophores (for review see [148]). Hydrogel immobilized liposomes had comparable amounts of AF488 encapsulated as liposomes prior immobilization.*

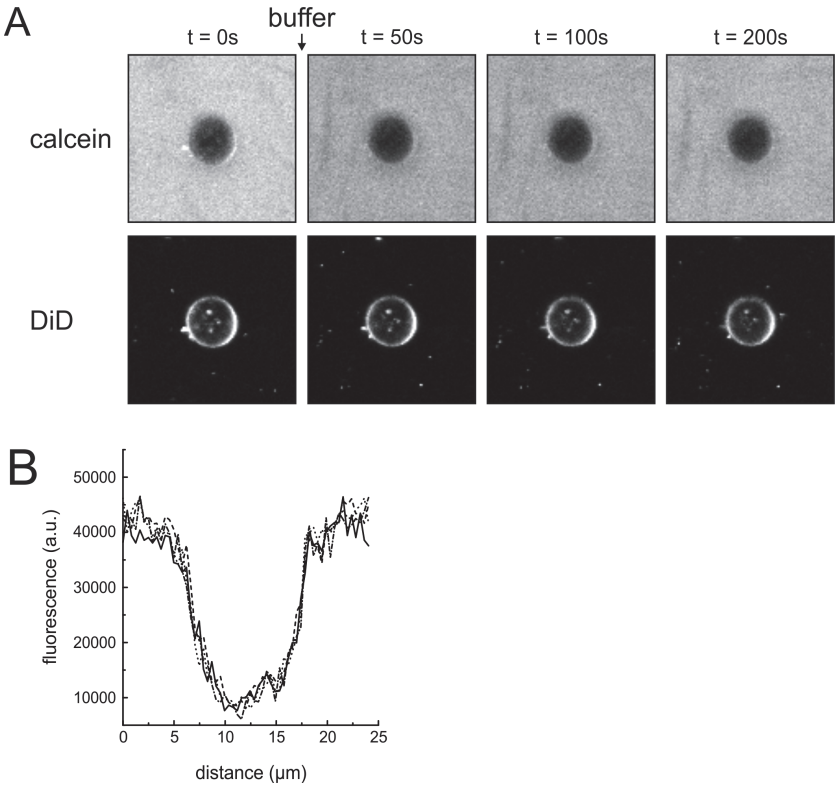

Figure S2: *The MscL channel remains in its closed state in absence of a trigger. A) MscL containing and DiD stained GUV at various time points after addition of buffer. B) Calcein fluorescence outside and inside the GUV was quantified by cross-sections through the center of the GUV depicted in A at the different time points; t = 0s (straight line), 50s (dash-dot), 100s (dot), 200s (dash).*

Author contributions

Liposome, PL and IMV immobilization as well as bulk and single PL *in vitro* protein translocation assays were performed by I. Kusters. The GUV studies were done by N. Mukherjee and A. Koçer. M. R. de Jong provided the hydrogelator and contributed to the development of the immobilization protocols. S. Tans, A. Koçer and A. J. M. Driessen supervised this study and contributed to the writing of the manuscript.

Acknowledgements

This work was funded by NanoNed (IK, MDJ, AJMD), a national nanotechnology program coordinated by the Dutch Ministry of Economical Affairs and the Zernike Institute for Advanced Materials (IK, AJMD), and by the Chemical Sciences division of The Netherlands Organization for Scientific Research (NWO-CW; IK, AJMD). Further, this project was supported by MEDITRANS Sixth Framework Programme (AK,NM), NWO VIDI (AK), ERC-Starting grant (AK).

CHAPTER 7

TOWARDS SINGLE MOLECULE OBSERVATIONS OF PROTEIN TRANSLOCATION

Ilja Kusters, Sander Tans and Arnold J.M. Driessen

Abstract

Bacterial protein secretion is mediated by the ATPase SecA that translocates proteins targeted for export through a protein-conducting channel, termed SecYEG. The mechanism of protein translocation has so far mostly been addressed with conventional biochemical assays that involve ensemble averaging. Here, we present *in vitro* protein translocation assays with single molecule sensitivity that represent a step towards the real time observation of single preproteins being translocated by the bacterial translocon. For the first time, protein translocation is visualized at the single vesicle level using an *in vitro* translocation assay with surface immobilized inner membrane vesicles (IMVs). In a second, discontinuous assay, protein translocation is analyzed at the single molecule level in free diffusing proteoliposomes (PLs) by means of Dual-color fluorescence-burst analysis (DCFBA).

Introduction

Protein transport across biological membranes is an essential process in all kingdoms of life. In bacteria, the majority of proteins that are destined for secretion are targeted to the highly conserved protein-conducting channel SecYEG. The motor protein SecA, associated with this heterotrimeric channel, utilizes ATP to drive the translocation of the so-called preproteins across the membrane. Bacterial protein secretion has been studied with a multitude of biochemical and structural techniques and this has led to a detailed understanding of many aspects of this process. However, despite two decades of research, several of the intimate details of the mechanism of SecA-mediated protein translocation remain unclear. Based on the observation that protein translocation occurs in steps of defined size, SecA was suggested to mechanically push the preprotein through the SecYEG channel [4-6]. This model was opposed by studies suggesting a Brownian ratchet mechanism where SecA merely facilitates channel opening and the preprotein moves by diffusion [125,127]. In analogy to the eukaryotic Hsp70 chaperone BiP, SecA is thought to prevent backsliding thereby providing directionality to the process. Various other models including the peristalsis and subunit recruitment model combine these two basic principles with other features (for review of translocation models see Chapter 1 and [126]). Conventional biochemical assays have, so far, been unsuccessful in elucidating the exact mode of preprotein movement inside the SecYEG channel. This is partially due to the ensemble averaging of these assays resulting from a multitude of parallel but not synchronous translocation reactions. Observing single polypeptide chains moving through SecYEG may therefore unravel dynamics and transient intermediate states that define the translocation process. Analysis of preprotein movement at the single molecule level will be pivotal for our understanding of the mechanism of SecA mediated protein translocation. Other controversial questions as to the oligomeric state of SecYEG during protein translocation may also be answered with single molecule techniques. The ultimate proof that SecYEG functions as a monomeric complex would be to detect single translocating channels. This may be achieved by determining the translocation activity of proteoliposomes (PLs) containing only a single SecYEG copy as suggested in a recent study. Here we describe two new, fluorescence based, *in vitro* protein translocation assays that reach single molecule resolution. First, a single vesicle translocation assay employs surface immobilized inner membrane vesicles (IMVs) to monitor protein translocation at the single vesicle level with a time resolution of several minutes in a laser scanning confocal setup. Employing TIRF microscopy to this assay would enable real time observations of single vesicle translocating preproteins *in vitro*. A second, discontinuous, assay has true single molecule sensitivity and allows a static but precise assessment of translocation activity in solution without eventually detrimental interactions of PLs with glass surfaces. Here, protein translocation is quantified by determination of the relative stoichiometry of co-migrating PLs and the fluorescently labeled model

preprotein proOmpA. This assay may prove a valuable tool for measuring the activity of single SecYEG PLs.

Results

Surface-Immobilization of IMVs and a single vesicle translocation assay

The protein conduction channel SecYEG was labeled with Cy5-maleimide on its periplasmic site at position C295 on SecY in intact *E. coli* cells. Inverted membrane vesicles (IMVs) from these cells were isolated and labeled with biotinyl-maleimide. Since SecYEG does not contain any cysteines on the exposed cytoplasmic site unidentified membrane proteins are biotinylated. Protein translocation activity was not affected by the biotinylation (data not shown). Fluorescent labeling of SecY was visualized by in gel fluorescence of IMVs on SDS-PAGE (Fig1A). SecY is labeled almost exclusively (compare with coomassie stained gel, Fig 1A). To view the IMVs in a confocal microscope the cover slip of a home build flow cell was incubated with biotinylated BSA and streptavidin (Fig 1b). The biotinylated IMVs bind with high efficiency to the BSA-biotin-streptavidin layer on the glass surface and immobilization is resistant against applied buffer flow. The Cy5 fluorophore (absorption maximum 650 nm) can be exited with a 523 nm laser when a very high light intensity is applied (two orders of magnitude higher than used for the Cy3 fluorophore). The observed fluorescent intensities of the IMVs vary considerably indicating a heterogeneous size and SecYEG distribution.

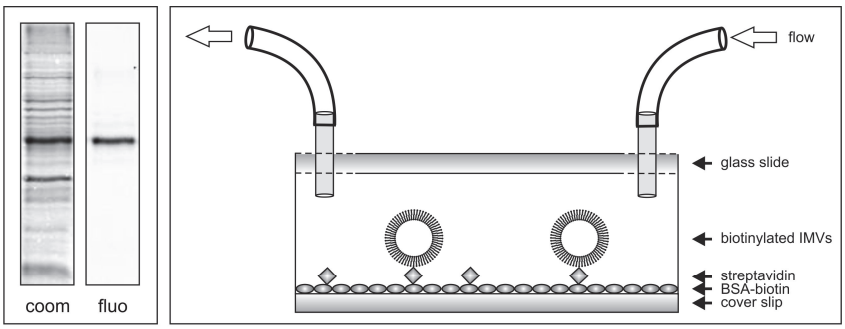

***Figure 1**: Inner membrane vesicles (IMVs) containing fluorescently labeled SecY are immobilized in a home built flow cell. A) SDS-PAGE of with IMVs containing over expressed and Cy-5 labeled SecYEG. In gel fluorescence (fluo) and coomassie stained gel. B) Schematic of a flow cell with immobilized IMVs.*

Photo bleaching of individual vesicles down to single bleaching steps allows an estimation of the number of embedded SecYEG channels, which ranges from dozens to a few hundred copies of SecYEG (data not shown). Protein translocation can be studied on the single vesicle level using precursor proteins labeled with a spectrally

separated fluorophore. ProOmpA, labeled with Cy3-maleimide at a unique cysteine, binds in the presence of the molecular chaperone SecB and SecA to SecYEG containing vesicles as evidenced by co-localization of Cy3 and Cy5 fluorescence (Fig 2A). When ATP is added the increase of the fluorescent intensity per vesicle is significantly higher (Fig 2B). Here, several turnovers of protein translocation lead to the accumulation of proOmpA-Cy3 inside the vesicles.

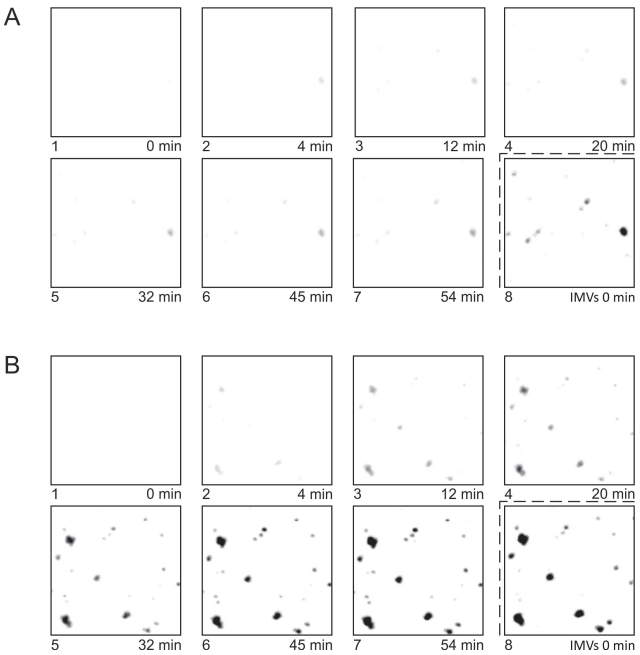

Figure 2: *ProOmpA-Cy3 binding to and translocation into surface immobilized IMVs. A) SecA dependent binding of proOmpA-Cy3 to IMVs in absence of ATP. 1-7: green fluorescence (570 nm) at different time intervals (4-10 min), 8: SecY-Cy5 containing IMVs are visible as red fluorescence (670nm at t = 0 min). B) In presence of ATP and SecA, translocation of proOmpA-Cy3 into SecY-Cy5 IMVs leads to higher accumulation of the preprotein compared to A). 9-15: green fluorescence (570 nm) at different time intervals (4-10 min), 8: IMVs are visible as red fluorescence (670 nm at t = 0 min). Pictures 1-7 and 9-15 have identical dynamic range.*

Protein translocation monitored by DCFBA

The number of SecYEG channels in IMVs is very high due to overexpression of the single cysteine SecY mutant together with SecEG. To monitor single molecule protein translocation events in vesicles, however, it is necessary to downscale the number of SecYEG channels to a few or even down to one channel per vesicle. This can be achieved by reconstitution of purified SecYEG into liposomes composed of synthetic or native lipid mixture at a very low protein to lipid ratio. As the resulting protein concentration drops to the nanomolar range, detection of proteins or even protein activity with biochemical methods becomes challenging. With fluorescence microscopy, however, even single fluorescently labeled proteins are detectable. Surface immobilization of SecYEG proteoliposomes (PLs) via biotin-streptavidin linkage as accomplished with IMVs would be ideal to monitor single molecule translocation events. Immobilization of PLs of *E. coli* lipids and SecYEG was as efficient as for IMVs. Under these conditions, no specific, SecA dependent, binding of proOmpA could be observed.

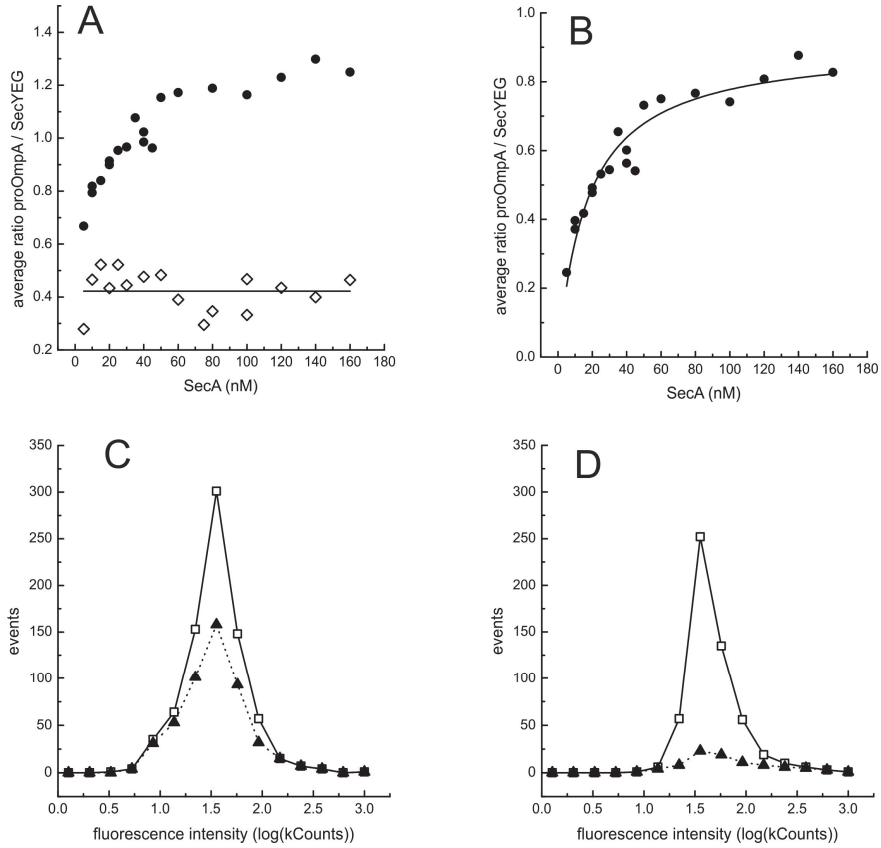

Figure 3: *In vitro protein translocation assayed by DCFBA. A) The average ratio of proOmpA-Atto647N/SecY-AF488A as an arbitrary value for translocation activity is plotted against the SecA concentration. Translocation reactions supplemented with ATP are indicated as black dots and not energized reactions as open diamonds. B) The background from non-specific co-migrating signals was subtracted and the resulting curve fitted using the Michaelis-Menten equation. C+D) Fluorescent intensities of fluorescence bursts of all PLs (open squares) and of PLs co-migrating with proOmpA signals (black triangles) in reactions supplemented with ATP (C) and in non energized reactions (D).*

Therefore, we set out to measure protein translocation in solution with PLs containing only few to single SecYEG channels. To this end, a discontinuous *in vitro* protein translocation assay was conducted with Atto647N labeled proOmpA and Alexa Fluor 488 labeled SecYEG reconstituted into liposomes of *E. coli* lipids. In a series of experiments, the SecA concentration was varied from 5-160 nM and the reactions were incubated with or without ATP. After non translocated proOmpA was digested by the addition of Proteinase K, the reactions were measured with a dual-color laser scanning confocal microscope. Fluorescent burst originating from the diffusing SecYEG-PLs and from proOmpA-Atto647N were recorded and analyzed by dual-color fluorescence burst analysis (DCFBA, for review see: [148]).

This method identifies overlapping peaks from co-migrating PLs and proOmpA and calculates the ratios of fluorescent intensities of proOmpA/SecYEG. The resulting average ratio is an arbitrary unit for the amount of proOmpA co-migrating with SecYEG. The reactions without ATP had a much lower average ratio of proOmpA/SecYEG compared to the reactions supplemented with ATP (Fig 3A). With increasing SecA concentrations, more proOmpA co-migrated with SecYEG in presence of ATP whereas the average ratio of the not energized reactions remained constant (Fig 3A). This background resulting from coincidental co-migration and non-specific binding of proOmpA-peptides to the PLs was averaged and subtracted from the ATP containing reactions. The resulting curve was fitted using the Michaelis-Menten equation and an apparent K_M of 17.1 nM +/- 2.2 nM was derived from the fit. The fraction of PLs active in protein translocation can be estimated by plotting the intensities of the fluorescent bursts of all PLs and of the PLs that co-migrate with a proOmpA-Atto647N signal above the arbitrary threshold. In the experiment with 160 nM SecA, 63% of all PL signals co-migrated with proOmpA-647N when ATP was added (Fig 3C) in contrast to only 16% of the PL signals in the non-energized reactions (Fig 3D). We conclude that protein translocation can be assayed at the single molecule level by quantifying the co-migration of PLs and proOmpA. In reactions energized with ATP not only more PLs co-migrate with a proOmpA-signal but also the ratio of proOmpA/SecYEG is significantly increased.

Discussion

Fluorescent labeling allows detecting single proteins and their activity without ensemble averaging by means of fluorescent microscopy. In order to observe single protein translocation events in a time resolved manner, the translocation machinery needs to remain in the observation area of a microscope throughout the whole process. Here, we show that functional immobilization of the SecYEG channel in its native lipid environment can be achieved via biotin-streptavidin linkage to the cover glass of a flow cell suitable for confocal or TIRF microscopy. IMVs with a specifically labeled single cysteine in a periplasmic loop of SecY can be obtained by whole cell labeling. A disadvantage of using IMVs is the uncontrollable and high number of SecYEG channels that is hampering single molecule observations. Reconstituting purified fluorescently labeled SecYEG into liposomes allows downscaling the number of channels per liposome. Immobilized PLs composed of *E. coli* lipids and SecYEG, however, were inactive in specific proOmpA binding and translocation. Possibly, due to the high concentration of the non-bilayer lipid phosphatidylethanolamine in *E. coli* polar lipid extract (67%), the PLs collapsed on the BSA coated surface. Other lipid mixtures that are compatible with SecYEG function and support membrane integrity such as mixtures with the bilayer lipid phosphatidylcholine may be better suitable for surface immobilization. However, immobilization of *E. coli* proteoliposomes was achieved recently on a surface carrying a supported lipid bilayer supplemented with biotinylated lipids [193].

In this study, protein translocation was assayed by counting the number of SecYEG containing PLs that occurred as fluorescent spots in a TIRF setup due to binding or translocation of fluorescently labeled proOmpA. External addition of a fluorescence quencher caused PL-fluorescence to disappear if no ATP was present and proOmpA was only bound to the outside of the PLs. However, no quantification of the fluorescent intensities of bound, translocated or quenched proOmpA was conducted ignoring fluorescence quenching above background. In contrast, the number of observed fluorescent spots were equaled to the total "fluorescence of vesicles" not taking the sum of fluorescent intensities of the PLs into account. Furthermore, although stated differently by the authors, a significant fraction of single SecYEG PLs (>15%) were active in protein translocation, i.e. were not quenched when ATP was present to fuel the translocation reaction. Also, the issue of SecYEG orientation was not taken into account, which being random, will reduce the number the active single SecYEG containing PLs. Evidence that the translocation of single or even few proOmpA molecules could be detected by this assay was also not demonstrated although in a bleaching experiment, fluorophores on SecYEG were counted. Surprisingly, no proOmpA binding to SecYEG was observed in presence of SecA contradicting previous studies ([2,56,200]. Similarly, in this study, no proOmpA binding was observed to surface immobilized PLs in presence of SecA although it is unclear if the PLs have retained their activity. However, surface immobilized IMVs were active in binding proOmpA in presence of SecA and absence of ATP (Fig 2A). Finally, in the study presented by Deville and co-workers, also the possibility of quenching upon translocation of the environment sensitive fluorophore Alexa Fluor 488 on proOmpA was not investigated. The similarly sensitive fluorophore Fluorescein is highly quenched when translocated proOmpA aggregates inside membrane vesicles ([149], I. Kusters unpublished results).

In order to observe protein translocation at the single molecule level the discontinuous *in vitro* translocation assay was combined with a recently developed fluorescence based technique called DCFBA [148]. This new assay blends detection with single molecule sensitivity and the efficiency of *in vitro* translocation of the model preprotein proOmpA in bulk, free from interference with surfaces. Upon addition of ATP, fluorescently labeled proOmpA is translocated by SecA into SecYEG containing PLs where it is protected against an externally added protease (for details see [211]). Traditionally, translocated proOmpA is visualized by in gel fluorescence on SDS-PAGE. The detection limit of gel-imaging techniques, however, renders it impossible to detect low protein concentrations. On the other hand, even single fluorescently labeled proteins diffusing through the confocal excitation volume of a fluorescence microscope will give rise to significant fluorescent bursts. DCFBA uses a quantitative analysis of these fluorescence bursts from individual PLs and proOmpA molecules of a translocation assay to determine the relative ratio of the co-migrating proteins. After protein translocation assays the average ratio of the fluorescent intensities of proOmpA-Atto647N / SecY-AF488 was found dramatically higher when ATP was

present compared to not energized reactions. With increasing concentrations of the motor protein SecA, the proOmpA/SecY ratio was found to rise when ATP was added. In absence of this energy source, the ratio of co-migrating proOmpA and SecY was constant. We conclude, that protein translocation can be assayed by quantifying the amount of co-migrating proOmpA and SecYEG using DCFBA. This method cannot distinguish between fully translocated preprotein or proOmpA derived peptides that are bound non-specifically to the outer surface of the PLs after protease digestion. Furthermore, the concentration of proOmpA in the translocation reactions of around 20 nM causes coincidental co-migration since at this concentration, in average, always at least one particle is present in the focal volume. It should be noted, however, that the substrate concentration was likely to be limiting. ProOmpA binding to SecYEG bound SecA was previously determined to occur with a K_d of around 35 nM [2]. As higher concentrations of fluorophores lead to substantial coincidental co-migration only 20 nM proOmpA was used in the experiments described. True kinetics may be obtained with saturating substrate concentrations and separation of non-bound proOmpA and PLs by sucrose gradient centrifugation. The single particle resolution of the DCFBA technique allows determining the fraction and intensity distribution of co-migrating particles. For the ATP containing reactions, up to 63% of the fluorescent burst originating from PLs co-migrated with a proOmpA signal. In the not energized reaction the number of co-migrating signals was found to be significantly lower (8-16%). Interestingly, PLs of all intensities were found co-migrating with proOmpA indicating that also PLs with few and single SecYEG are active in protein translocation.

Material and Methods

In vivo labeling of SecYEG

Labeling of whole cells was conducted as described elsewhere [237] with the following modifications. Overexpression of $SecYG_{295}C$ EG was achieved in *E. coli* SF100 cells transformed with the pET84 vector [211]. Cells from a 250 mL culture were pelleted and resuspended in 40 mL, 5 mM EDTA, 1 mM DTT, 0.4 M sucrose followed by 20 min incubation on ice. After recollection by a 20min centrifugation at 5300 rpm, SS35 rotor, cells were washed once with 50 mM Tris pH7.5, 0.4 M sucrose, 3 mM $MgCl_2$ and resuspended in the same buffer to an $OD_{600\ nm}$ of 40. Labeling with Cy5-maleimide was done for 2 hours on ice. Isolation of IMVs and visualization of in gel fluorescence is described elsewhere [211].

Surface immobilization of IMVs

Biotinylation of IMVs was achieved by incubation with 0.5mM 3-(N-maleimido-propinyl)-biocytin for 2 hours on ice. The reaction was quenched by addition of 5 mM DTT and free label was separated from the IMVs by ultracentrifugation and washing of the IMV pellet. For the home built flow cell, channels were cut into parafilm which

was sandwiched between a cover slip (24x50 mm) and a microscope glass slide by heating to 200°C on a heating plate. The top glass slide contained holes of 1 mm diameter at that aligned with the parafilm channels at the two extreme ends. The flow cell was fixed in a custom made sample holder and connected with flexible tubes to allow sample injection via syringes. The glass slides were cleaned by 1 h incubation with 2 % Helmanex in a sonicator bath followed by three washed with MilliQ water and another 1 h sonication in MilliQ. Coating of the glass surface with biotinylated BSA-streptavidin was achieved by incubating the flow cell for 30 min first with BSA (1 mg/mL)/BSA-biotin (0.1 mg/mL) followed by streptavidin (20 µg/mL) and a buffer wash. Immobilization of biotinylated IMVs on this surface was resistant against applied buffer flow.

Protein purification and in vitro protein translocation

Purification of SecA, SecB, SecYEG, proOmpA and labeling of the latter two as well as reconstitution of SecYEG into proteoliposomes is described elsewhere in detail [211]. The *in vitro* protein translocation assay was essentially performed as described [211] with the following modifications. A 50 µL translocation assay was divided in two 20 µL reactions of which one was supplemented with 2 mM ATP while to the other an equal volume of MilliQ water was added. SecA concentrations in the assays varied as indicated. After incubating the assays for 20 min at 37°C, Proteinase K was added to a final concentration of 0.4 mg/mL and incubation at 37°C was continued for 30 min.

Fluorescence measurements and DCFBA analysis

The dual-laser scanning confocal microscope and the DCFBA analysis is described in detail elsewhere [105,148].

Acknowledgements

This work was supported by NanoNed, a national nanotechnology program coordinated by the Dutch Ministry of Economical Affairs and the Zernike Institute for Advanced Materials, and by the Chemical Sciences division of The Netherlands Organization for Scientific Research (NWO-CW).

.

CHAPTER 8

A SYSTEMATIC ANALYSIS OF THE *IN VITRO* TRANSLOCATION OF FLUORESCENTLY LABELED PROOMPA CYSTEINE MUTANTS

Ilja Kusters, Janny de Wit, Sander Tans and Arnold J.M. Driessen

Introduction

Protein translocation in bacteria is mediated by a complex multi-protein machinery composed of the membrane embedded SecYEG channel, a molecular chaperone, SecB, and the motor protein SecA (for review see [258]). Proteins destined for secretion, termed preproteins, are transported across the membrane by the ATPase SecA that mediates their translocation through the protein conducting SecYEG channel. Translocation has been studied both at the genetic and biochemical level. In particular, two decades of *in vitro* studies on protein translocation have contributed to our understanding of the mechanism of this process [259]. Translocation of model preproteins into inverted inner membrane vesicles (IMVs) of *E. coli* or proteoliposomes containing purified and reconstituted SecYEG can be assayed discontinuously by a protease protection assay or in real time by fluorescence quenching [149,211]. In order to detect the translocated preprotein, radioactive labeling by incorporation of 35S-methionine in a coupled *in vitro* transcription/translocation system or by iodination of purified preprotein is often used. However, these methods are time consuming and inconvenient due to the use of radioactive materials. An alternative to radioactive labeling was introduced 2002 when de Keyzer et al. employed site specific labeling of preproteins with fluorescent probes [149]. In the discontinuous translocation assay, protease protected preproteins can be separated from the bulk fluorescence by SDS-PAGE and visualized by in gel fluorescence similar to the detection of radioactive labeled preproteins. The very efficient fluorescent labeling procedure which is applied after purification of the preproteins allows the generation of large quantities of labeled substrate and therefore enzymatic assays with an excess of substrate. A major advantage of fluorescently labeled preproteins lies in the use in time resolved fluorescent assays. Changes in fluorescence through environment depending quenching or Förstner resonance energy transfer (FRET) allow to monitor protein translocation in real time and to obtain true kinetics [52,149] (Kedrov, Kusters et al., submitted). Furthermore, due to advances in fluorescence spectroscopy, observations of single molecule translocation events are within reach. Previously, the commonly used model preprotein proOmpA was found to translocate less efficiently *in vitro* when it was labeled at residues within or close to the N-terminal signal sequence [149] or when multiple or bulky fluorophores were attached to certain positions of the polypeptide chain (J. G. de Wit, unpublished results). Here, we present a systematic study on the translocation efficiency of various proOmpA cysteine mutants with focus on the effect of (cysteine-) labeling position, number and size of the attached fluorophores.

Results

To study the effect of labeling position on the model preprotein proOmpA, a series of single cysteine mutants was constructed that enables the site specific labeling with fluorescent probes (Fig 1A). Cysteine residues were at positions 33 [149], 66, 108,

163, 198, 245, 290, 302, the latter two being the native cysteines of proOmpA (Fig 1A). The purified and urea dissolved proOmpA mutants were subjected to fluorescent labeling with cysteine specific maleimide derivatives of the fluorophores Fluorescein (Flu, MW 427.37 Da), Texas Red (TR, MW 728,83) and Alexa Fluor 568 (AF568, MW 880.92). As expected for unfolded proteins, the labeling efficiency for all cysteine mutants was virtually the same as determined by the ratio of fluorescent over coomassie stained protein bands (Fig 1B).

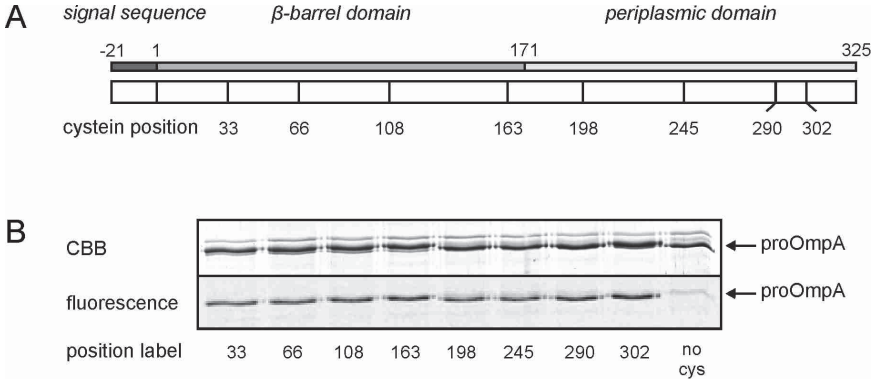

Figure 1: *Labeling efficiency of single cysteine mutants of proOmpA. A) Schematic of proOmpA single cysteine positions. B) Fluorescein labeling of different single cysteine mutants. The coomassie stained bands (CBB) are included as a control showing equal protein loading.*

The differently labeled proOmpA single cysteine mutants were tested for *in vitro* translocation activity with IMVs of *E. coli*. In comparison with the translocation efficiency of the C290 mutant, only proOmpA with fluorescein at position 66 and 245 translocated less efficiently (Fig 2). For Texas Red labeled proOmpA, a trend is noticeable that the translocation efficiency increases with the distance of the label attached towards the C-terminus. An exception to this trend is position 33 that allows reasonable translocation when labeled with Texas Red. ProOmpA mutants labeled with the bulky and negatively charged AF568 are not competent for *in vitro* translocation when the label is attached at positions 33, 66, 108 or 163 (Fig 2). Significant translocation activity can only be observed from position 198 onwards with an increased efficiency the further the label is attached to the C-terminus. Interestingly, translocation of proOmpA C198-AF568 results in formation of a stable intermediate visible as a band with lower molecular weight that is additional to the full length protein (Fig 2). After translocation, proOmpA C245-AF568 appears exclusively as an intermediate which is shorter than the full length protein but somewhat longer than the intermediate observed for the C198-AF568 mutant. Intermediates are also observed for the Flu and TR labeled proOmpA mutants with cysteines at positions 33, 66, 108, 168 and 198. The size of these intermediates is identical for all mutants and therefore independent of the labeling position. Unlike for the fluorescein or Texas Red

labeled proOmpA a significant difference in translocation efficiency is observed for the AF568 labeled C-terminal residues C290 and C302, the latter translocating with approximately 50% higher efficiency. Apparently, for AF568 labeled proOmpA the position of the label is not the only criteria determining translocation competence. Overall it seems that when bulky fluorophores are attached to proOmpA in the N-terminal region, translocation is inhibited.

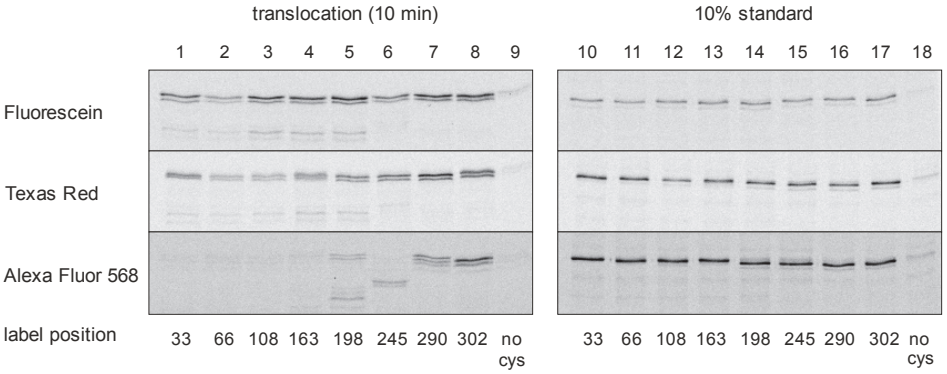

Figure 2: *Translocation of proOmpA single cysteine mutants labeled with different fluorescent probes into urea stripped IMVs.*

SecYEG channels with signal sequence suppressor mutations translocate preproteins with defective signal sequence (PrlA phenotype, [260]) and exhibit elevated translocation efficiency *in vitro* [149]. To study the effect of inhibitory labeling of the N-terminal AF568 labeled proOmpA mutants, *in vitro* translocation assays with IMVs containing PrlA4EG complexes were conducted. As described previously [149], the translocation efficiency is generally enhanced which is evident by comparison of the translocation of C290 and C302 labeled proOmpA into IMVs containing wild type SecYEG or PrlA4EG (Fig 3, compare lane 7 and 8 for SecYEG and PrlA4EG IMVs, respectively).

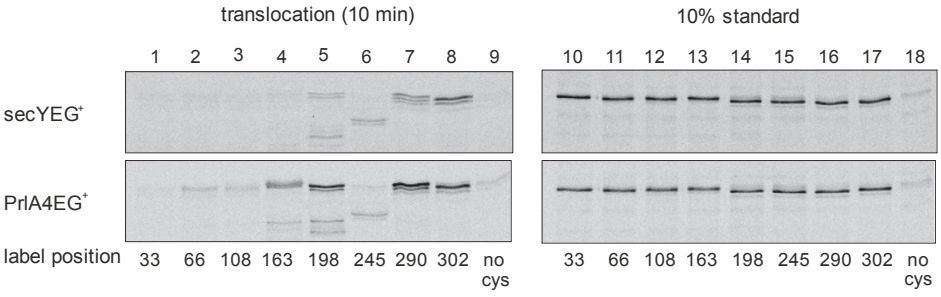

Figure 3: *Translocation of proOmpA-AF568 into SecYEG and PrlA4EG IMVs.*

Interestingly, also proOmpA mutants AF568-labeled in the N-terminal part at positions 66, 108 and 163 that are not translocated by WT-SecYEG show significant translocation activity across PrlA4EG complexes. Apparently, the SecYEG inherent proofreading mechanism that is disabled in PrlA4 mutants inhibits the translocation of proOmpA labeled at the N-terminal part with bulky and charged fluorophores.

A similar inhibitory effect of N-terminal labeling was observed with double and triple cysteine mutants of proOmpA that were labeled with fluorescein. When the first label was attached at residue 33 or 66, translocation was strongly inhibited in comparison to the single cysteine proOmpA C290 mutant (Fig 4). Double or triple cysteine mutants with the first label at position 108 translocated significantly better than the previous more N-terminal mutants (Fig 4, compare lanes 2-3 to 4 and 5-6 to 7, respectively).

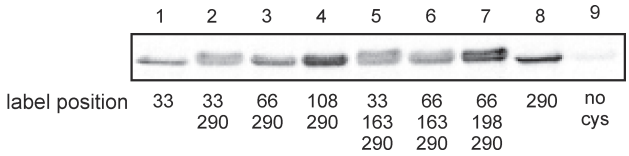

Figure 4: *Translocation of proOmpA single, double and triple cysteine mutants labeled with Fluorescein into IMVs.*

To investigate the effect of the number of fluorophores on translocation efficiency, single (C290), double (C108, C290 and C168, C290) and triple (C108, C198, C290) cysteine proOmpA mutants were labeled with FM. Increased labeling of proOmpA with multiple cysteines is visible as shift in the apparent molecular mass on SDS-PAGE (Fig 5 A). No double or triple bands occurred indicating full labeling of the cysteines. To further prove complete labeling, single, double and triple cysteine proOmpA mutants were labeled with the photo stable fluorophore Cy3 and bound via nonspecific interaction to the glass surface of a microscopic cover slip. By focusing the laser beam of a confocal microscope onto single surface attached proteins, bleaching curves could be recorded over time (Fig 5B). The number of bleaching steps was in agreement to the number of cysteines present in the proOmpA mutant. Thus, all cysteines were labeled stoichiometrically. Next, translocation of the proOmpA mutants was tested *in vitro*. To assure that the translocation reaction had not reached saturation levels, a kinetic translocation assay was conducted by stopping the reaction at different time points (Fig 6A). The reaction was starting to saturate after 8 minutes and was still clearly in the linear range after 6 minutes. Therefore, the translocation efficiency of the different mutants after 6 minutes was compared which displays a clear trend: the more fluorophores were attached proOmpA, the lower the translocation efficiency (Fig 6B). Furthermore, translocation inhibition was proportional to the number of fluorophores and independent on the position where the second fluorophore was attached. Thus, inhibition by multiple fluorophores appears to occur via a general, not site-specific, mechanism.

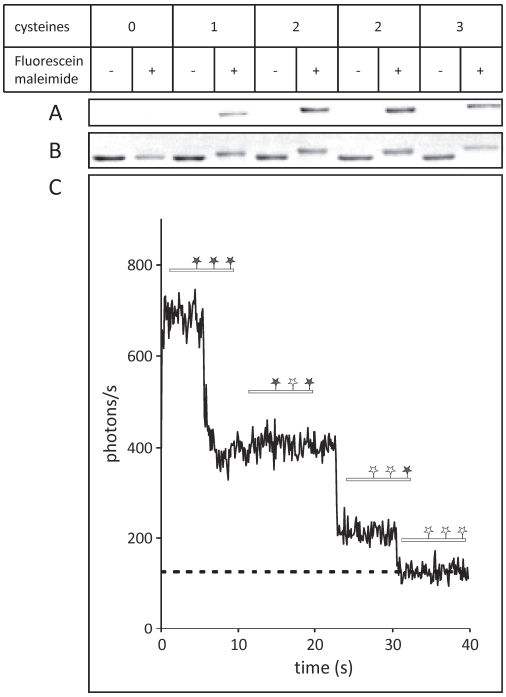

Figure 5: *Labeling efficiency of proOmpA single, double and triple cysteine mutants. A) Labeling of proOmpA with Fluorescein results in a shift on SDS-PAGE that is greater with the number of attached fluorophores. For double (lanes 6, 8) and triple (lane 10) labeled proOmpA no additional, lower molecular weight, bands occur. B) Bleaching of surface immobilized Cy3-labeled proOmpA$_{C108, C198, C290}$ in a confocal microscope. The individual fluorophores bleach in distinct steps*

Discussion

Fluorescent labeling of preproteins is a useful tool for *in vitro* studies on protein translocation as it enables to work with saturating substrate concentrations and avoids handling of radioactive materials. Moreover, it broadens the spectrum of biochemical and biophysical techniques that can be employed to study details of the translocation process. Cysteine specific labeling with fluorescent dyes is highly efficient for all tested positions on proOmpA which is likely due to the unfolded nature of the purified preprotein in high concentrations of urea (6-8 M). Through a yet undetermined mechanism, translocation of fluorescently labeled proOmpA is inhibited *in vitro* when the label is attached at certain positions, in particular at position near to the N-terminus, i.e., 4 [149] and 66, but also position 245 seems unfavorable (Fig 2). Additionally, the translocation efficiency drops with the bulkiness of the attached fluorophore (Fig 2). The latter effect becomes more prominent in combination with the site-specific inhibition. Especially, the translocation of N-terminal labeled proOmpA is strongly inhibited with bulky fluorophores (Fig 2). Interestingly, translocation of a proOmpA mutant labeled with the most bulky fluorophore AF568 at C245 results exclusively in a specific translocation intermediate indicating that translocation cannot be completed, and that a partially translocated preprotein is trapped in the channel. Cleavage of the not translocated part by the externally added protease results in the observed lower molecular mass band on SDS-PAGE.

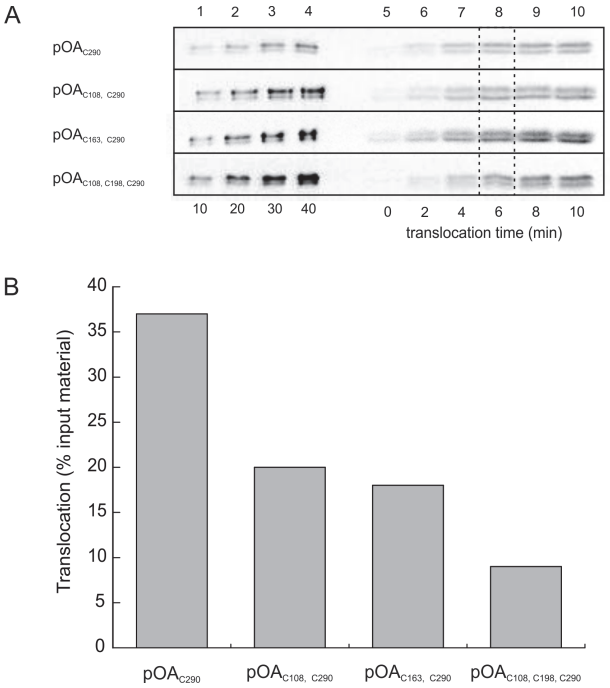

Figure 6: *Translocation efficiency of fluorescently labeled single, double and triple cysteine mutants.*

AF568 carries a single negative charge which could, besides the bulkiness, add to the observed inhibition. However, in a study that investigated the effect of long stretches of positively or negatively charged amino acids in proOmpA, multiple (>10) negative charges were necessary to significantly inhibit protein translocation *in vitro*. Therefore, the single negative charge on AF568 has most likely only a minor effect. The intermediates observed for proOmpA labeled with Flu and TR at positions 33-198 resemble the previously described intermediate of proOmpA termed I26 which occurs due to a hydrophobic patch at position 261-265 in the proOmpA molecule [261]. This hydrophobic patch appears to be a thermodynamic hurdle causing a transient delay or stop in translocation. SecYEG mutants with a PrlA4 phenotype were previously shown to allow translocation of a proOmpA mutant carrying a fluorescent probe at position 4 after the signal sequence. PrlA4 mutants were originally identified as suppressors of the translocation defects of preproteins with missing or defective signal sequences. In case of the enhanced translocation of C4 labeled proOmpA it seemed that also abnormal structural elements in the vicinity of the signal sequence are accepted by PrlA4. In this respect, this region presumably forms a hairpin-like structure with the signal sequence, and appears to be rather critical in the initiation of translocation. Here, we show that PrlA4EG restores translocation defects of several proOmpA mutants labeled with AF568 at various positions up to amino acid position 163, remote from the signal sequence. We conclude that PrlA4 mutations affect the proofreading throughout the entire translocation process rather than acting only on signal sequence

defects. Proofreading might be reminiscent of channel opening, and it has been suggested that the PrlA mutants exhibit a relaxed mechanism of channel opening. Many of the mutations cluster in the central constriction ring and the plug domain, and thus such mutations may give rise to a destabilized pore that would otherwise require the function of SecA in channel opening.

Translocation of double and triple labeled proOmpA mutants displayed a labeling position dependent inhibition similar to this observed for single labeled proOmpA. When the first fluorophore was attached close to the N-terminus at position 33 or 66, translocation was impaired severely. However, fluorescein at position 33 hardly inhibited translocation in the single cysteine proOmpA mutant. Possibly, the number of fluorophores adds another hurdle to the site (N-terminus) specific inhibition effect observed with fluorescent labeling, thus resulting in much lower translocation efficiency. ProOmpA can be labeled with fluorescent dyes in stoichiometric amounts respective to the number of the cysteines. This is visible by a shift in molecular mass on SDS-PAGE that is proportional to the number of attached fluorophores and the absence of additional bands that are expected with incomplete labeling. Strikingly, bleaching of surface attached multiple labeled proOmpA results in distinct bleaching events which number matches the number of cysteines in the preprotein. Translocation of multiple labeled proOmpA is less efficient than single labeled proOmpA and the level of inhibition is proportional to the number of attached fluorophores. Thus, bulky molecules attached to the preprotein present a general hurdle for the translocon, possibly by locally extending the thickness of the polypeptide chain, interfering with SecA function or because of space constraints in the SecYEG channel. Even though the kinetics of translocation of such multiple labeled preproteins is reduced, their translocation competence renders them suitable for further single molecule translocation investigations. .

Material and Methods

Purification of proOmpA, SecA, SecB, IMVs, fluorescent labeling of proOmpA and the discontinuous *in vitro* protein translocation assay is described in detail elsewhere [211]. In gel fluorescence of SDS-PAGE gels with fluorescently labeled proOmpA was visualized in a Roche Lumi Imager. Bleaching experiments with Cy3 labeled proOmpA were done in a home build confocal microscope employing a 523 nm Nd-Yttrium laser. Microscopic glass slides were cleaned by 30 min sonication in a 2% Hellmanex solution at 60°C followed by three times washing with MilliQ water and another 30 min sonication in MilliQ. Fluorescently labeled proOmpA was diluted in 8 M Urea, 50 mM Tris HCl pH8 and applied to a clean microscopic cover slip. Visualization of surface attached proOmpA was achieved by a surface scan (50x50 µm) and fluorescent spots were selected for fluorescent bleaching by focusing the laser beam on the particular spot and measuring the emitting fluorescence over time.

CHAPTER 9

SUMMARY

Summary and Concluding Remarks for Scientists

Summary for the Unacquainted

Samenvatting for Leken

Zusammenfassung für Laien

Summary and Concluding Remarks

For Scientists

Introduction

In all living organisms, proteins are synthesized inside the cells, in the cytoplasm. To function inside the various lipid enclosed compartments of eukaryotes or in the cell envelope and at the cell surface of bacteria and archaea, proteins need to be transported across the lipid membrane, which acts as a natural barrier for macromolecules. In bacteria, the major route for this vectorial transport process, called protein secretion or protein translocation, is the Sec-pathway (for review see chapter 1). It consists of a multi-protein machinery, termed translocon, that includes a highly conserved protein conducting membrane channel, SecYEG, the ATPase SecA and in some bacteria a molecular chaperone, SecB. This minimal translocon is capable of secreting proteins whereas for membrane protein insertion ribosomes and other membrane proteins, such as the insertase YidC, associate with the SecYEG channel. Proteins destined for secretion, the so called preproteins, are recognized by SecB at their N-terminal signal sequence and targeted to the SecYEG bound SecA motor protein. SecA mediates the translocation of preproteins through multiple cycles of ATP binding and hydrolysis. Since the mid 1980s, a multitude of biochemical and structural data have been published on a variety of mechanistic details of this multi-protein machinery. A milestone in the field has been the reconstitution of the translocon *in vitro* from purified components in 1990, a method that has been refined ever since (see chapter 2, 5-7). Yet, the mechanism of SecA mediated protein translocation is unknown. This is partially due to the intrinsic difficulty investigating the special environment of the translocon, the membrane-water interface. However, new developments in fluorescence microscopy lead the way for a detailed view on various aspects of the bacterial translocation machinery. In this thesis, new fluorescence based methods were applied and/or developed to investigate the oligomeric state of SecA and SecYEG during the protein translocation process. These methods may be applied to other systems that involve ligand-receptor interactions and variable oligomerization.

Dual-color fluorescence-burst analysis (DCFBA)

DCFBA was recently developed to quantify the efflux of fluorescently labeled particles out of membrane vesicles and was now modified to study ligand-receptor interaction and the oligomeric state of the receptor bound ligand (for review see chapter 3). In contrast to other similar methods, DCFBA not only determines the fraction of co-migrating particles but further quantifies the relative ratio or stoichiometry of the two, differently labeled, components. This is accomplished by identifying overlapping fluorescence bursts and calculating the ratio of fluorescence intensity of one fluorophore over the intensity of the second, spectrally well separated fluorophore. In this way the extend of membrane leakage of a fluorescent marker molecule or the amount of fluorescently labeled receptor bound to its membrane receptor can be quantified on freely diffusing particles. Another advantage of DCFBA

over other methods analyzing co-migrating particles, such as Fluorescence cross-correlation spectroscopy (FCCS), is that the size-distribution and varying number of fluorescent components per particle is not interfering with the analysis. This is important when (proteo-) liposomes are involved in the measurements as their size and number of embedded membrane proteins varies considerably. Thus, DCFBA is a new tool to investigate the oligomeric state of soluble ligands when bound to their membrane embedded receptor in equilibrium and at low nanomolar protein concentrations.

The oligomeric state of SecA

SecA is a soluble ATPase that exists as a homo-dimer in the cytosol and associates with the membrane channel SecYEG during protein translocation. Its oligomeric state when engaged in protein translocation has been controversial as several studies concluded that SecA may monomerize during protein translocation while other studies found SecA active as a dimer. Employing DCFBA and FCCS, the quaternary structure of SecA in solution and when bound to its membrane receptor SecYEG is investigated in chapter 4. SecA was confirmed to exist as a dimer in solution but the dissociation constant for this dimerization turned out to be very low (~ 0.74 nM) and was for the first time determined in equilibrium. Covalently crosslinked SecA was found to bind to SecYEG with an identical ratio as non crosslinked SecA indicating that the latter also binds as a dimer. Interestingly, at high salt concentrations, the non crosslinked SecA was found to bind as a monomer with similar dissociation constant as the crosslinked SecA dimer. This data suggest an asymmetric binding of the SecA dimer to SecYEG as one SecA protomer binds in a salt resistant and the other in a salt sensitive manner. Possibly, one SecA interacts directly with SecYEG whereas the second protomer binds to the SecYEG associated copy. This hypothesis was found to be compatible with the *T. maritima* SecA-SecYEG co-crystal and SecA dimer structures of *E. coli* and *B. subtilis* as well as several crosslinking studies. Previously, SecA was proposed to cycle between solution and the membrane interface. By conducting *in vitro* protein translocation experiments with limiting SecA concentrations, an apparent K_M of the reaction could be determined in chapter 4. Comparison of the binding affinity of SecA for SecYEG (~3.6 nM) to the apparent K_M (~ 100 nM) lead to the conclusion that membrane cycling of SecA is an important feature of the mechanism of protein translocation.

The oligomeric state of SecYEG

The protein conducting channel of bacteria, SecYEG, is a hetero-trimeric membrane protein complex that has been found to form higher oligomeric states, in particular dimers, in the membrane, in addition to the monomer. However, the functional oligomeric state during protein translocation is controversial. Employing reconstitution of fluorescently labeled SecYEG into liposomes followed by formation

of giant unilamellar vesicles (GUVs) allowed the assessment of the oligomeric state of SecYEG at the single molecule level (chapter 5). SecYEG was found to monomeric in presence or absence of the motor protein SecA and translocation ligands. Formation of a translocation intermediate of the fluorescently labeled fusion protein proOmpA-DhfR trapped inside SecYEG could be monitored by FRET in bulk and in GUVs by FCCS-FRET demonstrating the activity of the GUV embedded SecYEG channel. Moreover, the vast majority of correctly oriented SecYEG channels is active in the GUVs which further supports the observation that SecYEG functions as a monomer.

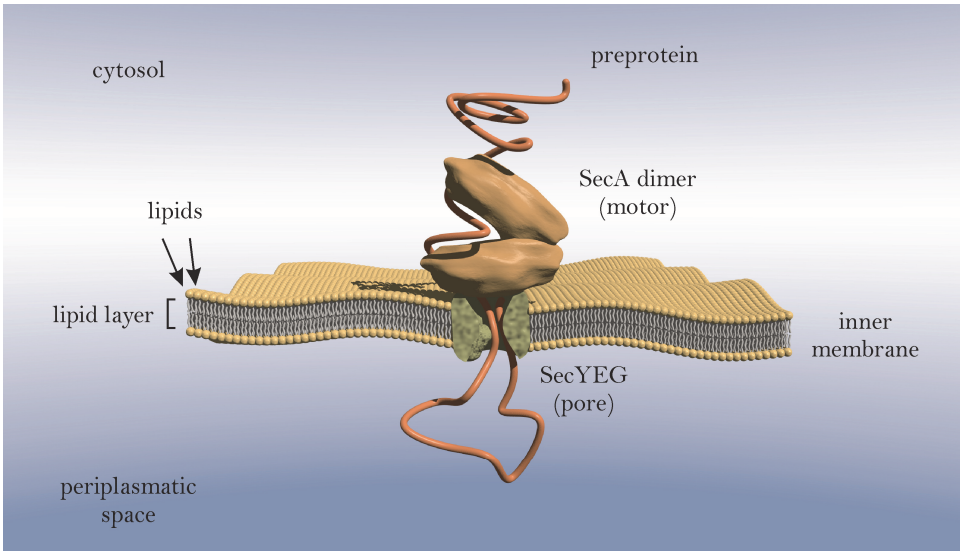

Figure 1: The bacterial protein secretion pathway. *The dimeric motor protein SecA drives translocation of an unfolded preprotein through the protein conducting membrane channel SecYEG.*

New tools to study protein translocation and membrane proteins at the single molecule level

Membrane proteins are intrinsically difficult to investigate due to the unique environment of the elastic and sensitive biological membrane. However, immobilization of membranes such that the embedded membrane proteins retain their function will open new ways to investigate this intriguing environment by means of fluorescence microscopy and other biophysical methods. Hydrogels composed of organic gelators that self assemble into nano-scaled fibers allow immobilizing membrane vesicles and (proteo-) liposomes without disturbing the membrane integrity (chapter 6). Moreover, the activity of soluble and membrane proteins is maintained when such proteins are trapped in the hydrogel as demonstrated by *in vitro* protein translocation and opening of the mechanosensitive channel of large conductance, MscL embedded in GUVs (chapter 6). An inherent disadvantage of gels is that transport of

molecules occurs solely by diffusion, complicating exchange or addition of substances such as ATP. Therefore, surface immobilization of inner membrane vesicles (IMVs) onto a glass surface of a flow cell suitable for microscopic studies was applied via biotin-streptavidin interaction in chapter 7. In this setup, protein translocation can be monitored by accumulation of fluorescently labeled proOmpA at the location of IMVs that contain SecYEG, labeled with a spectrally separated fluorophore. As the number of SecYEG channels in IMVs is high and difficult to control, surface immobilization of proteoliposomes (PLs) with a low copy number of SecYEG was tested. Unfortunately, the interaction of the PLs with the surface resulted in loss of activity. However, with this method, protein translocation can be studied on single vesicle level although it lacks single molecule sensitivity due to the high background binding of proOmpA to the IMVs. The detection limit for proteins and ensemble averaging in conventional biochemical assays hampers studies at very low (nanomolar) protein concentrations. Therefore, a new *in vitro* protein translocation assay in suspension was developed, based on co-migration of SecYEG containing PLs and fluorescently labeled proOmpA quantified by DCFBA (chapter 7). Due to the single particle resolution, not only the activity of a set of PLs can be tested but also the fraction of active PLs in the batch. The translocation activity of few to single-SecYEG PLs is evident as significantly higher amounts of proOmpA co-migrate with the PLs in presence of ATP compared to experiments without ATP. Although this discontinuous assay has true single molecule sensitivity for both SecYEG and proOmpA, it lacks time resolution. This assay may be useful for investigations of the activity of single-SecYEG PLs. Labeling components of the Sec-pathway with fluorescent probes has been a powerful tool in many protein translocation studies. In particular useful was the introduction of fluorescently labeled proOmpA as it allows detecting even single translocating preproteins. In previous studies, however, labeling of certain residues on proOmpA inhibited translocation *in vitro*. Therefore, we conducted a systematic study on the translocation of proOmpA labeled at various sites (chapter 8). Residues towards the N-terminus were sensitive to labeling with bulky fluorescent probes, a trend that was also visible when multiple residues were labeled. Furthermore, inhibition of translocation increased proportionally to the number of fluorophores attached to proOmpA. However, the advantages of fluorescently labeled preprotein outweigh this inhibition which exact mechanism is unknown.

Perspective

Analysis of movements of preproteins being transported across SecYEG will be pivotal to our understanding of the mechanism of protein translocation. As the ensemble averaging nature of conventional biochemical assays blurs details of this dynamic process, single molecule techniques may be powerful tools in elucidating further details. One way of monitoring single preproteins translocating may be by the use of Förstner Resonance Energy transfer (FRET) between fluorophores attached to proOmpA and SecYEG. During translocation, multiple donor fluorophores on

proOmpA may sequentially transfer their excitation energy to an acceptor fluorophore attached to the exit of the SecYEG pore. In this manner, preprotein movements could be analyzed at the single molecule level addressing questions as to the step size, processivity or intermediate states of protein translocation. For these experiments, however, it is essential for SecYEG channels to remain in the observation area of a microscope. Future efforts should focus on the functional immobilization of biological membranes with embedded SecYEG that is compatible with the other components of the *in vitro* translocation system.

Summary and Concluding Remarks

For the Unacquainted

Introduction

All living organisms are made of cells that are surrounded by a membrane that consists of water-repelling fatty molecules, the lipids (Figure 1). Higher organisms also have compartments inside their cells. The organelles are also enclosed by a lipid membrane. The membrane forms a barrier for large molecules such as proteins, DNA or nutrition molecules and prevents them from leaking from the cell or organelle. Some proteins, however, function inside of organelles, at the cell surface or outside the cell and need to be transported across the membrane barrier. For this reason, every cell has a specialized machinery to transport proteins across or into the lipid membrane. This machinery is made of proteins that are the main topic of this thesis (Figure 1).

Proteins fulfill many functions in the cell. Some are molecular machines such as enzymes and motor proteins and others form structures that create the different shapes cells can have. Another, specialized, subset of proteins is integrated into lipid membranes, the membrane proteins. Among other functions they are responsible for nutrition uptake into the cell, motility, sensing and interaction with the outside environment and communication with other cells. All proteins are synthesized at the ribosomes inside the cells, in the cytoplasm, but many need to be transported across or integrated into a lipid membrane. In bacteria, which are single cell organisms surrounded by one or two membranes, the major route for this protein export is called the Sec-pathway. This process, termed protein secretion or protein translocation, is described in detail in chapter 1. The Sec-pathway is a multi-protein machinery, the 'translocon', and consists of a membrane protein complex, SecYEG, that forms a water-filled channel in the membrane and a water-soluble motor protein, SecA (Figure 1B). This minimal translocon is capable of secreting proteins whereas for membrane protein insertion into the membrane, ribosomes and other membrane proteins associate with the SecYEG channel. Proteins destined for secretion, called preproteins, have a special amino-terminal amino-acid sequence, the signal sequence, which serves as recognition tag for the Sec-machinery. With the help of this signal sequence the preproteins are directed to the SecYEG bound SecA motor protein. SecA uses the biological fuel ATP as an energy source to transport the preprotein through the SecYEG channel to the other side of the membrane. How SecA does this is unknown although this process is topic of intense studies for at least a decade. In the cytoplasm, two SecA proteins attach to each other and form a so called dimer (two copies of the same protein are called a homo-dimer while a single copy is called monomer). The question whether SecA also stays a dimer when interacting with the membrane channel SecYEG during protein secretion or whether one SecA copy is released from the complex is a matter of controversy.

A milestone in the field has been the re-constitution of a functional Sec-pathway in a test tube ('*in vitro*') using isolated and purified components. For this method, first published in 1990, SecA and SecYEG containing membranes are separated from the

various other components of a cell, i.e. purified, and combined again in a test tube to perform the protein secretion reaction (see chapter 2, 5-7). Although many details of the translocation reaction could be unraveled with this method, the mechanism of SecA function remain unclear. This is partially due to the intrinsic difficulty of investigating the special environment of the translocon, the membrane - water interface. However, new developments in fluorescence microscopy lead the way for a detailed view on various aspects of the bacterial translocation machinery.

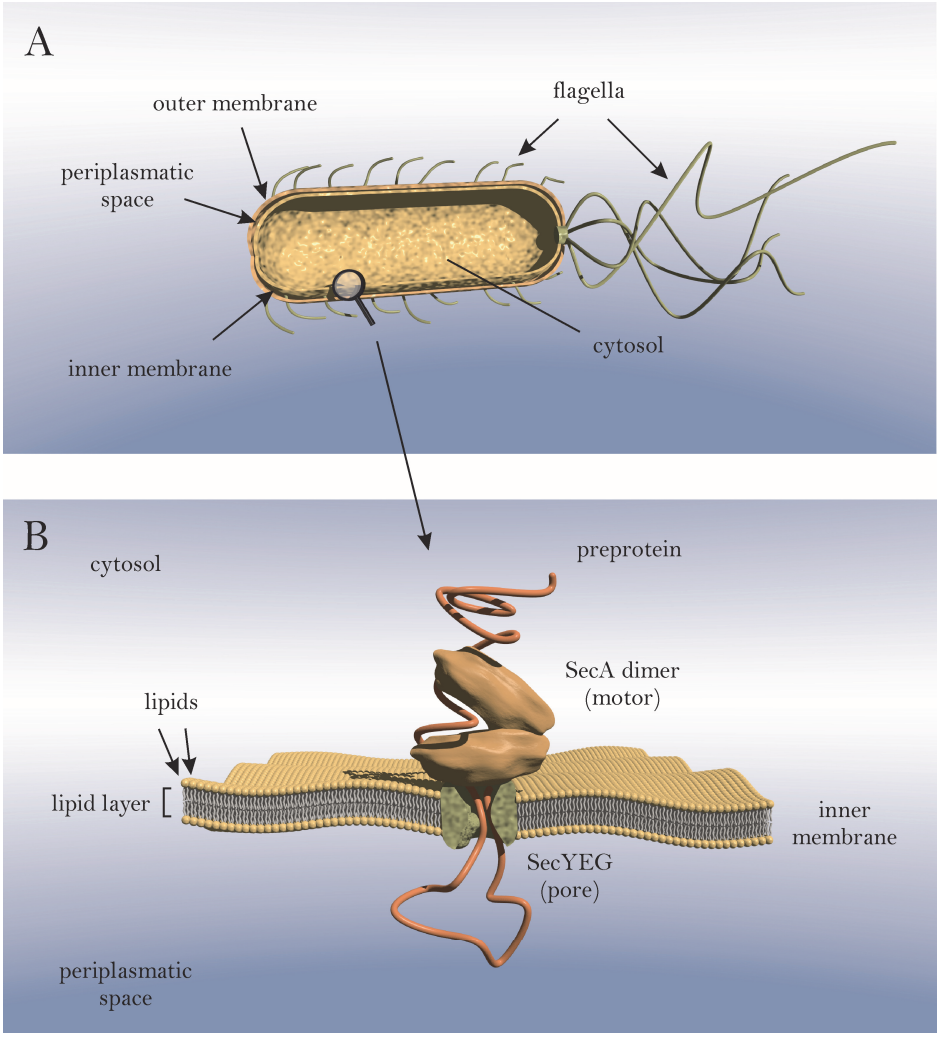

Figure 1: *The bacterium Escherichia coli and the bacterial protein secretion pathway. A) The bacterium E. coli has two membranes that are separated by a periplasmatic space. B) Translocation across the inner membrane is mediated by the Sec-machinery. The dimeric motor protein SecA drives translocation of a preprotein through the membrane channel SecYEG.*

In this thesis, new fluorescence based methods were applied and/or developed to investigate SecA and SecYEG during the protein translocation process. Here, the focus lies with the question whether SecA remains a dimer during protein translocation and whether SecYEG functions as monomer or dimer. The developed methods can now be applied to investigate other protein machineries with membrane proteins and soluble proteins that interact with each other.

Fluorescence and labeling with fluorescent dyes

Fluorescent molecules, called fluorophores, absorb light of a specific color (the excitation light). A very short time (nano seconds) after this, they release light of a different color (fluorescence). In a modern fluorescent microscope, the excitation light is filtered out and even single fluorescent molecules can be observed. These fluorophores can be attached to proteins in order to investigate the behavior of single fluorescently labeled proteins. In this thesis, SecA, SecYEG and the model preprotein proOmpA were fluorescently labeled.

Dual-color fluorescence-burst analysis (DCFBA)

In this thesis, DCFBA,method was modified to study the SecA-SecYEG interaction and to address the question whether SecA is a dimer or monomer when bound to SecYEG (for a detailed summary of DCFBA see chapter 3). DCFBA is a new tool to investigate interactions of membrane proteins and soluble proteins. At the same time, it can be used to determine whether a protein is a monomer or a dimer.

The oligomeric state of SecA

SecA is a soluble motor-protein that exists as a homo-dimer in the cytosol and associates with the membrane channel SecYEG during protein translocation. The phenomenon that several copies of proteins associate and form complexes is termed 'oligomeric state'. Using DCFBA and another method, Fluorescence cross-correlation spectroscopy (FCCS), the oligomeric state of SecA in solution and when bound to its membrane receptor SecYEG is investigated in chapter 4. SecA was confirmed to exist as a dimer in solution and found to also bind as a dimer to SecYEG. Interestingly, in the presence of high amounts of salt, SecA binds as a monomer to SecYEG and can be kept as a monomer in solution. This data suggest an asymmetric binding of the SecA dimer to SecYEG as one SecA binds in a salt resistant and the other in a salt sensitive manner. Possibly, one SecA interacts directly with SecYEG whereas the second protomer binds to the SecYEG associated copy (chapter 4, Fig. 8).

The oligomeric state of SecYEG

The protein conducting channel of bacteria, SecYEG, is a hetero-trimeric membrane protein complex (three different proteins associating to one complex) that has been found to form higher oligomeric states, in particular dimers, in the membrane. However, the functional oligomeric state during protein translocation is a topic of controversy. In chapter 5, fluorescently labeled SecYEG was investigated in the membrane. SecYEG was found to be monomeric in the presence or absence of the motor protein SecA and other translocation components.

New tools to study protein translocation and membrane proteins at the single molecule level

Membrane proteins are intrinsically difficult to investigate due to the unique environment of the elastic and sensitive biological membrane. However, immobilization of membranes such that the embedded membrane proteins retain their function will open new ways to investigate this intriguing environment by means of fluorescence microscopy and other biophysical methods. In chapter 6, hydrogels composed of organic gelators are used that self assemble into nano-scaled fibers and that allow immobilizing membranes and the membrane proteins within. Importantly, the activity of soluble and membrane proteins is maintained when such proteins are trapped in the hydrogel as demonstrated by *in vitro* protein translocation and opening of the mechanosensitive channel MscL (chapter 6).

To address different questions, membrane vesicles were immobilized on a glass surface in chapter 7. With this method, protein translocation could be monitored over a long time period on single membrane vesicles. Because these membrane vesicles contain many SecYEG channels, a new protein translocation assay was developed that allows detection of the activity of single SecYEG channels (chapter 7).

Labeling components of the Sec-pathway with fluorescent probes has been a powerful tool in many protein secretion studies. In particular useful was the introduction of fluorescently labeled proOmpA as it allows detecting even single translocating preproteins. In previous studies, however, fluorescent labeling of certain proOmpA mutants caused a reduction of protein translocation activity. Therefore, we conducted a systematic study on this matter (chapter 8).

Perspective

In order to understand the way how the Sec-machinery exactly works, more details of this process need to be unraveled. However, conventional methods cannot resolve such details because too many molecules are observed at the same time. By fluorescent microscopy single fluorescently labeled proteins can be detected and to followed in time. Thus, fluorescent microscopy may give us insights into the mechanism of protein secretion and functioning of the SecA motor protein. Thereby, analysis of movements

of preproteins being transported across SecYEG will be important and can be addressed by fluorescence microscopy. For these experiments, however, it is essential for SecYEG channels to remain in the observation area of a microscope. Future efforts should focus on the functional immobilization of biological membranes with embedded SecYEG that is compatible with the other components of the *in vitro* protein translocation system.

SAMENVATTING

Voor Leken

Introductie

Alle levende organismen zijn opgebouwd uit cellen die omgeven zijn door een membraan die bestaat uit vetmoleculen, de lipiden (figuur 1). Eukaryoten hebben ook compartimenten binnenin de cel, de organellen, die ook omsloten worden door een lipide membraan. Deze membranen vormen een barrière voor grote moleculen zoals eiwitten, DNA of bouwsteenmoleculen zodat deze niet uit de cel lekken. Sommige eiwitten functioneren in organellen, aan het celoppervlak of buiten de cel en moeten over deze membraan barrière worden getransporteerd. Hiervoor heeft elke cel een gespecialiseerd complex om eiwitten over of in de membraan te transporteren. Dit complex bestaat uit eiwitten en is het hoofdonderwerp van dit proefschrift.

Eiwitten voeren veel functies uit in de cel. Sommigen zijn moleculaire machines zoals enzymen en motoreiwitten en anderen vormen structuren die de vorm van de cel bepalen. Weer een andere subset van eiwitten, de membraaneiwitten, is geïntegreerd in de lipide membraan. Zij zijn onder andere verantwoordelijk voor voedingsopname in de cel, beweegbaarheid, detectie en communicatie met andere cellen. Alle eiwitten worden gesynthetiseerd door de ribosomen in de cel, in het cytoplasma, maar veel worden getransporteerd over of geïnserteerd in de lipide membraan. In bacteriën, eencellige organismen omringd door 1 of 2 membranen, is de hoofdroute voor dit eiwittransport de zogenaamde Sec-route (figuur 1A).

Dit proces, genaamd eiwitsecretie of eiwittranslocatie, is in hoofdstuk 1 in detail beschreven. De Sec-route is een multi-eiwit complex, genaamd het translocon en bestaat uit een membraaneiwit complex, SecYEG, dat een water-gevuld kanaal vormt in de membraan en een water oplosbaar motor eiwit, SecA (figuur 1B). Het minimale translocon is in staat om eiwitten te transporteren, maar voor membraaneiwitinsertie zijn ribosomen en andere membraaneiwitten geassocieerd aan SecYEG nodig. Eiwitten bestemd voor uitscheiding, zogenaamde precursoreiwitten, hebben een speciale N-terminale aminozuur sequentie, die dient als herkenningspunt voor het Sec mechanisme. Met behulp van deze signaal sequentie kunnen de precursoreiwitten worden gedirigeerd naar het SecYEG gebonden SecA motoreiwit. SecA gebruikt de biologische brandstof ATP als energiebron om het precursoreiwit door het SecYEG kanaal te transporteren naar de andere kant van de membraan.

Hoe SecA dit doet is grotendeels onbekend, hoewel intensief onderzoek is verricht aan dit onderwerp. In het cytoplasma hechten twee SecA eiwitten zich aan elkaar en vormen een dimeer (2 kopieën van hetzelfde eiwit vormen een homodimeer en een enkele kopie wordt een monomeer genoemd). De vraag of hetzelfde SecA ook een dimeer blijft als het een interactie aangaat met het SecYEG kanaal tijden eiwittranslocatie of wanneer een SecA wordt losgelaten is een onderwerp van controverse.

Een mijlpaal in het veld was de reconstitutie van de Sec-route in een reageerbuis (*'in vitro'*) met geïsoleerde componenten. Voor deze methode, voor het eerst

gepubliceerd in 1990, werden SecA en SecYEG bevattende membranen gezuiverd en weer gecombineerd in een reageerbuis om eiwittranslocatie uit te voeren (zie hoofdstuk 2, 5-7). Hoewel veel details aangaande de functie van het translocon opgehelderd konden worden, de details hoe SecA functioneert bleven onduidelijk. Dit komt gedeeltelijk door de intrinsieke moeilijkheid om de speciale omgeving van het translocon te bestuderen, het grensvlak tussen de membraan en het water. Nieuwe ontwikkelingen in fluorescentie microscopie maken het echter mogelijk om verschillende aspecten van het bacteriële translocatie mechanisme te bekijken in detail.

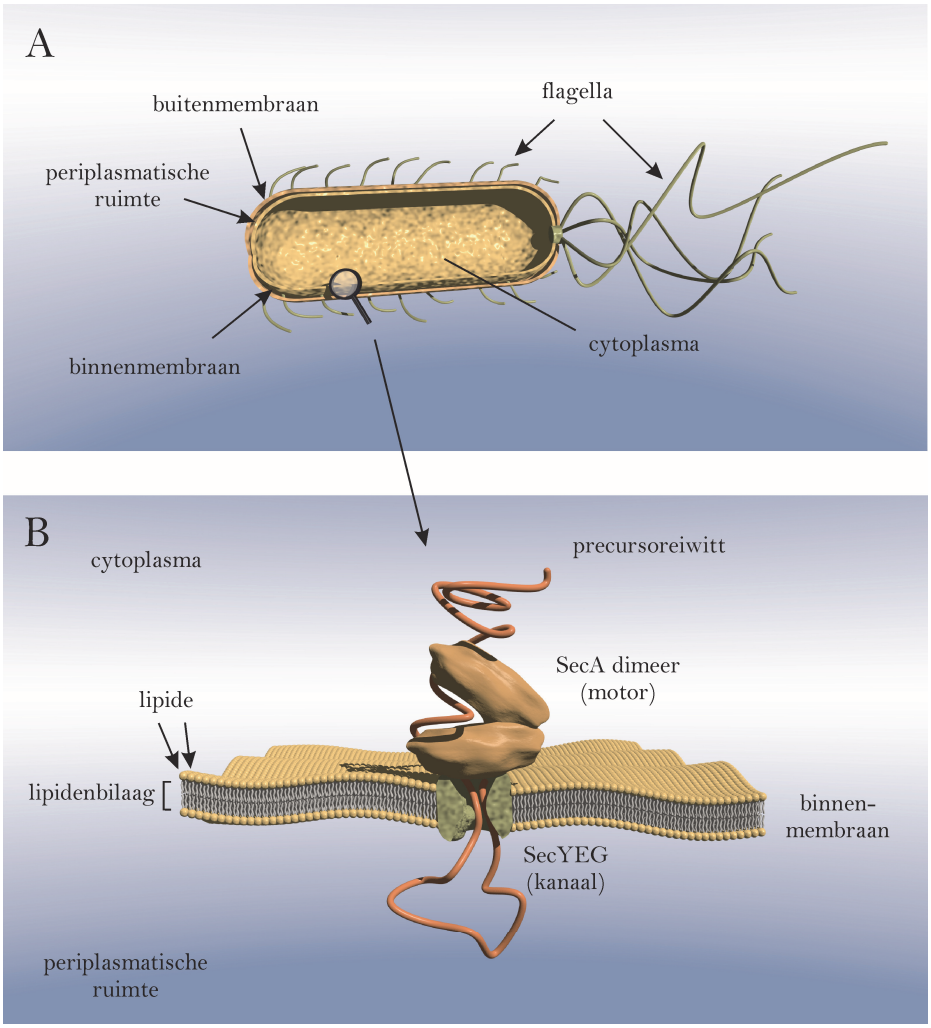

Figuur 1: *Het bacterie Escherichia coli en de bacteriële eiwitsecretie route. A) E. coli beschikt over twee membranen die gescheiden worden door de periplasmatische ruimte. B) Het transport van eiwitten over de binnenmembraan wordt gemedieerd door de Sec-machinerie. Het dimere motoreiwit SecA drijft de translocatie van een precursoreiwit door het membraankanaal SecYEG.*

In dit proefschrift worden nieuwe methoden gebaseerd op fluorescentie toegepast en/of ontworpen om SecA en SecYEG te onderzoeken tijdens het eiwittranslocatie proces. De focus ligt op de vraag of het SecA een dimeer blijft tijdens eiwit translocatie en of SecYEG functioneert als een monomeer of een dimeer. De methoden die ontworpen zijn kunnen worden toegepast om andere eiwitcomplexen te bestuderen met membraaneiwitten en oplosbare eiwitten die interactie met elkaar aangaan.

Fluorescentie en labelen met fluorescente kleurstoffen

Fluorescente moleculen, zogenaamde fluoroforen, absorberen licht van een bepaalde kleur (het excitatie licht). Een hele korte tijd hierna (nanoseconden), laten zij het licht in een andere kleur weer los (fluorescentie). In een moderne fluorescente microscoop wordt het excitatie licht eruit gefilterd en kan zelfs een enkel fluorescent molecuul worden geobserveerd. Deze fluoroforen kunnen aan eiwitten gekoppeld worden en hierdoor kan het gedrag van een enkel fluorescent gemerkt eiwit bestudeerd worden. In dit proefschrift worden SecA, SecYEG en het precursor eiwit proOmpA fluorescent gemerkt.

Tweekleuren fluorescentie-uitbarsting analyse (DCFBA)

In dit proefschrift werd de DCFBA methode gemodificeerd om SecA-SecYEG interactie te bestuderen en de vraag te onderzoeken of SecA een dimeer of een monomeer is wanneer het gebonden is aan SecYEG (voor een gedetailleerde samenvatting van DCFBA, zie hoofdstuk 3). DCFBA is een nieuwe methodiek om interacties te onderzoeken tussen membraaneiwitten en oplosbare eiwitten. Op hetzelfde moment kan worden bepaald of het eiwit een monomeer of een dimeer is.

De oligomere toestand van SecA

SecA is een oplosbaar motoreiwit dat als een homodimeer bestaat in het cytosol en geassocieerd is met het membraankanaal SecYEG tijdens eiwittranslocatie. Dit fenomeen dat enkele kopieën van eiwitten associëren en complexen vormen wordt de 'oligomere toestand' genoemd. Door gebruik van DCFBA en een andere methode, fluorescentie kruis-correlatie spectroscopie (FCCS), worden de oligomere toestand van SecA in oplossing en gebonden aan SecYEG bestudeerd in hoofdstuk 4. Het werd bevestigd dat SecA als een dimeer bestaat in oplossing en ook als een dimeer bindt aan SecYEG. Interessant was dat SecA als een monomeer bindt aan SecYEG en als een monomeer in oplossing kan bestaan in aanwezigheid van hoge zout concentraties. Deze data suggereert een asymmetrische binding van het SecA dimeer aan SecYEG, aangezien 1 SecA kopie bindt op een zoutresistente manier en de ander op een zoutgevoelige. Mogelijkerwijs bindt 1 SecA direct aan het SecYEG en de tweede protomeer aan het SecYEG gebonden SecA molecuul. (Hoofdstuk 4, Fig. 8)

De oligomere toestand van SecYEG

Het eiwittranslocatiekanaal van bacteriën, SecYEG, is een heterotrimeer membraaneiwit complex (drie verschillende eiwitten associëren tot 1 complex) dat volgens onderzoeken bestaat in hogere oligomere toestanden, voornamelijk dimeren. Maar de functionele oligomere toestand tijdens eiwittranslocatie is een controversieel aspect van studie. In hoofdstuk 5 werd fluorescent gemertk SecYEG onderzocht in de membraan. SecYEG werd als monomeer gevonden in de aanwezigheid en afwezigheid van het motoreiwit SecA en andere translocatie componenten.

Nieuwe tools om eiwittranslocatie en membraaneiwitten op een enkel molecuul niveau te bestuderen

Membraaneiwitten zijn intrinsiek moeilijk te bestuderen door de unieke omgeving van het elastische en gevoelige biologische membraan. Maar immobilisatie van membranen zodat membraaneiwitten hun functie behouden zal de weg openen om deze intrigerende omgeving te bestuderen met fluorescentie microscopie en andere biofysische methoden. In hoofdstuk 6 worden hydrogelen, bestaand uit organische chelatoren, gebruikt die zichzelf opbouwen tot vezels op nanoschaal en die het mogelijk maken membranen te immobiliseren met de membraaneiwitten erin. Belangrijk is dat de activiteit van oplosbare en membraaneiwitten behouden blijft wanneer ze gevangen worden in de hydrogel zoals we laten zien door *in vitro* eiwit translocatie en het openen van het mechanosensitieve MscL kanaal (hoofdstuk 6).

Om verschillende vragen te beantwoorden werden membraanvesikels geïmmobiliseerd op een glazen oppervlak in hoofdstuk 7. Met deze methode kon eiwittranslocatie voor een lange periode bekeken worden in enkele membraanvesikels. Omdat deze membraan vesikels veel SecYEG kanalen bevatten, werd een nieuwe translocatie assay ontwikkeld die het mogelijk maakt om de activiteit van een enkel SecYE kanaal te detecteren (hoofdstuk 7).

Het labelen van componenten van de Sec-route met fluorescente merkers is een krachtige tool geweest in veel eiwitsecretie onderzoeken. De introductie van het fluorescent gelabelde proOmpA was bijzonder bruikbaar, omdat het mogelijk werd om enkel getransloceerde precursor eiwitten te detecteren. In eerdere onderzoeken veroorzaakte het fluorescent merken van bepaalde proOmpA mutanten een reductie in eiwit translocatie activiteit. Daarom hebben we hierop een systematisch onderzoek uitgevoerd (hoofdstuk 8).

Perspectief

Om te begrijpen hoe het Sec systeem precies werkt, moeten er meer details opgehelderd worden. Maar conventionele methodes kunnen deze details niet bekijken omdat teveel moleculen worden geobserveerd in dezelfde tijd. Door fluorescentie microscopie kunnen enkele fluorescent gelabelde eiwitten gedetecteerd worden en

gevolgd in de tijd. Dus fluorescentie microscopie kan ons inzicht verschaffen in het mechanisme van eiwit secretie en het functioneren van het SecA motoreiwit. Daarbij zullen analyses van de beweging van precursor eiwitten die getransporteerd worden door SecYEG belangrijk zijn en die kunnen bekeken worden met fluorescentie microscopie. Maar voor deze experimenten is het noodzakelijk dat SecYEG in het observatiegebied van de microscoop blijft. Toekomstige inspanningen zullen zich moeten richten op functionele immobilisatie van biologische membranen met daarin SecYEG en moeten verdere gedetailleerde studies van het *in vitro* eiwit translocatie systeem mogelijk maken op enkel molecuul niveau.

Deutsche Zusammenfassung

Für Laien

Einführung

Alle Lebewesen sind aus Zellen aufgebaut, die von Membranen umgeben sind, die aus wasserabstossenden Fettmolekülen, den Lipiden, bestehen (Abbildung 1). Höhere Organismen haben auch gesonderte Räume innerhalb ihrer Zellen. Diese sogenannten Organellen sind auch von Lipidmembranen umschlossen. Biologische Membranen sind Barrieren für grössere Moleküle, wie Proteine, DNA oder Nahrungsmoleküle und verhindern, dass diese die Zelle oder Organelle verlassen. Einige Proteine haben aber Funktionen innerhalb von Organellen, an der Zelloberfläche oder ganz ausserhalb von Zellen und müssen daher über die Membranbarriere hinweg transportiert werden. Um diese Proteine an ihre zugehörigen Stellen zu bringen, hat jede Zelle eine spezialisierte Maschinerie, die Proteine über oder in die Lipidmembran transportieren. Diese Maschinerie ist auch aus Proteinen aufgebaut und ist das Hauptthema dieser Doktorarbeit.

Proteine haben viele verschiedene Funktionen in den Zellen. Einige sind molekulare Maschinen und Motorproteine und andere bilden Strukturen, die die verschiedenen Formen erzeugen, die eine Zelle haben kann. Eine andere, spezialisierte Kategorie von Proteinen, ist direkt in die Lipidmembran integriert, die Membranproteine. Sie sind zum Beispiel für die Nahrungsaufnahme in die Zelle, Bewegung, Erkennung und Interaktion mit der Umgebung sowie für die Kommunikation mit anderen Zellen verantwortlich.

Alle Proteine werden an den Ribosomen innerhalb der Zelle, im Zytosol, synthetisiert, aber viele müssen durch eine Membran transportiert oder in sie integriert werden. In Bakterien, das sind einzellige Lebewesen, die von einer oder zwei Membranen umgeben sind (Abbildung 1A), werden die meisten Proteine über den sogenannten Sec-Weg ausgeschleust. Dieser Prozess, Proteinsekretion oder Proteintranslokation genannt, wird detailliert in Kapitel 1 dieser Arbeit beschrieben. Der Sec-Weg besteht aus einer Multiproteinmaschinerie, dem 'Translokon', die aus einem Membranproteinkomplex, SecYEG, das eine wassergefüllte Pore in der Membran bildet und einem wasserlöslichen Motorprotein, SecA, aufgebaut ist (Abbildung 1B). Dieses minimale Translokon is fähig, Proteine zu sekretieren wohingegen für die Integration von Membranproteinen in die Membran, Ribosomen und andere Membranproteine mit der SecYEG Pore zusammenarbeiten.

Proteine, die für die Sekretion bestimmt sind, werden Preproteine genannt und haben eine spezielle Aminosäuresequenz, die Signalsequenz, die als Erkennungssignal für die Sec-Maschinerie dient. Mit Hilfe dieser Sequenz werden Preproteine zu dem SecYEG gebundenen SecA Motorprotein geleitet. SecA nutzt den biologischen "Treibstoff" ATP als Energiequelle, um Preproteine durch die SecYEG Pore auf die andere Seite der Membran zu transportieren. Wie SecA dies tut, ist unbekannt, obwohl dieser Prozess seit mindestens einem Jahrzehnt Gegenstand intensiver Untersuchungen ist. Im Zytosol von Bakterien heften sich zwei SecA Proteine aneinander und bilden einen sogenannten Dimer (zwei gleiche Proteine, die

aneinander gebunden sind nennt man Homodimer, während ein einzelnes Protein Monomer genannt wird). Die Frage, ob SecA auch ein Dimer bleibt, wenn es mit der Membranpore SecYEG interagiert, oder ob SecA während der Proteinsekretion als Monomer agiert, ist Gegenstand controverser Debatten.

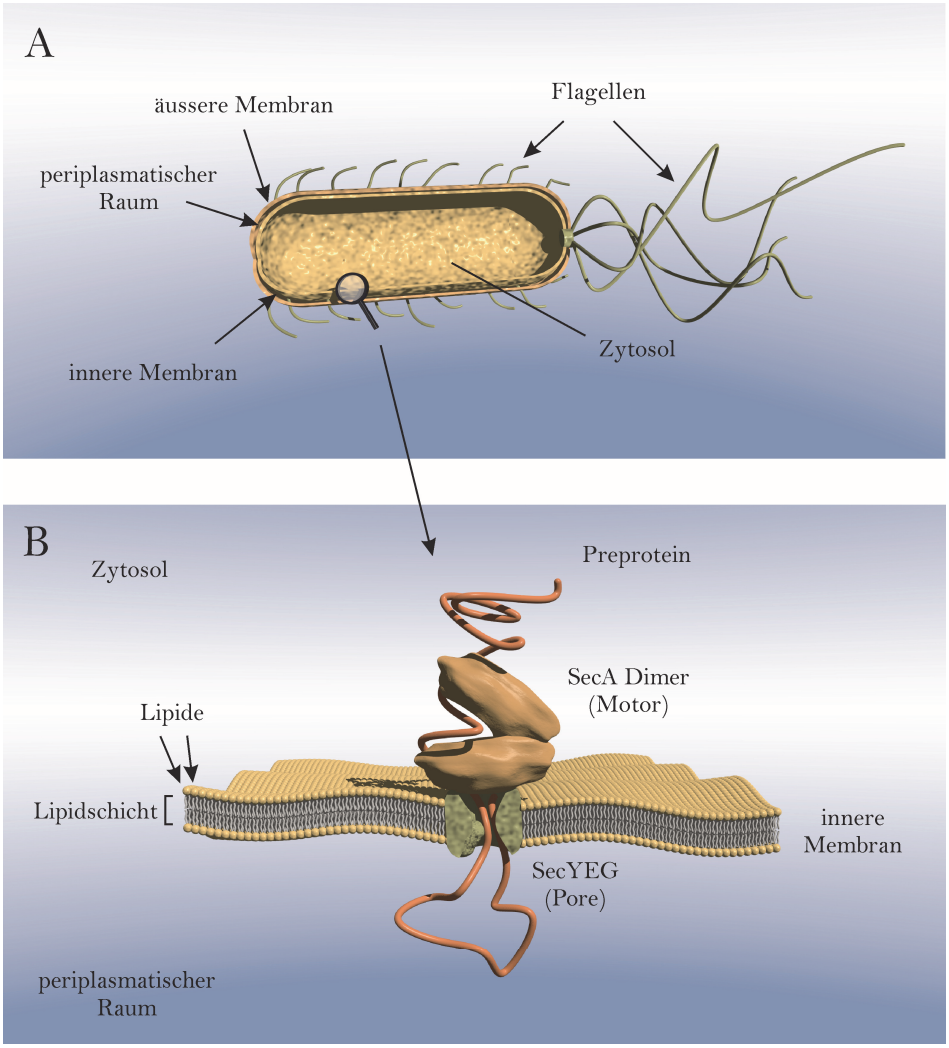

Abbildung 1: *Das Bakterium Escherichia coli und der Proteinsekretionsweg. A) Das Bakterium Escherichia coli hat zwei Membranen, die durch einen periplasmatischen Raum getrennt sind. B) Translokation über die innere Membran wird durch die Sec-Machinerie bewerkstelligt. Das dimere Motorprotein SecA transportiert Preproteine durch die Membranpore SecYEG.*

Ein Meilenstein in diesem Fachgebiet war die Rekonstitution einer funktionierenden Sec-Maschinerie im Reagenzglas (*'in vitro'*) mit isolierten und gereinigten Komponenten. Für diese Methode, erstmals publiziert 1990, werden SecA und SecYEG beinhaltende Membranen von den verschiedenen anderen Komponenten einer Zelle getrennt, d. h. gereinigt, und wieder im Reagenzglas kombiniert, um die Proteinsekretionsreaktion auszuführen (siehe Kapitel 2, 5-7). Obwohl durch diese Methode viele Details der Proteintranslokationsreaktion aufgedeckt werden konnten, bleibt der genaue Mechanismus der Arbeitsweise von SecA unklar. Das ist teilweise bedingt durch die inhärente Schwierigkeit, das spezielle Umfeld des Translokons, die Membran – Wasser Grenzfläche, zu untersuchen. Allerdings bieten neue Entwicklungen in der Fluoreszenzmikroskopie Möglichkeiten, verschiedene Aspekte der bakteriellen Translokationsmaschinerie detailliert zu untersuchen.

In dieser Doktorarbeit wurden neue fluoreszenzbasierte Methoden angewandt und/oder entwickelt, um SecA und SecYEG während des Proteintranslokationsprozesses zu beobachten. Der Fokus hier liegt in der Frage, ob SecA während der Translokation ein Dimer bleibt und ob SecYEG als Monomer oder Dimer arbeitet. Die hier entwickelten Methoden können nun auf andere Proteinmaschinerien angewendet werden, in denen Membranproteine und lösliche Proteine miteinander interagieren.

Fluoreszenz und Markierung mit fluoreszierenden Farbstoffen

Fluoreszierende Moleküle, genannt Fluorophore, absorbieren Licht von bestimmter Farbe (das Anregungslicht). Eine sehr kurze Zeit später (Nanosekunden), geben sie Licht einer anderen Farbe ab (Fluoreszenzlicht). Moderne Fluoreszenzmikroskope können das Anregungslicht rausfiltern und sogar einzelne Farbstoffmoleküle können beobachtet werden. Diese Fluoreszenzfarbstoffe können fest an Proteine angeheftet werden, um das Verhalten von einzelnen fluoreszenzmarkierten Proteinen zu untersuchen. In dieser Arbeit wurden SecA, SecYEG und das Modellpreprotein proOmpA mit Fluoreszenzfarbstoffen markiert.

Zweifarben Fluoreszenzausbruchanalyse (Dual-color fluorescence-burst analysis, DCFBA)

In dieser Arbeit wurde die Methode DCFBA modifiziert, um die SecA-SecYEG Interaktion zu untersuchen und um die Frage, ob SecA ein Dimer bleibt, wenn es an SecYEG bindet, zu beantworten (für eine detaillierte Zusammenfassung der DCFBA-Methode siehe Kapitel 3). DCFBA ist ein neue Methode, um die Interaktion von Membranproteinen mit löslichen Proteinen zu beobachten. Gleichzeitig kann bestimmt werden, ob ein Protein ein Monomer oder Dimer ist.

Der oligomere Zustand von SecA

SecA ist ein lösliches Motorprotein, das als Homodimer im Zytosol existiert und das während der Proteintranslokation an die Membranpore SecYEG bindet. Das Phänomen, dass mehrere individuelle Proteine sich zusammenlagern und Komplexe bilden, wird "oligomerer Zustand" genannt. Der oligomere Zustand von SecA in Lösung und gebunden an den Membranrezeptor SecYEG wurde in Kapitel 4 mit DCFBA und einer anderen Methode, Fluoreszenz Kreuz-Korrelationsspektroskopie (FCCS), untersucht. Es konnte bestätigt werden, dass SecA in Lösung ein Dimer ist und ausserdem auch als Dimer an SecYEG bindet. Interessanterweise bindet SecA als Monomer an SecYEG, wenn hohe Salzkonzentrationen anwesend sind. Diese Daten legen nahe, dass SecA assymetrisch mit SecYEG interagiert, da Bindung des SecA Monomers salz-resistent ist und Bindung des zweiten SecA salz-empfindlich ist. Möglicherweise kontaktiert ein SecA SecYEG direkt, während das andere SecA an das schon SecYEG gebundene SecA bindet (Kapitel 4, Abbildung 8).

Der oligomere Zustand von SecYEG

Die proteindurchlässige Pore der Bakterien, SecYEG, ist ein heterotrimerer Membranproteinkomplex (drei verschiedene Proteine lagern sich zu einem Komplex zusammen), der in der Membran auch in höheren oligomeren Formen, vor allem als Dimer, beobachtet wurde. Allerdings ist der funktionelle oligomere Zustand von SecYEG während der Proteintranslokation Gegenstand von kontroversen Debatten. In Kapitel5 wurde fluoreszenzmarkiertes SecYEG in Membranen untersucht. SecYEG war ein Monomer in An- oder Abwesenheit des Motorproteins SecA und anderer Komponenten des Translokationsapparates.

Neue Werkzeuge, um Proteintranslokation und Membranproteine auf Einzelmolekülniveau zu untersuchen

Untersuchungen an Membranproteinen werden erschwert durch das einzigartige Umfeld der elastischen und empfindlichen biologischen Membran. Allerdings würde die Immobilisierung von biologischen Membranen, in einer Art und Weise, dass die eingebetteten Membranproteine ihre Funktion behalten, neue Wege eröffnen, dieses interessante Umfeld durch Fluoreszenzmikroskopie und andere biophysikalischen Methoden zu untersuchen. In Kapitel 6 wurden erstmalig Hydrogele aus organischen Gelatoren benutzt, die sich selbst zu wenigen nanometer dünnen Fasern verbinden und die in der Lage sind, Membranen und die beinhalteten Membranproteine zu immobilisieren. Hierbei war es wichtig zu beobachten, dass sowohl lösliche als auch Membranproteine im Gel aktiv waren, was durch *in vitro* Proteintranslokation und Öffnung der mechanosensitiven Membranpore MscL gezeigt wurde (Kapitel 6).

Um andere Fragestellungen zu behandeln, wurden Membranvesikel auf einer Glasoberfläche immobilisiert (siehe Kapitel 7). Mit dieser Methode konnte

Proteintranslokation an einzelnen Membranvesikeln über eine lange Zeitspanne beobachtet werden. Weil diese Membranvesikel ziemlich viele SecYEG Poren hatten, wurde eine neue *in vitro* Proteintranslokationsmethode entwickelt, mit der die Aktivität von einzelnen SecYEG Poren erkennbar ist (Kapitel 7).

Fluoreszenzmarkierung von Komponenten des Sec-Wegs hat sich als nützliches Werkzeug für die Untersuchung der Proteinsekretionsreaktion erwiesen. Besonders nützlich war dabei die Fluoreszenzmarkierung des Preproteins proOmpA, da es sogar die Erkennung von einzelnen Preproteinen ermöglicht. In früheren Studien wurde allerdings bemerkt, dass die Fluoreszenzmarkierung von bestimmten proOmpA Mutanten eine Reduktion der Proteintranslokationaktivität hervorrufen kann. Daher wurde eine systematische Untersuchung dieses Phänomens in Kapitel 8 durchgeführt.

Ein Ausblick

Um zu verstehen, wie genau die Sec-Maschinerie funktioniert, müssen mehr Details dieses Prozesses aufgedeckt werden. Allerdings können konventionelle Methoden nicht diese Details klären, da zu viele Moleküle gleichzeitig beobachtet werden. Mit Hilfe von Fluoreszenzmikroskopie hingegen können sogar einzelne fluoreszenzmarkierte Proteine sichtbar gemacht und über einen gewissen Zeitraum beobachtet werden. Daher kann die Fluoreszenzmikroskopie uns Einsicht in den Mechanismus der Proteinsekretion und Funktionsweise des SecA Motorproteins geben. Dabei werden die Analyse von Bewegungen des Preproteins innerhalb der SecYEG Pore während des Sekretionsprozesses wichtig sein, die mit Fluoreszenzmikroskopie beobachtet werden können. Für diese Experimente wird es essentiell sein, dass einzelne SecYEG Poren im Beobachtungsfeld des Mikroskops verbleiben. Zukünftige Studien sollen sich auf die funktionelle Immobilisierung von biologischen Membranen mit integrierten SecYEG konzentrieren, die kompatibel mit den anderen Komponenten des *in vitro* Proteintraslokationsmaschinerie sind.

Appendix

Acknowledgements

I would like to start by thanking my parents who always supported me whatever I had put in my mind of what I want to become in life. Believing in learning by doing I was able to test engineering, music, chemistry and finally found my home in microbiology. Thank you so much for the support all this time including bringing fire wood from Düsseldorf to Greifswald so that I don't freeze during the grim eastern winter.

Thanks to Janine Kirstein and Ulf Gerth, my supervisors of my masters study in the lab of Prof. M. Hecker, I felt fit to try my luck abroad and to continue some *in vitro* work.

Arnold impressed me right from the start by replying the next day of my application email with two job offers, one on filamentous fungi and one with *E. coli*. Obviously, I picked the latter one. Since then he has kept this amazing response time even on midnight emails. Thank you very much for this always accessible and very motivating supervision and giving me the opportunity and support to do this very exciting research. I always appreciated the relaxed and funny atmosphere in discussions and meetings with you and find working with you as a boss very enjoyable.

Without Geert van den Bogaart, the SecA-DCFBA project would have been impossible and I would like to thank him for his help, enthusiasm and optimism in this project. Thank you also, Geert, for introducing me to the fascinating world of POV-Ray.

Thank you Faizah for choosing me as your top-master supervisor and thereby initiating the SecA-DCFBA project which turned out to be the main project of this thesis.

Janny and Greetje, thank you for your patience and answers to the hundreds of (mostly stupid) questions that I had during my PhD. Without you, this work would have been very difficult.

My paranimfen Andy and Jelger I would like to thank for the bizarre working environment that always let me feel being with, well, special people. It was lots of fun sharing an office with you despite Jelgers lack of musical instinct.

Thank you Jeanine and Alexej for the many intriguing scientific discussions and after work beers. Herfita, Patrick and Stef (yes, I mention you all together in one sentence) thanks for the many enjoyable activities and beers that we had together and that are unforgettable connected to my PhD!

Victor, thank you for the continuous checking on my survival in the microscope room and lighten my otherwise dark days (by opening the door and saying "Survive?").

Also many thanks for help with the microscope and your patience in trying to explain the mysteries of fluorescence to a biologist.

Also thanks to 'Mr. Schedule' Jacek and Anne for help with the microscope.

Nobina, Armagan and Menno, thank you very much for the inspiring collaboration in the hydrogel project. I really enjoyed this interdisciplinary work and hope that the hydrogel story continues.

I would like to thank Sander Tans for the long lasting collaboration and the unique experience to work at the AMOLF institute. I learned a lot from our discussions.

To mention all the occasions on which members of Molmic have helped me, lifted my spirit or brought me back on my feet again would require to cut down the remaining woods of Holland to make more paper. Therefore only a global, nevertheless heart-full thanks to everybody!

The path of Samta that I am following since a few years has brought me the balance that I was striving for and that now fulfills me. Samta, thank you for bringing peace and equanimity into my, our, live. I am also thankful to your parents who supported you in coming to the Netherlands. Without them, I would have never met you.

"Until he extends the circle of his compassion to all living things, man will not himself find peace." Albert Schweitzer (The Philosophy of Civilisation)

List of publications

Kusters, I., Mukherjee, N., de Jong, M., Tans, S., Koçer, A., and Driessen, A. (2011) Taming membranes: Functional immobilization of biological membranes in hydrogels, *PLOS one* , in press

Kusters, I. and Driessen, A.J.M (2011) SecA, a remarkable nanomachine, *Cellular and Molecular Live Sciences*, 2011, DOI 10.1007/s00018-011-0681-y

Kusters, I., van den Bogaart, G., Kedrov, A., Krasnikov, V., Fulyani, F., Poolman, B., and Driessen, A. (2011) Quaternary structure of SecA in solution and bound to SecYEG probed at the single molecule level, *Structure*. 19:430-9

Kusters, I., van den Bogaart, G., de Wit, J., Krasnikov, V., Poolman, B., and Driessen, A. (2010) Purification and functional reconstitution of the bacterial protein translocation pore, the SecYEG complex, *Methods Mol Biol 619*, 131-143.

van den Bogaart, G., **Kusters, I.**, Velasquez, J., Mika, J. T., Krasnikov, V., Driessen, A , and Poolman, B. (2008) Dual-color fluorescence-burst analysis to study pore formation and protein-protein interactions, *Methods 46*, 123-130.

Gerth, U., Kock, H**., Kusters, I.**, Michalik, S., Switzer, R. L., and Hecker, M. (2008) Clp-dependent proteolysis down-regulates central metabolic pathways in glucose-starved Bacillus subtilis, *J Bacteriol 190*, 321-331.

List of co-authors and collaborators

Department of Molecular Microbiology

Prof. Dr. Arnold Driessen[1]

Dr. Alexej Kedrov[1]

Janny G. de Wit[1]

Department of Membrane Enzymology

Dr. Geert van den Bogaart[2,3]

Faizah Fulyani[2]

Nobina Mukherjee[2]

Dr. Armagan Koçer[2]

Jacek T. Mika[2]

Jeanette Velásquez[2]

Prof. Dr. Bert Poolman[2]

Department of Optical Condensed Matter Physics

Dr. Viktor Krasnikov[4,5]

AMOLF institute

Prof. Dr. Ir. Sander J. Tans[6]

BiOMaDe Technology Foundation

Dr. Menno R. de Jong[7]

1 Department of Microbiology, Groningen Biomolecular Sciences and Biotechnology Institute, and Zernike Institute for Advanced Materials

2 Department of Membrane Enzymology, Groningen Biomolecular Sciences and Biotechnology Institute, Netherlands Proteomics Centre, and Zernike Institute for Advanced Materials, University of Groningen, Nijenborgh 4, 9747 AG Groningen, The Netherlands

3 Present address: Max Planck Institute for Biophysical Chemistry, Department of Neurobiology, Am Fassberg 11, Go¨ ttingen D-37077 Germany

4 Department of Optical Condensed Matter Physics, University of Groningen, Nijenborgh 4, 9747 AG Groningen, The Netherlands

5 Present address: Department of Single-Molecule Biophysics, the Zernike Institute for Advanced Materials, University of Groningen, Nijenborgh 4, 9747 AG Groningen, The Netherlands

6 AMOLF institute, Science Park 104, 1098 XG Amsterdam, the Netherlands

7 BiOMaDe Technology Foundation, Nijenborgh 4, 9749 AG Groningen, The Netherlands

References

1. Josefsson LG, Randall LL (1981) Processing in vivo of precursor maltose-binding protein in Escherichia coli occurs post-translationally as well as co-translationally. J Biol Chem 256 (5):2504-2507

2. Hartl FU, Lecker S, Schiebel E, Hendrick JP, Wickner W (1990) The binding cascade of SecB to SecA to SecY/E mediates preprotein targeting to the E. coli plasma membrane. Cell 63 (2):269-279

3. Fekkes P, de Wit JG, van der Wolk JP, Kimsey HH, Kumamoto CA, Driessen AJ (1998) Preprotein transfer to the Escherichia coli translocase requires the co-operative binding of SecB and the signal sequence to SecA. Mol Microbiol 29 (5):1179-1190

4. Economou A, Wickner W (1994) SecA promotes preprotein translocation by undergoing ATP-driven cycles of membrane insertion and deinsertion. Cell 78 (5):835-843

5. Schiebel E, Driessen AJ, Hartl FU, Wickner W (1991) Delta mu H+ and ATP function at different steps of the catalytic cycle of preprotein translocase. Cell 64 (5):927-939

6. van der Wolk JP, de Wit JG, Driessen AJ (1997) The catalytic cycle of the escherichia coli SecA ATPase comprises two distinct preprotein translocation events. EMBO J 16 (24):7297-7304

7. Egea PF, Stroud RM, Walter P (2005) Targeting proteins to membranes: structure of the signal recognition particle. Curr Opin Struct Biol 15 (2):213-220

8. Gumbart J, Schulten K (2007) Structural determinants of lateral gate opening in the protein translocon. Biochemistry 46 (39):11147-11157

9. Breyton C, Haase W, Rapoport TA, Kuhlbrandt W, Collinson I (2002) Three-dimensional structure of the bacterial protein-translocation complex SecYEG. Nature 418 (6898):662-665

10. Murphy CK, Beckwith J (1994) Residues essential for the function of SecE, a membrane component of the Escherichia coli secretion apparatus, are located in a conserved cytoplasmic region. Proc Natl Acad Sci U S A 91 (7):2557-2561

11. Van den Berg B, Clemons WM, Jr., Collinson I, Modis Y, Hartmann E, Harrison SC, Rapoport TA (2004) X-ray structure of a protein-conducting channel. Nature 427 (6969):36-44

12. Smith MA, Clemons WM, Jr., DeMars CJ, Flower AM (2005) Modeling the effects of prl mutations on the Escherichia coli SecY complex. J Bacteriol 187 (18):6454-6465

13. Flower AM (2007) The SecY translocation complex: convergence of genetics and structure. Trends Microbiol 15 (5):203-210

14. Bessonneau P, Besson V, Collinson I, Duong F (2002) The SecYEG preprotein translocation channel is a conformationally dynamic and dimeric structure. EMBO J 21 (5):995-1003

15. Duong F (2003) Binding, activation and dissociation of the dimeric SecA ATPase at the dimeric SecYEG translocase. EMBO J 22 (17):4375-4384

16. Tziatzios C, Schubert D, Lotz M, Gundogan D, Betz H, Schagger H, Haase W, Duong F, Collinson I (2004) The bacterial protein-translocation complex: SecYEG dimers associate with one or two SecA molecules. J Mol Biol 340 (3):513-524

17. Mitra K, Schaffitzel C, Shaikh T, Tama F, Jenni S, Brooks CL, 3rd, Ban N, Frank J (2005) Structure of the E. coli protein-conducting channel bound to a translating ribosome. Nature 438 (7066):318-324

18. Meyer TH, Menetret JF, Breitling R, Miller KR, Akey CW, Rapoport TA (1999) The bacterial SecY/E translocation complex forms channel-like structures similar to those of the eukaryotic Sec61p complex. J Mol Biol 285 (4):1789-1800

19. Manting EH, van Der Does C, Remigy H, Engel A, Driessen AJ (2000) SecYEG assembles into a tetramer to form the active protein translocation channel. EMBO J 19 (5):852-861

20. Scheuring J, Braun N, Nothdurft L, Stumpf M, Veenendaal AK, Kol S, van der Does C, Driessen AJ, Weinkauf S (2005) The oligomeric distribution of SecYEG is altered by SecA and translocation ligands. J Mol Biol 354 (2):258-271

21. Hanein D, Matlack KE, Jungnickel B, Plath K, Kalies KU, Miller KR, Rapoport TA, Akey CW (1996) Oligomeric rings of the Sec61p complex induced by ligands required for protein translocation. Cell 87 (4):721-732

22. Beckmann R, Bubeck D, Grassucci R, Penczek P, Verschoor A, Blobel G, Frank J (1997) Alignment of conduits for the nascent polypeptide chain in the ribosome-Sec61 complex. Science 278 (5346):2123-2126

23. Beckmann R, Spahn CM, Eswar N, Helmers J, Penczek PA, Sali A, Frank J, Blobel G (2001) Architecture of the protein-conducting channel associated with the translating 80S ribosome. Cell 107 (3):361-372

24. Menetret JF, Neuhof A, Morgan DG, Plath K, Radermacher M, Rapoport TA, Akey CW (2000) The structure of ribosome-channel complexes engaged in protein translocation. Mol Cell 6 (5):1219-1232

25. Hamman BD, Chen JC, Johnson EE, Johnson AE (1997) The aqueous pore through the translocon has a diameter of 40-60 A during cotranslational protein translocation at the ER membrane. Cell 89 (4):535-544

26. Osborne AR, Rapoport TA (2007) Protein translocation is mediated by oligomers of the SecY complex with one SecY copy forming the channel. Cell 129 (1):97-110

27. du Plessis DJ, Berrelkamp G, Nouwen N, Driessen AJ (2009) The lateral gate of SecYEG opens during protein translocation. J Biol Chem 284 (23):15805-15814

28. Becker T, Bhushan S, Jarasch A, Armache JP, Funes S, Jossinet F, Gumbart J, Mielke T, Berninghausen O, Schulten K, Westhof E, Gilmore R, Mandon EC, Beckmann R (2009) Structure of monomeric yeast and mammalian Sec61 complexes interacting with the translating ribosome. Science 326 (5958):1369-1373

29. Zimmer J, Nam Y, Rapoport TA (2008) Structure of a complex of the ATPase SecA and the protein-translocation channel. Nature 455 (7215):936-943

30. Deville K, Gold VA, Robson A, Whitehouse S, Sessions RB, Baldwin SA, Radford SE, Collinson I (2011) The oligomeric state and arrangement of the active bacterial translocon. J Biol Chem 286 (6):4659-4669

31. Mori H, Ito K (2006) Different modes of SecY-SecA interactions revealed by site-directed in vivo photo-cross-linking. Proc Natl Acad Sci U S A 103 (44):16159-16164

32. van der Sluis EO, Nouwen N, Koch J, de Keyzer J, van der Does C, Tampe R, Driessen AJ (2006) Identification of two interaction sites in SecY that are important for the functional interaction with SecA. J Mol Biol 361 (5):839-849

33. Tsukazaki T, Mori H, Fukai S, Ishitani R, Mori T, Dohmae N, Perederina A, Sugita Y, Vassylyev DG, Ito K, Nureki O (2008) Conformational transition of Sec machinery inferred from bacterial SecYE structures. Nature 455 (7215):988-991

34. Nagamori S, Nishiyama K, Tokuda H (2002) Membrane topology inversion of SecG detected by labeling with a membrane-impermeable sulfhydryl reagent that causes a close association of SecG with SecA. J Biochem 132 (4):629-634

35. Mori H, Ito K (2001) An essential amino acid residue in the protein translocation channel revealed by targeted random mutagenesis of SecY. Proc Natl Acad Sci U S A 98 (9):5128-5133

36. de Keyzer J, Regeling A, Driessen AJ (2007) Arginine 357 of SecY is needed for SecA-dependent initiation of preprotein translocation. FEBS Lett 581 (9):1859-1864

37. Cheng Z, Jiang Y, Mandon EC, Gilmore R (2005) Identification of cytoplasmic residues of Sec61p involved in ribosome binding and cotranslational translocation. J Cell Biol 168 (1):67-77

38. Raden D, Song W, Gilmore R (2000) Role of the cytoplasmic segments of Sec61alpha in the ribosome-binding and translocation-promoting activities of the Sec61 complex. J Cell Biol 150 (1):53-64

39. Menetret JF, Schaletzky J, Clemons WM, Jr., Osborne AR, Skanland SS, Denison C, Gygi SP, Kirkpatrick DS, Park E, Ludtke SJ, Rapoport TA, Akey CW (2007) Ribosome binding of a single copy of the SecY complex: implications for protein translocation. Mol Cell 28 (6):1083-1092

40. Kuhn P, Weiche B, Sturm L, Sommer E, Drepper F, Warscheid B, Sourjik V, Koch HG (2011) The bacterial SRP receptor, SecA and the ribosome use overlapping binding sites on the SecY translocon. Traffic

41. Heinrich SU, Mothes W, Brunner J, Rapoport TA (2000) The Sec61p complex mediates the integration of a membrane protein by allowing lipid partitioning of the transmembrane domain. Cell 102 (2):233-244

42. Plath K, Mothes W, Wilkinson BM, Stirling CJ, Rapoport TA (1998) Signal sequence recognition in posttranslational protein transport across the yeast ER membrane. Cell 94 (6):795-807

43. Egea PF, Stroud RM (2010) Lateral opening of a translocon upon entry of protein suggests the mechanism of insertion into membranes. Proc Natl Acad Sci U S A 107 (40):17182-17187

44. Harris CR, Silhavy TJ (1999) Mapping an interface of SecY (PrlA) and SecE (PrlG) by using synthetic phenotypes and in vivo cross-linking. J Bacteriol 181 (11):3438-3444

45. Tam PC, Maillard AP, Chan KK, Duong F (2005) Investigating the SecY plug movement at the SecYEG translocation channel. EMBO J 24 (19):3380-3388

46. Lycklama ANJA, Bulacu M, Marrink SJ, Driessen AJ (2010) Immobilization of the plug domain inside the SecY channel allows unrestricted protein translocation. J Biol Chem 285 (31):23747-23754

47. Maillard AP, Lalani S, Silva F, Belin D, Duong F (2007) Deregulation of the SecYEG translocation channel upon removal of the plug domain. J Biol Chem 282 (2):1281-1287

48. Saparov SM, Erlandson K, Cannon K, Schaletzky J, Schulman S, Rapoport TA, Pohl P (2007) Determining the conductance of the SecY protein translocation channel for small molecules. Mol Cell 26 (4):501-509

49. Junne T, Schwede T, Goder V, Spiess M (2006) The plug domain of yeast Sec61p is important for efficient protein translocation, but is not essential for cell viability. Mol Biol Cell 17 (9):4063-4068

50. Li W, Schulman S, Boyd D, Erlandson K, Beckwith J, Rapoport TA (2007) The plug domain of the SecY protein stabilizes the closed state of the translocation channel and maintains a membrane seal. Mol Cell 26 (4):511-521

51. Junne T, Schwede T, Goder V, Spiess M (2007) Mutations in the Sec61p channel affecting signal sequence recognition and membrane protein topology. J Biol Chem 282 (45):33201-33209

52. Bol R, de Wit JG, Driessen AJ (2007) The active protein-conducting channel of Escherichia coli contains an apolar patch. J Biol Chem 282 (41):29785-29793

53. Bieker-Brady K, Silhavy TJ (1992) Suppressor analysis suggests a multistep, cyclic mechanism for protein secretion in Escherichia coli. EMBO J 11 (9):3165-3174

54. Danese PN, Silhavy TJ (1998) Targeting and assembly of periplasmic and outer-membrane proteins in Escherichia coli. Annu Rev Genet 32:59-94

55. Duong F, Wickner W (1999) The PrlA and PrlG phenotypes are caused by a loosened association among the translocase SecYEG subunits. EMBO J 18 (12):3263-3270

56. van der Wolk JP, Fekkes P, Boorsma A, Huie JL, Silhavy TJ, Driessen AJ (1998) PrlA4 prevents the rejection of signal sequence defective preproteins by stabilizing the SecA-SecY interaction during the initiation of translocation. EMBO J 17 (13):3631-3639

57. Nouwen N, de Kruijff B, Tommassen J (1996) prlA suppressors in Escherichia coli relieve the proton electrochemical gradient dependency of translocation of wild-type precursors. Proc Natl Acad Sci U S A 93 (12):5953-5957

58. Lill R, Dowhan W, Wickner W (1990) The ATPase activity of SecA is regulated by acidic phospholipids, SecY, and the leader and mature domains of precursor proteins. Cell 60 (2):271-280

59. Karamanou S, Gouridis G, Papanikou E, Sianidis G, Gelis I, Keramisanou D, Vrontou E, Kalodimos CG, Economou A (2007) Preprotein-controlled catalysis in the helicase motor of SecA. EMBO J 26 (12):2904-2914

60. Driessen AJ, Nouwen N (2008) Protein translocation across the bacterial cytoplasmic membrane. Annu Rev Biochem 77:643-667

61. Miller A, Wang L, Kendall DA (2002) SecB modulates the nucleotide-bound state of SecA and stimulates ATPase activity. Biochemistry 41 (16):5325-5332

62. Vrontou E, Economou A (2004) Structure and function of SecA, the preprotein translocase nanomotor. Biochim Biophys Acta 1694 (1-3):67-80

63. Gouridis G, Karamanou S, Gelis I, Kalodimos CG, Economou A (2009) Signal peptides are allosteric activators of the protein translocase. Nature 462 (7271):363-367

64. Eser M, Ehrmann M (2003) SecA-dependent quality control of intracellular protein localization. Proc Natl Acad Sci U S A 100 (23):13231-13234

65. Akita M, Shinkai A, Matsuyama S, Mizushima S (1991) SecA, an essential component of the secretory machinery of Escherichia coli, exists as homodimer. Biochem Biophys Res Commun 174 (1):211-216

66. Moran U, Phillips R, Milo R (2010) SnapShot: key numbers in biology. Cell 141 (7):1262-1262 e1261

67. Matsuyama S, Kimura E, Mizushima S (1990) Complementation of two overlapping fragments of SecA, a protein translocation ATPase of Escherichia coli, allows ATP binding to its amino-terminal region. J Biol Chem 265 (15):8760-8765

68. Sardis MF, Economou A (2010) SecA: a tale of two protomers. Mol Microbiol 76 (5):1070-1081

69. Musial-Siwek M, Rusch SL, Kendall DA (2007) Selective photoaffinity labeling identifies the signal peptide binding domain on SecA. J Mol Biol 365 (3):637-648

70. Gelis I, Bonvin AM, Keramisanou D, Koukaki M, Gouridis G, Karamanou S, Economou A, Kalodimos CG (2007) Structural basis for signal-sequence recognition by the translocase motor SecA as determined by NMR. Cell 131 (4):756-769

71. Papanikou E, Karamanou S, Baud C, Frank M, Sianidis G, Keramisanou D, Kalodimos CG, Kuhn A, Economou A (2005) Identification of the preprotein binding domain of SecA. J Biol Chem 280 (52):43209-43217

72. Cooper DB, Smith VF, Crane JM, Roth HC, Lilly AA, Randall LL (2008) SecA, the motor of the secretion machine, binds diverse partners on one interactive surface. J Mol Biol 382 (1):74-87

73. Fekkes P, van der Does C, Driessen AJ (1997) The molecular chaperone SecB is released from the carboxy-terminus of SecA during initiation of precursor protein translocation. EMBO J 16 (20):6105-6113

74. Zhou J, Xu Z (2003) Structural determinants of SecB recognition by SecA in bacterial protein translocation. Nat Struct Biol 10 (11):942-947

75. Fekkes P, de Wit JG, Boorsma A, Friesen RH, Driessen AJ (1999) Zinc stabilizes the SecB binding site of SecA. Biochemistry 38 (16):5111-5116

76. Breukink E, Nouwen N, van Raalte A, Mizushima S, Tommassen J, de Kruijff B (1995) The C terminus of SecA is involved in both lipid binding and SecB binding. J Biol Chem 270 (14):7902-7907

77. Papanikou E, Karamanou S, Economou A (2007) Bacterial protein secretion through the translocase nanomachine. Nat Rev Microbiol 5 (11):839-851

78. Koonin EV, Gorbalenya AE (1992) Autogenous translation regulation by Escherichia coli ATPase SecA may be mediated by an intrinsic RNA helicase activity of this protein. FEBS Lett 298 (1):6-8

79. Cordin O, Banroques J, Tanner NK, Linder P (2006) The DEAD-box protein family of RNA helicases. Gene 367:17-37

80. Mitchell C, Oliver D (1993) Two distinct ATP-binding domains are needed to promote protein export by Escherichia coli SecA ATPase. Mol Microbiol 10 (3):483-497

81. Ye J, Osborne AR, Groll M, Rapoport TA (2004) RecA-like motor ATPases--lessons from structures. Biochim Biophys Acta 1659 (1):1-18

82. Sato K, Mori H, Yoshida M, Mizushima S (1996) Characterization of a potential catalytic residue, Asp-133, in the high affinity ATP-binding site of Escherichia coli SecA, translocation ATPase. J Biol Chem 271 (29):17439-17444

83. Sianidis G, Karamanou S, Vrontou E, Boulias K, Repanas K, Kyrpides N, Politou AS, Economou A (2001) Cross-talk between catalytic and regulatory elements in a DEAD motor domain is essential for SecA function. EMBO J 20 (5):961-970

84. Papanikolau Y, Papadovasilaki M, Ravelli RB, McCarthy AA, Cusack S, Economou A, Petratos K (2007) Structure of dimeric SecA, the Escherichia coli preprotein translocase motor. J Mol Biol 366 (5):1545-1557

85. Hunt JF, Weinkauf S, Henry L, Fak JJ, McNicholas P, Oliver DB, Deisenhofer J (2002) Nucleotide control of interdomain interactions in the conformational reaction cycle of SecA. Science 297 (5589):2018-2026

86. Karamanou S, Vrontou E, Sianidis G, Baud C, Roos T, Kuhn A, Politou AS, Economou A (1999) A molecular switch in SecA protein couples ATP hydrolysis to protein translocation. Mol Microbiol 34 (5):1133-1145

87. Keramisanou D, Biris N, Gelis I, Sianidis G, Karamanou S, Economou A, Kalodimos CG (2006) Disorder-order folding transitions underlie catalysis in the helicase motor of SecA. Nat Struct Mol Biol 13 (7):594-602

88. Vrontou E, Karamanou S, Baud C, Sianidis G, Economou A (2004) Global co-ordination of protein translocation by the SecA IRA1 switch. J Biol Chem 279 (21):22490-22497

89. Mori H, Ito K (2006) The long alpha-helix of SecA is important for the ATPase coupling of translocation. J Biol Chem 281 (47):36249-36256

90. Economou A (2008) Structural biology: Clamour for a kiss. Nature 455 (7215):879-880

91. Woodbury RL, Hardy SJ, Randall LL (2002) Complex behavior in solution of homodimeric SecA. Protein Sci 11 (4):875-882

92. Driessen AJ (1993) SecA, the peripheral subunit of the Escherichia coli precursor protein translocase, is functional as a dimer. Biochemistry 32 (48):13190-13197

93. Wang HW, Chen Y, Yang H, Chen X, Duan MX, Tai PC, Sui SF (2003) Ring-like pore structures of SecA: implication for bacterial protein-conducting channels. Proc Natl Acad Sci U S A 100 (7):4221-4226

94. Chen Y, Tai PC, Sui SF (2007) The active ring-like structure of SecA revealed by electron crystallography: conformational change upon interaction with SecB. J Struct Biol 159 (1):149-153

95. Chen Y, Pan X, Tang Y, Quan S, Tai PC, Sui SF (2008) Full-length Escherichia coli SecA dimerizes in a closed conformation in solution as determined by cryo-electron microscopy. J Biol Chem 283 (43):28783-28787

96. Shilton B, Svergun DI, Volkov VV, Koch MH, Cusack S, Economou A (1998) Escherichia coli SecA shape and dimensions. FEBS Lett 436 (2):277-282

97. Bu Z, Wang L, Kendall DA (2003) Nucleotide binding induces changes in the oligomeric state and conformation of Sec A in a lipid environment: a small-angle neutron-scattering study. J Mol Biol 332 (1):23-30

98. Sharma V, Arockiasamy A, Ronning DR, Savva CG, Holzenburg A, Braunstein M, Jacobs WR, Jr., Sacchettini JC (2003) Crystal structure of Mycobacterium tuberculosis SecA, a preprotein translocating ATPase. Proc Natl Acad Sci U S A 100 (5):2243-2248

99. Vassylyev DG, Mori H, Vassylyeva MN, Tsukazaki T, Kimura Y, Tahirov TH, Ito K (2006) Crystal structure of the translocation ATPase SecA from Thermus thermophilus reveals a parallel, head-to-head dimer. J Mol Biol 364 (3):248-258

100. Zimmer J, Li W, Rapoport TA (2006) A novel dimer interface and conformational changes revealed by an X-ray structure of B. subtilis SecA. J Mol Biol 364 (3):259-265

101. Wowor AJ, Yu D, Kendall DA, Cole JL (2011) Energetics of SecA Dimerization. J Mol Biol

102. de Keyzer J, van der Sluis EO, Spelbrink RE, Nijstad N, de Kruijff B, Nouwen N, van der Does C, Driessen AJ (2005) Covalently dimerized SecA is functional in protein translocation. J Biol Chem 280 (42):35255-35260

103. Or E, Boyd D, Gon S, Beckwith J, Rapoport T (2005) The bacterial ATPase SecA functions as a monomer in protein translocation. J Biol Chem 280 (10):9097-9105

104. Ding H, Mukerji I, Oliver D (2003) Nucleotide and phospholipid-dependent control of PPXD and C-domain association for SecA ATPase. Biochemistry 42 (46):13468-13475

105. Kusters I, van den Bogaart G, Kedrov A, Krasnikov V, Fulyani F, Poolman B, Driessen AJ (2011) Quaternary Structure of SecA in Solution and Bound to SecYEG Probed at the Single Molecule Level. Structure 19 (3):430-439

106. Benach J, Chou YT, Fak JJ, Itkin A, Nicolae DD, Smith PC, Wittrock G, Floyd DL, Golsaz CM, Gierasch LM, Hunt JF (2003) Phospholipid-induced monomerization and signal-peptide-induced oligomerization of SecA. J Biol Chem 278 (6):3628-3638

107. Or E, Navon A, Rapoport T (2002) Dissociation of the dimeric SecA ATPase during protein translocation across the bacterial membrane. EMBO J 21 (17):4470-4479

108. Jilaveanu LB, Oliver D (2006) SecA dimer cross-linked at its subunit interface is functional for protein translocation. J Bacteriol 188 (1):335-338

109. Wang H, Na B, Yang H, Tai PC (2008) Additional in vitro and in vivo evidence for SecA functioning as dimers in the membrane: dissociation into monomers is not essential for protein translocation in Escherichia coli. J Bacteriol 190 (4):1413-1418

110. Jilaveanu LB, Zito CR, Oliver D (2005) Dimeric SecA is essential for protein translocation. Proc Natl Acad Sci U S A 102 (21):7511-7516

111. Randall LL, Crane JM, Lilly AA, Liu G, Mao C, Patel CN, Hardy SJ (2005) Asymmetric binding between SecA and SecB two symmetric proteins: implications for function in export. J Mol Biol 348 (2):479-489

112. Mao C, Hardy SJ, Randall LL (2009) Maximal efficiency of coupling between ATP hydrolysis and translocation of polypeptides mediated by SecB requires two protomers of SecA. J Bacteriol 191 (3):978-984

113. Randall LL, Crane JM, Liu G, Hardy SJ (2004) Sites of interaction between SecA and the chaperone SecB, two proteins involved in export. Protein Sci 13 (4):1124-1133

114. Suo Y, Hardy SJ, Randall LL (2011) Orientation of SecA and SecB in complex, derived from disulfide cross-linking. J Bacteriol 193 (1):190-196

115. Tani K, Tokuda H, Mizushima S (1990) Translocation of ProOmpA possessing an intramolecular disulfide bridge into membrane vesicles of Escherichia coli. Effect of membrane energization. J Biol Chem 265 (28):17341-17347

116. Driessen AJ (1992) Precursor protein translocation by the Escherichia coli translocase is directed by the protonmotive force. EMBO J 11 (3):847-853

117. Fak JJ, Itkin A, Ciobanu DD, Lin EC, Song XJ, Chou YT, Gierasch LM, Hunt JF (2004) Nucleotide exchange from the high-affinity ATP-binding site in SecA is the rate-limiting step in the ATPase cycle of the soluble enzyme and occurs through a specialized conformational state. Biochemistry 43 (23):7307-7327

118. Chun SY, Randall LL (1994) In vivo studies of the role of SecA during protein export in Escherichia coli. J Bacteriol 176 (14):4197-4203

119. Nouwen N, Berrelkamp G, Driessen AJ (2007) Bacterial sec-translocase unfolds and translocates a class of folded protein domains. J Mol Biol 372 (2):422-433

120. van Dalen A, Killian A, de Kruijff B (1999) Delta psi stimulates membrane translocation of the C-terminal part of a signal sequence. J Biol Chem 274 (28):19913-19918

121. Driessen AJ, Wickner W (1991) Proton transfer is rate-limiting for translocation of precursor proteins by the Escherichia coli translocase. Proc Natl Acad Sci U S A 88 (6):2471-2475

122. Nishiyama K, Fukuda A, Morita K, Tokuda H (1999) Membrane deinsertion of SecA underlying proton motive force-dependent stimulation of protein translocation. EMBO J 18 (4):1049-1058

123. Shiozuka K, Tani K, Mizushima S, Tokuda H (1990) The proton motive force lowers the level of ATP required for the in vitro translocation of a secretory protein in Escherichia coli. J Biol Chem 265 (31):18843-18847

124. Nouwen N, Berrelkamp G, Driessen AJ (2009) Charged amino acids in a preprotein inhibit SecA-dependent protein translocation. J Mol Biol 386 (4):1000-1010

125. Simon SM, Peskin CS, Oster GF (1992) What drives the translocation of proteins? Proc Natl Acad Sci U S A 89 (9):3770-3774

126. Tomkiewicz D, Nouwen N, Driessen AJ (2007) Pushing, pulling and trapping--modes of motor protein supported protein translocation. FEBS Lett 581 (15):2820-2828

127. Liang FC, Bageshwar UK, Musser SM (2009) Bacterial Sec protein transport is rate-limited by precursor length: a single turnover study. Mol Biol Cell 20 (19):4256-4266

128. Tomkiewicz D, Nouwen N, van Leeuwen R, Tans S, Driessen AJ (2006) SecA supports a constant rate of preprotein translocation. J Biol Chem 281 (23):15709-15713

129. Uchida K, Mori H, Mizushima S (1995) Stepwise movement of preproteins in the process of translocation across the cytoplasmic membrane of Escherichia coli. J Biol Chem 270 (52):30862-30868

130. Erlandson KJ, Miller SB, Nam Y, Osborne AR, Zimmer J, Rapoport TA (2008) A role for the two-helix finger of the SecA ATPase in protein translocation. Nature 455 (7215):984-987

131. Patel SS, Donmez I (2006) Mechanisms of helicases. J Biol Chem 281 (27):18265-18268

132. Velankar SS, Soultanas P, Dillingham MS, Subramanya HS, Wigley DB (1999) Crystal structures of complexes of PcrA DNA helicase with a DNA substrate indicate an inchworm mechanism. Cell 97 (1):75-84

133. Osborne AR, Clemons WM, Jr., Rapoport TA (2004) A large conformational change of the translocation ATPase SecA. Proc Natl Acad Sci U S A 101 (30):10937-10942

134. Korolev S, Hsieh J, Gauss GH, Lohman TM, Waksman G (1997) Major domain swiveling revealed by the crystal structures of complexes of E. coli Rep helicase bound to single-stranded DNA and ADP. Cell 90 (4):635-647

135. Lohman TM, Bjornson KP (1996) Mechanisms of helicase-catalyzed DNA unwinding. Annu Rev Biochem 65:169-214

136. Wong I, Lohman TM (1992) Allosteric effects of nucleotide cofactors on Escherichia coli Rep helicase-DNA binding. Science 256 (5055):350-355

137. Musial-Siwek M, Rusch SL, Kendall DA (2005) Probing the affinity of SecA for signal peptide in different environments. Biochemistry 44 (42):13987-13996

138. Jilaveanu LB, Oliver DB (2007) In vivo membrane topology of Escherichia coli SecA ATPase reveals extensive periplasmic exposure of multiple functionally important domains clustering on one face of SecA. J Biol Chem 282 (7):4661-4668

139. Economou A, Pogliano JA, Beckwith J, Oliver DB, Wickner W (1995) SecA membrane cycling at SecYEG is driven by distinct ATP binding and hydrolysis events and is regulated by SecD and SecF. Cell 83 (7):1171-1181

140. Bechtluft P, Nouwen N, Tans SJ, Driessen AJ (2010) SecB--a chaperone dedicated to protein translocation. Mol Biosyst 6 (4):620-627

141. Engelman DM, Steitz TA (1981) The spontaneous insertion of proteins into and across membranes: the helical hairpin hypothesis. Cell 23 (2):411-422

142. Cannon KS, Or E, Clemons WM, Jr., Shibata Y, Rapoport TA (2005) Disulfide bridge formation between SecY and a translocating polypeptide localizes the translocation pore to the center of SecY. J Cell Biol 169 (2):219-225

143. Joly JC, Wickner W (1993) The SecA and SecY subunits of translocase are the nearest neighbors of a translocating preprotein, shielding it from phospholipids. EMBO J 12 (1):255-263

144. Brundage L, Hendrick JP, Schiebel E, Driessen AJ, Wickner W (1990) The purified E. coli integral membrane protein SecY/E is sufficient for reconstitution of SecA-dependent precursor protein translocation. Cell 62 (4):649-657

145. Lecker S, Lill R, Ziegelhoffer T, Georgopoulos C, Bassford PJ, Jr., Kumamoto CA, Wickner W (1989) Three pure chaperone proteins of Escherichia coli--SecB, trigger factor and GroEL--form soluble complexes with precursor proteins in vitro. EMBO J 8 (9):2703-2709

146. van der Wolk JP, Klose M, de Wit JG, den Blaauwen T, Freudl R, Driessen AJ (1995) Identification of the magnesium-binding domain of the high-affinity ATP-binding site of the Bacillus subtilis and Escherichia coli SecA protein. J Biol Chem 270 (32):18975-18982

147. van der Does C, Manting EH, Kaufmann A, Lutz M, Driessen AJ (1998) Interaction between SecA and SecYEG in micellar solution and formation of the membrane-inserted state. Biochemistry 37 (1):201-210

148. van den Bogaart G, Kusters I, Velasquez J, Mika JT, Krasnikov V, Driessen AJ, Poolman B (2008) Dual-color fluorescence-burst analysis to study pore formation and protein-protein interactions. Methods 46 (2):123-130

149. De Keyzer J, Van Der Does C, Driessen AJ (2002) Kinetic analysis of the translocation of fluorescent precursor proteins into Escherichia coli membrane vesicles. J Biol Chem 277 (48):46059-46065

150. Brogden KA (2005) Antimicrobial peptides: pore formers or metabolic inhibitors in bacteria? Nat Rev Microbiol 3 (3):238-250

151. Alber F, Dokudovskaya S, Veenhoff LM, Zhang W, Kipper J, Devos D, Suprapto A, Karni-Schmidt O, Williams R, Chait BT, Sali A, Rout MP (2007) The molecular architecture of the nuclear pore complex. Nature 450 (7170):695-701

152. Kass RS (2005) The channelopathies: novel insights into molecular and genetic mechanisms of human disease. J Clin Invest 115 (8):1986-1989

153. Smisterova J, van Deemter M, van der Schaaf G, Meijberg W, Robillard G (2005) Channel protein-containing liposomes as delivery vehicles for the controlled release of drugs-optimization of the lipid composition. J Control Release 101 (1-3):382-383

154. Hancock RE, Sahl HG (2006) Antimicrobial and host-defense peptides as new anti-infective therapeutic strategies. Nat Biotechnol 24 (12):1551-1557

155. Cruickshank CC, Minchin RF, Le Dain AC, Martinac B (1997) Estimation of the pore size of the large-conductance mechanosensitive ion channel of Escherichia coli. Biophys J 73 (4):1925-1931

156. Krantz BA, Melnyk RA, Zhang S, Juris SJ, Lacy DB, Wu Z, Finkelstein A, Collier RJ (2005) A phenylalanine clamp catalyzes protein translocation through the anthrax toxin pore. Science 309 (5735):777-781

157. Movileanu L, Schmittschmitt JP, Scholtz JM, Bayley H (2005) Interactions of peptides with a protein pore. Biophys J 89 (2):1030-1045

158. Huang C (1969) Studies on phosphatidylcholine vesicles. Formation and physical characteristics. Biochemistry 8 (1):344-352

159. Finkelstein MC, Weissmann G (1979) Enzyme replacement via liposomes. Variations in lipid compositions determine liposomal integrity in biological fluids. Biochim Biophys Acta 587 (2):202-216

160. Allen TM, Cleland LG (1980) Serum-induced leakage of liposome contents. Biochim Biophys Acta 597 (2):418-426

161. Weinstein JN, Yoshikami S, Henkart P, Blumenthal R, Hagins WA (1977) Liposome-cell interaction: transfer and intracellular release of a trapped fluorescent marker. Science 195 (4277):489-492

162. van den Bogaart G, Krasnikov V, Poolman B (2007) Dual-color fluorescence-burst analysis to probe protein efflux through the mechanosensitive channel MscL. Biophys J 92 (4):1233-1240

163. Petrasek Z, Schwille P (2008) Precise measurement of diffusion coefficients using scanning fluorescence correlation spectroscopy. Biophys J 94 (4):1437-1448

164. van den Bogaart G, Mika JT, Krasnikov V, Poolman B (2007) The lipid dependence of melittin action investigated by dual-color fluorescence burst analysis. Biophys J 93 (1):154-163

165. Knol J, Sjollema K, Poolman B (1998) Detergent-mediated reconstitution of membrane proteins. Biochemistry 37 (46):16410-16415

166. Schwille P, Meyer-Almes FJ, Rigler R (1997) Dual-color fluorescence cross-correlation spectroscopy for multicomponent diffusional analysis in solution. Biophys J 72 (4):1878-1886

167. Winkler T, Kettling U, Koltermann A, Eigen M (1999) Confocal fluorescence coincidence analysis: an approach to ultra high-throughput screening. Proc Natl Acad Sci U S A 96 (4):1375-1378

168. Heinze KG, Rarbach M, Jahnz M, Schwille P (2002) Two-photon fluorescence coincidence analysis: rapid measurements of enzyme kinetics. Biophys J 83 (3):1671-1681

169. Yao J, Larson DR, Vishwasrao HD, Zipfel WR, Webb WW (2005) Blinking and nonradiant dark fraction of water-soluble quantum dots in aqueous solution. Proc Natl Acad Sci U S A 102 (40):14284-14289

170. Li H, Ying L, Green JJ, Balasubramanian S, Klenerman D (2003) Ultrasensitive coincidence fluorescence detection of single DNA molecules. Anal Chem 75 (7):1664-1670

171. Green JJ, Ladame S, Ying L, Klenerman D, Balasubramanian S (2006) Investigating a quadruplex-ligand interaction by unfolding kinetics. J Am Chem Soc 128 (30):9809-9812

172. James JR, White SS, Clarke RW, Johansen AM, Dunne PD, Sleep DL, Fitzgerald WJ, Davis SJ, Klenerman D (2007) Single-molecule level analysis of the subunit composition of the T cell receptor on live T cells. Proc Natl Acad Sci U S A 104 (45):17662-17667

173. Heinze KG, Koltermann A, Schwille P (2000) Simultaneous two-photon excitation of distinct labels for dual-color fluorescence crosscorrelation analysis. Proc Natl Acad Sci U S A 97 (19):10377-10382

174. Kucerka N, Tristram-Nagle S, Nagle JF (2005) Structure of fully hydrated fluid phase lipid bilayers with monounsaturated chains. J Membr Biol 208 (3):193-202

175. Tristram-Nagle S, Petrache HI, Nagle JF (1998) Structure and interactions of fully hydrated dioleoylphosphatidylcholine bilayers. Biophys J 75 (2):917-925

176. Agosto MA, Ivanovic T, Nibert ML (2006) Mammalian reovirus, a nonfusogenic nonenveloped virus, forms size-selective pores in a model membrane. Proc Natl Acad Sci U S A 103 (44):16496-16501

177. Campbell RE, Tour O, Palmer AE, Steinbach PA, Baird GS, Zacharias DA, Tsien RY (2002) A monomeric red fluorescent protein. Proc Natl Acad Sci U S A 99 (12):7877-7882

178. Shattil SJ, Cunningham M, Wiedmer T, Zhao J, Sims PJ, Brass LF (1992) Regulation of glycoprotein IIb-IIIa receptor function studied with platelets permeabilized by the pore-forming complement proteins C5b-9. J Biol Chem 267 (26):18424-18431

179. Dimitrov DS, Sowers AE (1990) Membrane electroporation--fast molecular exchange by electroosmosis. Biochim Biophys Acta 1022 (3):381-392

180. Sauer H, Pratsch L, Peters R (1991) A microassay for the pore-forming activity of complement, perforin, and other cytolytic proteins based on confocal laser scanning microscopy. Anal Biochem 194 (2):418-424

181. Matsuzaki K, Yoneyama S, Miyajima K (1997) Pore formation and translocation of melittin. Biophys J 73 (2):831-838

182. Bohrer MP, Deen WM, Robertson CR, Troy JL, Brenner BM (1979) Influence of molecular configuration on the passage of macromolecules across the glomerular capillary wall. J Gen Physiol 74 (5):583-593

183. Doeven MK, Folgering JH, Krasnikov V, Geertsma ER, van den Bogaart G, Poolman B (2005) Distribution, lateral mobility and function of membrane proteins incorporated into giant unilamellar vesicles. Biophys J 88 (2):1134-1142

184. Gasteiger E, Hoogland C, Gattiker A, Duvaud S, Wilkins MR, Appel RD, Bairoch A, Walker (Ed.) JM (2005). The Proteomics Protocols Handbook, Springer-Verlag, Heidelberg, Germany:pp. 571–607

185. Colletier JP, Chaize B, Winterhalter M, Fournier D (2002) Protein encapsulation in liposomes: efficiency depends on interactions between protein and phospholipid bilayer. BMC Biotechnol 2:9

186. Lichtenberg D, Barenholz Y (1988) Liposomes: preparation, characterization, and preservation. Methods Biochem Anal 33:337-462

187. Kirby CJ, Gregoriadis G (1984) Preparation of liposomes containing factor VIII for oral treatment of haemophilia. J Microencapsul 1 (1):33-45

188. Moscho A, Orwar O, Chiu DT, Modi BP, Zare RN (1996) Rapid preparation of giant unilamellar vesicles. Proc Natl Acad Sci U S A 93 (21):11443-11447

189. Limpert E, Stahel WA, Abbt M (2001) Log-normal distributions across the sciences. Bioscience 51 (5):341-352

190. Elson EL, Magde D (1974) Fluorescence correlation spectroscopy. I. Conceptual basis and theory. Biopolymers 13:1-27

191. Aragon SR, Pecora R (1976) Fluorescence correlation spectroscopy as a probe of molecular dynamics. J Chem Phys 64:1791–1803

192. Digman MA, Sengupta P, Wiseman PW, Brown CM, Horwitz AR, Gratton E (2005) Fluctuation correlation spectroscopy with a laser-scanning microscope: exploiting the hidden time structure. Biophys J 88 (5):L33-36

193. Sukharev SI, Blount P, Martinac B, Blattner FR, Kung C (1994) A large-conductance mechanosensitive channel in E. coli encoded by mscL alone. Nature 368 (6468):265-268

194. Yoshimura K, Batiza A, Kung C (2001) Chemically charging the pore constriction opens the mechanosensitive channel MscL. Biophys J 80 (5):2198-2206

195. Habermann E (1972) Bee and wasp venoms. Science 177 (46):314-322

196. Raghuraman H, Chattopadhyay A (2007) Melittin: a membrane-active peptide with diverse functions. Biosci Rep 27 (4-5):189-223

197. Ambroggio EE, Separovic F, Bowie JH, Fidelio GD, Bagatolli LA (2005) Direct visualization of membrane leakage induced by the antibiotic peptides: maculatin, citropin, and aurein. Biophys J 89 (3):1874-1881

198. Lee MT, Hung WC, Chen FY, Huang HW (2008) Mechanism and kinetics of pore formation in membranes by water-soluble amphipathic peptides. Proc Natl Acad Sci U S A 105 (13):5087-5092

199. Geertsma ER, Nik Mahmood NA, Schuurman-Wolters GK, Poolman B (2008) Membrane reconstitution of ABC transporters and assays of translocator function. Nat Protoc 3 (2):256-266

200. de Keyzer J, van der Does C, Kloosterman TG, Driessen AJ (2003) Direct demonstration of ATP-dependent release of SecA from a translocating preprotein by surface plasmon resonance. J Biol Chem 278 (32):29581-29586

201. Mori H, Tsukazaki T, Masui R, Kuramitsu S, Yokoyama S, Johnson AE, Kimura Y, Akiyama Y, Ito K (2003) Fluorescence resonance energy transfer analysis of protein translocase. SecYE from Thermus thermophilus HB8 forms a constitutive oligomer in membranes. J Biol Chem 278 (16):14257-14264

202. van der Sluis EO, Nouwen N, Driessen AJ (2002) SecY-SecY and SecY-SecG contacts revealed by site-specific crosslinking. FEBS Lett 527 (1-3):159-165

203. Veenendaal AK, van der Does C, Driessen AJ (2001) Mapping the sites of interaction between SecY and SecE by cysteine scanning mutagenesis. J Biol Chem 276 (35):32559-32566

204. Doyle SM, Braswell EH, Teschke CM (2000) SecA folds via a dimeric intermediate. Biochemistry 39 (38):11667-11676

205. Bacia K, Schwille P (2007) Practical guidelines for dual-color fluorescence cross-correlation spectroscopy. Nat Protoc 2 (11):2842-2856

206. Weinkauf S, Hunt JF, Scheuring J, Henry L, Fak J, Oliver DB, Deisenhofer J (2001) Conformational stabilization and crystallization of the SecA translocation ATPase from Bacillus subtilis. Acta Crystallogr D Biol Crystallogr 57 (Pt 4):559-565

207. Girard P, Prost J, Bassereau P (2005) Passive or active fluctuations in membranes containing proteins. Phys Rev Lett 94 (8):088102

208. Karamanou S, Sianidis G, Gouridis G, Pozidis C, Papanikolau Y, Papanikou E, Economou A (2005) Escherichia coli SecA truncated at its termini is functional and dimeric. FEBS Lett 579 (5):1267-1271

209. Or E, Rapoport T (2007) Cross-linked SecA dimers are not functional in protein translocation. FEBS Lett 581 (14):2616-2620

210. van der Does C, de Keyzer J, van der Laan M, Driessen AJ (2003) Reconstitution of purified bacterial preprotein translocase in liposomes. Methods Enzymol 372:86-98

211. Kusters I, van den Bogaart G, de Wit J, Krasnikov V, Poolman B, Driessen A (2010) Purification and functional reconstitution of the bacterial protein translocation pore, the SecYEG complex. Methods Mol Biol 619:131-143

212. Veldhuis G, Hink M, Krasnikov V, van den Bogaart G, Hoeboer J, Visser AJ, Broos J, Poolman B (2006) The oligomeric state and stability of the mannitol transporter, EnzymeII(mtl), from Escherichia coli: a fluorescence correlation spectroscopy study. Protein Sci 15 (8):1977-1986

213. Driessen AJ (2001) SecB, a molecular chaperone with two faces. Trends Microbiol 9 (5):193-196

214. Boy D, Koch HG (2009) Visualization of distinct entities of the SecYEG translocon during translocation and integration of bacterial proteins. Mol Biol Cell 20 (6):1804-1815

215. Yahr TL, Wickner WT (2000) Evaluating the oligomeric state of SecYEG in preprotein translocase. EMBO J 19 (16):4393-4401

216. Alami M, Dalal K, Lelj-Garolla B, Sligar SG, Duong F (2007) Nanodiscs unravel the interaction between the SecYEG channel and its cytosolic partner SecA. EMBO J 26 (8):1995-2004

217. Walde P, Cosentino K, Engel H, Stano P (2010) Giant vesicles: preparations and applications. Chembiochem 11 (7):848-865

218. Garcia-Saez AJ, Carrer DC, Schwille P (2010) Fluorescence correlation spectroscopy for the study of membrane dynamics and organization in giant unilamellar vesicles. Methods Mol Biol 606:493-508

219. van Voorst F, de Kruijff B (2000) Role of lipids in the translocation of proteins across membranes. Biochemical Journal 347 (Pt. 3):601-612

220. van der Does C, Swaving J, van Klompenburg W, Driessen AJ (2000) Non-bilayer lipids stimulate the activity of the reconstituted bacterial protein translocase. J Biol Chem 275 (4):2472-2478

221. Gold VA, Robson A, Bao H, Romantsov T, Duong F, Collinson I (2010) The action of cardiolipin on the bacterial translocon. Proc Natl Acad Sci U S A 107 (22):10044-10049

222. Reeves JP, Dowben RM (1969) Formation and properties of thin-walled phospholipid vesicles. J Cell Physiol 73 (1):49-60

223. Ramadurai S, Holt A, Krasnikov V, van den Bogaart G, Killian JA, Poolman B (2009) Lateral diffusion of membrane proteins. J Am Chem Soc 131 (35):12650-12656

224. Saffman PG, Delbruck M (1975) Brownian motion in biological membranes. Proc Natl Acad Sci U S A 72 (8):3111-3113

225. Krichevsky O, Bonnet G (2001) Fluorescence correlation spectroscopy: the technique and its applications Reports on progress in physics 65 (2):251-297

226. Matsuyama S, Akimaru J, Mizushima S (1990) SecE-dependent overproduction of SecY in Escherichia coli. Evidence for interaction between two components of the secretory machinery. FEBS Lett 269 (1):96-100

227. Arkowitz RA, Joly JC, Wickner W (1993) Translocation can drive the unfolding of a preprotein domain. EMBO J 12 (1):243-253

228. Dekker C, de Kruijff B, Gros P (2003) Crystal structure of SecB from Escherichia coli. J Struct Biol 144 (3):313-319

229. Tang Y, Pan X, Tai PC, Sui SF (2010) The structure of SecB/OmpA as visualized by electron microscopy: The mature region of the precursor protein binds asymmetrically to SecB. Biochem Biophys Res Commun 393 (4):698-702

230. Kaufmann A, Manting EH, Veenendaal AK, Driessen AJ, van der Does C (1999) Cysteine-directed cross-linking demonstrates that helix 3 of SecE is close to helix 2 of SecY and helix 3 of a neighboring SecE. Biochemistry 38 (28):9115-9125

231. Doeven MK, van den Bogaart G, Krasnikov V, Poolman B (2008) Probing receptor-translocator interactions in the oligopeptide ABC transporter by fluorescence correlation spectroscopy. Biophys J 94 (10):3956-3965

232. Garcia-Saez AJ, Ries J, Orzaez M, Perez-Paya E, Schwille P (2009) Membrane promotes tBID interaction with BCL(XL). Nat Struct Mol Biol 16 (11):1178-1185

233. Rusch SL, Kendall DA (2007) Oligomeric states of the SecA and SecYEG core components of the bacterial Sec translocon. Biochim Biophys Acta 1768 (1):5-12

234. Baneyx F, Georgiou G (1990) In vivo degradation of secreted fusion proteins by the Escherichia coli outer membrane protease OmpT. J Bacteriol 172 (1):491-494

235. Hanahan D (1983) Studies on transformation of Escherichia coli with plasmids. J Mol Biol 166 (4):557-580

236. Kusters I, van den Bogaart G, Kedrov A, Krasnikov V, Fulyani F, Poolman B, Driessen AJ (2011) Quaternary structure of SecA in solution and bound to SecYEG probed at the single molecule level. Structure:in press

237. Slotboom DJ, Sobczak I, Konings WN, Lolkema JS (1999) A conserved serine-rich stretch in the glutamate transporter family forms a substrate-sensitive reentrant loop. Proc Natl Acad Sci U S A 96 (25):14282-14287

238. Hutschenreiter S, Tinazli A, Model K, Tampe R (2004) Two-substrate association with the 20S proteasome at single-molecule level. EMBO J 23 (13):2488-2497

239. Crowe LM, Mouradian R, Crowe JH, Jackson SA, Womersley C (1984) Effects of carbohydrates on membrane stability at low water activities. Biochim Biophys Acta 769 (1):141-150

240. van den Bogaart G, Hermans N, Krasnikov V, de Vries AH, Poolman B (2007) On the decrease in lateral mobility of phospholipids by sugars. Biophys J 92 (5):1598-1605

241. Bakheet TM, Doig AJ (2009) Properties and identification of human protein drug targets. Bioinformatics 25 (4):451-457

242. Bagatolli LA (2006) To see or not to see: lateral organization of biological membranes and fluorescence microscopy. Biochim Biophys Acta 1758 (10):1541-1556

243. Joo C, Balci H, Ishitsuka Y, Buranachai C, Ha T (2008) Advances in single-molecule fluorescence methods for molecular biology. Annu Rev Biochem 77:51-76

244. Toprak E, Selvin PR (2007) New fluorescent tools for watching nanometer-scale conformational changes of single molecules. Annu Rev Biophys Biomol Struct 36:349-369

245. Tamm LK, McConnell HM (1985) Supported phospholipid bilayers. Biophys J 47 (1):105-113

246. Wagner ML, Tamm LK (2000) Tethered polymer-supported planar lipid bilayers for reconstitution of integral membrane proteins: silane-polyethyleneglycol-lipid as a cushion and covalent linker. Biophys J 79 (3):1400-1414

247. Sackmann E (1996) Supported membranes: scientific and practical applications. Science 271 (5245):43-48

248. Sackmann E, Tanaka M (2000) Supported membranes on soft polymer cushions: fabrication, characterization and applications. Trends Biotechnol 18 (2):58-64

249. Richter RP, Berat R, Brisson AR (2006) Formation of solid-supported lipid bilayers: an integrated view. Langmuir 22 (8):3497-3505

250. Lin CW, Yan F, Shimamura S, Barg S, Shyng SL (2005) Membrane phosphoinositides control insulin secretion through their effects on ATP-sensitive K+ channel activity. Diabetes 54 (10):2852-2858

251. Deville K, Gold VA, Robson A, Whitehouse S, Sessions RB, Baldwin SA, Radford SE, Collinson I (2010) The oligomeric state and arrangement of the active bacterial translocon. J Biol Chem

252. Meleard P, Bagatolli LA, Pott T (2009) Giant unilamellar vesicle electroformation from lipid mixtures to native membranes under physiological conditions. Methods Enzymol 465:161-176

253. Hamai C, Cremer PS, Musser SM (2007) Single giant vesicle rupture events reveal multiple mechanisms of glass-supported bilayer formation. Biophys J 92 (6):1988-1999

254. Brizard A, Stuart M, van Bommel K, Friggeri A, de Jong M, van Esch J (2008) Preparation of nanostructures by orthogonal self-assembly of hydrogelators and surfactants. Angew Chem Int Ed Engl 47 (11):2063-2066

255. Girard P, Pecreaux J, Lenoir G, Falson P, Rigaud JL, Bassereau P (2004) A new method for the reconstitution of membrane proteins into giant unilamellar vesicles. Biophys J 87 (1):419-429

256. Dudia A, Kocer A, Subramaniam V, Kanger JS (2008) Biofunctionalized lipid-polymer hybrid nanocontainers with controlled permeability. Nano Lett 8 (4):1105-1110

257. Kocer A, Walko M, Feringa BL (2007) Synthesis and utilization of reversible and irreversible light-activated nanovalves derived from the channel protein MscL. Nat Protoc 2 (6):1426-1437

258. du Plessis DJ, Nouwen N, Driessen AJ The Sec translocase. Biochim Biophys Acta

259. Muller M, Blobel G (1984) In vitro translocation of bacterial proteins across the plasma membrane of Escherichia coli. Proc Natl Acad Sci U S A 81 (23):7421-7425

260. Emr SD, Hanley-Way S, Silhavy TJ (1981) Suppressor mutations that restore export of a protein with a defective signal sequence. Cell 23 (1):79-88

261. Sato K, Mori H, Yoshida M, Tagaya M, Mizushima S (1997) Short hydrophobic segments in the mature domain of ProOmpA determine its stepwise movement during translocation across the cytoplasmic membrane of Escherichia coli. J Biol Chem 272 (9):5880-5886